CRANFIELD INSTITUTE OF TECHNOLOGY

SCHOOL OF MECHANICAL ENGINEERING

Ph.D THESIS

Academic Year 1976 - 1979

D.J. NEVRALA

Modelling of Air Movements in Rooms

Supervisor: S.D. Probert

April 1979

SUMMARY

The assessment of room air movements, in all but elementary cases, relies on investigations using either full-size mock-ups or scaled models. Temperature considerations severly limit the maximum geometric scale factor.

A solution is offered by which accurate predictions of the air flows in full-size air-conditioned rooms may be obtained from observations made with small models if certain criteria are satisfied. The maximum geometric scale-factor can be increased to 8.5, while limiting the maximum working temperature in the model to 100°C, by replacing the convective currents with wall jets of a similar velocity profile, volume flow, momentum flux and heat content. A further improvement may be achieved if the scale-factor adopted for the jet nozzle is smaller than the geometric scale-factor. This approach can lead to scale-factors exceeding 11.8.

Theoretical studies have shown the replacement of convective currents by plane jets is feasible. In the course of the study, detailed investigations of areas important for the aimsof the project but where there is a dearth of relevant information, were undertaken.

To test the validity of predictions and to establish necessary empirical factors, a range of measurements of convective currents and their replacement jets were carried out. The results showed that a virtual identity of maximum profile velocity, momentum flux and volume flow at the replacement cross-section could be achieved.

Based on measured empirical factors, a simple procedure, valid for the majority of practical applications, by which replacement jets can be calculated directly from convective surface parameters is given.

Thus, the aim of this study, namely the worthwhile use of a small model which can be constructed cheaply, has been achieved.

ACKNOWLEDGEMENTS

This study originated while the author was working with the Heating and Ventilating Research Association, but due to the pressure of other duties remained incomplete for several years. It was resurrected and completed with the generous financial aid of the British Gas Corporation and the helpful guidance of the Cranfield Institute of Technology during the last three years. To all of these organisations, I wish to express my sincere gratitude.

CONTENTS

FIGURES

Part 1

Part 2

TABLES

PART 1. MODELLING OF AIR MOVEMENTS IN ROOMS

PART 1. MODELLING OF AIR MOVEMENTS IN ROOMS

1.1 Background

1.1.1 Comfort and energy conservation

Space-conditioning systems, whether for the full air-conditioning of an office or industrial plant, or for the warm-air heating of a domestic environment, are usually prescribed and designed without sufficient attention being devoted to local air movements within the confined spaces. However, comfort conditions for human habitation are normally specified in terms of temperature and air velocity (1)-(11). Also, at a selected position in any conditioned space, the local temperature and air velocity are dependent on a number of factors including the room size, the air supply flow rate and velocity, the supply-return air temperature differential, the positions of the supply orifices and the presence of humans (12)-(33).

Properly controlled air movements in a room are desirable in creating a pleasant environment. Some of the more sophisticated 'comfort' indices take into account the influence of air speed, as well as surface and air temperatures and humidity (5)(34)(35). However, even when buildings are designed so as to satisfy these criteria, their subsequent occupants will sometimes be uncomfortable. If there are insufficient air movements, the environment will appear 'stuffy' whereas at the other extreme, complaints may arise due to the presence of 'draughts'. In industry, besides the comfort of personnel, the efficient removal of pollutants from the work area in a manner that avoids disturbing the technological process is an important consideration..

The human body generates its own convective boundary layer and this mollifies the discomforting effects of external air currents. Also, some parts of a human are more sensitive to ambient air movements than others - for example, air speeds of about 0.15 ms^{-1} can be perceived by one's bare ankles whereas about double this value is necessary for detection at face level.

Because of rapidly increasing fuel charges (i.e. since November 1973), better thermal insulation of buildings has been given a higher priority, and this trend will probably continue. Thus the ratio of fabric to ventilation heat losses from the average house has decreased. Whereas for the traditional house the ventilation heat loss amounted to less than 20 per cent of the total heat loss, in a well-insulated dwelling it may contribute more than 50 per cent. Thus it is now desirable, in order to achieve an even greater degree of energy thrift, to optimize the air-movement patterns in occupied zones, so avoiding local overheating which sometimes occurs in an endeavour to combat the effects of draughts.

Unfortunately, conventional methods adopted in design are largely empirical, being based on previous experience. Lack of theoretical guidance has led to some space-conditioning systems being designed so that they are either inadequate in their performance or inefficient

with respect to the energy that is expended to satisfy the comfort requirements. Thus it is desirable to consider, and if necessary for formulate, criteria to aid in the systemization of the design process.

Design depends upon knowledge gained from experimentation, but the latter can be accomplished economically only if worthwhile information can be interpreted from measurements on models. Thus it is necessary to devise realistic conditions, which the tests on the model must satisfy, in order to reveal the desired information concerning the behaviour of the full-size system. Such a formulation is attempted in this chapter.

1.1.2 Air movements

Room-air movements arise either because of the non-uniform temperatures of the surfaces involved or due to the air in the enclosure being replaced, the resulting complicated flow patterns being a consequence of the interaction between inertia, viscous and buoyancy forces. For the small air velocities (<0.3 ms^{-1}) normally encountered in rooms, not one of these forces predominates. So a general, exact solution of the equations describing the flow patterns is extremely difficult to obtain, especially if realistic boundary conditions (e.g. to take account of obstacles and unusual room shapes) are imposed. Thus calculations for real systems are usually confined to predicting the 'throw' of jets issuing from terminal devices; throw being defined as the distance from the terminal orifice to where the break-up of the jet ensues.

For important projects, physical models are usually built so that the air movements involved may be observed and, where necessary, corrective design modifications introduced. Often, full-scale mock-ups are needed, e.g. for operating theatres in hospitals, space capsules or even trains (36). However, the construction of large mock-ups is expensive and time-consuming but unfortunately, to date, scaling factors make quantitative predictions from small-scale models of doubtful value.

No simple but essential breakthrough has occurred concerning the analytical approach and thus it is worthwhile to look afresh at what possibilities modelling techniques can offer. The ideal would be to use small (e.g. one-tenth full-size) inexpensive models capable of revealing accurate flow patterns for the full-size system. To be inexpensive, the technique could only involve cheap, readily available materials and modelling fluids. Also, the maximum permitted temperatures for the model would be critical, both from considerations of operation and safety. It is envisaged, however, that the use of small models may require the adoption of more sophisticated techniques for temperature and velocity measurements (e.g. non-perturbing methods such as Mach-Zehnder interferometry and laser-Doppler anemometry) than are common at present for air-conditioning studies.

1.1.3 Notation

A_{eff} Effective outlet area (see Figure 1.1), m^2

Ar Archimedes number for the flow

$$\left(= \frac{Gr}{Re^2} = \frac{gl\beta\Delta t}{v^2}\right)$$

b,h Width and vertical extent, respectively, of the air inlet grille (see Figure 1.1), m

C Constant

C_p Specific heat of the fluid at constant pressure, J kg^{-1} $^oC^{-1}$

d_h Hydraulic diameter of the considered room, m

D_m Coefficient of diffusion for the fluid in the model, m^2 s^{-1}

F Area of section of the room (see Figure 1.1), m^2

g Local acceleration due to gravity, ms^{-2}

Gr Grashof number for the flow $\left(= \frac{gl^3\beta\Delta t}{v^2}\right)$

K Constant in equation (1-11)

l Characteristic dimension of the flow system, m

l' Fictitious length, m

m,n,p Dimensions of the considered rectangular room (see Figure 1.1), m

M Momentum of the flow, kg ms^{-1}

Nu Nusselt number for the flow $\left(= \frac{\alpha l}{\lambda}\right)$

Pe Péclet number for the flow $\left(= Re.Pr = \frac{vl}{\alpha}\right)$

Pr Prandtl number for the flow $\left(= \frac{\nu}{\alpha}\right)$

Ra Rayleigh number for the flow (= Gr.Pr)

Re Reynolds number for the flow $\left(= \frac{vl}{\nu}\right)$

S Geometric scale factor

S_T Temperature scale factor

S_l Outlet scale factor

t Temperature, ^oC

T	$\frac{1}{2}(T_1 + T_2)$, K
v	Velocity of the flow, ms^{-1}
V	Volume flow rate, $m^3\ s^{-1}$
α	Thermal diffusivity of the fluid $\left(= \frac{\lambda}{\rho C_p}\right)$, $m^2\ s^{-1}$
β	Coefficient of expansion of the fluid $\left(= \frac{1}{T}\right)$, K^{-1}
Δ	Difference between two values of a variable
λ	Thermal conductivity of the fluid, $W\ m^{-1}\ K^{-1}$
ν	Kinematic viscosity of the fluid, $m^2\ s^{-1}$
ρ	Density of the fluid, $kg\ m^{-3}$

Subscripts

a	With respect to ambient conditions
corr	Corrected value
i	With respect to initial jet condition
JET	Referring to wall jet
1	Nozzle
L	Laminar flow convective current
m	Model
max	Maximum value
o	Referring to full-size system
T	Turbulent flow convective current
w	Heated wall (e.g. Δt_w represents the temperature difference between the heated surface and the ambient air)
1,2	With respect to the two conditions 1 or 2 respectively

Superscripts

-	Mean value
'	Fictitious

1.2 Modelling Theory

A theory should enable one to reduce the number of experimental observations necessary to describe adequately the behaviour of the considered system (see Figure 1.1) as well as to permit the use of a scale-model rather than a full-size mock-up for predictive purposes.

A laminar velocity field, formed under the influence of inertia and viscous forces, can be described by the Navier-Stokes differential equations (37). If a temperature field is superimposed, the resultant bouyancy forces affect the system and the equations have to be extended by a further term ($g\rho\beta\Delta t$) to account for the additional vertical flows. The presence of turbulent flows poses an even more difficult situation to cope with mathematically, because both the local velocities and temperatures vary irregularly. As an approximation, the Navier-Stokes equations are usually rewritten using time-average values of the variables. However, to solve the equations it becomes necessary to know in advance the relationships between the variations and the average values. To date, only semi-empirical methods of solution for practical systems have been proposed.

The equations of motion and energy transfer can be solved merely for idealized situations in which it is justifiable for some of the terms in the equations to be neglected. Nevertheless, by dealing with such simplified abstractions from reality it is possible to develop criteria for similarity of both the velocity and temperature fields between the model and the full-size system. Deduction of the necessary conditions for similarity of flows is facilitated by non-dimensionalizing all the variables in the modified Navier-Stokes equations. (Similarity of the velocity fields is attained when, for all geometrically similar positions in the flows, the ratio of the velocities in the model and full-size system is constant. An analogous situation applies with respect to the temperature distributions in the flows, but the constant will be different from that for the identical position in the velocity fields).

In order to achieve similarity of flows, three conditions have to be satisfied:

(1) the inertia and viscous condition i.e.

$$Re = \text{constant} \quad \ldots (1.1)$$

(2) the bouyancy condition, i.e.

$$Ar = \text{constant} \quad \ldots (1.2)$$

(3) the temperature distribution condition, i.e.

$$Pe = \text{constant} \quad \ldots (1.3)$$

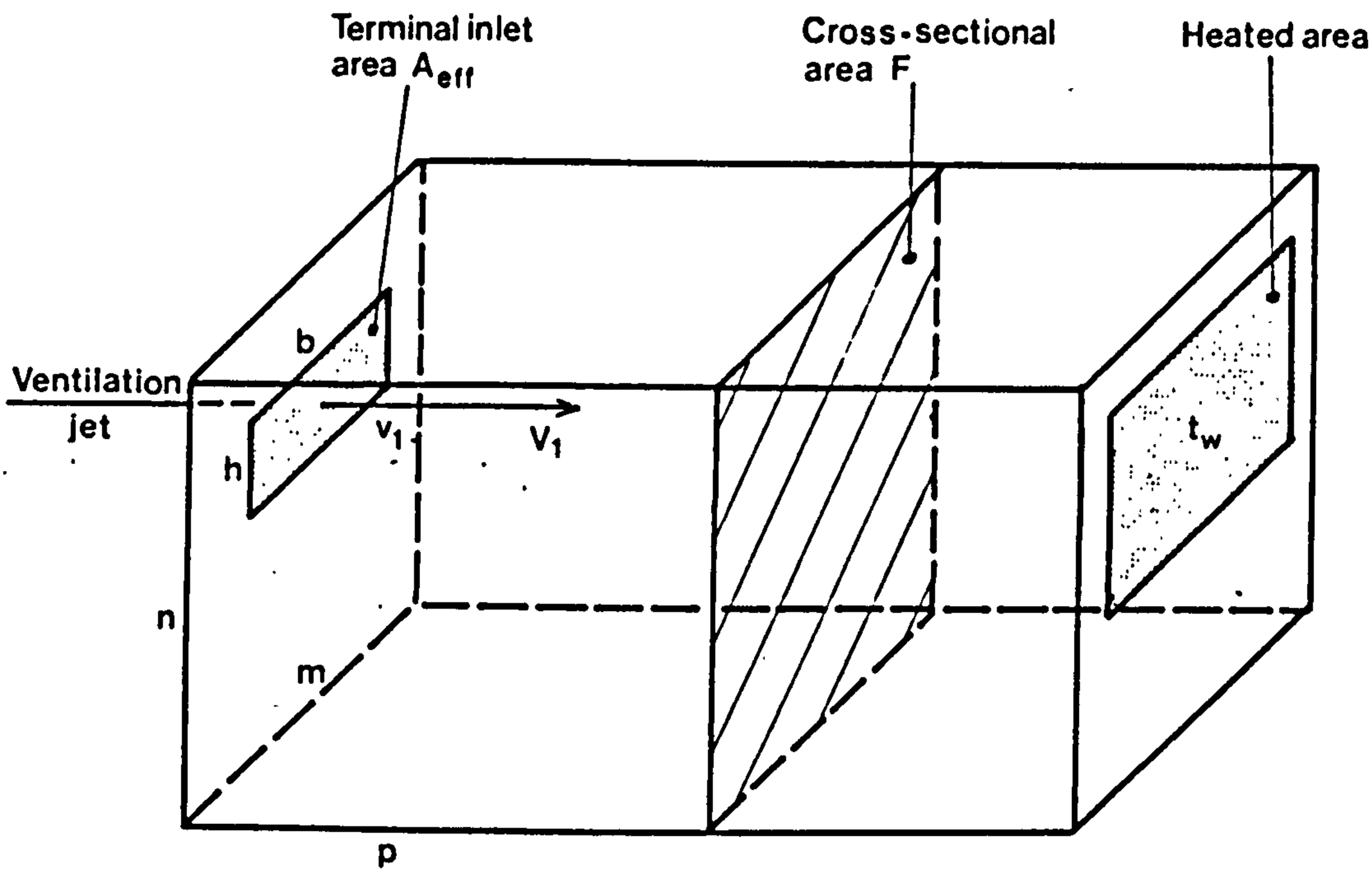

Fig.1.1. GEOMETRICAL AND FLOW PARAMETERS FOR A VENTILATED RECTANGULAR ROOM WITH A HEATED AREA ON THE VERTICAL WALL

It is also necessary to comply with three boundary conditions - geometric, hydrodynamic and thermal. If the model is an accurately scaled replica of the original, then compliance with the geometric condition is assured. For a room enclosed by solid walls, the hydrodynamic boundary condition is automatically fulfilled. In contrast, however, the thermal boundary condition is much more difficult to satisfy because the thermal parameters can usually only be stated for some of the involved surfaces. The temperature distributions over the remaining surfaces will depend upon the heat flows through these surfaces. In order to achieve complete thermal similarity, all the heat flows and radiation exchanges in the original would have to be known in order to reproduce appropriately scaled representations of them in the model.

Room-air movements are influenced not only by inertia and friction, but also by the forces of bouyancy, and, to achieve similarity, conditions (1) Re = constant and (2) Ar = constant have to be satisfied. Buoyancy forces are determined by the temperature field, and, therefore, to obtain similarity of velocity fields, similarity of temperature fields must also be achieved, i.e. condition (3) must be satisfied. But the Peclet number

$$Pe = Re.Pr \qquad \ldots (1.4)$$

where the Prandtl number

$$Pr = \frac{\nu}{\alpha} = \frac{\nu\rho C_p}{\lambda} \qquad \ldots (1.5)$$

is entirely dependent of parameters that describe the physical properties of the fluid. Within the limited temperature and pressure ranges normally encountered for air flow in rooms, these parameters remain approximately invariant.

1.2.1 Use of identical fluids in the model and full-size systems

This is the simplest way of achieving invariance of Pr. Also, condition (1) can then be simplified. If the subscript 'o' is used to denote values in the original, full-size system and 'm' those for the model, the first condition can be presented as

$$Re = \frac{v_o l_o}{\nu_o} = \frac{v_m l_m}{\nu_o} \qquad \ldots (1.6)$$

but with the same fluid in both situations this simplifies to

$$v_o l_o = v_m l_m \qquad \ldots (1.7)$$

If a scale factor is defined by

$$S = \frac{l_o}{l_m} \qquad \ldots (1.8)$$

then

$$v_m = S v_o \qquad \ldots (1.9)$$

The second similarity condition, equation (1.2), can be expressed as

$$\frac{g l_o \Delta t_o}{v_o^2 T_o} = \frac{g l_m \Delta t_m}{v_m^2 T_m} \qquad \ldots (1.10)$$

where $\Delta t = (T_1 - T_2)$; $T_1 > T_2$; $T = \frac{1}{2}(T_1 + T_2)$; T_1 and T_2 are two characteristic temperature of the system. Substituting from equations (1.8) and (1.9) into (1.10) with some rearrangement gives

$$\frac{S^3(T_{10} - T_{20})}{T_{10} + T_{20}} = \frac{(T_{1m} - T_{2m})}{T_{1m} + T_{2m}} = \frac{K}{2} \qquad \ldots (1.11)$$

and so

$$T_{1m} = \left(\frac{2 + K}{2 - K}\right) T_{2m} \qquad \ldots (1.12)$$

Thus, for $K = 2, T_{1m} \to \infty$, and it therefore represents the condition for maximum possible S. Making this substitution into equation (1.11) reveals that

$$S_{max} = \left(\frac{T_{10} + T_{20}}{T_{10} - T_{20}}\right)^{\frac{1}{3}} \qquad \ldots (1.13)$$

For typical conditions, T_{10} = 310 K and T_{20} = 290 K, and so S_{max} = 3.11. But this implies that $T_1 \to \infty$. If, however, the maximum temperature permitted in the model is 100°C (i.e. T_{1m} = 373 K) and we choose $T_{2m} = T_{20}$ = 293 K, then the practical maximum scale factor decreases to 1.54. However, the reduction in costs achievable using models with scale factors of this magnitude, as opposed to full-scale mock-ups, is only modest.

1.2.2 Use of different fluids in the model and full-size systems

To comply with condition (3), namely that the Péclet numbers should be identical for the model and the full-size system flows, and if Re also has to be invariant, then the Prandtl numbers must also be equal. As room-air movements are being considered, the fluid in the full-size system will always be air. Its temperature, even in extreme cases, will only vary between 0°C and 50°C, for which its Prandtl number has the values of 0.707 and 0.698 respectively (38).

An extensive search for a fluid with even an approximately similar value of Pr as that for air and which would also satisfy practical limitations imposed by temperature, pressure, safety in use, availability and price has failed (39)-(42). For example, for water at 0°C, Pr equals 13.7, whereas at 100°C it has fallen to 1.75 and decreases to a minimum of 0.86 at about 250°C. Transformer oil is even less suitable, because its Prandtl number drops from 250 to 80 as the temperature rises from 40°C to 100°C (43).

An alternative approach would be to use solutions of different densities in the model in order to simulate the required differences of air density as caused by the non-uniform temperature field in the full-size system. Then, the coefficient of thermal diffusivity for the air would have to be replaced by the diffusion coefficient D_m, of the dissolved substance and, therefore,

$$Pr = \text{constant} = \frac{\nu_o}{\alpha_o} = \frac{\nu_m}{D_m} \qquad \ldots (1.14)$$

Again, an exhaustive search (ranging from saline solutions to benzine, for which $180 < (\nu_m/D_m) < 1900$) has failed to reveal a suitable fluid.

Rydberg (44) concluded that provided the flows start from rest and that the model is not of too small dimensions (i.e. for those situations in which the heat transmission and material exchange depend almost entirely on the flow), then a difference in the values of ν_o/α_o and ν_m/D_m can be tolerated. This approach is suitable for the study of the intermittent ventilation of rooms, such as when windows are suddenly opened wide, but would be inappropriate in the study of room-air movements generated by air jets and heated surfaces.

1.2.3 Modelling with turbulent conditions applying in the room

Air movements in closed rooms are predominantly turbulent, the turbulence being of low frequency and comparatively high amplitude. Turbulence occurs not only at the boundaries of the jet but throughout the room. Also, any heat sources in the room tend to increase the general level of turbulence. Under such conditions, the influence of viscous forces is restricted predominantly to the boundary regions and they play a relatively minor role in determining the overall air-movement patterns. Thus, invariance of Re between the model and full-size flows is not essential. Müllejans (45) and

van Gunst et al (46) have corroborated this and shown that air-movement patterns in rooms ventilated by jets and having heated surfaces are independent of Re and rely solely on Ar. Therefore, the only similarity condition that has to be satisfied for turbulent conditions is

$$Ar = \frac{g\Delta t\beta l}{v^2} = \text{constant} \qquad \ldots (1.15)$$

Müllejans also advocated the use of a reference velocity, v', defined as

$$v' = \frac{V_1}{F} \qquad \ldots (1.16)$$

where (see Figure 1.1) V_1 is the inlet volume flow and F is the cross-sectional area of the room. He asserted that the reference velocities both in the full-size system and the model should be equal, i.e.

$$v'_o = v'_m = \text{constant} \qquad \ldots (1.17)$$

Based on this assumption and equations (1.8), (1.10) and (1.12), it can be deduced that

$$S\frac{\Delta t_o}{T_o} = \frac{\Delta t_m}{T_m} = K \qquad \ldots (1.18)$$

and

$$S = \frac{K}{2}\frac{(T_{10} + T_{20})}{(T_{10} - T_{20})} \qquad \ldots (1.19)$$

But $K \leqslant 2$, as deduced from equation (1.12). Therefore,

$$S_{max} = \frac{(T_{10} + T_{20})}{(T_{10} - T_{20})} \qquad \ldots (1.20)$$

For the same typical temperatures assumed earlier, namely T_{10} = 310 K and T_{20} = 290 K, S_{max} = 30. When a realistic value for t_{1m} is assumed, namely 100°C, along with a value for t_{2m} of 20°C, the practical maximum scale factor is reduced to 3.64. This is 2.36 times the value if invariance of Reynolds number is also a necessary condition.

The reference velocity as defined by equation (1.16) can be expressed as

$$v' = \frac{\text{number of changes per second x m.n.p}}{m.n}$$

$$= \text{number of air changes per second x p} \qquad \ldots (1.21)$$

where m, n and p are the orthogonal dimensions of the room through which air is flowing. However, v' provides no indication of the influences of inlet velocity or nozzle configuration. To help remedy this, Müllejans (45) introduced a corrected Archimedes number:

$$Ar_{corr} = \left(\frac{b.h}{d_h^2}\right) Ar \qquad \ldots (1.22)$$

where b and h are the dimensions of the inlet grille (see Figure 1.1) and d_h is the hydraulic diameter of the room. So

$$d_h = \frac{2mn}{m + n} \qquad \ldots (1.23)$$

If d_h is used as a reference length and, in order to be able to consider more complicated terminal devices, b.h is expressed as A_{eff}, equation (1.22) can then be rewritten as

$$Ar_{corr} = \frac{g d_h \beta \Delta t}{v'^2} \left(\frac{A_{eff}}{d_h^2}\right) = \frac{g(A_{eff}/d_h)\beta\Delta t}{v'^2} \qquad \ldots (1.24)$$

Thus the use of a corrected Archemedes number, involving the reference length

$$l' = \frac{A_{eff}}{d_h} \qquad \ldots (1.25)$$

will make some allowance for the inlet condition and the room size. Also, for similarity of flows in the model and the full-size systems,

$$Ar_{corr} = \frac{g l' \beta \Delta t}{v'^2} = \text{constant} \qquad \ldots (1.26)$$

1.3 New Possibilities for Modelling Room-Air Movements

In Section 1.2.1, it was seen that permitted temperature considerations limit severely the maximum scale factor. Some easing of the difficulty would, however, ensue if the convective currents generated by warm surfaces could be simulated by wall jets. Another simplifying possibility would be to restrict the requirement for similarity between both the velocity and temperature fields in the model and full-size system to only the occupied zone, i.e. a deformation of the inlet conditions would be allowable.

1.3.1 Replacing a convective current by a wall jet

It is suggested that the air flow from a heated surface can be simulated by a jet of similar velocity profile, volume flow, momentum flux and heat content. According to (37), the mean temperature of a

convective current, measured as the difference between the moving stream and ambient air temperature, is for turbulent flow

$$\overline{\Delta t_T} = 0.236\ \Delta t_w \qquad \ldots (1.27)$$

and for laminar flow

$$\overline{\Delta t_L} = 0.400\ \Delta t_w \qquad \ldots (1.28)$$

where Δt_w is the temperature difference between the heated surface and the ambient air. Purely laminar flow ($Ra < 5 \times 10^8$) is less likely to occur in practice, and so turbulent flows will be considered in the following discussion.

Although the replacement wall jet would have the same heat content and therefore the same mean temperature as the original convective current, the ratio of the mean to maximum absolute temperatures of the profile would be more favourable. The highest temperature in a convective current occurs at the heated surface. The highest temperature in the replacement wall jet is the initial temperature of the air issuing from the slot: in the initial region of a jet it would be identical with the maximum of the temperature profile. Calculations, based on equations in (24) and (47), for the intended applications indicate that the relative mean temperature of the replacement jet, $\overline{\Delta t_{JET}}$, is about 0.7 times the relative initial temperature, $\Delta t_{i,JET}$.

If the maximum temperature in the model is constrained to be 100°C, and $\overline{\Delta t_T} = \overline{\Delta t_{JET}} = 0.7\ \Delta t_{i,JET}$, Ta = 20°C and $\Delta t_{i,JET}$ = (100 - 20)°C = 80°C, then a wall jet not exceeding this temperature could represent a heated surface in the model with a temperature of

$$t_w = \frac{0.7\ \Delta t_{i,JET}}{0.236} + 20 = 257^oC \qquad \ldots (1.29)$$

By considering the same typical conditions as previously, namely t_{10} = 40°C and $t_{20} = t_{2m}$ = 20°C, but with t_{1m} = 250°C, then equation (1.29) would suggest that

$$\frac{\Delta t_m}{T_m} = 0.56 = S^3 \frac{\Delta t_o}{T_o} \qquad \ldots (1.30)$$

i.e. a maximum permitted basic scale factor of 2.04. For a turbulent flow in the room,

$$\frac{\Delta t_m}{T_m} = 0.56 = S \frac{\Delta t_o}{T_o} \qquad \ldots (1.31)$$

and so the maximum permitted scale factor would be 8.5.

A minor weakness of this method of modelling is that extra air is introduced into the room. However, as this amount is relatively minute, the consequent distortion of the room air-flow pattern would be insignificant.

1.3.2 Modified-nozzle scale-factor method

In most cases where air is introduced into rooms, the area A_{eff} of the nozzle is negligible compared with cross-sectional area, F, of the room. Thus a moderate deformation of the nozzle's dimensions in relation to those for the geometric scale-model should yield satisfactory results, because the flow pattern is, within a restricted range, independent of Re, being solely a function of Ar (45)(46). For the turbulent flow resulting from the interaction of the jets and convective current, then via equation (1.24).

$$\frac{\Delta t_o}{T_o} \frac{b_o h_o (m_o + n_o)}{2 m_o n_o} = \frac{\Delta t_m}{T_m} \frac{b_m h_m (m_m + n_m)}{2 m_m n_m} \qquad \ldots (1.32)$$

assuming that $A_{eff} = b.h$, $d_h = 2mn/(m + n)$ and $v' = \text{constant}$.

Let us also make the additional assumptions

$$(a) \quad \frac{\Delta t_m}{T_m} = S_T \frac{\Delta t_o}{T_o} \qquad \ldots (1.33)$$

where S_T is the temperature scale-factor, and

$$(b) \quad S_1 = \frac{b_o}{b_m} = \frac{h_o}{h_m} \qquad \ldots (1.34)$$

where S_1 is the nozzle scale-factor.

Substituting from equations (1.33) and (1.34) into (1.32) gives

$$\frac{\Delta t_o}{T_o} \frac{b_o h_o (m_o + n_o)}{2 m_o n_o} = S_T \frac{\Delta t_o}{T_o} \frac{b_o h_o}{S_1^2} \frac{(m_o + n_o)}{2 m_o n_o} S \qquad \ldots (1.35)$$

because

$$\frac{m_m}{m_o} = \frac{n_m}{n_o} = S$$

Thus

$$\frac{S_T S}{S_1^2} = 1 \qquad \ldots (1.36)$$

The maximum working temperature that can be used in the model limits the temperature scale factor S_T. As an example, consider again the situation in which the convective current has been replaced by a wall jet whose maximum temperature is 100°C. This represents a model surface with t_{1m} = 250°C, the other temperatures being t_{10} = 40°C and $t_{20} = t_{2m}$ = 20°C. The temperature scale-factor is again

$$S_T = \frac{\Delta t_m}{T_m} \frac{T_o}{\Delta t_o} = 8.5 \qquad \ldots (1.37)$$

The new limiting factor imposed on the maximum geometrical scale-factor, S, determines how far the nozzle dimensions need to be deformed in relation to the rest of the model. Let us assume a conservative value for S_1, say 0.85S, which if substituted into equation (1.36) along with S_T = 8.5 leads to S_{max} = 11.8.

Table 1.1. Parameters for the model as functions of the scale factors.

Parameter	According to theory		
	B	Tu	Ne
$m_m(n_m, p_m)$	$\frac{m_o}{S}$	$\frac{m_o}{S}$	$\frac{m_o}{S}$
$b_m(h_m)$	$\frac{b_o}{S}$	$\frac{b_o}{S}$	$\frac{b_o}{\sqrt{S_T S}}$
$A_{eff,m}$	$\frac{A_{eff,o}}{S^2}$	$\frac{A_{eff,o}}{S^2}$	$\frac{A_{eff,o}}{S_T S}$
V_{1m}	$\frac{V_{10}}{S}$	$\frac{V_{10}}{S^2}$	$\frac{V_{10}}{S^2}$
v_{1m}	$v_{10} S$	v_{10}	$v_{10} \frac{S_T}{S}$
v'_m	$v'_o S$	v'_o	v'_o
l'_m	$\frac{l'_o}{S}$	$\frac{l'_o}{S}$	$\frac{l'_o}{S_T}$
M_{1m}	M_{10}	$\frac{M_{10}}{S^2}$	$M_{10} \frac{S_T}{S^3}$

Key on following page

The following key applies: B...basic modelling theory, Tu... turbulent room theory, Ne...modified-nozzle scale-factor theory.

The parameters shown in parentheses should be treated in a similar manner to that indicated in the appropriate row of the table.

All the parameters of interest would be influenced by the proposed approach. For instance, from equation (1.36),

$$A_{eff,m} = b_m.h_m = \frac{b_o h_o}{S_1^2} = \frac{A_{eff,o}}{S_T S} \qquad \ldots (1.38)$$

$$b_m = \frac{b_o}{\sqrt{S_T.S}} \quad \text{and} \quad h_m = \frac{h_o}{\sqrt{S_T.S}}$$

If

$$V_{1m} = \frac{V_{10}}{S^2} \quad \text{and} \quad v_{10} = \frac{V_{10}}{A_{eff,o}}$$

and then the initial velocity of the jet is

$$v_{1m} = \frac{V_{1m}}{A_{eff,m}} = \frac{V_{10}}{A_{eff,o}} \frac{S_T.S}{S^2} = v_{10} \frac{S_T}{S} \qquad \ldots (1.39)$$

The volume rate of flow through the nozzle will be

$$V_{1m} = v_{1m} b_m h_m = v_{10} \frac{S_T}{S} \frac{b_o h_o}{S_T S} = \frac{V_o}{S^2} \qquad \ldots (1.40)$$

The fictitious reference length of equation (1.25) would be modified in the following way:

$$l'_m = \frac{A_{eff,m}}{d_{h,m}} = \frac{A_{eff,o}}{S_T S} \frac{S}{d_{h,o}} = \frac{l_o}{S_T} \qquad \ldots (1.41)$$

For momentum, if S_o took on a specific value, say S_1, then

$$\frac{M_{1m}}{M_{10}} = \frac{v_{1m} V_{1m}}{v_{10} V_{10}} \qquad \ldots (1.42)$$

Therefore

$$M_{1m} = \frac{S_T}{S^3} M_{10} \qquad \ldots (1.43)$$

Table 1.2. Collation of maximum scale factors obtained from previous examples.

Theory used	S_{max}
B	1.54
B_{JET}	2.04
Tu	3.64
Tu_{JET}	8.5
Ne_{JET}	11.8

The subscript 'JET' implies that a wall jet has been used to simulate the convective current.

This modified-nozzle method could lead to greater flexibility in the modelling of room-air movements for those cases where the ratio S_1/S is not critical and could result in even higher permitted geometrical scale-factors than evaluated in the above example.

1.4 Conclusions

Accurate predictions of the air flows in full-size air-conditioned rooms may be obtained from observations made with small models if certain criteria are satisfied. The maximum geometric scale-factor can be increased to 8.5, while limiting the maximum working temperature in the model to 100°C, by replacing the convective currents with wall jets of a similar velocity profile, volume flow, momentum flux and heat content. A further improvement may be achieved if the scale-factor adopted for the jet nozzle is smaller than the geometric scale-factor. This approach can lead to scale-factors exceeding 11.8. Thus, the aim namely the worthwhile use of a small model which can be constructed cheaply, can be achieved.

REFERENCES

(1) HOUGHTEN, F.C. and YAGLOU, C.P. 'Determination of the comfort zone', Trans. A.S.H.V.E. 1923 29, 361.

(2) MISSENARD, A. 'On thermally equivalent environments', J.I.H.V.E. 1959 27, 231.

(3) BEDFORD, T. Environment warmth and its measurement 1946 (H.M.S.O., London).

(4) I.H.V.E. Guide.

(5) A.S.H.R.A.E. Guide.

(6) HOUGHTEN, F.C., GUTBERLET, C. and WITKOWSKI, E. 'Draft temperatures and velocities in relation to skin temperature and feeling of warmth', A.S.H.V.E. Trans. 1938 44, 289-308.

(7) RYDBERG, J. and NORBACK, P.E.R. 'Air distribution and drafts', A.S.H.V.E. Trans. 1949 55, 225-240.

(8) STRAUB, H.E. 'Principles of room air distribution', Heat. Pip. Air Condit. 1969 41 (No. 4), 122-128.

(9) DIN 1946, Ventilation systems (VDI ventilation rules) June 1962.

(10) McNALL, P.E. and NEVINS, R.G. 'A critique of ASHRAE comfort standard', ASHRAE Journal 1968, 99-102.

(11) McINTYRE, D.A. "a guide to thermal comfort', Appl. Ergonomics 973 4 (No. 2), 66-72.

(12). RYDBERG, J. 'Perforated ceilings for air injection', Kylteknisk Tidskrift 1963 (No. 2), 31-38.

(13) RYDBERG, J. 'Cooling effects and air quantities permissible in space air distribution', Kylteknisk Tidskrift 1963 (no. 3) 49-52.

(14) LINKE, W. 'Aspects of jet ventilation', Kaltetechnik -Klinatisierung 1966 18 (No. 3), 122-126 (HVRA Translation 103).

(15) YOUSOUFIAN, H.H. 'Diffusion and distribution from ceiling and wall outlets', Heat Pip. Air Condit. 1966 38 (No. 4), 124-131.

(16) Guide and data book: systems and equipment 1967 (ASHRAE, New York).

(17) DAWS, L.F. 'Movement of air streams indoors', Building Research Station, Research Paper 66 August 1967.

(18) STOECKER, W.F. Principles for air conditioning practice 1968 (Industrial Press, New York).

(19) HOWARTH, A.T. An investigation of factors affecting air movement in mechanically ventilated rooms M.Phil. Thesis, University of Nottingham 1970.

(20) JACKMAN, P.J. 'Air movement in rooms with side-wall mounted grilles - a design procedure', HVRA Laboratory Report No. 65 1970.

(21) HOWARTH, A.T., MORTON, A.S. and SHERRATT, A.F.C. 'A new method of comfort heating with warm air', Conference on heat and mass transfer by combined forced and natural convection I.Mech.E., Manchester University, Sept. 1971.

(22) JACKMAN, P.J. 'Air movement in rooms with sill-mounted grilles - a design procedure', HVRA Laboratory Report No. 71 1971.

(23) NEVINS, R.G. 'Air distribution research', ASHRAE Journal 1971, 63.

(24) BATURIN, V.V. Fundamentals of industrial ventilation Third Edition, 1972 (Pergamon Press, Oxford).

(25) NEVINS, R.G. and MILLER, P.L. 'Analysis, evaluation and comparison of room air distribution performance - a summary', ASHRAE Trans. 1972 78, 235-242.

(26) JACKMAN, P.J. 'Air movement in rooms with ceiling-mounted diffusers', HVRA Laboratory Report No. 81 1973.

(27) HOLMES, M.J. and CAYGILL, C. 'Air movement in rooms with low air supply rates', HVRA Laboratory Report No. 84 1974.

(28) CROOME-GALE, D.J. and ROBERTS, B.M. Air conditioning and ventilation of buildings 1975 (Pergamon Press, Oxford).

(29) HOLMES, M.J. 'Room air distribution with variable air volume supply systems', HVRA Project Report 15/107 1974.

(30) HOLMES, M.J. 'Designing variable volume systems for room air movement', HVRA Applications Guide, 1/74 1974.

(31) CONRAD, O. 'Untersuchung Über das Verhalten zweier gegeneinander Strömender Wandstrablen', Gesundheits-Ingenieur 1972 93, 10.

(32) HOLMES, M.J. and JONES, T.J. 'A laboratory investigation into the effect of cold windows on room air distribution from ceiling diffusers', HVRA Project Report 15/101 October 1975.

(33) HOLMES, J.M. 'Room air movement with ceiling-mounted diffusers', BSRIA Applications Guide 275/1975.

(34) FANGER, P.O. Thermal comfort 1973 (McGraw-Hill, New York).

(35) JOKL, M. 'The physiological requirements for thermal comfort to be met by heating systems', Paper CIB Commission W45 Symposium September, 1972.

(36) STANLEY, E.E., SHORTER, D.N. and COUSINS, P.J. 'A laboratory study of the downward displacement systems of ventilation in operating theatres', HVRA Laboratory Report No. 19 March 1964.

(37) KAYS, W.M. Convective heat and mass transfer 1966 (McGraw Hill, New York).

(38) CHYSKÝ, J. Vlhký vzduch-podklady pro výpočet úprav vzduchu, ZTV/3 1969 12.

(39) KAYE, G.W.C. and LABY, T.H. Tables of physical and chemical constants 1973 (Longmans).

(40) Handbook of chemistry and physics 1976-77, 57th Edition (CRC Press).

(41) American Institute of Physics Handbook 1972, 3rd Edition (McGraw-Hill, New York).

(42) REID, C.R. and SHERWOOD, T.K. Properties of gases and liquids; their examination and correlation 1966 (McGraw-Hill, New York).

(43) MICHEJEV, M.A. Heat transfer 1949 (Gosenergoizdat, Moscow-Leningrad).

(44) RYDBERG, J. 'Model experiments relating to ventilation by windows', V.V.S. Stockholm, No. 2 1945 (D.S.E.R./B.R.S. Library Communication 401, 1953).

(45) MÜLLEJANS, H. Uber die Ahnlichkeit der Nichtisothermen Strömung und den Wärmeübergang in Räumen mit Strahllüftung 1966 (Westdeutscherverlag, Köln und Opladen).

(46) VAN GUNST, E., ERKELENS, P.J. andCOENDERS, W.P.J. 'Some results of investigations regarding the supply of cooled air in a test room', 4th International Congress on Heating and Air Conditioning Paris, 1967.

(47) BILLINGTON, N.S. 'Air movement over hot or cold surfaces', HVRA Report No. 29, January 1966.

PART 2 FEASIBILITY OF THE REPLACEMENT OF NATURAL CONVECTIVE CURRENTS BY WALL JETS WHEN ATTEMPTING TO MODEL ROOM AIR MOVEMENTS

CONTENTS

NOTATION

a	Constant	
a	Coefficient of turbulence	
a_i	Coefficient of turbulence in the initial region	
a_m	Coefficient of turbulence on the main region	
a_ρ	Acceleration due to forces of buoyancy	ms^{-2}
A	Constant	
Ar	Archimedes number $\left\{= \frac{Gr}{Re^2}\right\}$	
b_o	Nozzle aperture half-width	m
c	Constant	
c_p	Specific heat	$J\ kg^{-1}\ {}^0K^{-1}$
C	Constant	
F	Function	
g	Acceleration due to gravity	ms^{-2}
Gr	Grashof number	
h	Heat transfer coefficient	$Wm^{-1}\ {}^0K^{-1}$
h*	Transverse distance across flow of shear layer measured from a point where $v = v_o$	m
$h_{0.5}$	Length scale; value of h* where $v = 0.5\ v_o$	m
H	Vertical dimension of convection surface	m
K	Room air turbulence maximum velocity factor	$\left\{K = \frac{v_e}{v_{max}}\right\}$
K_V	Room air turbulence volume factor $\left\{K_V = \frac{V_e}{V_c}\right\}$	
K_M	Room air turbulence momentum flux factor $\left\{K_M = \frac{M_e}{M_c}\right\}$	
K_Q	Room air turbulence heat flux factor $\left\{K_Q = \frac{Q_e}{Q_c}\right\}$	
l	Length of element	m
l_o	Distance of apparent source of jet from nozzle	m
L_i	Length of initial region	m

M	Momentum flux	$kgms^{-2}$ per m run
Nu	Nusselt number	
p	Pressure differential	N/ms^{-2}
Pr	Prandtl number	
q	Local rate of heat flow	$W\ m^{-2}$
Q	Heat content of convective or jet flow	W per m run
$\dot{Q}$	Heating power	W per m run
Ra	Rayleigh number (=Gr Pr)	
Re	Reynolds number	
S	Distance of nozzle from edge of convective surface	m
Δt	Temperature differential	^oC
x	Vertical distance from the starting point of boundary layer	m
x	Distance from nozzle	m
v	Velocity of the flow	ms^{-1}
v^*	Characteristic velocity	ms^{-1}
v_{ar}	Mean arithmetic velocity	ms^{-1}
v_{sq}	Mean square velocity	ms^{-1}
V	Volume flow	m^3s^{-1} per m run
v_m	Velocity scale; maximum value of jet velocity profile	ms^{-1}
w	Buoyancy component of velocity	ms^{-1}
y	Transverse distance across flow	m
$y_{0.5}$	Length scale; value of y where $v = 0.5\ v_m$	m
α	Constant	
α	Thermal diffusitivity	m^2s^{-1}
β	Coefficient of expansion	K^{-1}
β_o	Correction coefficient for momentum	

δ	Width of boundary layer	m
λ	Thermal conductivity	$Wm^{-1}{}^{o}K^{-1}$
μ	Dynamic viscosity	$Ns\ m^{-2}$
ν	Kinematic viscosity	m^2s^{-1}
ρ	Density	kgm^{-3}
τ	Time	s
τ_L	Laminar sheer stress	Nm^{-2}
τ_T	Turbulent sheer stress	Nm^{-2}
ϕ	Function	
Φ	Ratio of mean arithmetic velocity to maximum velocity $\left\{ \Phi = \frac{v_{o_{ar}}}{v_{o_{max}}} \right\}$	
Ψ	Ratio of mean square velocity to maximum velocity $\left\{ \Psi = \frac{v_{o_{sq}}}{v_{o_{mx}}} \right\}$	

Subscripts

a	With respect to ambient conditions
c	Convective current
e	Denotes presence of room air turbulence
J	Related to isothermal jet values
L	Laminar
m	With respect to maximum value of velocity profile
max	Maximum value of convective velocity profile
o	With respect to nozzle conditions
S	Replacement jet values at x = H
T	Total
T	Turbulent

w With respect to surface generating convective currents

x In the x-direction

y In the y-direction

ρ Related to buoyancy generated values

Superscripts

— Mean value

' Corrected value

PART 2 FEASIBILITY OF THE REPLACEMENT OF NATURAL CONVECTION CURRENTS BY WALL JETS WHEN ATTEMPTING TO MODEL ROOM AIR MOVEMENTS

2.1 INTRODUCTION

Although the lack of reliable theoretical guidance makes the use of models in the study of room air movements attractive, temperature considerations severly limit the scale factor[1]. The problem is the cost of the relatively large scale, if not full scale, mock-ups made necessary by the restricted maximum practicable operational temperature in the model. It has been suggested[2] that accurate predictions of the air flows (well removed from the original perturbation) in full-scale space conditioned rooms may be obtained from observations made with small models if the convective currents in the model are replaced by wall jets of suitable thermal and aerodynamic characteristics. The advantage of using a replacement wall jet having the same volume flow, momentum flux and heat content would be that whilst the impact of the replacement jet on the room air movement pattern would be essentially the same as that due to the original convective current, the maximum temperature in the model would be far lower. The highest temperature in a convective current occurs at the heated surface (Fig. 2.1), but if it is replaced be a wall jet having an identical mean temperature, and therefore heat content, the highest temperature will be the temperature of the air issuing from the slot (Fig. 2.2). Thus a wall jet in the initial region, where no decay in the core temperature is presumed, would evidently be most advantageous.

Considerable scope exists for the application of the principle of replacement of convective currents by wall jets in a model. In general, room air movements are generated by convective currents which are stimulated by surfaces at temperatures that differ from the mean room air temperature. The temperatures of the jets also usually differ from the mean room air temperature. A typical example of warm surfaces leading to convective currents that interact with cool jets, is the summer air-conditioning situation, when the heat flows into the enclosure through external walls and windows and is transported away by the air-conditioning system. Up to now research into room air movements has concentrated on this aspect. The winter situation can be even more complex. Convection currents are stimulated not only by cool walls and windows, but also by the warm surfaces of heat emitters. The need to conserve energy has led to high levels of insulation, and resulted in changes in the thermal characteristics of structures[3]. Better space conditioning systems will have to be designed in order to provide acceptable levels of thermal comfort and their success will, to a much higher degree than hitherto, depend on a detailed knowledge of room air movements [4] [5].

When modelling situations where convective currents from cool surfaces interact with warm currents or jets, the replacement of convective currents by wall jets has a further advantage. It is more convenient to provide cool air for the replacement wall jet than to cool surfaces in the model to far lower temperatures required to generate an equivalent convective current. Even at relatively modest sub-zero

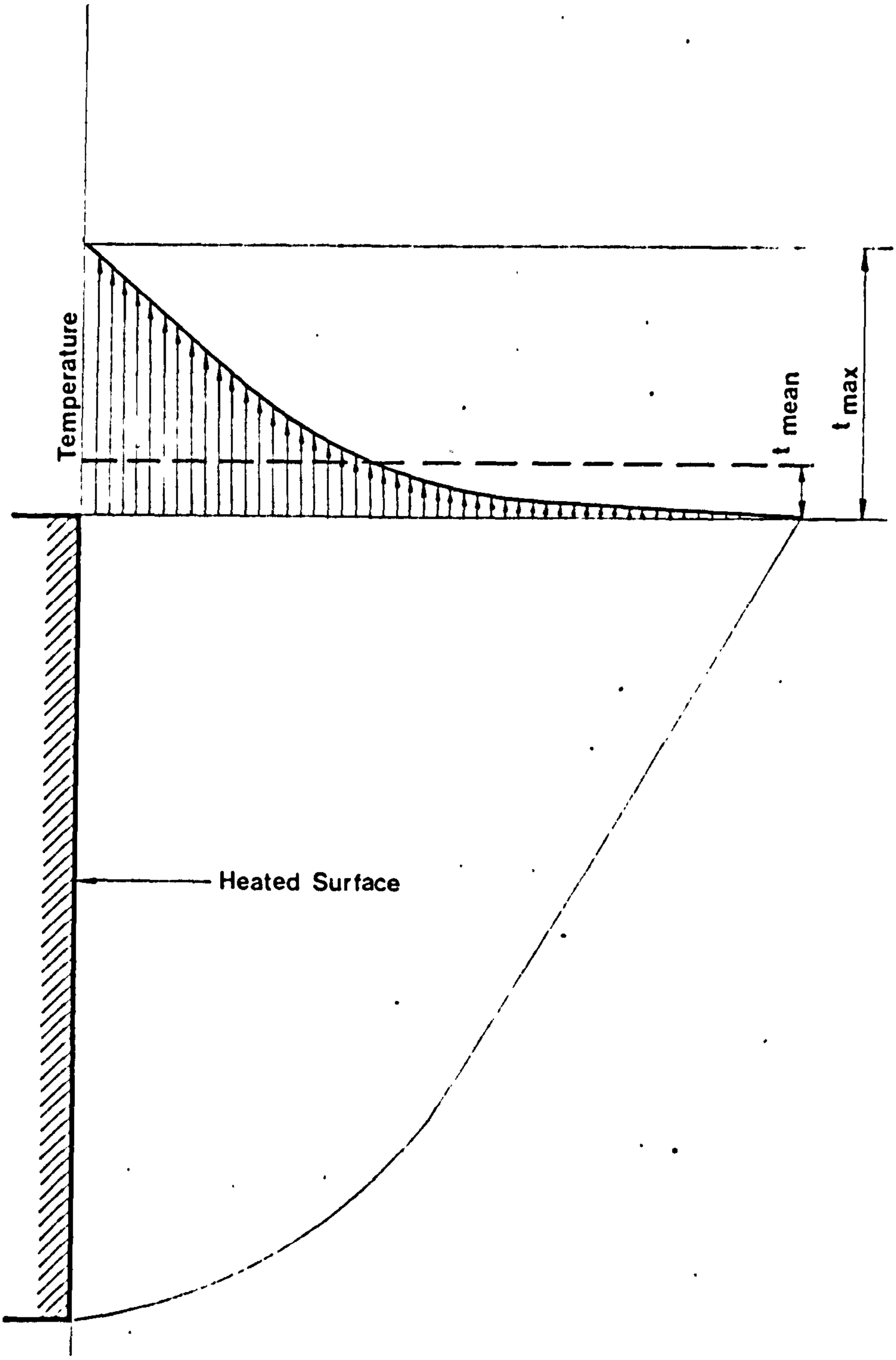

Fig. 2.1. TEMPERATURE PROFILE OF A CONVECTIVE CURRENT

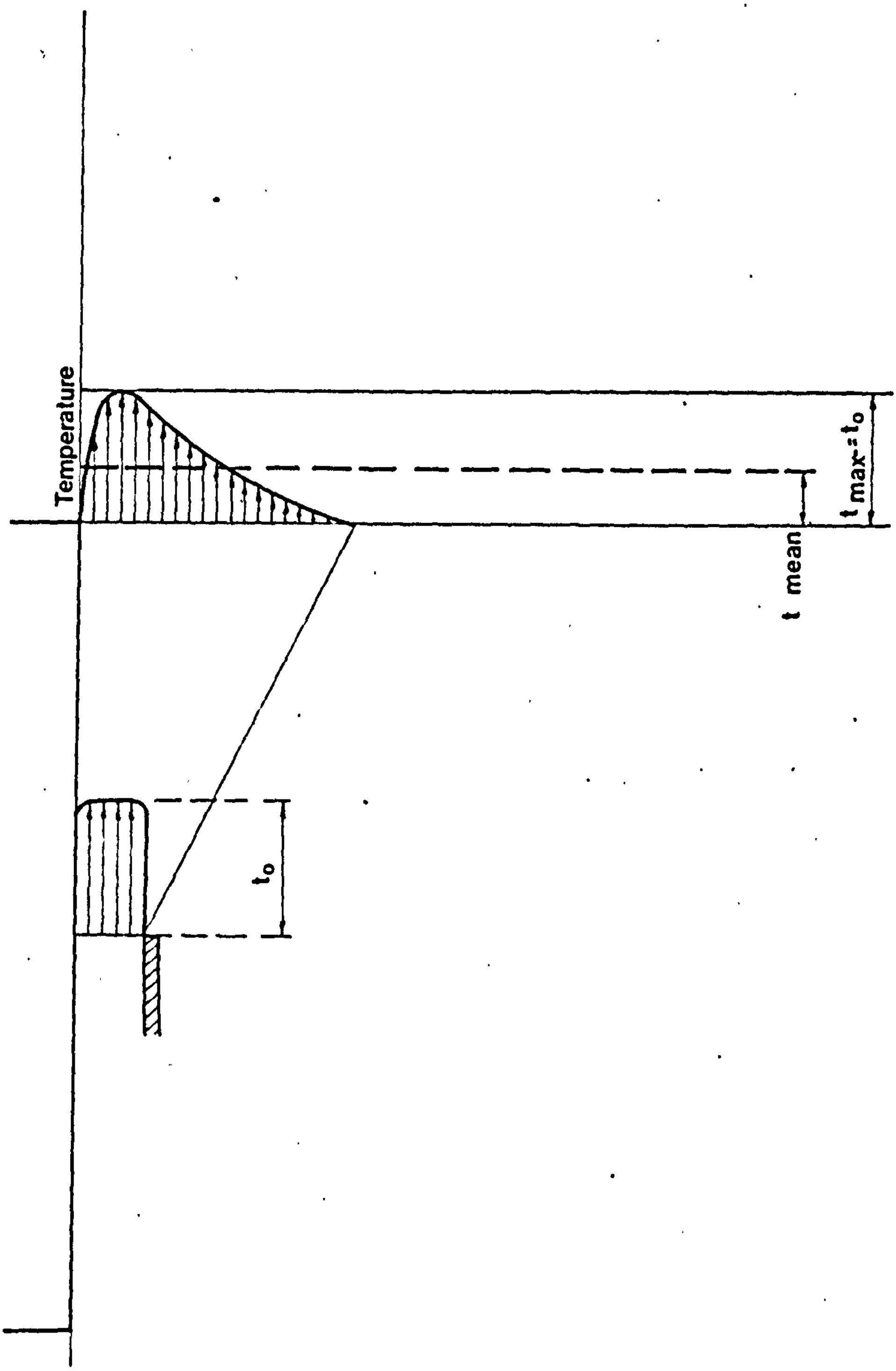

Fig.2.2. TEMPERATURE PROFILE OF A REPLACEMENT WALL JET

temperatures, condensation would pose a problem, if extreme precautions were not taken.

It may be convenient to divide into three steps the theoretical approach to the replacement of convective currents in models by wall jets. The first step is to find suitable theoretical expressions for the parameters that describe a convective current leaving a heated or cooled surface. The second step is to define a relationship between the parameters that describe a wall jet and its initial velocity, temperature and width as well as the relative position of the slot. The third and final step is to derive a relationship between the length and surface temperatures of the surface generating the convective current and the initial parameters of the replacement wall jet.

2.2 NATURAL CONVECTIVE CURRENTS

A survey of the literature [6-20] has revealed a varying degree of agreement between theoretically predicted parameters of convective currents and the experimental results. These divergencies can be accounted for mainly by errors introduced by the individual experimental techniques and by different ambient air conditions encountered in the course of the experiments.

Transition from laminar to turbulent flow depends primarily upon the height and relative temperature of the heated or cooled surface, the Rayleigh number, Ra, being usually preferred to express this relationship. Laminar flow according to Billington[6] occurs if $Ra < 5 \times 10^8$, whereas Cheesewright[7] considers $Ra = 1.4 \times 10^9$ as the beginning of transition, because it was at this value that significant fluctuations in the boundary layer first appeared. Fully established turbulent flow occurs at Ra values between $Ra > 10^9$ and $Ra > 6 \times 10^9$, depending on author and criteria employed.

Fig. 2.3 shows how the Ra number changes with height and relative temperature, Δt, of the heated or cooled surface. Also shown in the graph are the ranges of Ra numbers associates with the most common sources of convective currents in buildings. Walls, because of their height, would inevitably generate turbulent flows. The standard form of radiators, would on the other hand generate laminar flows. Windows and higher heat emitters occupy a zone of uncertainty. In practice, the level of room turbulence will be higher than that encountered in the experimental situation, (because of furnishings, presence of humans, etc.), and it is therefore probable that transition will occur at correspondingly lower Ra numbers. The values quoted by Billington[6], i.e. laminar flow for $Ra < 5 \times 10^8$ and turbulent flow for $Ra > 10^9$ should therefore be more appropriate to realistic situations.

Convective currents on leaving the vicinity of the heated or cooled surfaces interact with other flows and influence the room air movement patterns. The parameters that describe the impact of a flow are the volume flow, momentum flux and the heat content - these can be

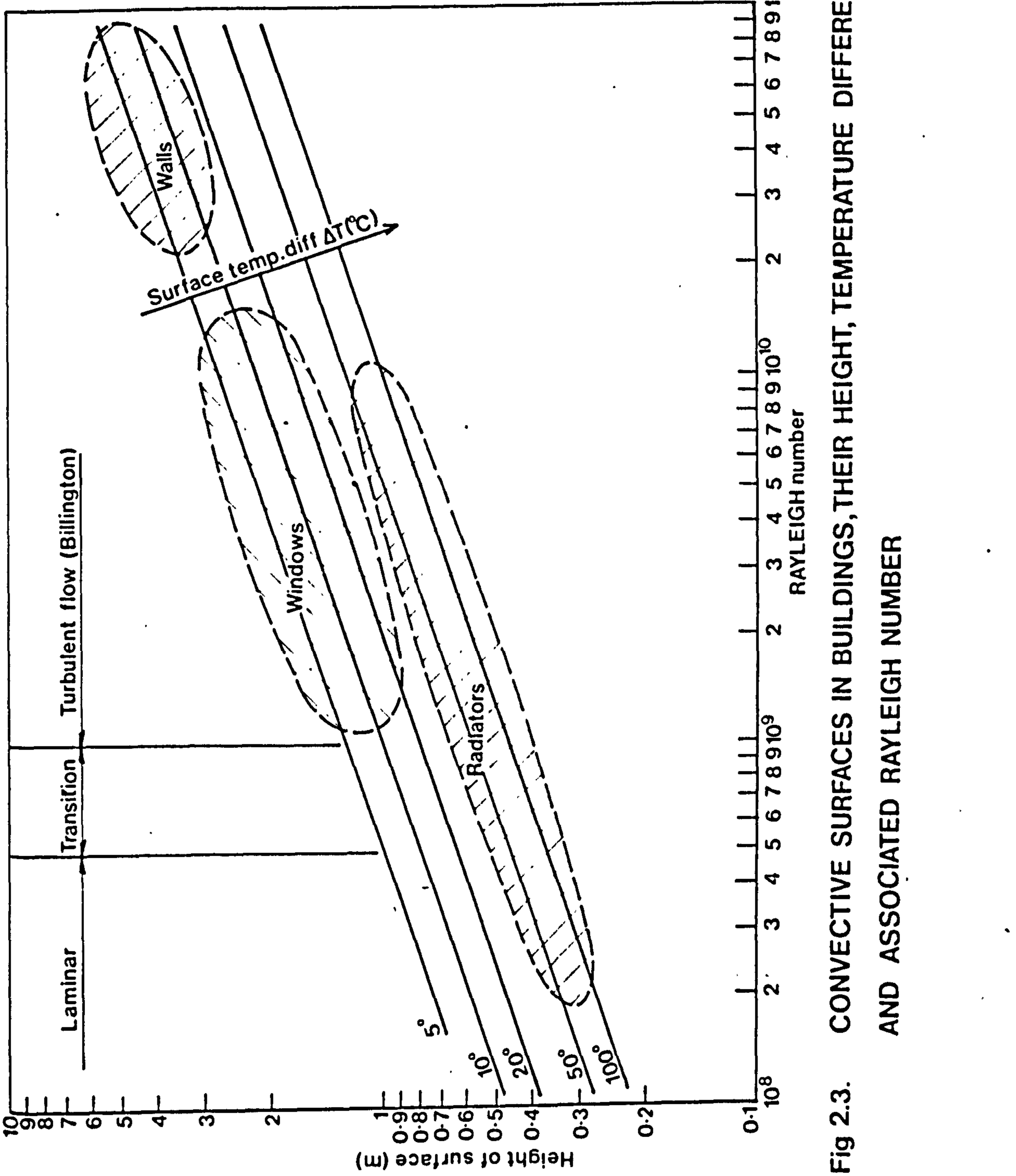

Fig 2.3. CONVECTIVE SURFACES IN BUILDINGS, THEIR HEIGHT, TEMPERATURE DIFFERENCE AND ASSOCIATED RAYLEIGH NUMBER

deduced from the know velocity and temperature profiles of the stream (Fig. 2.4).

2.2.1. Laminar flow

The velocity profile of a convective current resulting from the presence of a heated or cooled surface at a homogeneous temperature can be expressed by an equation that takes the form [6 10 12]

$$v = v^* \frac{y}{\delta} (1 - \frac{y}{\delta})^2 \quad \ldots (2.1)$$

where v^* is a characteristic velocity and δ is the width of the boundary layer. Maximum velocity along the profile will occur at a distance y from the surface where $\frac{dv}{dy} = 0$, which yields a value of $y_{max} = \frac{\delta}{3}$. Substituting into equation (2.1).

$$v_{max} = 0.148\ v^* \quad \ldots (2.2)$$

and therefore

$$v = 6.75\ v_{max} \frac{y}{\delta} (1 - \frac{y}{\delta})^2$$

The temperature profile can be described by a simple expression

$$\Delta t = \Delta t_w (1 - \frac{y}{\delta})^2 \quad \ldots (2.3)$$

where Δt_w is the temperature differential between the surface and ambient air temperature.

By introducing equations (2.3) and (2.4) into the equation of flow for the boundary layer, it is possible to express the maximum velocity, v_{max}, and the width of the boundary layer, δ, as a function of the relative surface temperature, Δt_w, and the distance along the surface from the starting point of the boundary layer, x. Namely

$$v_{max} = 0.766 (0.952 + \frac{\nu}{\alpha})^{-0.5} (g\beta)^{0.5} x^{0.5} \Delta t_w^{0.5} \ldots (2.5)$$

and

$$\delta = 3.93 (\frac{\nu}{\alpha})^{-0.5} (0.952 + \frac{\nu}{\alpha})^{0.25} (\frac{g\beta}{\nu^2})^{-0.25} x^{0.25} \Delta t_w^{-0.25} (2.6)$$

or in non-dimentionised form

$$Re_{max} = 0.766 (0.952 + Pr)^{-0.5} Gr^{0.5} \quad \ldots (2.7)$$

and

$$\frac{\delta}{x} = 3.93\ Pr^{-0.5} (0.952 + Pr)^{0.25} Gr^{-0.25} \quad \ldots (2.8)$$

The range of temperatures encountered in room air movements in practice is relatively limited. If, for example, values expressing the physical properties of air at 293 K are substituted into equations (2.5) much simplified expressions will result, namely

$$v_{max} = 0.108 x^{0.5} \Delta t_w^{0.5} \quad \ldots (2.9)$$

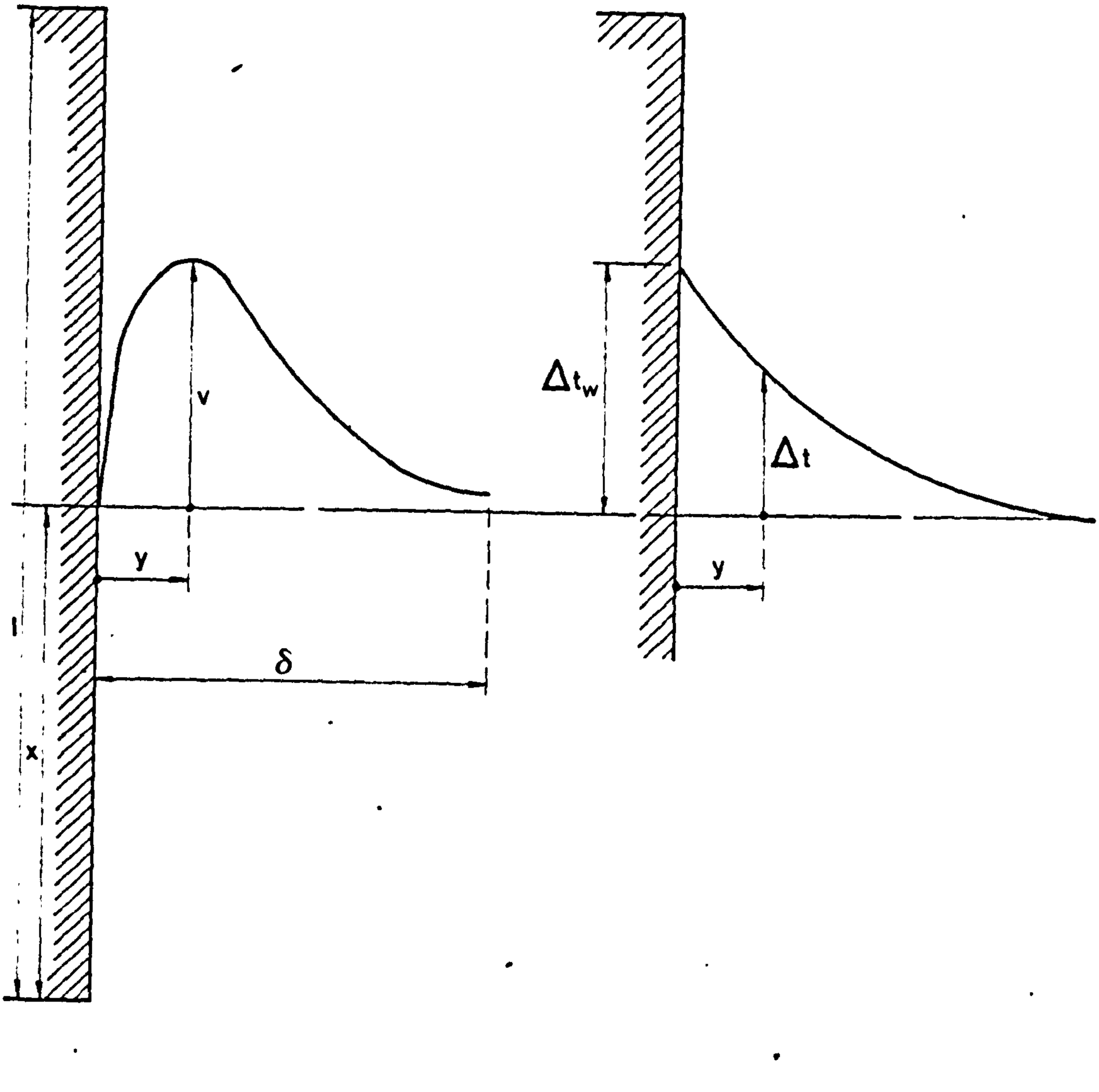

Fig.2.4. CONVECTIVE CURRENT NOMENCLATURE

$$\delta = 4.93 \times 10^{-2} \times {}^{0.25}\Delta t_W^{0.25} \qquad \ldots (2.10)$$

The error introduced by the use of the above simplified equations should be negligible as the values of physical properties of air vary only slightly over the encountered temperature range.

The main parameters that govern the impact of a flow on room air movements - volume flow V, momentum flux M and the heating in power Q can now also be expressed as functions of the relative surface temperature and the distance along the surface.

The volume flow, V, is

$$V = {}_0\int^{\delta} v \, dy \qquad \ldots (2.11)$$

Substituting from equation (2.1) and integrating gives

$$V = 0.083 \, v^* \delta \qquad \ldots (2.12)$$

or substituting equation (2.2), (2.9) and (2.10) reveals that

$$V = 3 \times 10^{-3} \times {}^{0.75} \Delta t_W^{0.25} \qquad \ldots (2.13)$$

The momentum flow can be expressed as

$$M = {}_0\int^{\delta} \rho v^2 \, dy \qquad \ldots (2.14)$$

and by substituting and integrating

$$M = 2.49 \times 10^{-4} \times^{1.25} \Delta t_W^{0.75} \rho \qquad \ldots (2.15)$$

The heating power of a convective stream is

$$\dot{Q} = {}_0\int^{\delta} \rho . c_p . v . \Delta t \, dy \qquad \ldots (2.16)$$

and substituting from equations (2.1), (2.2), (2.4), (2.9) and (2.10) and integrating gives

$$\dot{Q} = 1.2 \times 10^{-3} \times^{0.75} \Delta t_W^{1.25} \rho c_p \qquad \ldots (2.17)$$

and the mean temperature of the stream $\overline{\Delta t}$ is therefore

$$\overline{\Delta t} = \frac{\dot{Q}}{\rho c_p} \qquad \ldots (2.18)$$

substituting equation (2.13) and (2.17) and rearranging yields

$$\overline{\Delta t} = 0.4 \, \Delta t_W \qquad \ldots (2.19)$$

which indicates that the mean temperature of the stream is dependent solely upon the relative surface temperature.

2.2.2. Turbulent flow

Although the velocity and temperature profiles of turbulent convective

currents differ in shape from laminar profiles, they can be described by essentially the same type of equations. If the velocity profile is expressed as

$$v = v^* \left(\frac{y}{\delta}\right)^{\frac{1}{7}} \left(1 - \frac{y}{\delta}\right)^4 \quad \ldots (2.20)$$

the maximum velocity, v_{max}, will occur where $\frac{dv}{dy} = 0$, i.e. at $y = \frac{\delta}{29}$

and substituting into equation (2.20) leads to

$$v_{max} = 0.535\ v^* \quad \ldots (2.21)$$

Again, as for laminar flow, introducing equations (2.20), (2.21) and the expression of the temperature profile

$$\Delta t = \Delta t_w \left(1 - \left(\frac{y}{\delta}\right)^{\frac{1}{7}}\right) \quad \ldots (2.22)$$

into the turbulent flow equation for the boundary layer, it is possible to express the maximum velocity, v_{max}, and the width of the boundary layer, δ, as a function of the relative surface temperature, Δt_w, and the distance along the surface, x.

This relationship can either be expressed in non-dimensional forms

$$\dot{Re}_{max} = 0.64\ G_r^{\ 0.5}(1+0.49Pr^{0.66\dot{}})^{-0.5} \quad \ldots (2.23)$$

and

$$\frac{\delta}{x} = 0.57\ G_r^{-0.1}Pr^{-0.5\dot{3}}(1 + 0.49\ Pr^{0.66\dot{}})^{0.1} \ldots (2.24)$$

or in simplified expressions

$$v_{max} = 0.1 \times^{0.5} \Delta t_w^{0.5} \quad \ldots (2.25)$$

and $$\delta = 0.11 \times^{0.7} \Delta t_w^{0.1} \quad \ldots (2.26)$$

for which values for the physical properties of air at 20°C and 1 atmosphere pressure have been substituted.

Volume flow, momentum flux and the heating power are defined, as previously, in integral forms by equations (2.11),(2.14) and (2.16). By substituting equations (2.20), (2.21), (2.22), (2.25) and (2.26) as appropriate and integrating, they can be expressed as functions of the relative surface temperature and the distance along the surface, i.e.

$$V = 2.94 \times 10^{-3} \times^{1.2} \Delta t_w^{0.4} \quad \ldots (2.27)$$

$$M = 2.01 \times 10^{-4} \times^{1.7} \Delta t_w^{0.9}\ \rho \quad \ldots (2.28)$$

and $$\dot{Q} = 0.694 \times 10^{-3} \times^{1.2} \Delta t_w^{1.4}\ \rho\ c_p \quad \ldots (2.29)$$

It is also useful to define the mean arithmetic velocity, v_{ar}, and the mean square velocity, v_{sq}, as these concepts will be used later when a relationship between convective currents and the replacement jets is derived.

The mean arithmetic velocity is defined as

$$v_{ar} = \frac{\text{Volume Flow}}{\text{Area of Stream}} = \frac{\dot{V}}{\delta \times l} \qquad \ldots (2.30)$$

and the mean square velocity is

$$v_{sq} = \frac{\text{Momentum Flux}}{\text{Mass Flow}} = \frac{M}{\rho V} \qquad \ldots (2.31)$$

The expressions for the mean arithmetic and mean square velocity have therefore also been included in Table 2.1.

For completeness, formulae for the coefficient of heat transfer, h, the local rate of heat flow $\dot{q}$ as well as the Nusselt number are given below.

The average value of the coefficient of heat transfer is

$$\bar{h} = \frac{\dot{Q}}{\Delta t_w \, x} \qquad \ldots (2.32)$$

The local rate of heat flow, $\dot{q}$, is derived from the condition

$$\dot{q} = -\lambda \left(\frac{d\Delta t}{dy}\right)_w \qquad \ldots (2.33)$$

for y = 0. Hence, if $q = h\Delta t_w$,

$$h = \frac{\dot{q}}{\Delta t_w} = -\lambda \left(\frac{d\Delta t}{dy}\right)_w \Delta t_w^{-1} \qquad \ldots (2.34)$$

and

$$Nu = \frac{hx}{\lambda} = \left(\frac{d\Delta t}{dy}\right)_w \times \Delta t_w^{-1} \qquad \ldots (2.35)$$

2.2.3 Resumé

A literature survey has shown that there is no data available on the influence of room air movements on convective currents. In particular the transition from laminar to turbulent flow may be influenced by room turbulence, and it is in this region that convective currents generated by a number of the most common sources of thermal flows lie. The values quoted by Billington[6] (laminar flow $Ra < 5 \times 10^8$, turbulent flow $Ra > 10^9$) should be the more appropriate to realistic situations.

Equations describing parameters of natural convective currents, both in the laminar and turbulent regions, have been calculated. Physical properties of air at 20°C and atmosphere pressure have been used to derive simplified equations to be used in the calculation of replacement jets. All equations are summarised in Table 2.1. The simplified equations are valid for air temperatures not too widely different from those used in their calculations. In other cases the non-dimensional expressions should be used. It is also important to note that all the formulae are valid for Prandtl numbers close to unity. This condition is automatically fulfilled when air is the fluid as the Pr number of air varies little (0.69–0.73) for the temperature range encountered in the study of room air movements.

The area that warrants experimental investigation is the influence of room turbulence on the main parameters of convective currents.

TABLE 2.1 Natural convection. Simplified formulae valid for air temperatures near 20°C and normal atmospheric pressure. For other cases use dimensionless formulae.

$\Delta tw = T_w - T_a$ (m); ρ(kg-m$^-$); c_p (J kg^{-1}K^{-1}); x (m)

LAMINAR			
	General	Simplified	Unit
v_{max}	$0.148v^*$	$0.108x^{0.5}\Delta t_w^{0.5}$	ms^{-1}
Re_{max}	$0.766(0.952+Pr)^{-0.5}Gr^{0.5}$		-
v^*	$6.75\ v_{max}$		ms^{-1}
δ		$4.93x10^{-2}x^{0.25}\Delta t_w^{-0.25}$	m
$\frac{\delta}{x}$	$3.93Pr^{-0.5}(0.952+Pr)^{0.25}Gr^{-0.25}$		-
V	$0.083v^*\delta$	$3x10^{-3}x^{0.75}\Delta t_w^{0.25}$	m^3s^{-1}*
M	$0.953x10^{-2}v^{*2}\delta\rho$	$2.49x10^{-4}x^{1.25}\Delta t_w^{0.75}\rho$	$kgms^{-2}$*
v_{ar}	$0.5625\ v_{max}$		ms^{-1}
v_{sq}	$0.77\ v_{max}$		ms^{-1}
$\overline{\Delta t}$	$0.4\ \Delta t_w$		°C
$\dot{Q}$	$\rho c_p\ \overline{\Delta t}\ \dot{V}$	$1.2x10^{-3}x^{0.75}\Delta t_w^{1.25}\rho c_p$	W*
	$0.679(0.952+Pr)^{-0.25}Pr.Gr.\lambda$		W*
Nu	$0.508Pr^{0.5}(0.952+Pr)^{-0.25}Gr^{0.25}$		-
	$0.377Gr^{0.25}$		-
$\overline{Nu}$	$1.\dot{3}\ Nu$		-
h	$Nu\ \lambda x^{-1}$	$0.9x10^{-3}x^{-0.25}\Delta t_w^{0.25}\rho c_p$	$Wm^{-2}K^{-1}$
$\bar{h}$	$1.\dot{3}\ h$		$Wm^{-2}K^{-1}$
$\dot{q}$	$h\Delta t_w$	$0.9x10^{-3}x^{-0.25}\Delta t_w^{1.25}\rho c_p$	Wm^{-2}

* per m run

TEXT BOUND INTO

THE SPINE

ABLE 2.1 continued.

TURBULENT			
	General	Simplified	Unit
$_{max}$	$0.535v^*$	$0.1x^{0.5}\Delta t_w^{0.5}$	ms^{-1}
e_{max}	$0.64(1+0.49Pr^{0.66})^{-0.5}Gr^{0.5}$		-
	$1.87\ v_{max}$		ms^{-1}
	$0.11x^{0.7}\Delta t_w^{-0.1}$		m
	$0.57Pr^{-0.53}(1+0.49Pr^{0.66})^{0.1}Gr^{-0.1}$		-
	$0.142v^*\delta$	$2.94x10^{-3}x^{1.2}\Delta t_w^{0.4}$	m^3s^{-1}*
	$0.0523v^*\delta\rho$	$2.01x10^{-4}x^{1.7}\Delta t_w^{0.9}\rho$	$kgms^{-2}$*
r	$0.27\ v_{max}$		ms^{-1}
q	$0.658\ v_{max}$		ms^{-1}
	$0.236\Delta t_w$		^oC
	$c_p\overline{\Delta t}\ V\rho$	$0.694x10^{-3}x^{1.2}\Delta t_w^{1.4}\rho c_p$	W*
	$0.0227(1+0.49Pr^{0.66})^{-0.4}Pr^{0.46}Gr^{0.4}\lambda$		W*
	$0.0301Pr^{0.46}(1+0.49Pr^{0.66})^{-0.4}Gr^{0.4}$		-
	$0.0227Gr^{0.4}$		-
	$0.8\dot{3}\ Nu$		-
	$Nu\ \lambda x^{-1}$	$0.834x10^{-3}x^{0.2}\Delta t_w^{0.4}\rho c_p$	$Wm^{-2}K^{-1}$
	$0.83\ h$		$Wm^{-2}K^{-1}$
	$h\Delta t_w$	$0.834x10^{-3}x^{0.2}\Delta t_w^{0.4}\rho c_p$	Wm^{-2}

per m run

2.3 REPLACEMENT JETS

In the overwhelming majority of cases, where room air movements are studied, the convective current will be substituted by a plane wall jet. In some instances, such as a free standing panel radiator, a plane jet would be the appropriate replacement. In 2.2 the parameters describing convective currents have been determined.

In this chapter 2.3 the most appropriate expressions for plane jets and plane wall jets will be identified to enable a theoretical attempt, in the following chapter 2.4 to be made at establishing parameters of replacement jets directly from the relative temperature differential and physical size of surfaces generating convective currents.

As has been shown, the convective currents, that are to be replaced by jets, could be either in the turbulent or in the laminar region, and will, of course, be at a different temperature to that of the ambient air.

2.3.1. Plane jets.

The theory of plane jets, especially turbulent plane jets, has been well established[21-34]. Theoretical predictions in the fully developed flow region are in good agreement with experimental results[22, 34-41].

The evolution of a submerged jet, Fig. 2.5, issuing from a nozzle can be conveniently divided into four separate zones[42,43]. The first zone, or initial region, is characterised by the axial velocity throughout its length being constant, equal approximately to the mean velocity in the nozzle, and a wedge shaped core of undiminished mean velocity surrounded by a mixing layer. The second zone or transitional region, is where the axial velocity changes slowly. For jets issuing from circular or square nozzles, this region is relatively short[43] reaching only to a distance equivalent to eight diameters from the nozzle. The velocity changes more slowly in cases of rectangular jets[44]. For high aspect ratio slots, the region reaches approximately to four times the width and breadth[43]. The axial velocity falls according to $\frac{v_m}{v_o} = f(\frac{1}{\sqrt{x}})$. The third zone or main region, is where turbulence has become uniform in character and the axial velocity diminishes according to $v_m/v_o = f(\frac{1}{x})$. The fourth or end region, is characterised by a rapid decay of the axial velocity and the jet disintegrates into small eddies.

For jets issuing from long narrow nozzles, i.e. plane jets, the second region is the most important: for, as observations have confirmed,[43 45] it extends until the jet finally disintegrates. It is therefore possible for plane jets to simplify Fig. 2.5 and to analyse their development in only two zones as shown in Fig. 2.6. The first zone is the initial, or flow development, region and the

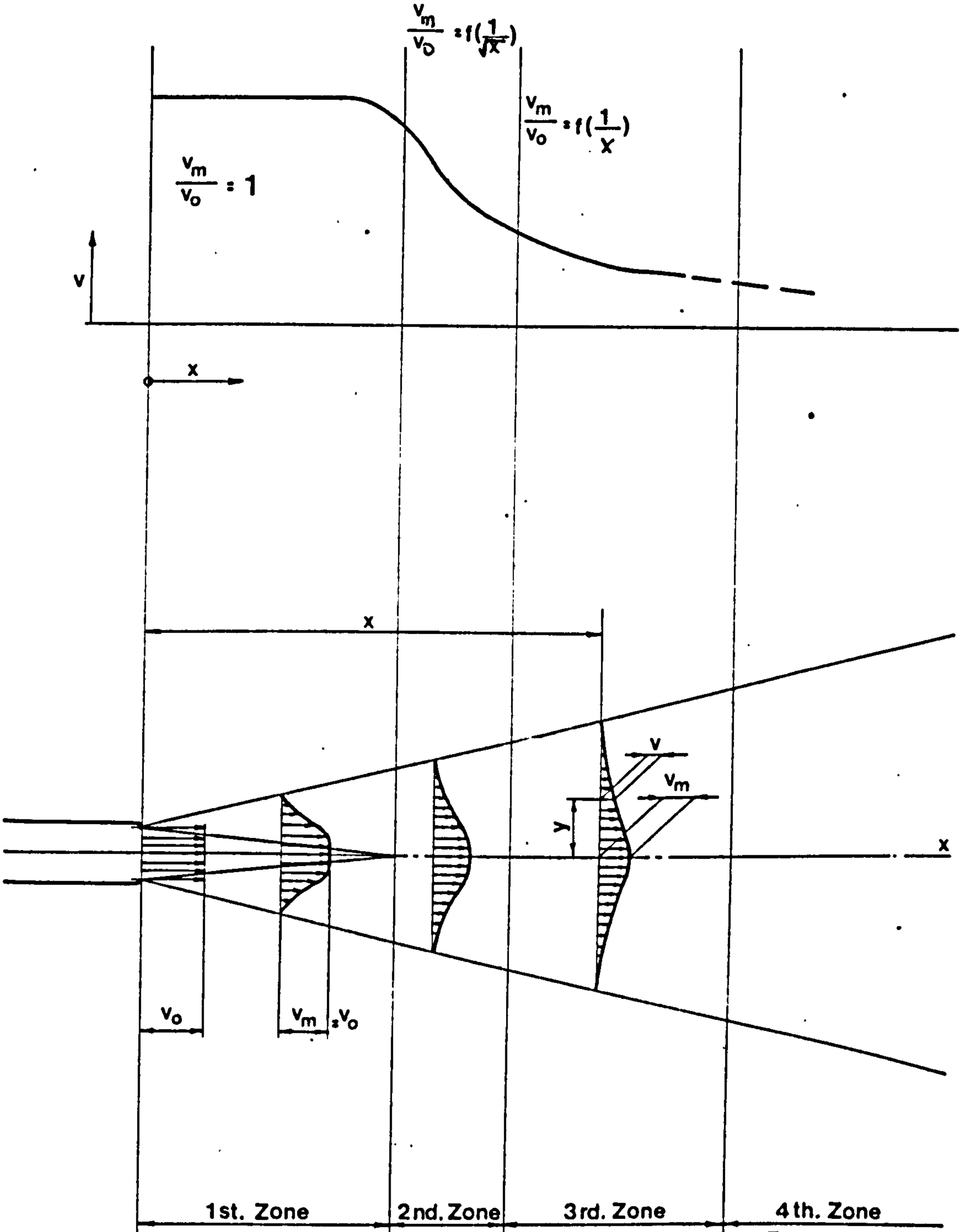

Fig. 2.5. DEFINITION SKETCH OF FREE JETS

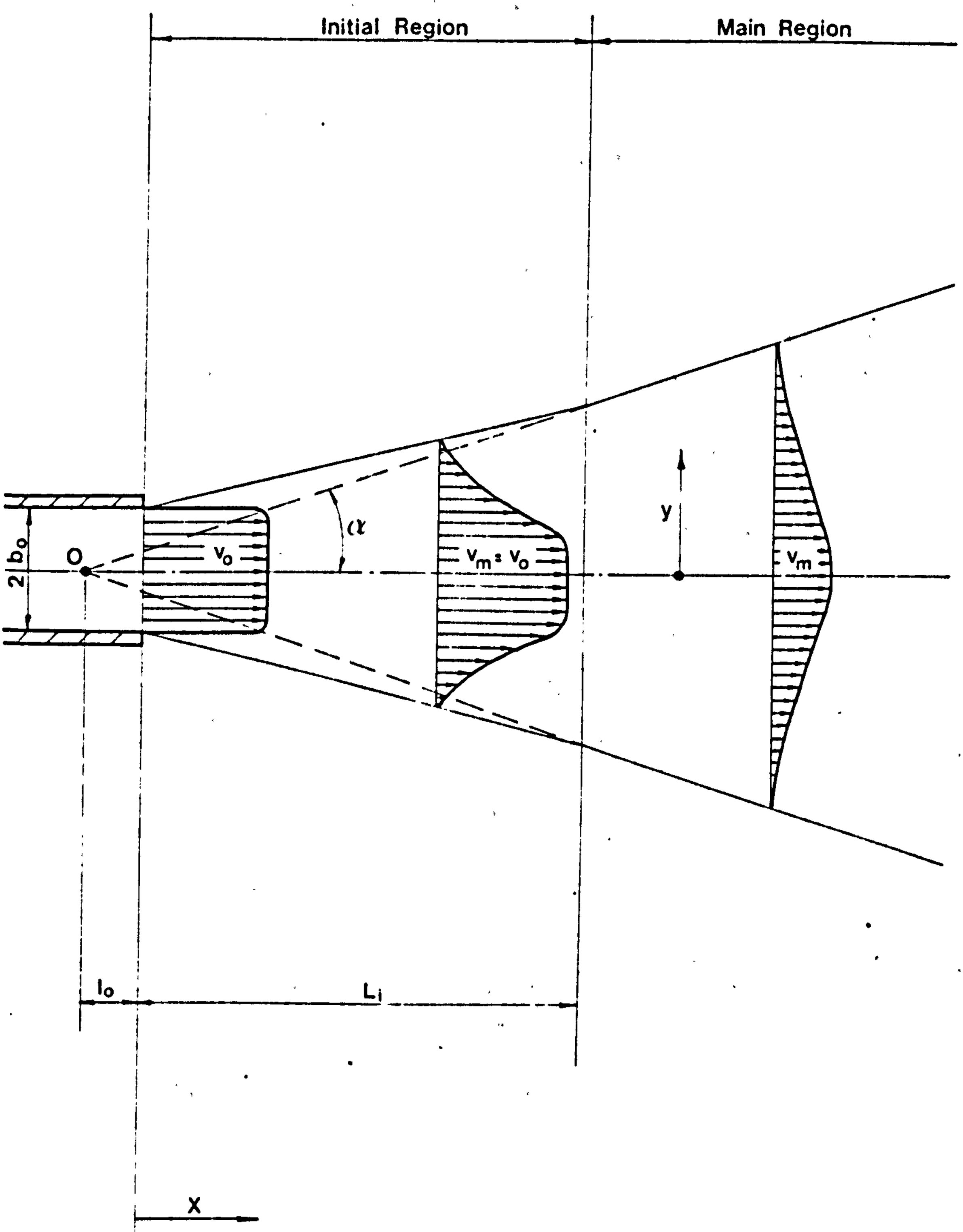

Fig. 2.6. REPRESENTATION OF PLANE TURBULENT FREE JETS

second zone becomes the main region where the flow has become fully developed - the axial velocity diminishing according to $v_m/v_o = f(\frac{1}{\sqrt{x}})$

2.3.1.1. Main Region

In the fully developed flow region experimental observations have shown that plane jets observe certain characteristic laws. The width of the jet increases proportionally with distance from the nozzle and the jet apparently emanates from a line source usually situated at a distance, l_o, behind the nozzle. The axial velocity decreases with distance from the nozzle. Velocity profiles at successive normal cross sections, when plotted in dimensionless co-ordinates, are identical, as shown in Fig. 2.7 where Frothmann experimental results[35] are plotted. The two non-dimensionalising qualities, usually referred to as the velocity scale and the length scale, are v_m, the maximum velocity, and $y_{0.5}$, i.e. the value of y where v is equal to half the maximum velocity. This similarity also applies to temperature profiles of non-isothermal plane jets[41].

In order to use these similarity profiles for solving any particular problem, it is necessary to predict the manner of variation of the non-dimensionalised quantities.

The general equations of motion in the Cartesian system, i.e. the Navier-Stokes equations and the continuity equation [25 46], can be simplified for a two-dimensional steady flow, where the flow in the x-direction is generally much greater than in the y-direction and the pressure gradient in the axial direction is neglected, to the form

$$v_x \frac{\partial v_x}{\partial x} + v_y \frac{\partial v_x}{\partial x} = \frac{1}{\rho} \frac{\partial}{y} (\tau_L + \tau_T) \quad \ldots (2.36)$$

$$\frac{\partial v_x}{\partial x} + \frac{\partial v_y}{\partial y} = 0$$

where v_x and v_y are the mean velocities in the x and y co-ordinate directions and τ_L and τ_T are, respectively, the laminar and turbulent sheer stresses. In free turbulent flow, due to the absence of solid boundaries, τ_T is much larges than τ_L and hence it is reasonable to neglect τ_L.

For a free, plane jet issuing into a large stagnant environment and expanding under zero pressure gradient, the momentum flux of such a jet, issuing from a nozzle $2b_o$ wide and assuming a uniform exit velocity of v_o, is $M_o = 2\rho b_o v_o^2$ and therefore, if $M_o = M$ = Constant

$$M_o = 2\rho b_o v_o^2 = 2\int_o^\infty \rho v^2 dy \quad \ldots (2.38)$$

Momentum flux effectively replaces individual values of b_o and v_o as a parameter controlling the behaviour of plane jets. Because the momentum flux of flows are important parameters governing room air movement patterns, first priority should be given to obtaining as near as possible an identity of the values of momentum flux of the convective currents and the replacement jets.

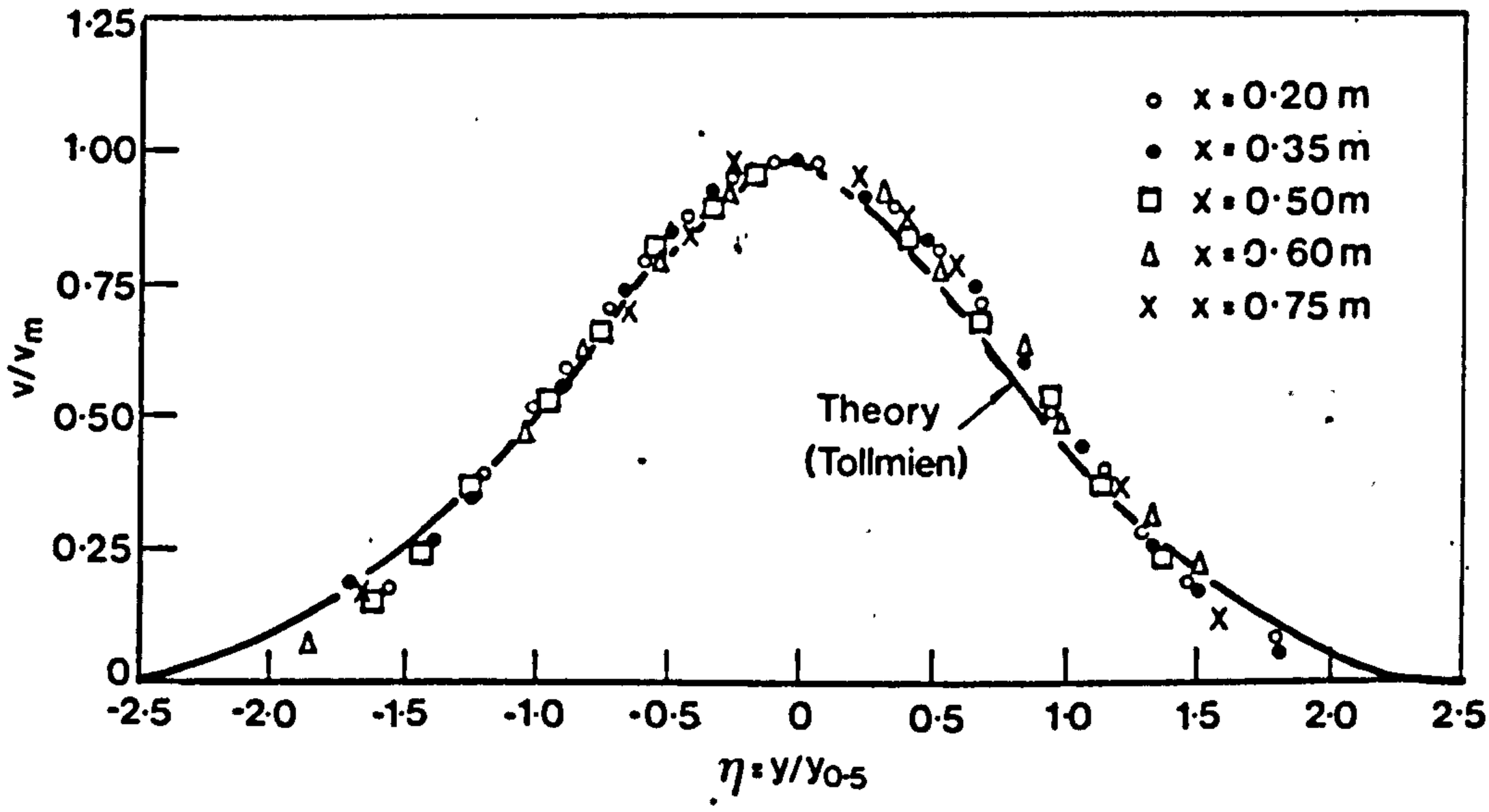

Fig.2.7. VELOCITY DISTRIBUTION FOR PLANE TURBULENT FREE JETS-FÖRTHMANN RESULTS AND TOLLMIEN PREDICTION

M = constant implies that

$$\frac{d}{dx} \int_0^\infty v^2 \, dy = 0 \qquad \ldots (2.39)$$

i.e. that the rate of change of the momentum flux in the x-direction is zero. Fig. 2.7 shows that $\frac{v}{v_m} = f(\frac{y}{y_{0.5}})$

Substituting into equation (2.39) gives

$$\frac{d}{dx} \int_0^\infty \rho v_m^2 \cdot y_{0.5} \, f^2(\frac{y}{y_{0.5}}) \, d \, (\frac{y}{y_{0.5}}) = 0 \qquad \ldots (2.40)$$

The expression $f^2(\frac{y}{y_{0.5}}) \, d \, (\frac{y}{y_{0.5}})$ is, by definition, invarient and therefore

$$\frac{d}{dx} (v_m^2 \, y_{0.5}) = 0 \qquad \ldots (2.41)$$

This implies that $(v_m^2 \, y_{0.5})$ is independent of x; $v_m^2 \, y_{0.5} \propto x^0$.

Assuming a simple exponential expressions for the scale factors, $v_m \propto x^a$ and $y_{0.5} \propto x^b$, results in

$$2a + b = 0 \qquad \ldots (2.42)$$

A similarity analysis of the equations of motion (2.36) and (2.37), assuming $\tau/\rho \, v_m^2 = f \, (y/y_{0.5})$ based on experimental observations and dimensional considerations, results in a = -0.5 and b = 1. This is in agreement with the observed behaviour of plane jets, i.e. $v_m/v_0 = f(\frac{1}{\sqrt{x}})$

The same conclusions can be reached on the basis of the entrainment hypothesis or other considerations.

To obtain a theoretical velocity the equations of motion (2.36) (2.37) would have to be solved. The equations contain three unknows -v_x, v_y and τ - and therefore one more equation is required.

Tollmien[21] used the Prandtl mixing length formula to obtain the required extra equation and numerically solved the resulting non-linear second order differential[28 46] equation

$$F''^2 + FF' = 0 \qquad \ldots (2.43)$$

where $v/v_m = F' \, (\phi)$ and $\phi = \frac{y}{ax}$. The constant a is an experimentally determined coefficient that relates to the construction and shape of the nozzle and defines the degree of turbulence. For the boundary condition $\frac{v}{v_m} = 0$, $\phi = 2.4$ and for $\frac{v}{v_m} = 0.5$, a value of $\phi = 0.955$ is obtained. Görtler[23] based his analysis on the "new" kinematic eddy viscosity theory. Other solutions were based on the application of the vorticity transfer theory[24 29 30] and Reichardt's molecular analogy theory [20 25 26].

A comparison of experimental results [35 36 37 38 39] and theoretical

predictions shows that the Görtler solution gives a slightly better fit near the axis of the jet, whereas the Tollmien solution is generally preferred in the outer region[46]. It has been found that experimental velocity (and temperature) distributions can be represented satisfactorily by a Gaussian curve[38]

$$\frac{v}{v_m} = \exp\ (-A\ (\frac{y}{x})^2) \qquad \ldots\ (2.44)$$

where A was found to range from 71 to 75 or

$$\frac{v}{v_m} = \exp - 0.639\ (\frac{y}{y_{0.5}})^2 \qquad \ldots\ (2.45)$$

Using the experimental results of Förthmann[35] and others, Abramovich[28] found that the coefficient a varied from 0.09 to 0.12, depending on the aspect ratio and the construction of the nozzle. The lower values are appropriate for convergent nozzles and lower aspect ratios[47]. Experimental results of Reichardt[37] indicate a value of a = 0.13, which is in agreement with results reported by Newman[48] for large values of $\frac{x}{b_o}$. For smaller values of $\frac{x}{b_o}$ lower values of a = 0.08 were found. Zijnen[38] also found that a varied with the aspect ratio of the nozzle. Results of studies of cold air jets issuing from linear slots by O'Callaghan, Probert and Newbert[41] indicate that the coefficient of turbulence, a, varies with the Reynolds number of the nozzle ($Re = \frac{2b_o' v_o}{\nu_o}$) as shown in Fig.2.8. The value of the turbulence coefficient increases with decreasing Reynolds number, significantly for $Re < 2 \times 10^3$.

Once the relationship of the variation of velocity (and temperature) with x and y has been defined, it is possible to deduce all the required parameters of the plane jet. The Tollmien solution leads to an expression for the axial, and therefore the maximum, velocity in relation to the initial velocity

$$\frac{v_m}{v_o} = \frac{1.21}{\sqrt{\frac{a}{b_o} x + 1_o}} \qquad \ldots\ (2.46)$$

The above expression, and the subsequent equations, are valid for uniform initial velocity and temperature profiles in the nozzle.

If $\Phi = 2.4$ for $\frac{v}{v_m} = 0$ then the angle of divergence of the jet is

$$\tan \alpha = 2.4a \qquad \ldots\ (2.47)$$

and therefore the distance of the apparent source of the jet from the nozzle exit is

$$1_o = 0.416 \frac{b_o}{a} \qquad \ldots\ (2.48)$$

The half width of the jet is

$$\frac{b_x}{b_o} = 2.4\ (\frac{ax}{b_o} + 0.416) \qquad \ldots\ (2.49)$$

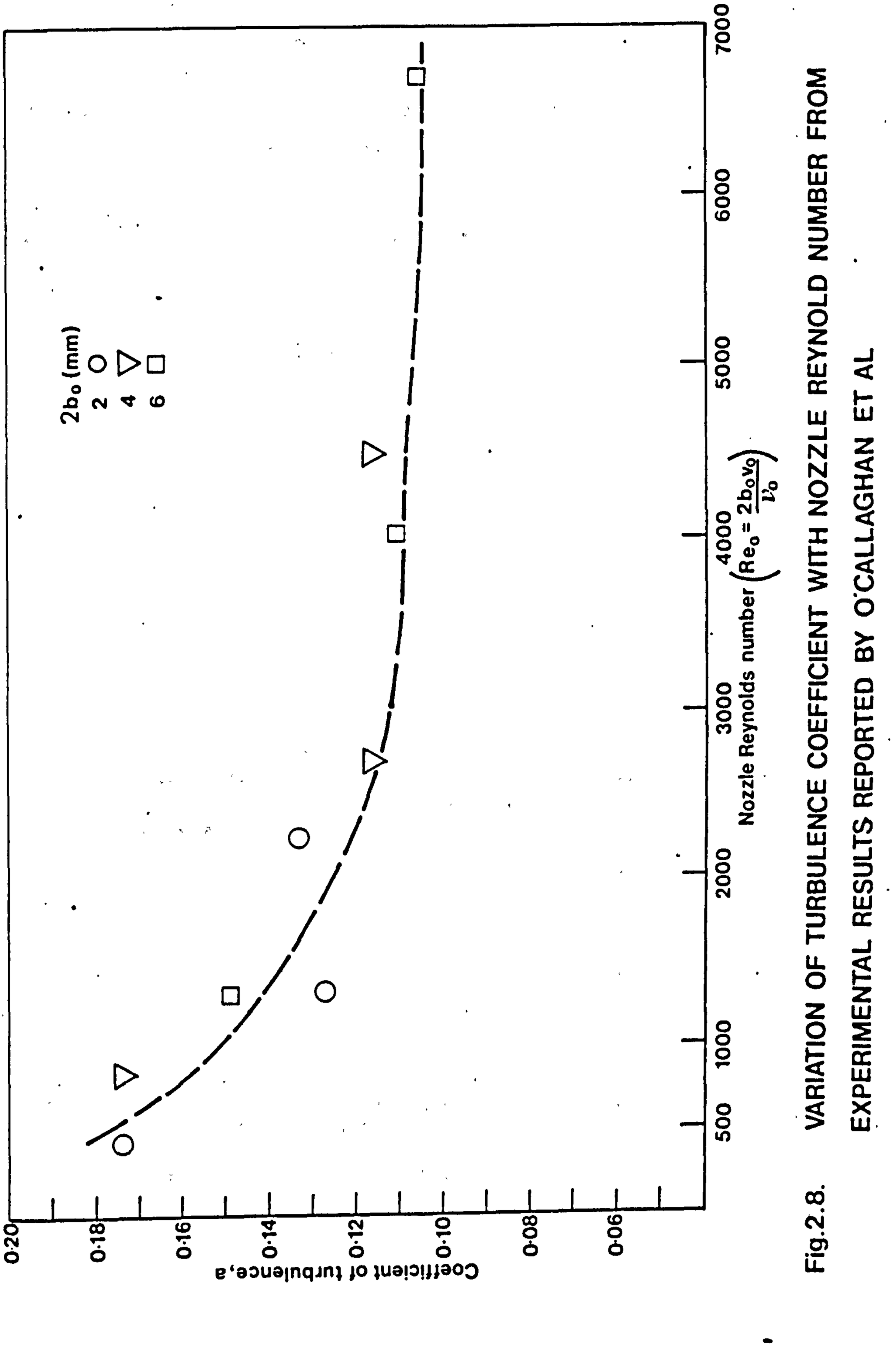

Fig.2.8. VARIATION OF TURBULENCE COEFFICIENT WITH NOZZLE REYNOLD NUMBER FROM EXPERIMENTAL RESULTS REPORTED BY O'CALLAGHAN ET AL

Equation (2.46) can then be rewritten

$$\frac{v_m}{v_o} = \frac{1.2}{\sqrt{\frac{ax}{bo} + 0.416}} \qquad \ldots (2.50)$$

Volume flow, adapted from Abramovich, is

$$\frac{V_x}{V_o} = 1.2\sqrt{\frac{ax}{b_o} + 0.416} \qquad \ldots (2.51)$$

and the expressions for the mean arithmetic velocity and the mean square velocity, as defined by equation (2.30) and (2.31), are therefore

$$\frac{v_{ar}}{v_o} = \frac{0.49}{\sqrt{\frac{ax}{b_o} + 0.416}} \qquad \ldots (2.52)$$

and

$$\frac{V_{sq}}{V_o} = \frac{V_o}{V_x} = \frac{0.82}{\sqrt{\frac{ax}{b_o} + 0.416}} \qquad \ldots (2.53)$$

Since the variation of velocity in a jet is controlled by the transverse movement of eddies, which are the agent for the transfer of mass and heat, the variation of the mean temperature of non-isothermal jets is assumed to be governed by the same laws as that of the mean square velocity, i.e.

$$\frac{\overline{\Delta t_x}}{\Delta t_o} = \frac{\overline{t_x - t_a}}{t_o - t_a} = \frac{v_{sq}}{v_o} = \frac{V_o}{V_x} \qquad \ldots (2.54)$$

Mean temperature is defined as the ratio of heat content to mass flow. The heat content of the jet is therefore also constant, i.e. $Q_x = Q_o = \text{Constant}$.

The Tollmien solution predicts that the temperature profile will vary in the same manner as the velocity profile, namely

$$\frac{\Delta t}{\Delta t_m} = \frac{v}{v_m} \qquad \ldots (2.55)$$

Other theoretical predictions [27] [29] [30] however lead to

$$\frac{\Delta t}{\Delta t_m} = \sqrt{\frac{v}{v_m}} \qquad \ldots (2.56)$$

Experimental observations[41] have shown that the square root relationship is, for practical purposes, the better description. A comparison of predicted and experimental profiles is shown in Fig. 2.9. Zijnen[38] devised a more complex empirical equation

$$\frac{\Delta t}{\Delta t_m} = \left(1 + 30\left(\frac{y}{x+\ell_o}\right)^2 + 2200\left(\frac{y}{x+T_o}\right)^4 - 30000\left(\frac{y}{x+T_o}\right)^6\right)\exp\left[-75\left(\frac{y}{x+x_o}\right)^2\right] \qquad (2.56a)$$

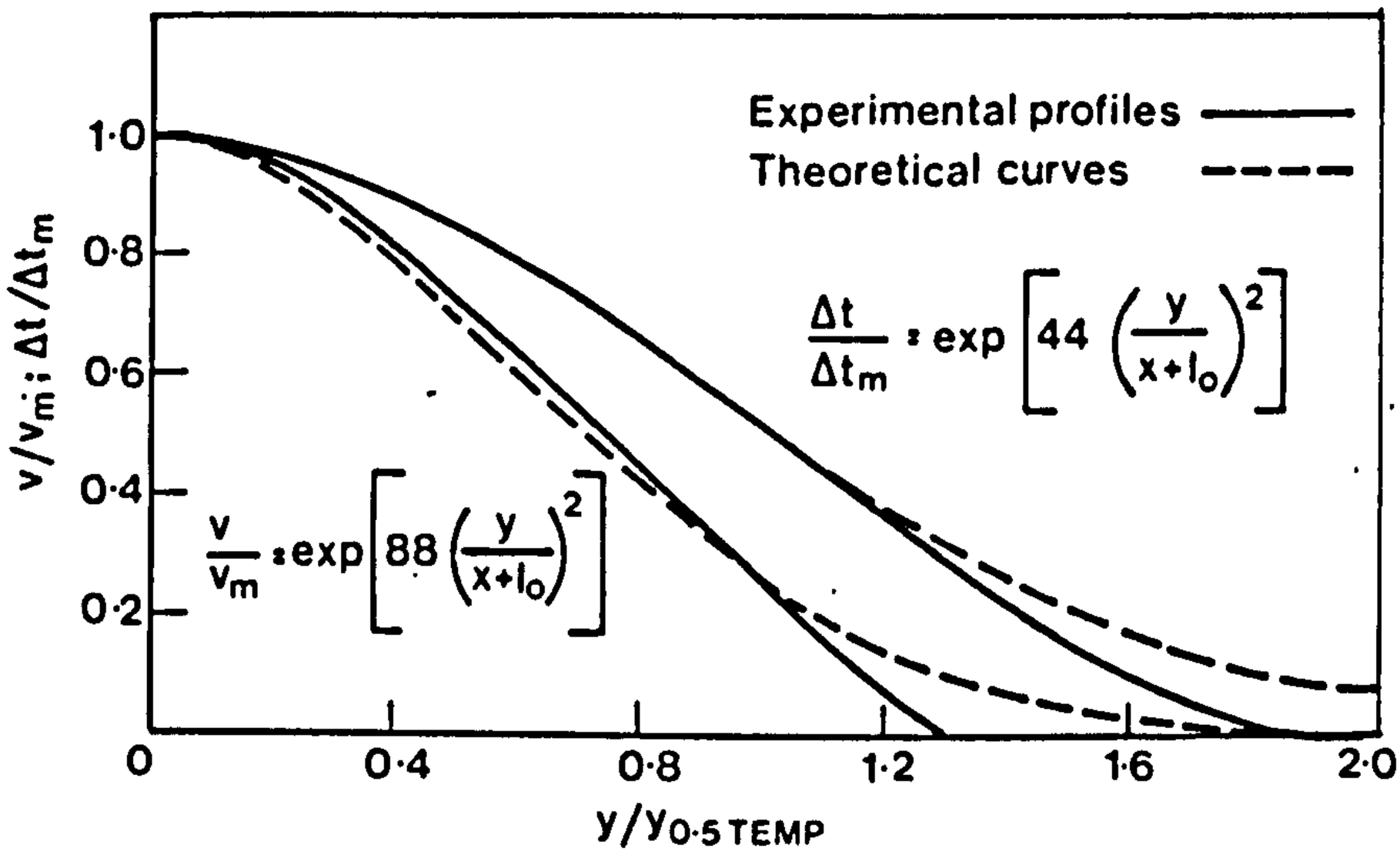

Fig.2.9. VELOCITY AND TEMPERATURE PROFILES OF JETS: COMPARISON OF EXPERIMENTAL DATA WITH PREDICTIONS

The temperature decay along the centre line of a non-isothermal jet, because the thermally peturbed layer spreads faster than the momentum disturbed layer, will not be identical with the velocity decay. An expresssion for moderate temperature differentials has been formulated by Abramovich

$$\frac{\Delta t_m}{\Delta t_o} = 0.73 \frac{v_m}{v_o} \qquad \ldots (2.57)$$

An empirical equation formulated by Zijnen[38]

$$\frac{\Delta t_m}{\Delta t_o} = \frac{2.828}{\sqrt{\frac{x}{b_o} + 1.2}} \qquad \ldots (2.57a)$$

results in an identical ratio as in equation (2.57) when compared with equation (2.46) for a = 0.1.

In Fig. 2.10 equation (2.57) has been plotted against experimental values obtained by O'Callaghan, Probert and Newbert. The graph shows that the experimental results are distributed equally around the Abramovich formula, indicating that equation (2.57) can be used for predictive calculations.

More recent data published by Abramovich[22 45] gives the formulae for the parameters of a plane jet in the main region in a modified form. The formula for the axial velocity

$$\frac{v_m}{v_o} = \frac{3.8\sqrt{\beta_o}}{\sqrt{\frac{x}{b_o} + \frac{\ell_o}{b_o}}} \qquad \ldots (2.58)$$

and the volume flow

$$\frac{V_x}{V_o} = 0.375 \sqrt{\beta_o}\sqrt{b\frac{x}{b_o} + \frac{\ell_o}{b_o}} \qquad \ldots (2.59)$$

contain a correction coefficient β_o for momentum and the relative distance of the source of the jet, l_o/b_o, has to be known. The modified·

formulae and the original equations lead to identical answers for uniform initial conditions and a value of the coefficient of turbulence a = 0.09 -0.1. The coefficient β_o is approximately

$$\beta_o = 1 - 0.22 \frac{\delta_o}{b_o} \qquad \ldots (2.59a)$$

where δ_o is the boundary layer thickness in the initial cross section of the jet.

The modified expression for the mean temperature of the jet takes into account experimental observations that heat and mass transfer and the transfer of momentum are not synonymous by introducing a temperature dependent term

$$\frac{\overline{\Delta t_x}}{\Delta t_o} = \frac{V_o}{V_x}\sqrt{\frac{T_a}{T_o}} \qquad \ldots (2.60)$$

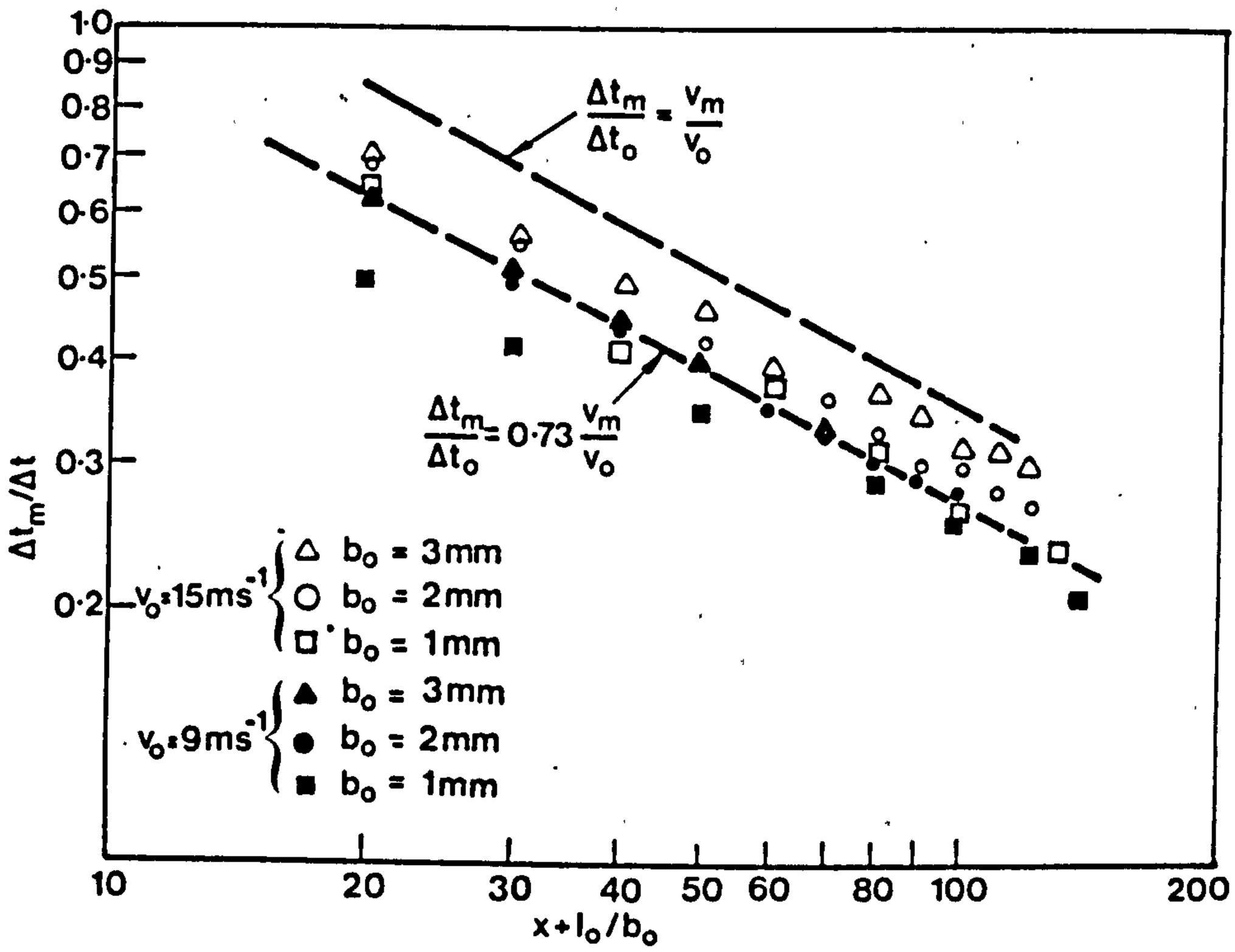

Fig. 2.10. TEMPERATURE DECAY ALONG THE CENTRE LINE OF JETS; COMPARISON OF EXPERIMENTAL DATA WITH PREDICTIONS

For temperature differentials encountered when modelling room air movements, the value of the temperature correcting factor would be between 0.9 and 0.97.

The temperature decay along the centre line of the jet is expressed as

$$\frac{\Delta t_m}{\Delta t_o} = 0.86 \frac{v_x}{v_o}\sqrt{\frac{T_a}{T_o}} \qquad \ldots (2.61)$$

For moderate temperature differentials, equation (2.61) would give a higher value than that predicted via equation (2.57), as shown in Fig. 2.10. Equation (2.57) gives a better fit to the experimental results.

As has been mentioned the relative value of the apparent source of the jet l_o/b_o has to be known in order to make use of the modified formulae, and it is suggested that for uniform initial profiles the value $l_o/b_o \simeq 0$. For practical applications such as air conditioning, this assumption is acceptable, because the error in design calculations resulting from any inaccuracy is negligible. However for calculations of replacement jets, the error may be more significant. The variation of the distance of the apparent source from the nozzle exit with the nozzle Reynolds number for a number of slot widths and initial velocities, calculated from measurements made by O'Callaghan, Probert and Newbert[41], is shown in Fig. 2.11. Also plotted in the graph are values of l_o/b_o calculated according to equation (2.48) for values of a obtained from Fig. 2.8 for appropriate Reynolds numbers. It can be seen that, for this particular nozzle geometry, equation (2.48) for $Re > 2 \times 10^3$ is in good agreement with the magnitude of the measured values, but the trend of l_o/b_o with Re is slightly in the opposite direction. At Reynolds numbers of circa 1000 a step change occurs. The probable cause of this sudden change is the laminar flow which occurs in the initial region of the jet resulting in the location of the apparent source of the jet moving downstream of the nozzle. Zijnen[38] found $l_o = 1.2\ b_o$ for higher nozzle Reynolds numbers ($Re > 10^4$), which gives some support to the trend shown by the experimental data in Fig. 2.11.

2.3.1.2.. Initial Region

The initial region, Fig. 2.5, is characterised by having a core where the jet retains its original properties. With increasing distance from the nozzle the original material in the core gradually becomes diffused due to mixing with the surround air. Up to the point of disappearance of the core, the axial velocity remains unchanged.

The initial region, or the flow development region, can also be described as a core surrounded by two plane sheer layers; its length depending on how quickly turbulence can penetrate to the axis of the jet.

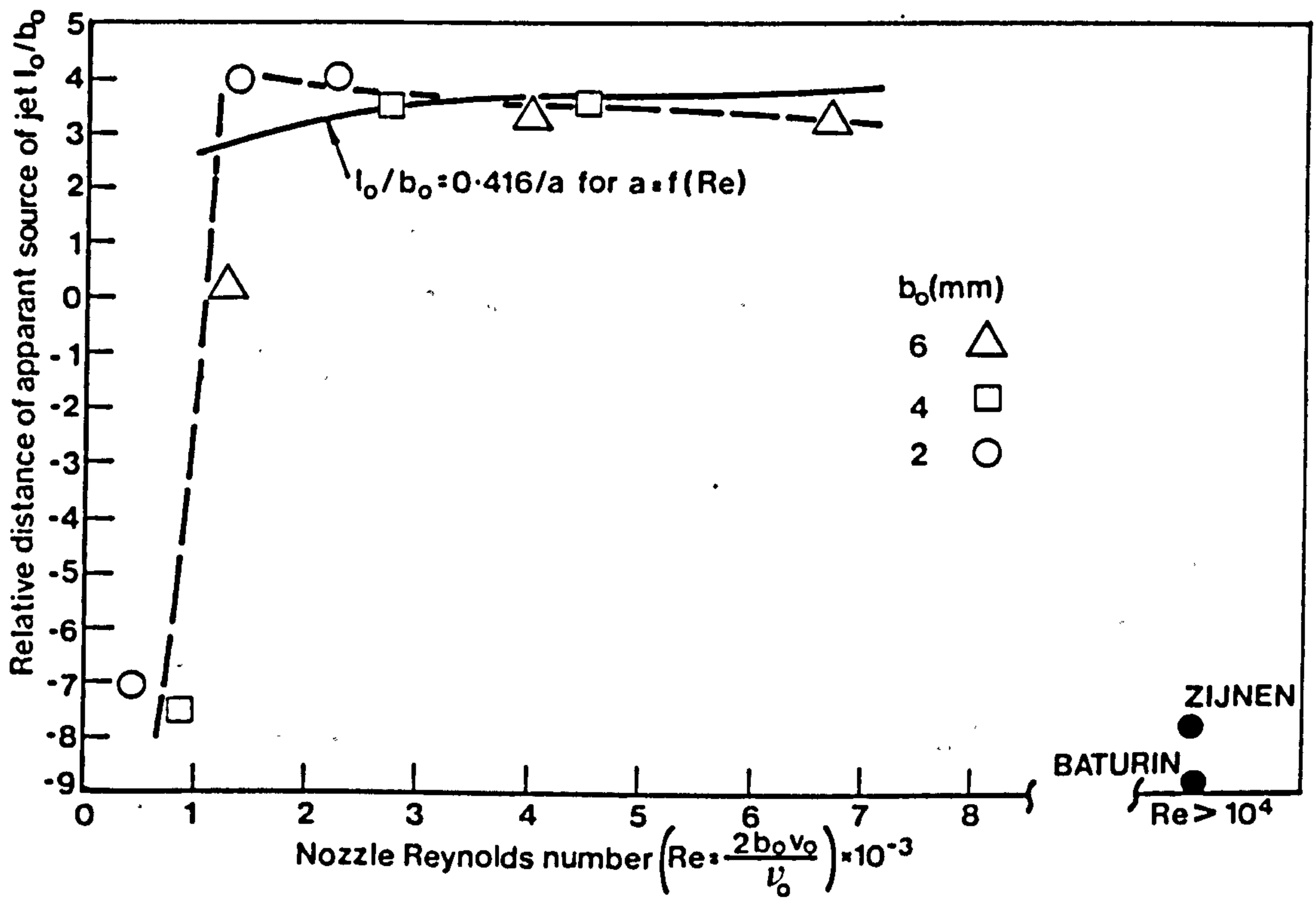

Fig.2.11. VARIATION WITH REYNOLDS NUMBER OF RELATIVE DISTANCE OF APPARENT SOURCE OF JETS FROM NOZZLE EXIT

Shear layers, see Fig. 2.12, display similar properties as plane jets. The thickness of the shear layer increases continuously with x and the velocity profiles are similar, but not symmetrical with respect to the x-axis. When successive velocity profiles are plotted in dimensionless co-ordinates they are identical, as in Fig. 2.13 where the Liepmann-Laufer[49] observations are shown. The distance h* (see Fig.2.12) is measured from the point where $v = v_o$ and the length scale is $h^*_{0.5}$, i.e. the distance h* where $v = 0.5\ v_o$.

To solve the equations of motion (2.36) and (2.37) for the plane shear layer, as previously, one more equation is required. Tollmien[21] constructed the third equation using the Prandtl mixing length theorem, and solved the general equation.

$$\frac{v}{v_o} = F'(\phi) \qquad \ldots (2.62)$$

where $\phi = \frac{y}{ax}$. The co-ordinates x and y are shown in Fig. 2.14 and a is an empirical constant. Using boundary conditions Tollmien found for $\frac{v}{v_o} = 1$, $\phi = 0.981$; for $\frac{v}{v_o} = 0$, $\phi_2 = 2.04$; and for $\frac{v}{v_o} = 0.5$, $\phi_{0.5} = 0.346$. Görtler[23] employed the constant eddy viscosity model to obtain a solution. Both the Tollmien and Görtler solutions agree reasonably well with experimental observations [25 36 49 50], and when replotted in uniform co-ordinates show only a small difference when compared with velocity profiles of plane jets.

Leipmann and Laufer[49] found that the value of the empirical constant in the Tollmien solution to be a = 0.084, which is in agreement with Newman[48] for small values of x/b_o, whereas Albertson et al[36] found a = 0.09. Taking a mean value of a = 0.087, the thickness of the shear layer is found to be

$$b_s = a\ x\ (\phi - \phi_2) = 0.263x \qquad \ldots (2.63)$$

and the angles of spread of the shear layer are $\alpha_1 = 4.90^o$ and $\alpha_2 = 10^o$.

The length of this initial region is

$$L_i = \frac{b_o}{a\phi_1} = 1.02\ \frac{b_o}{a} \qquad \ldots (2.64)$$

which for the mean value of a gives $L_i = 12\ b_o$. Baturin[45] quotes a slightly higher value of $L_i = 14.4$ for uniform outlet velocity profiles and $l_o = 0$.

If the value of ϕ_2 is known, the half width of the jet in the initial region can be calculated from

$$\frac{b_x}{b_o} = 1 + 2.04\ \frac{ax}{b_o} \qquad \ldots (2.65)$$

Integration of the expression for volume flow results in

$$\frac{V_x}{V_o} = 1 + 0.43\ \frac{ax}{b_o} \qquad \ldots . (2.66)$$

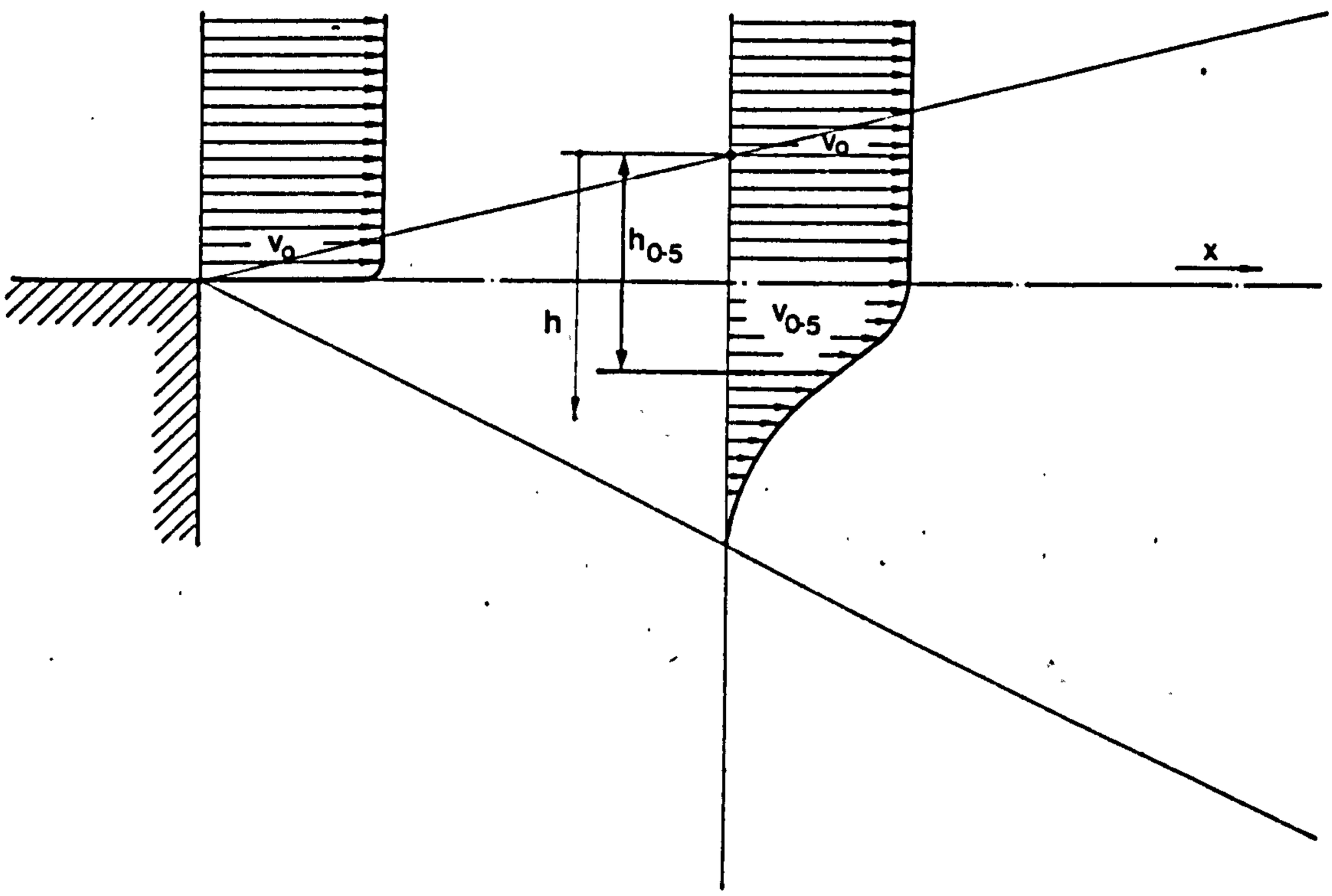

Fig. 2.12. REPRESENTATION OF PLANE TURBULENT SHEAR LAYERS

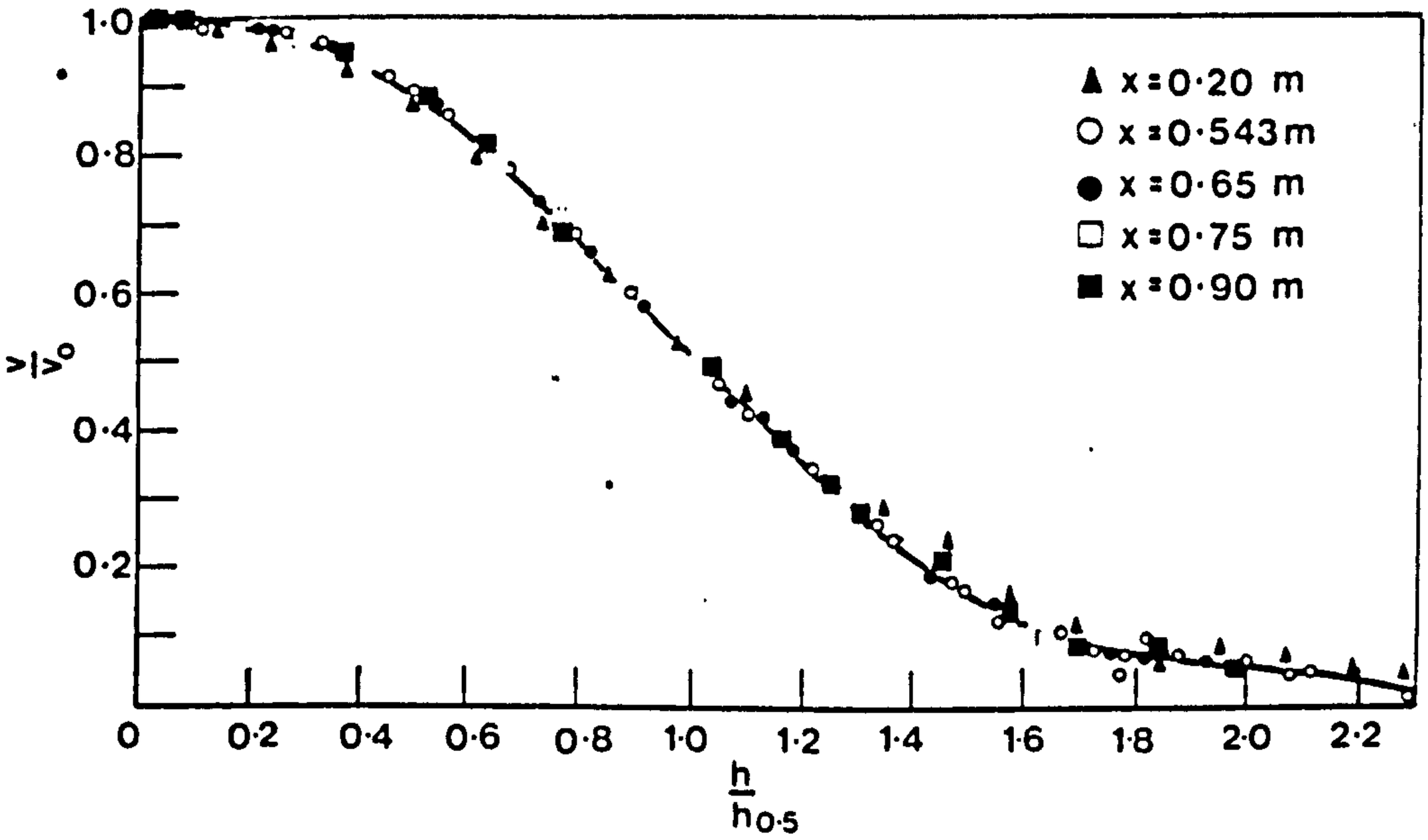

Fig.2.13. SIMILARITY OF VELOCITY PROFILES OF PLANE SHEAR LAYERS (LIEPMAN AND LANFER)

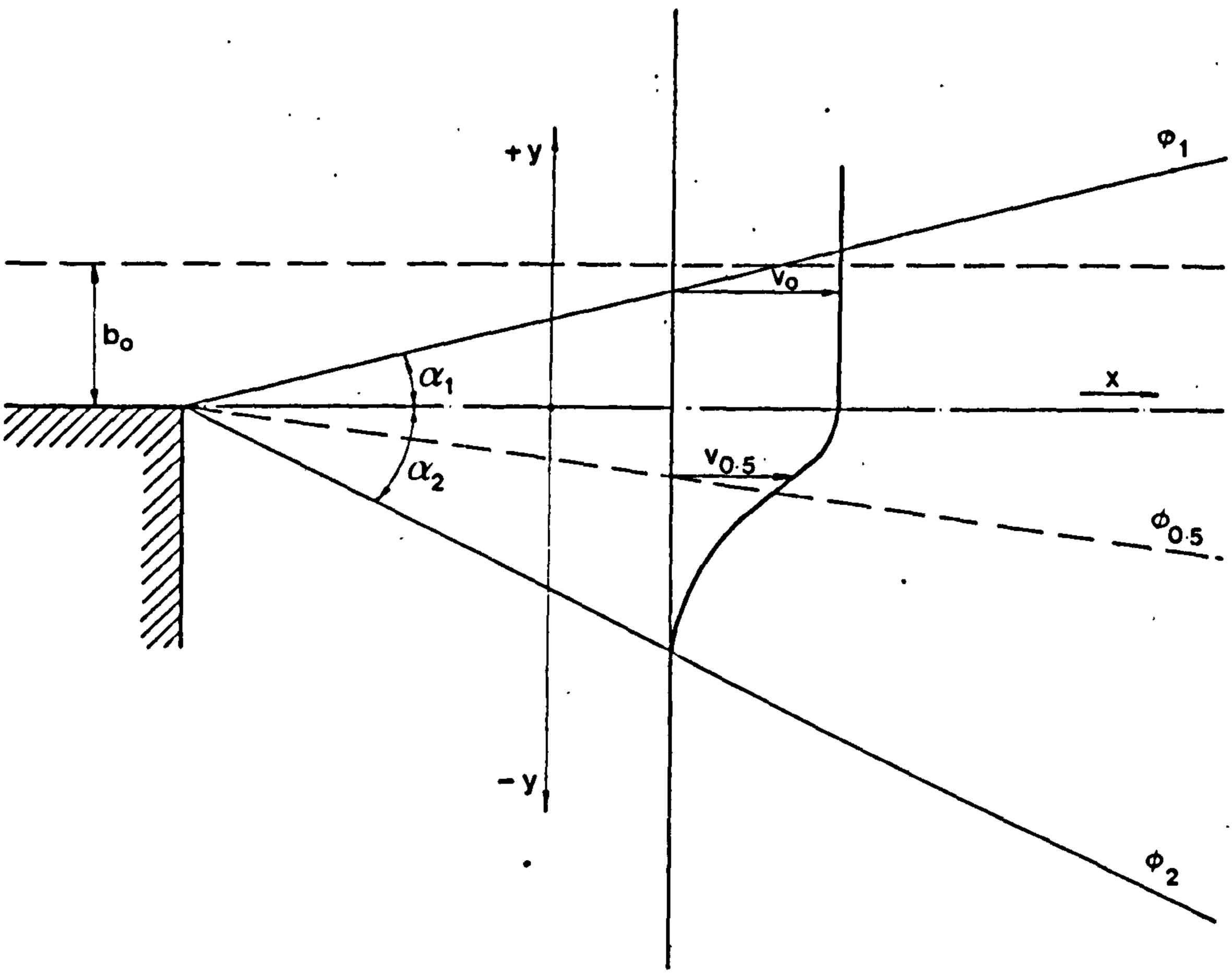

Fig.2.14. DEFINITION SKETCH OF PLANE TURBULENT SHEAR LAYER

and therefore the mean square velocity

$$\frac{v_{sq}}{v_o} = \frac{V_o}{V_x} = \frac{1}{1 + 0.43 \frac{ax}{b_o}} \qquad \ldots (2.67)$$

and the mean arithmetic velocity

$$\frac{v_{ar}}{V_o} = \frac{\overline{\frac{V_o}{V_x}}}{\overline{\frac{b_x}{b_o}}} = \frac{1 + 0.43 \overline{\frac{b_o}{ax}}}{1 + 2.04 \frac{ax}{b_o}} \qquad \ldots (2.68)$$

If the heating power of a jet is assumed constant and the transfers of heat and mass synomynous, equation (2.54) also applies in this initial region. There is some evidence that a more rapid decay of temperature than velocity occurs in the initial region of a jet. Frean and Billington[51], in their study of non-isothermal jets from a sharp-edged square orifice showed that the fall in temperature appears to take place right from the outlet and that the temperature core length was less precisely defined. The length of the temperature core was circa three quarters of the velocity core. Fig. 2.15, based on data obtained by O'Callaghan, Probert and Newbert in their study of non-isothermal plane jets [41], suggests that the centreline temperature decay begins at approximately seven tenths the distance where the decay of velocity is first noticed.

If the initial regions is treated as a shear layer, a discontinuity could occur at a point where the main region begins; the discontinuity being caused by the small difference in the velocity (and temperature) profiles (see Fig. 2.16). A discontinuity would not occur at only one specific condition, i.e. $\tan\alpha_i = \tan\alpha_M$ or

$$\frac{a_i}{a_M} = \frac{2.4}{2.04} = 1.176 \qquad \ldots (2.69)$$

where a_i is the coefficient of turbulence in the initial region and a_M in the main region. Equation (2.69) demands that $a_i > a_M$, by circa 18%. Experimentally obtained values indicate, for high nozzle Reynolds numbers, an opposite trend: the values range from 0.09 to 0.13 for the main region and 0.08 to 0.09 for the initial region.

One way of overcoming the discontinuity is to assume a constant value of boundary ϕ and of the coefficient of turbulence a for the whole jet, usually equal to the main region values. This approach is justified in technical practice where the initial region is of little importance, and any error due to such a simplification is well within design accuracy. To achieve such harmony the value of 2.4 should be substituted for 2.04 in equation (2.65) and (2.68).

A more accurate approach may be necessary if plane jets are to be used to replace convective currents. One possibility is to move the apparent source of the jet 0, see Fig. 2.17, by a distance Δl_o to a new position 0' located at a distance l_o' from the nozzle exit, so as to achieve an identical half-width of the jet at a distance L_i, i.e. at the end of the initial region. From geometrical considerations, using equations (2.48) (2.49), (2.64, (2.65) and the values of $\phi_i = 2.04$ and $\phi_M = 2.4$, it can

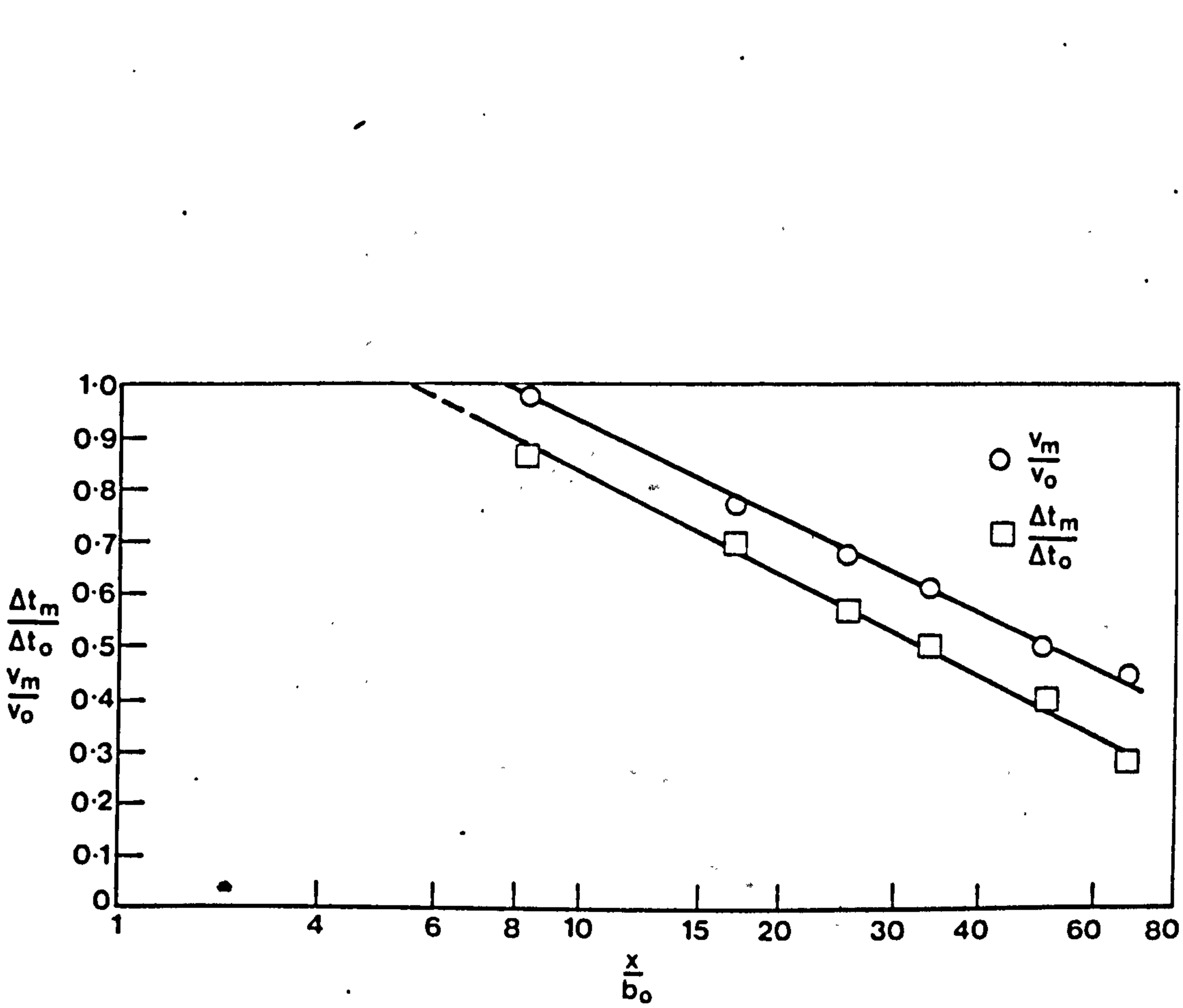

Fig.2.15. VELOCITY AND TEMPERATURE DECAYS ALONG THE CENTRE LINE OF JETS

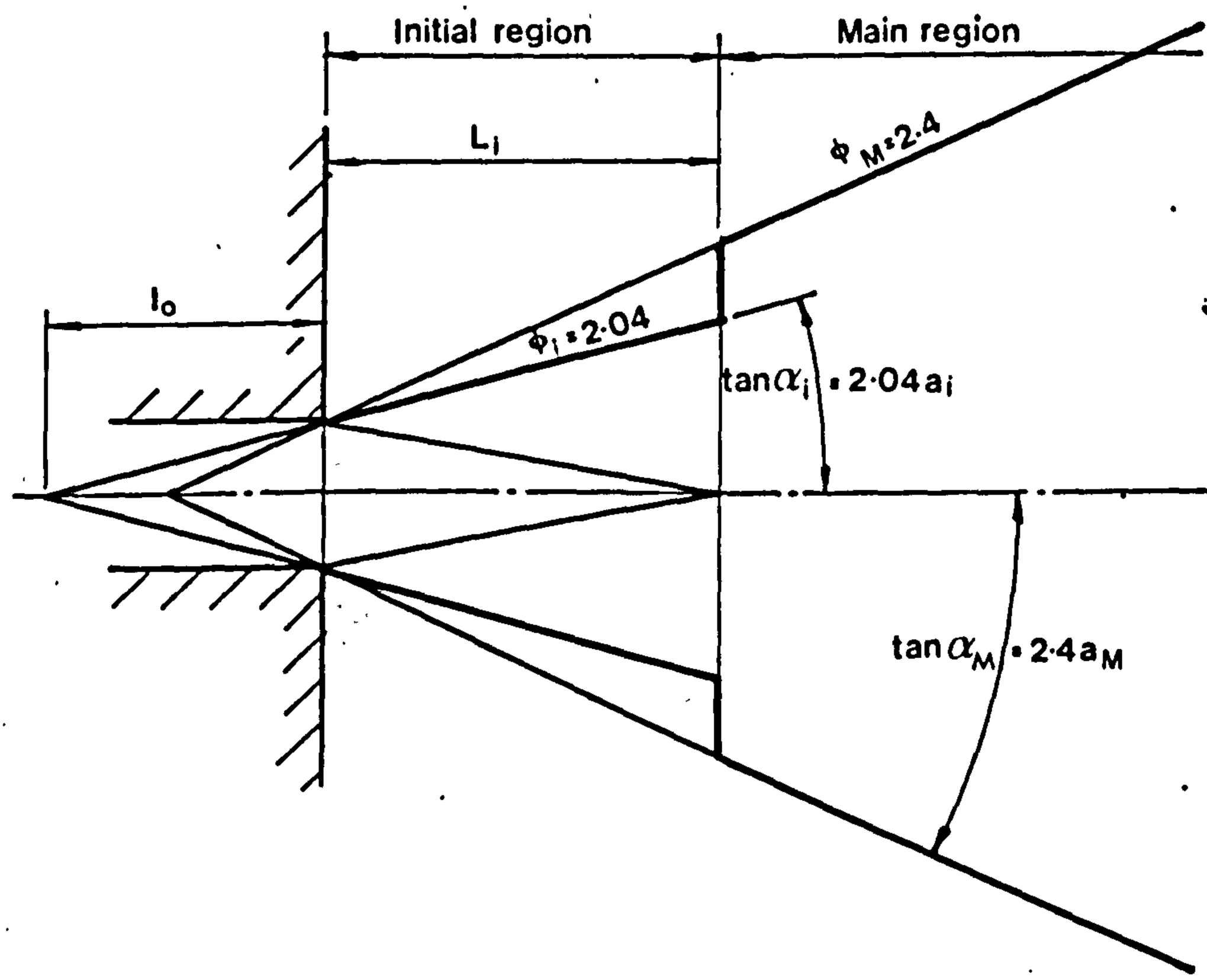

Fig. 2.16. DEFINITION SKETCH OF INITIAL REGION

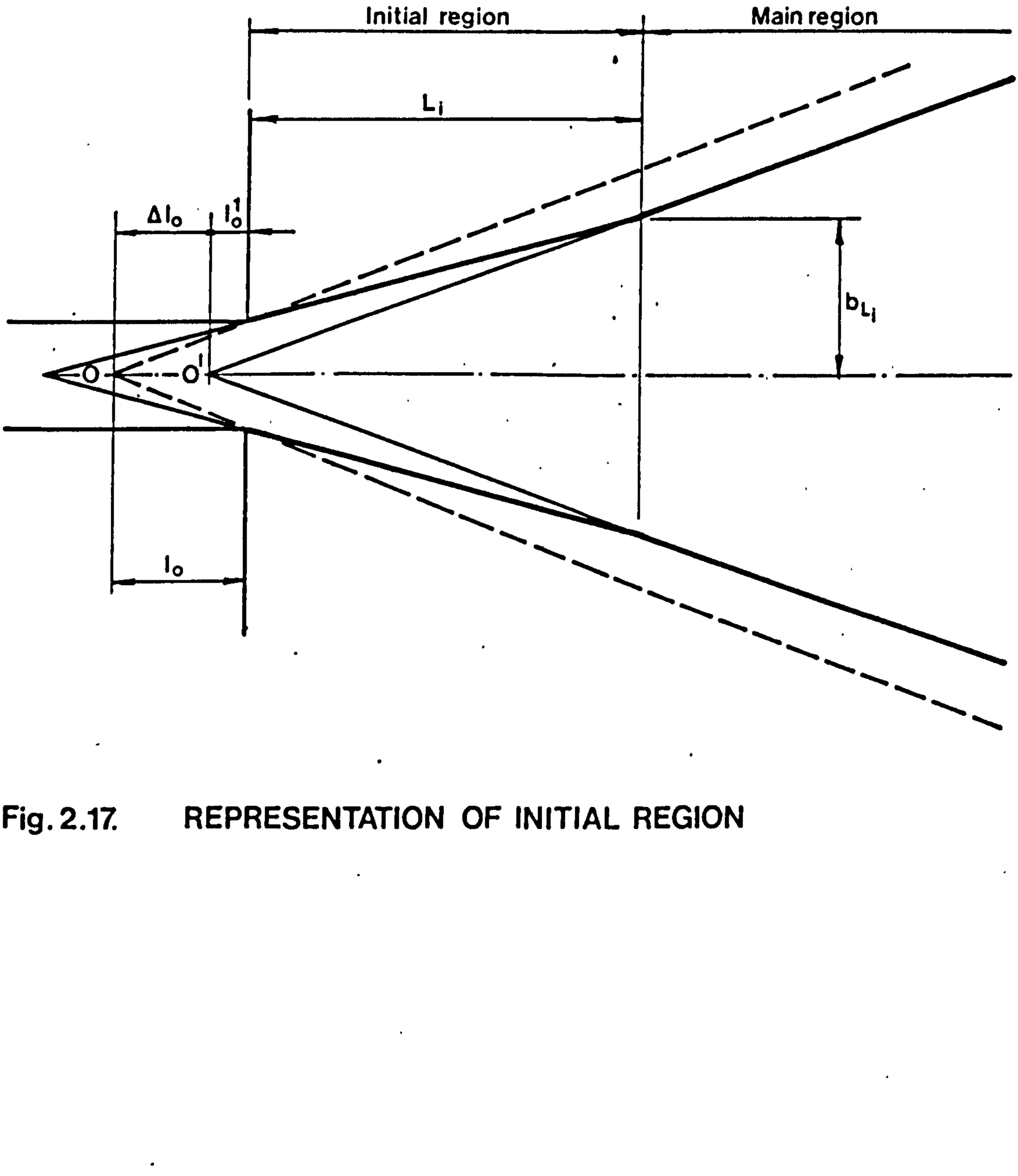

Fig. 2.17. REPRESENTATION OF INITIAL REGION

be shown that

$$\Delta l_o = 1.02\left\{\frac{b_o}{a_M}\ \frac{a_M}{a_j} - 0{,}85\right\} \qquad \ldots (2.69a)$$

The new location of the apparent source of the jet, 0' is therefore located at a distance l'_o from the nozzle exit given by

$$l_o' = l_o - \Delta l_o \qquad \ldots (2.70)$$

and substituting equations (2.48) and (2.69a)this becomes

$$l_o' = \frac{b_o}{a_M}\left\{1.283 - 1.02\ \frac{a_M}{a_j}\right\} \qquad \ldots (2.71)$$

For example, substituting the mean values of $a_M = 0.1$ and $a_j = 0.087$ into equation (2.71) results in the apparent source of the jet being displaced from $l_o = 4.16\ b_o$, as per equation (2.48) to $l_o' = 1.11\ b_o$.

Experimental results, as plotted in Fig. 2.8, indicate that the coefficient of turbulence in the main region decreases with increasing Re number. If this is so, then, with regard to equation (2.48), the relative distance of the apparent source of the jet from the nozzle, l_o/b_o, should increase with increasing nozzle Reynolds number. However, experimental data for low Reynolds numbers, as plotted in Fig. 2.11, shows an opposite trend; a decrease in the value of l_o/b_o with increasing Reynolds numbers. Based on experimental results as relatively high Re numbers, Zijnen observed $l_o/b_o = 1.2$ and Baturin suggested that, for uniform initial conditions, the value of $l_o/b_o \simeq 0$.

Such behaviour, contrary to expected trends, may be explained with the help of equation (2,71). Taking the experimental data of O'Callaghan et al, as plotted in Fig. 2.8 and Fig. 2.11, it is possible, using equation (2.71) to evaluate the value of the coefficient of turbulence in the initial region, a_j. The calculated values of a_j, as well as the original data, are plotted in Fig. 2.18. In the graph in Fig. 2.18a, the value of a_j rises more sharply than that of a_M, with decreasing Re numbers, until a point is reached where the value of a_j decreases very rapidly. This occurs at approximately $Re = 2 \times 10^3$. There is some evidence that for certain nozzle conditions the value of a_j is greater than a_M[52].

The sharp fall of the value of the coefficient of turbulence in the initial region can be explained by the onset of laminar flow in at least a part of the initial region. For this part of the function $a_j = f(Re)$, i.e. for $Re < 2 \times 10^3$, the value a_j must be a mean value over two distant sections of the initial region, as illustrated in Fig. 2.19. The relative lengths of the laminar and turbulent sections will obviously also vary with the nozzle Reynolds number. The value of the laminar section coefficient of turbulence, a_L, should be relatively insensitive to the Reynolds number. A visual evaluation of temperature perturbation interferograms[41] indicates an approximate value of $a_L = 0.05$.

On the right hand side of Fig. 2.18a is shown, as previously mentioned, the range of typical experimental values of a_M and a_j for higher nozzle Reynolds numbers. Applying equation (2.71) to these values results in

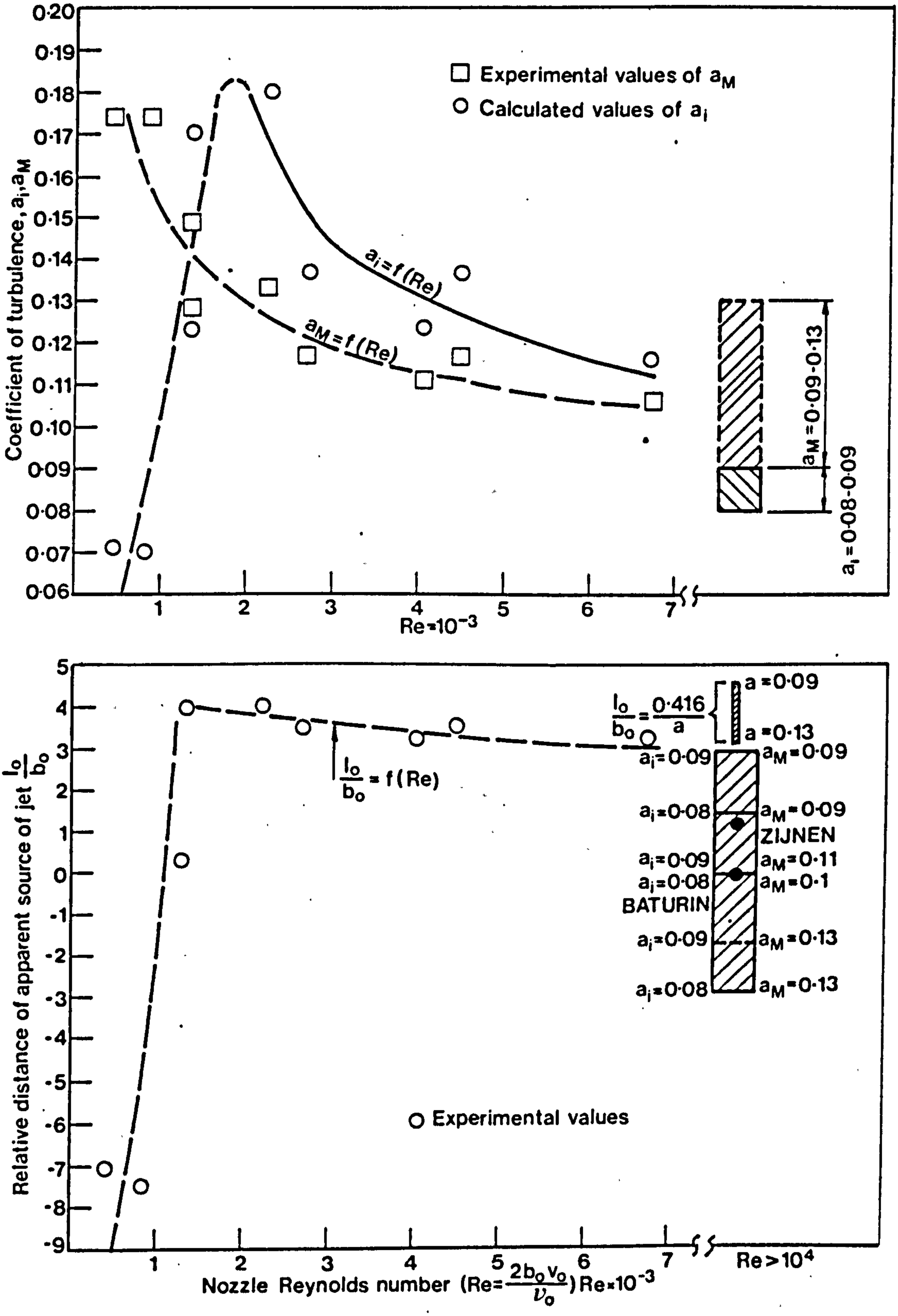

Fig.2.18. VARIATION WITH NOZZLE REYNOLDS NUMBER OF THE COEFFICIENT OF TURBULENCE a_i & a_M & OF RELATIVE DISTANCE OF SOURCE OF JET l_o/b_o

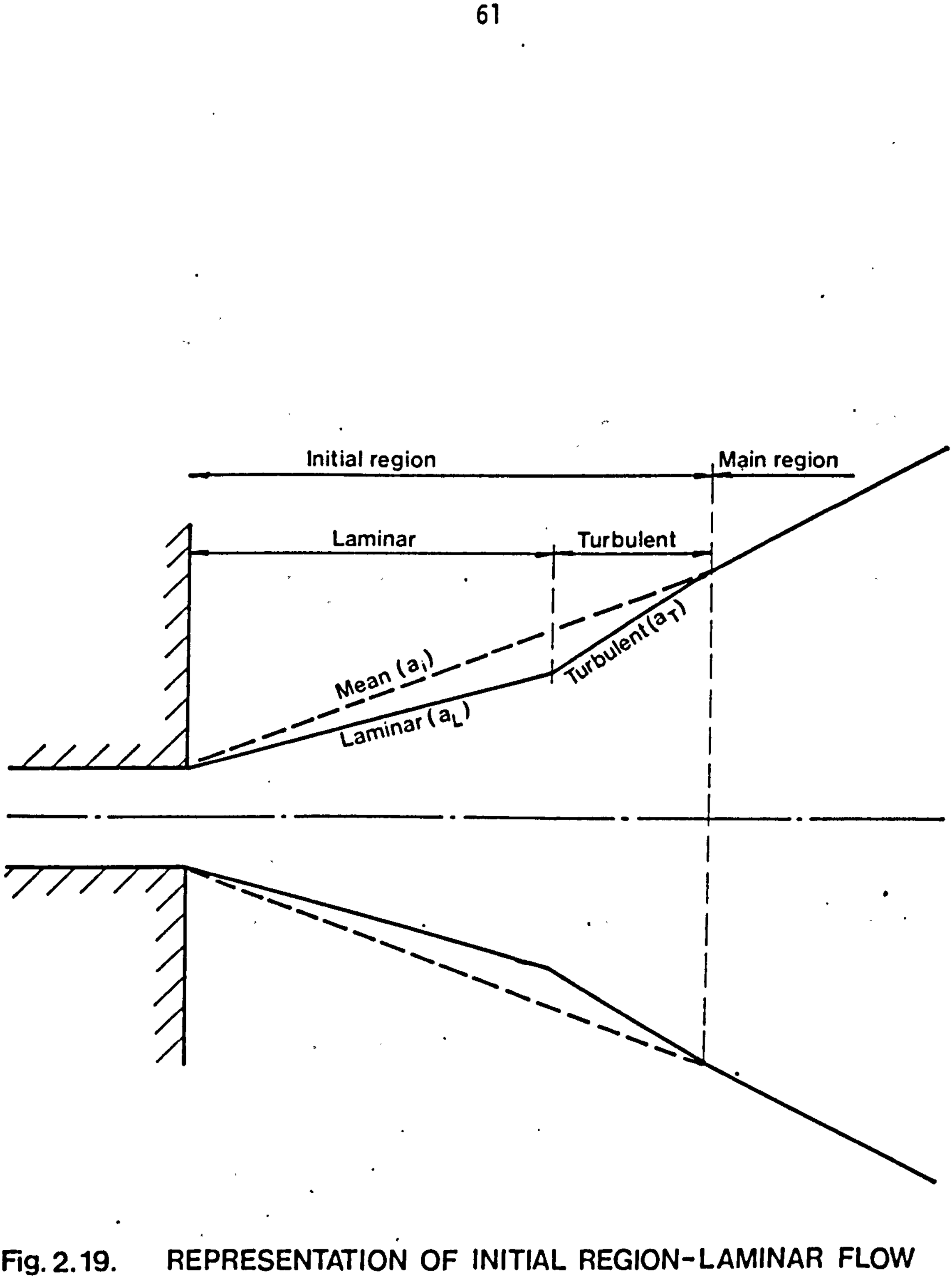

Fig. 2.19. REPRESENTATION OF INITIAL REGION-LAMINAR FLOW

a range of possible relative distances of the apparent source of the jet from the nozzle, l_o/b_o, as shown on the right hand side of Fig. 2.18b. There are two main points to be made. The first is that all the values of l_o/b_o calculated according to equation (2.71) lie below those calculated using equation (2.48). The second point is that it is possible to achieve $l_o/b_o = 0$ with a combination of the most commonly quoted values of a_M and a_j, namely $a_M = 0.1 \rightarrow 0.11$ and $a_j = 0.08 \rightarrow 0.09$. This supports the recommendation, appropriate to high nozzle numbers, that for uniform initial conditions $\frac{l_o}{b_o} \simeq 0$.

Based on a theoretical analysis of the flow in the wake behind a plate, Abramovich[22] obtained, for non-uniform initial velocity profiles, a relationship for the length of the initial region.

$$L_i' = L_i - 2.7\delta_o \qquad \ldots (2.72)$$

where δ_o is the boundary layer thickness in the initial cross section of the jet. For the extreme condition when the entire initial section is occupied by the boundary layer, i.e. $\delta_o = b_o$, the length of the initial region would be $\simeq 9\ b_o$ instead of $\simeq 12\ b_o$ obtained from equation (2.64).

The position of the apparent source of the jet is also affected by non-uniform initial conditions, moving further upstream by approximately the same distance as the initial region has been shortened.

2.3.2 Plane wall jets.

A plane wall jet is, in essence, a special case of a plane jet being discharged from a nozzle tangentially on to a smooth flat plate which is submerged in a semi-finite expanse of identical fluid. A plane wall jet is shown schematically in Fig. 2.20. In the initial region not only does a shear layer develop on the fluid side, but a boundary layer develops on the wall side. The main region is characterised by the disappearance of the potential core, which occurs at a point, L_j, where the developing boundary layer meets the penetrating shear layer. The velocity profiles, as expected, show a similarity in the developed stage of the jet when the appropriate scale factors are applied. Fig. 2.21 shows a dimensionless velocity profile based on Förthmanns[35] experimental observations for values of $x/b_o > 20$. The velocity scale factor is v_m and the length scale factor is $y_{0.5}$. Further experiments on wall jets have been made by Zerbe and Selna[53], Sigala[54], Meyers et al[55], Schwarz and Cosart[56] and a comprehensive bibliography has been compiled by Rajaratnam and Subramanya[57] and by Gauntner, Livingood and Hrycak[58].

Theoretical considerations, following closely the arguments for plane free jets, lead to similar simplified equations of motion (equations (2.36) and (2.37)). The integral momentum equation leads to an identical solution as equation (2.42) if, as a first approximation, a zero change in the momentum flux in the x-direction, as expressed by equation (2.39), is assumed. A similarity analysis results, therefore, in $a = -0.5$ and $b = 1$ for the assumed simple exponential expressions for

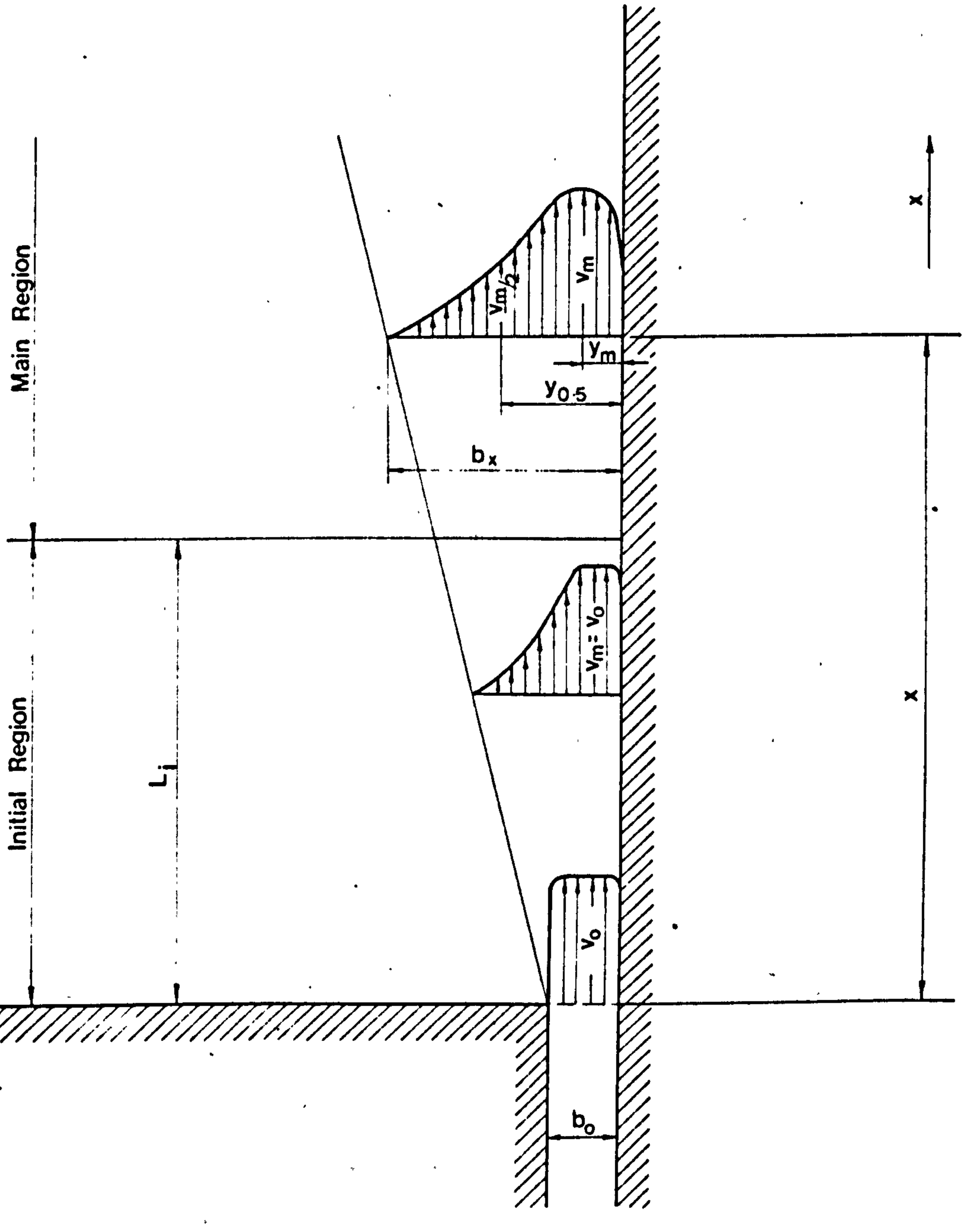

Fig.2.20. DEFINITION SKETCH OF PLANE WALL JET

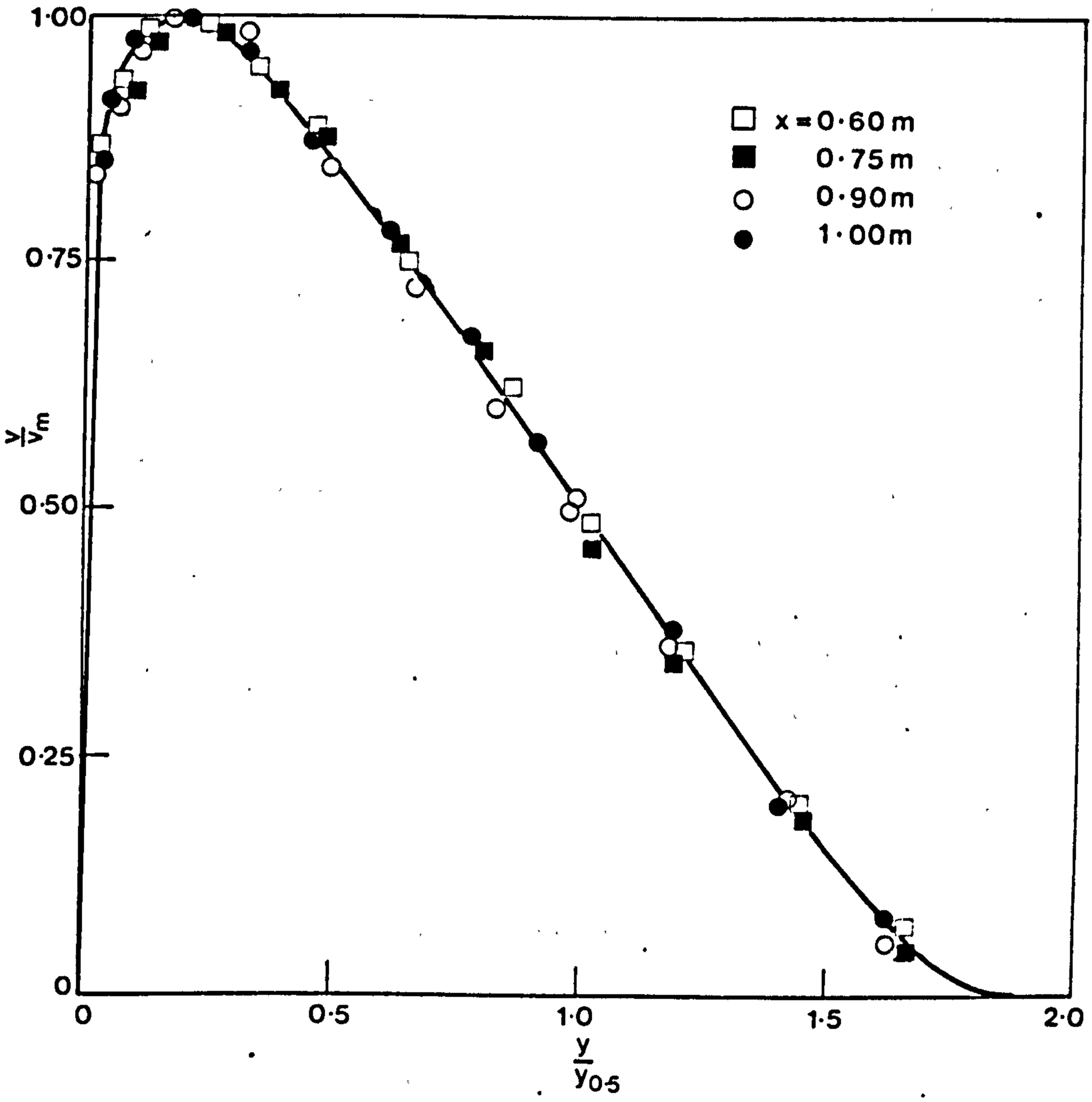

Fig.2.21. SIMILARITY OF VELOCITY PROFILES IN PLANE WALL JETS (FORTHMANN)

the scale factors, $v_m \propto x^a$ and $y_{0.5} \propto x^b$. This does not strictly apply, and if the presence of the wall shear stress term τ_o is not ignored, equations (2.39) becomes

$$\frac{d}{dx} \int_0^\infty \rho v^2 \, dy = - \tau_o \qquad \ldots (2.73)$$

The presence of the sheer stress term will evidently reduce the exponent a to less than -0.5. If $\tau_o \propto x^c$ is assumed then, with regard to equation (2.73),

$$2a + b - 1 = c \qquad \ldots (2.74)$$

which, for b = 1, we have that 2b = c. If the first approximation, a = -0.5, is accepted then c = -1. Thus for plane turbulent wall jets $v_m \propto 1/\sqrt{x}$; $y_{0.5} \propto x$ and $\tau_o \propto 1/x$.

Glauert [59] sought a theoretical solution of the boundary layer calculations according to which the form of velocity distribution across the jet would not vary along its length. For laminar flow Glauert obtained a similarity solution explicitly. For turbulent flow, molecular viscosity has to be replaced by eddy viscosity varying in a plausible manner over the velocity profile. In the boundary layer an eddy viscosity based on Blasius's one-fourth power friction formula for turbulent flow in pipes, which implies $v \propto y^{1/7}$, was used, whereas Prandtl's hypothesis for free turbulent flow, and therefore constant eddy viscosity, was assumed in the outer layer. The solutions were then matched at their boundaries. However, this approach implies that complete similarity of velocity profiles is not possible as the shape of the profile is influenced by a Reynolds number dependent constant, α. Fortunately the profile is relatively insensitive to a change in the value of α and therefore, within attainable practical accuracy, the profiles could be considered similar. The part of the velocity profile beyond the velocity maximum shows such an extreme insensitivity that the outer part of the profile, especially of a laminar wall jet, is virtually the same as that of a plane jet.

Experimental observations of Bakke[60], Meyers et al[55] and Schwarz and Cosart[56]have shown that the velocity gradient near the wall is greater than predicted by Glauert. The velocity distribution in the boundary layer is better described by $v \propto y^{1/14}$. It was also found that the turbulent shear stress was not zero at the velocity extreme, but at a point closer to the wall.

Meyers et al[55] found that for $\frac{y\ v_*}{\nu} > 10$ the logarithmetic law is valid in the form

$$\frac{v}{v_*} = 5.6 \log \left(\frac{y\ v_*}{\nu} \right) + 4.9 \qquad \ldots (2.75)$$

where $v_* = \sqrt{\tau_o/\rho}$. Different values of the constants have been found by Mathieu and Tailland[61] namely 4.45 and 10.3 respectively.

For lower values of $\frac{y\ v_*}{\nu}$ a simpler law applies:-

$$\frac{v}{v_*} = \frac{y\ v_*}{\nu} \qquad \ldots (2.76)$$

Verhoff[62] found an empirical equation to describe the similarity curve

$$\frac{v}{v_m} = 1.48 \left(\frac{y}{y_{0.5}}\right)^{1/7} \left[1 - \text{erf}\left\{0.68 \left(\frac{y}{y_{0.5}}\right)\right\}\right] \qquad \ldots (2.77)$$

An average curve of velocity decay of a number of available observations [54 55 56 63 64] is plotted in Fig. 2.22. The average curve is well described by the equation

$$\frac{v_m}{v_o} = \frac{C}{\sqrt{\frac{x}{b_o}}} \qquad \ldots (2.78)$$

where C = 3.5. The value of the constant C is well within the range of experimental values obtained for plane free jets. To be comparable with equation (2.46) the constant C can also be expressed as

$$C = \frac{1.21}{a} \qquad \ldots (2.79)$$

where a is the coefficient of turbulence. The mean value of this experimentally derived coefficient is usually quoted as a = 0.1 for plane jets. Substituting this value into equation (2.79) results in C = 3.83. This may indicate that the influence of the wall could, on the average, reduce the maximum velocity by circa 8% when compared with a plane free jet of 2 b_o nozzle width.

Because of the growth of the boundary layer the length of the initial region will also be affected. Evaluation of the one-seventh power law equation for Re = 10^4 and Re = 10^5 results in $L_i = 6.1b_o$ and $L_i = 6.7b_o$. These values are in good agreement with experimental observations.

Rajaratnam[46] obtained an expression for volume flow

$$\frac{V_x}{V_o} = 1 + 0.04\ \frac{x}{b_o} + 0.0046 \left(\frac{x}{b_o}\right)^{0.8} \qquad \ldots (2.80)$$

which gives identical results to those calculated with equation (2.66) for a = 0.1 and only approximately 3% higher than for a = 0.087, which is the mean value for shear layers.

For the purposes of calculation of replacement jets, wall jets can be calculated as for plane free jets of a nozzle width of $2b_o$. The error, especially in the initial region, is negligible. The only parameter that is significantly affected by the presence of the wall is the length of the initial region. The roughness of the wall surface has an effect on the growth of the boundary layer and velocity decay. It is of benefit, when considering replacement jets, to use smooth wall surfaces and thereby increase the predictability of calculations.

2.3.3. Influence of buoyancy forces

By definition, replacement jets will be non-isothermal. They will

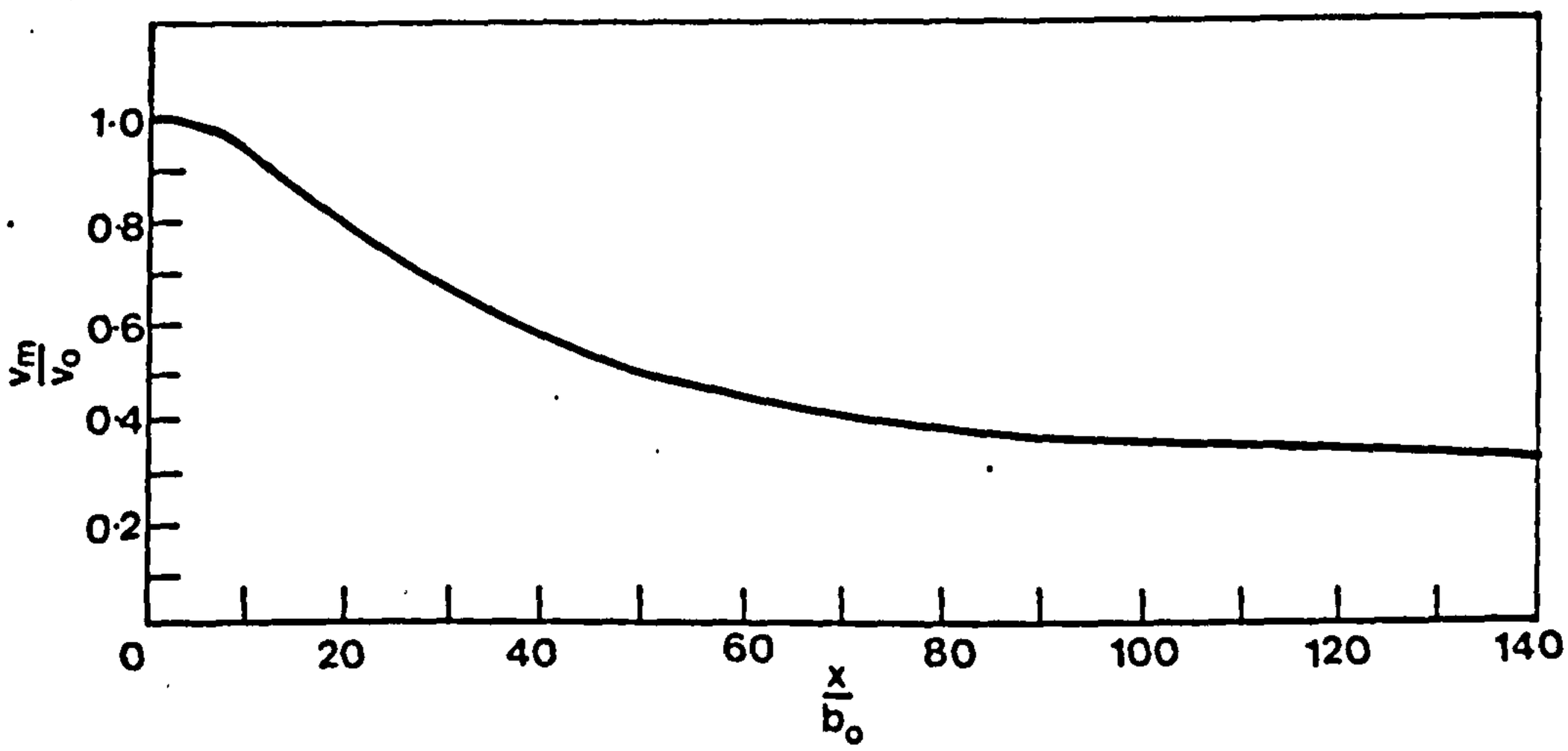

Fig.2.22. VELOCITY DECAY OF WALL JETS - AVERAGE OF A NUMBER OF OBSERVATIONS

either be heated jets discharged vertically upwards or cold jets downwards, i.e. in both cases the Archimedean forces of buoyancy will be acting in the direction of the initial flow from the jet nozzle.

Buoyancy forces will influence all parameters of the jet. The basic principle that describes the actions of Archimedean forces is simple, but the whole phenomenon of non-isothermal vertical jets is extremely complex. Not only do the temperature and velocity vary along both the x and y axes but their variations are themselves functions of buoyancy To further complicate matters, the energy generated by Archimedean forces can be dissipated by an increase in momentum flux, volume flow, friction on the wall surface and in the mixing layer. Some of the enery dissipated as friction will be transformed into heat and thereby further complicate the issue.

Although there is a considerable amount of theoretical and experimental information available concerning the behaviour of isothermal jets, there is comparatively little which deals with air streams initially at higher or lower temperatures than the surrounding air. The published information is exclusively concerned with problems that are encountered in the ventilation or air conditioning of spaces and therefore concentrates on the problem of curvature of the centre line of a jet. The jet is usually introduced into a room horizontally, or at an angle moderately different from horizontal. In order to be in a position to judge the importance of buoyancy forces in the calculation of replacement jets, two simplified cases will be examined; a more indepth study for this purpose would not be warranted.

In the first case the effect of buoyancy on centre line velocity is examined. The velocity along the centreline of a heated plane jet issuing vertically from a linear slot will be higher, due to the forces of bouyancy acting in the direction of the initial flow, than predicted for an equivalent isothermal jet. An element of the jet would have reached x' instead of x, see Fig. 2.23, in an equivalent length of time. The velocity at x' is a summation of two components

$$v_m' = v_m + w \qquad \ldots (2.81)$$

where v_m is the velocity of an equivalent isothermal jet at point x, and can therefore be calculated according to equation (2.50) if $x > L_j$, i.e. in the main region, or if $x < L_j$ then $v_m = v_o$. The buoyancy component, w, can be expressed as

$$w = \int_0^\tau a \, \rho \, d\tau \qquad \ldots (2.82)$$

where a is the acceleration due to buoyancy as defined by the Archimedean Law

$$a_\rho = g \frac{\rho_a - \rho_m}{\rho_a} = g \frac{T_m - T_a}{T_a} \qquad \ldots (2.83)$$

In the above expression g is the acceleration due to gravity and ρ_m and T_m are the density and absolute temperature of the centreline of the jet, i.e. the maximum values, and ρ_a and T_a the density and

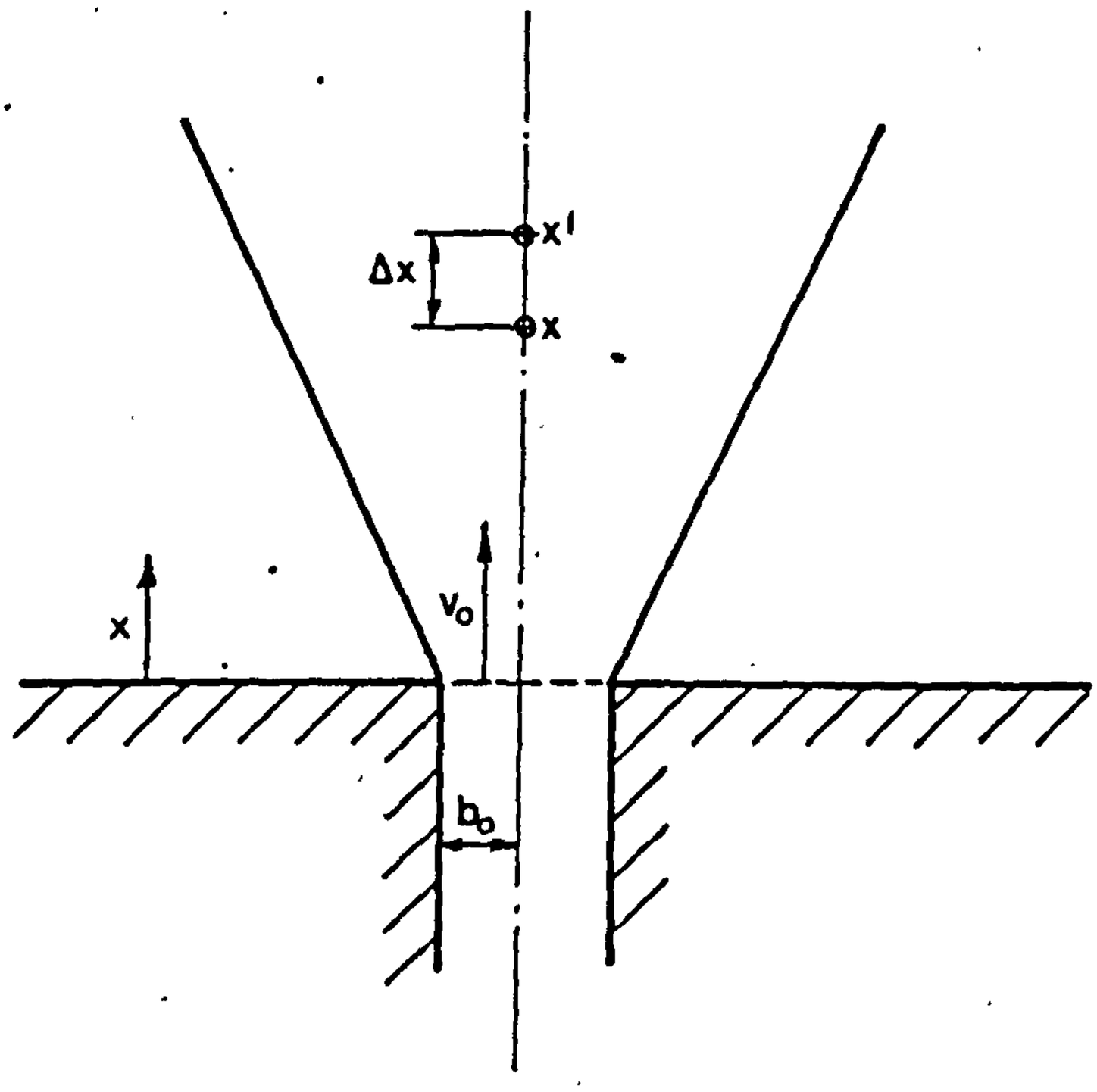

Fig.2.23. DEFINITION SKETCH OF THE EFFECT OF BUOYANCY FORCES

absolute temperature of the ambient air. If $d\tau = \frac{dx}{v_m}$, substituting equation (2.83 for a_ρ, equation (2.82) can be rewritten

$$w = {}_0\int^x g \frac{T_m - T_a}{T_a} \frac{1}{v_m} dx \qquad \ldots (2.84)$$

For the main region of the jet, an expression for $(T_m - T_a)$ can be found in equation (2.57). Substitution and integration yields

$$w = 0.73 \frac{g}{v_o} \left(\frac{T_o - T_a}{T_a}\right) \qquad \ldots (2.85)$$

or

$$\frac{w}{v_o} = 0.73\, Ar_o \frac{x}{b_o} \qquad \ldots (2.86)$$

where the Archimedean number for the flow at the nozzle

$$Ar_o = \frac{g\, b_o (T_o - T_a)}{v_o^2 T_a} \qquad \ldots (2.87)$$

The additional length an element would have travelled, $\Delta x = x' - x$, can now be found

$$\Delta x = {}_0\int^\tau w\, d\tau \qquad \ldots (2.88)$$

Substituting equation (2.85) for w, $d\tau = \frac{dx}{v_m}$ and equation (2.50) for v_m; after integration

$$\Delta x = 0.243 \frac{g}{v_o^2} \frac{(T_o - T_a)}{T_a} \left(\frac{b_o}{a}\right)^2 \left\{\left(\frac{ax}{b_o} + 0.416\right)^{2.5} - 0.693 \left(\frac{ax}{b_o} + 0.416\right)^{1.5} + 0.0743\right\} \qquad \ldots (2.89)$$

If it is assumed that $l_o = 0$; an alternative, less accurate, equation can be obtained, namely

$$\frac{\Delta x}{x} = 0.243 \sqrt{a}\, Ar_o \left(\frac{x}{b_o}\right)^{1.5}. \qquad \ldots (2.90)$$

In the initial region of the jet, where $v_m = v_o$ and $\Delta t_m = \Delta t_o$ is assumed, the corresponding equations are

$$w = \frac{g}{v_o} \frac{T_o - T_a}{T_a} x \qquad \ldots (2.91)$$

or

$$\frac{w}{v_o} = Ar_o \frac{x}{b_o} \qquad \ldots (2.92)$$

and

$$\Delta x = 0.5 \frac{g}{v_o^2} \frac{T_o - T_a}{T_a} x^2 \qquad \ldots (2.93)$$

or

$$\frac{\Delta x}{x} = 0.5\, Ar_o \frac{x}{b_o} \qquad \ldots (2.94)$$

Values of centreline w and Δx calculated according to the above equations should always be greater than those actually observed because the

equations do not take into account friction and mass interchange with the rest of the jet moving at a lower velocity. For this reason when used to evaluate the effect of buoyancy on the centreline velocity of non-isothermal vertical jets, the answers will always be conservative. The equations indicate that both the buoyancy component of velocity, w, and the additional length travelled, Δx, are extremely sensitive to the initial velocity in the nozzle and to a lesser degree to the initial temperature differential. For example, jet parameters of $b_o = 0.005m$, $\Delta t_o = 20^oC$, $T_o = 293^oK$ and an initial velocity $v_o = 1.0$ m/s will result in a relative rise in centreline velocity, $\frac{w}{v_o}$, at the end of th initial region ($L_1 = 12b_o$) of only 4%, whereas jet parameters of $b_o = 0.01m$, $\Delta t_o = 40^oC$ and $v_o = 0.5m/s$ (same initial flow rate at a higher temperature) will result in $\frac{w}{v_o} = 0.64$, i.e. a rise of 64%.

The growth of $\frac{w}{v}$ and $\frac{\Delta x}{x}$ is slower in the main region of the jet. The relative buoyancy component of the vertical centreline velocity $\frac{w}{v_o}$ for values of $\frac{x}{b_o} > L_i$ can be calculated directly if equations (2.86) and (2.92) are combined to give

$$\frac{w}{v_o} = Ar_o \left(\frac{L_i}{b_o} + 0.73 \frac{x-L_i}{b_o} \right) \quad \ldots (2.95)$$

Similarly the relative additional length, $\frac{\Delta x}{x}$, can be calculated if equations (2.90) and (2.94) are combined so producing

$$\frac{\Delta x}{x} = Ar_o \left[0.5 \frac{L_i}{b_o} + 0.243 \sqrt{a} \left(\frac{x-L_i}{b_o}\right)^{1.5} \right] \quad \ldots (2.96)$$

Using equation (2.95) for the same jet parameters as used in the above example but $x/b_o = 50$, the respective rise in centreline velocity would be 13% and 213%. The first value, 13% is more reliable because the currently accepted threshold velocity of 0.25 m/s[51] occurs at $x/b_o = 226$, whereas in the second case the threshold velocity has been reached and therefore the disruptive influence of all the factors not taken into account by the equations may predominate.

To gain an appreciation of how buoyancy affects the whole jet some radical simplifying conditions will have to be imposed. The first, and most important, is that all energy added by Archimedean forces to the jet will be transformed into additional momentum of the jet. This is probably true for the core of the jet which is unaffected by mass exchange with the ambient air. Therefore

$$M = M_J + M_\rho \quad \ldots (2.97)$$

where M is the total momentum of the non-isothermal vertical jet, M_J is the momentum of an equivalent isothermal jet and M_ρ is the buoyancy generated component. The momentum of an isothermal jet is by definition constant and therefore equal to $M_o = \rho V_o v_o$. The determination of the buoyancy generated component M_ρ, is more difficulat. Previous discussion has shown that there are a number of reasons why replacement jets should be designed to keep the values S, as shown in Fig. 2.2, as small as possible in order to maximise the temperature advantage of replacement jets and to minimise departures from calculated values.

All further discussion will therefore be concerned with the region where the profile is just fully developed, i.e. $x \propto L_1$.

A factor that should not be dismissed carelessly is the additional length travelled Δx. If it were not taken into account, the prediction would be for conditions at a distance of $(x + \Delta x)$ instead of x from the nozzle. For the two sets of parameters used in the previous examples equation (2.94) would give relative additional lengths of 2%, for the high nozzle velocity, and 32% for the low nozzle velocity and higher initial temperature case.

To be in a position to ascertain the magnitude of the buoyancy generated component of momentum flow, M_ρ, in essence a buoyancy mean square velocity component, v_{sq_ρ}, has to be found. The overall square velocity v_{sq_T} is

$$v_{sq_T} = v_{sq_J} + v_{sq_\rho} = \frac{V_o}{V} v_o + \frac{V_e}{V} w_{sq} \quad \ldots (2.98)$$

where v_{sq_J} is the isothermal value and V_e is the "effective" volume of the jet that is subject to the action of buoyancy forces. Buoyancy, to be effective, has to be able to influence an element of the jet for a sustained period. The initial volume issuing from the nozzle would theoretically comply as it is influenced by gravitational forces for the whole interval, but, due to the exchange of matter that is associated with turbulent flows in shear layers, the actual "effective volume" will be less. For lack of information a conservative estimate $V_e = 0.8\ V_o$ is adopted.

In order to calculate the buoyancy component of the mean square velocity w_{sq}, assumptions have to be made about how the effective volume, V_e, would have to be moved from the nozzle to x under isothermal conditions. Because of the general uncertainty, the mean arithmetic velocity (as expressed by equation (2.68)) can be considered as sufficiently accurate if x/b_o is moderate. Although the mean arithmetic velocity strictly applies to the total volume, i.e. both the primary and entrained component, in the initial region this discrepancy can be neglected. The first step in the calculation, as has been mentioned, is to anticipate the lengthening of the trajectory due to buoyancy. For this purpose, equation (2.93) is satisfactory and the corrected value

$$x' = x - 0.5 \frac{g}{v_o^2} \frac{T_o - T_a}{T_a} x^2 \quad \ldots (2.99)$$

is used. Substituting equation (2.83), where equation (2.54) and (2.66) have been used to express the temperature differential, into (2.82); utilising equation (2.68) in $d\tau = \frac{dx}{V}$ and rearranging and integrating gives

$$w_{sq} = \frac{g}{v_o} \left(\frac{T_o - T_a}{T_a}\right) \frac{b_o}{0.43a} \left[3.744 \left(1 + 0.43 \frac{ax'}{b_o}\right)^{-1} + 4.744 \log_e \left(1 + 0.43 \frac{ax'}{b_o}\right) - 3.774\right]$$

$$\ldots (2.100)$$

When equations (2.100) and (2.98) are applied to the two sets of parameters the two results are widely divergent. In the first case having the higher initial velocity but identical V_o (x/b_o = 12, v_o = 1m/s, b_o = 0.005 m and Δt_o = 20°C) the influence of buoyancy is negligible. The isothermal square velocity, v_{sq_J} = 0.66 m/s, is only raised by 6.4% and $\frac{\Delta x}{x}$ is only 2%. In the second case ($\frac{x}{b_o}$ = 12, v_o = 0.5 m/s, b_o = 0.01 m and Δt_o = 40°C) the effect is significant; v_{sq_J} = 0.37 m/s is raised by 61% to a value of v_{sq_T} = 0.6m/s. These values would have been even higher if a correction of $\frac{\Delta x}{x}$ = 32% had not been made thereby effectively reducing $\frac{x}{b_o}$ to a value of 8.14.

Buoyancy could have a beneficial effect on the sensitivity of sizing of replacement jets in the initial region. If the nozzle width is oversized, i.e. the initial velocity and momentum flux are lower than they should be, buoyancy will have more time to exert its influence and thereby raise the momentum flux and maximum velocity at the replacement cross-section. If the initial velocity is higher then the effect of buoyancy will be negligible.

The acceleration of the jet may also affect its angle of spread and therefore the coefficient of turbulence a. From simple geometric considerations, the modified coefficient of urbulence is

$$a' = \frac{a}{1 + \frac{\Delta x}{x}} \qquad \ldots (2.101)$$

If a = 0.09 and $\frac{\Delta x}{x}$ = 0.32, as in the second example, the modified coefficient of turbulence a' = 0.68. Such behaviour could result in a substantial lengthening of the initial region from $12b_o$ to $16b_o$ for plane jets and from $7b_o$ to $10b_o$ for wall jets.

2.3.4. Resumé

In this chapter the most appropriate expressions for replacement jets were identified and where not readily available, an effort has been made to deduce such formulae theoretically or from existing experimental data. To maintain the temperature differential advantage gained when convective currents are replaced by non-isothermal jets, it is essential to minimise the distance from the nozzle to the cross-section where the substitution takes place, i.e. from the nozzle to where the edge of the original convective surface would have been. Primarily for this reason, an emphasis has been placed on the analysis of the behaviour od jets near the end of the initial region, especially as there is a dearth of readily available relevant published information. This is hardly surprising, as most of the information available is connected with the most frequent technical applications of jets, such as air-conditioning, and therefore some aspects, important to replacement jets, are not considered at all or the information is incomplete.

The initial region was examined in greater detail, with an emphasis on flows at low nozzle Reynolds numbers, and an attempt was made to reconcile apparently conflicting data concerning the coefficient of turbulence, the position of the apparent source of the jet and the length of the initial region.

A review of wall jets has resulted in the conclusion that, for the purposes of the calculation of replacement jets, wall jets can be treated as plane free jets of twice the nozzle width. The only parameter that is significantly affected by the presence of a wall is the length of the initial region.

The most appropriate formulae for the calculation of replacement jets are tabulated in Table 2.2. The decision which to include, where alternatives were available, was difficult, as a balance had to be achieved between accuracy, and usually complexity, and the need for clarity required for the practical task of predicting what would be suitable replacement wall jets. In some instances, for example the formula governing the decay of axial temperature, the simpler expression described more accurately the available experimental results.

By definition, the replacement jet will be non-isothermal, discharged vertically, and the direction of initial flow of the jet and of the buoyancy forces will be coincidental. There is a dearth of information on this specific problem. Although the basic principle, the action of Archimedean force, is simple to understand, the whole phenonenon is extremely complex. A theoretical study has shown that for low initial velocities and higher temperature differentials buoyancy forces could modify the jet, even in the initial region. Fortunately, buoyancy could also act as a stabilising force and make the calculation of replacements jets less sensitive. Further experimental work is necessary. Approximate formulae for the assessment of buoyancy on replacement jets are tabulated in Table 2.3.

TABLE 2.2 Formulae for parameters of plane jets in the initial and main region. Wall jets are treated as plane jets where b_o is the width of the wall jet nozzle. Formulae presume uniform initial conditions.

Parameter	Initial Region	Main Region	Unit
Coefficient of turbulence a	For $Re>10^4$, a_i=0.08-0.09 For $Re<6.10^3$ see Fig.2.18	smaller values of $\frac{x}{b_o}$; a_M=0.09-0.11 larger values of $\frac{x}{b_o}$; a_M up to 0.13	-
Angle of spread tan α	$2.04a_i$	$2.4a_M$	
Apparent source l_o	$0.49 \frac{b_o}{a_i}$	$\frac{b_o}{a_M}(1.283-1.02 \frac{a_M}{a_i})$	m
Initial region L_i - plane jet	$1.02 \frac{b_o}{a_i}$; Non-uniform nozzle profile	$L_i - 2\delta_o$ where δ_o = nozzle boundary layer thickness	m
- wall jet	$0.6 L_i$		m
- temperature core	$0.7 L_i$		m
axial velocity $\frac{v_m}{v_o}$	1	$1.2 (\frac{ax}{b_o} + 0.416)^{-0.5}$	
axial temperature $\frac{\Delta t_w}{\Delta t_o}$	1	$0.73 \frac{v_m}{v_o}$	
volume flow $\frac{V_x}{V_o}$	$1 + 0.43 \frac{ax}{b_o}$	$1.2 (\frac{ax}{b_o} + 0.416)^{0.5}$	
mean arithmetic velocity $\frac{v_{ar}}{v_o}$	$\frac{1 + 0.43\frac{ax}{b_o}}{1 + 2.04 \frac{ax}{b_o}}$	$0.49 (\frac{ax}{b_o} + 0.416)^{-0.5}$	
mean square velocity $\frac{v_{sq}}{v_o}$	$(1 + 0.43 \frac{ax}{b_o})^{-1}$	$0.82 (\frac{ax}{b_o} + 0.416)^{-0.5}$	

mean temperature $\frac{\overline{\Delta t_x}}{\Delta t_o}$	$\frac{V_o}{V_x}$	$\frac{V_o}{V_x}\left(\frac{T_a}{T_o}\right)^{0.5}$	
half-width $\frac{b_x}{b_o}$	$1 + 2.04\,\frac{ax}{b_o}$	$2.4\left(\frac{ax}{b_o} + 0.416\right)$	m.

TABLE 2.3 Approximate formulae for the assessment of the effects of buoyancy on non-isothermal vertical jets; the directions of initial flow of jet and buoyancy forces being coincidental. Values are relative to equivalent isothermal values.

Parameter	Symbol	Initial Region	Main Region	Unit
Additional length travelled by centre-line element	Δx	$0.5 \frac{g}{v_o^2} \frac{T_o - T_a}{T_a} x^2$	see main text equation 2.89	m
Relative additional length	$\frac{\Delta x}{x}$	$0.5\, Ar_o \frac{x}{b_o}$	$Ar_o \left[0.5(\frac{L_i}{b_o}) + 0.243\, a^{0.5} (\frac{x-L_i}{b_o})^{1.5}\right]$	
Relative additional centre-line velocity at $x + \Delta x$	$\frac{w}{v_o}$	$Ar_o \frac{x}{b_o}$	$Ar_o \left[\frac{L_i}{b_o} + 0.73 \frac{(x-L_i)}{b_o}\right]$	
Additional mean square velocity at x, initial region	w_{sq}	$\frac{g}{v_o} \frac{(T_o - T_a)}{T_a} \frac{b_o}{0.43a} \left[3.744 (1 + 0.43 \frac{ax'}{b_o})^{-1} + 4.744 \log_e (1+0.43 \frac{ax'}{b_o}) - 3.774\right]$ where $x' = x - \Delta x$		
Modified coefficient of turbulence	a'	$\frac{a}{1+\frac{\Delta x}{x}}$		

2.4 THEORETICAL CALCULATION OF THE REPLACEMENT JET FROM CONVECTIVE SURFACE PARAMETERS.

The problem that has to be solved before non-isothermal jets are used to replace convective currents in models is the prediction of the basic parameters of the replacement jet, i.e. initial velocity, temperature and width and position of the nozzle, from the vertical dimension and surface temperature of the convective surface. The jet replacing the convective current, in order to be effective, has to influence room air movements in an identical way as the original convective current. To conform to this condition the following parameters, in order of their importance, will have to be identical as accurately as possible - momentum flux, maximum velocity and the mean temperature, defined as the ratio of heat content to mass flow. The similarity of the velocity and temperature profilesis to a certain extent given if the above parameters are identical.

2.4.1. Fundamental calculation

Consider a convective surface having a height H and a surface temperature differential Δt_w. These two values are sufficient to define all the parameters of a convective current leaving the top edge of a heated surface (or the bottom edge of a cooled surface), as given in Table 2.1. The nozzle of the replacement jet will be at a distance S, see Fig. 2.24, from the top edge of the original heated surface and will have a nozzle width b_o and an initial velocity v_o. As previously mentioned, in order to maximise the temperature advantage of replacing a convective current by a non-isothermal jet, flow in the initial region will be considered. Uniform initial conditions are assumed, i.e. $v_o = var_o = vsq_o$.

Flow in the initial region assumes $v_m = v_o$. If the maximum velocity of the replacement jet velocity profile, v_m is required to be identical with the maximum value of the convective velocity profile. v_{max}, i.e. $v_m = v_{max}$, then

$$v_o = v_m \qquad \ldots (2.102)$$

The boundary layer thickness is also assumed identical - $b_s = \delta$. Using expressions from Table 2.2.

$$\frac{var_s}{v_o} = \frac{1 + 0.43 \frac{aS}{b_o}}{1 + 2.04 \frac{aS}{b_o}} \qquad \ldots (2.103)$$

$$\frac{vsq_s}{v_o} = \left(1 + 0.43 \frac{aS}{b_o}\right)^{-1} \qquad \ldots (2.104)$$

$$\frac{\delta}{b_o} = 1 + 2.04 \frac{aS}{b_o} \qquad \ldots (2.105)$$

By substituting equation (2.103) and (2.104) into (2.105) it can be shown that

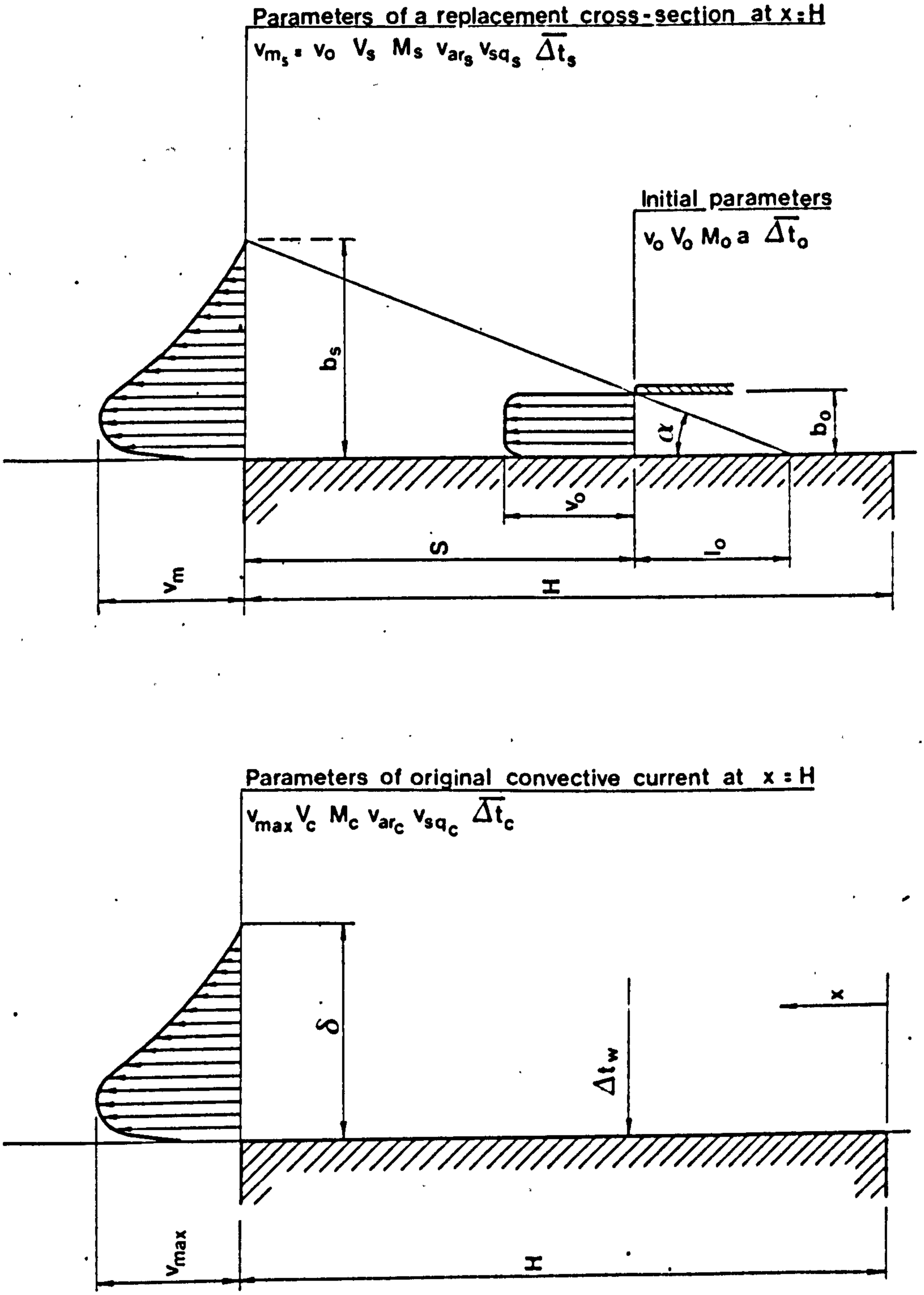

Fig.2.24. DEFINITION SKETCH OF CONVECTIVE SURFACE AND REPLACEMENT JET

$$b_o = \delta \frac{v_{ar_s} \quad v_{sq_s}}{v_o^2} \qquad \ldots (2.106)$$

The condition of equivalent momentum flux demands that $v_{sq_s} = v_{sq_c}$ and if $v_{ar_s} = v_{ar_c}$ is also assumed, by substitution for v_{sq_c} and v_{ar_c} from Table 2.1, for turbulent flow conditions of the original convective current the nozzle width of the replacement jet can be defined as

$$b_{o_T} = 0.178\ \delta \qquad \ldots (2.107)$$

and for laminar flow

$$b_{o_L} = 0.433\ \delta \qquad \ldots (2.108)$$

Initial volume flow, $V_o = b_o\ v_o$, is then

$$V_{o_T} = 0.178\ v_{max}\ \delta \qquad \ldots (2.109)$$

or

$$V_{o_L} = 0.433\ v_{max}\ \delta \qquad \ldots (2.110)$$

and the momentum flux, $M = V_o\ v_o\ \rho$, is

$$M_T = 0.178\ v_{max}^2\ \delta \qquad \ldots (2.111)$$

or

$$M_L = 0.433\ v_{max}^2\ \delta \qquad \ldots (2.112)$$

The mean temperature of the convective stream and the replacement jet are also required to be identical at x = H. The mean temperature of the jet can be expressed as

$$\frac{\overline{\Delta t_s}}{\overline{\Delta t_o}} = \frac{v_{sq_s}}{v_o} \qquad \ldots (2.113)$$

If $\overline{\Delta t_s} = \overline{\Delta t_c}$, $v_{sq_s} = v_{sq_c}$ and $v_o = v_{max}$; by substituting expressions for $\overline{\Delta t_c}$ and v_{sq_c} from Table 2.1 into equation (2.113) the initial temperature differential for turbulent flow becomes

$$\Delta t_{o_T} = 0.354\ \Delta t_w \qquad \ldots (2.114)$$

and for laminar flow

$$\Delta t_{o_L} = 0.52\ \Delta t_w \qquad \ldots (2.115)$$

Once the nozzle width, b_o, and the boundary layer thickness at x = H, b = δ, areknown, the distance of the nozzle from the top edge can be calculated from the angle of spread of the jet, viz.,

$$\tan\alpha = \frac{\delta}{s + l_o} = \frac{b_o}{l_o} \qquad \ldots (2.116)$$

and by rearranging

$$S = \frac{1}{\tan\alpha} \ (\delta - b_o) \qquad \ldots (2.117)$$

If $\tan\alpha = 2.04\ a_i$, for turbulent flow, substituting equation (2.107) for b_o, leads to

$$S_T = 0.4\ \frac{\delta}{a_i} \qquad \ldots (2.118)$$

and for laminar flow, using equation (2.108)

$$S_L = 0.28\ \frac{\delta}{a_i} \qquad \ldots (2.119)$$

The variation of the initial velocity v_o, and width b_o of the replacement jet with the vertical dimension H and surface temperature differential Δt_w of the original convective surface is shown graphically in Fig.2.25. Equation (2.25) was used to calculate the maximum velocity of the convective profile as a check of the Ra numbers. This confirmed that for all values shown in the graph the original convective flow was turbulent. The nozzle width was calculated according to the equation (2.107) and (2.26). The graph shows that the nozzle width b_o is more sensitive to the vertical dimension H of the original convective surface and less to the surface temperature differential, whereas the opposite is true of the initial velocity. Also plotted in the graph is the locus of points where the nozzle Reynolds number is $Re = 2 \times 10^3$. An ambient temperature of 20^oC was used throughout this calculation. As a generalisation, laminar flow in the nozzle of the replacement jet can be expected if the vertical dimensions of the original convective surface is less than 2 metres.

More detailed plots of the variations of nozzle velocity and width for smaller values of H are given in Fig. 2.26 and Fig. 2.27 respectively. Laminar flow on the original convective surface is presumed if $Ra < 5 \times 10^8$. The appropriate equations for the calculation of nozzle width are (2.108) and (2.10) and initial velocity (2.9). Turbulent flow is assumed for $Ra > 10^9$. The discontinuity caused by a change from laminar to turbulent flow on the original convective surface is more evident in the nozzle width than in the initial velocity.

Windows and heating surfaces are the most common components that generate convective currents significant enough to influence room air movement patterns. The effects of walls, especially if well insulated can usually be neglected. It is therefore the convective currents generated by scaled down windows and heating surfaces that will most frequently be replaced by wall jets when attempting to model room air movements. Scale factors of between S = 1 and S = 10, resulting from the application of modelling rules as set our in Part 1, when applied to typical windows (H = 1 to 2 m; $\Delta t_w = 10^oC$) and radiators (H = 0.5 to 1.0 m; $\Delta t_w = 60^oC$) yield a surprisingly narrow range of replacement jet parameters - v_o = 0.3 to 0.9 m/s and b_o = 0.003 to 0.025 m. The nozzle Reynolds numbers indicate that the flow in the nozzle will, as a rule, be laminar. The only exceptions are full scale, or near full scale, replacement jets for radiators. The above values of nozzle width and initial velocity should present no problems in their applications in practice.

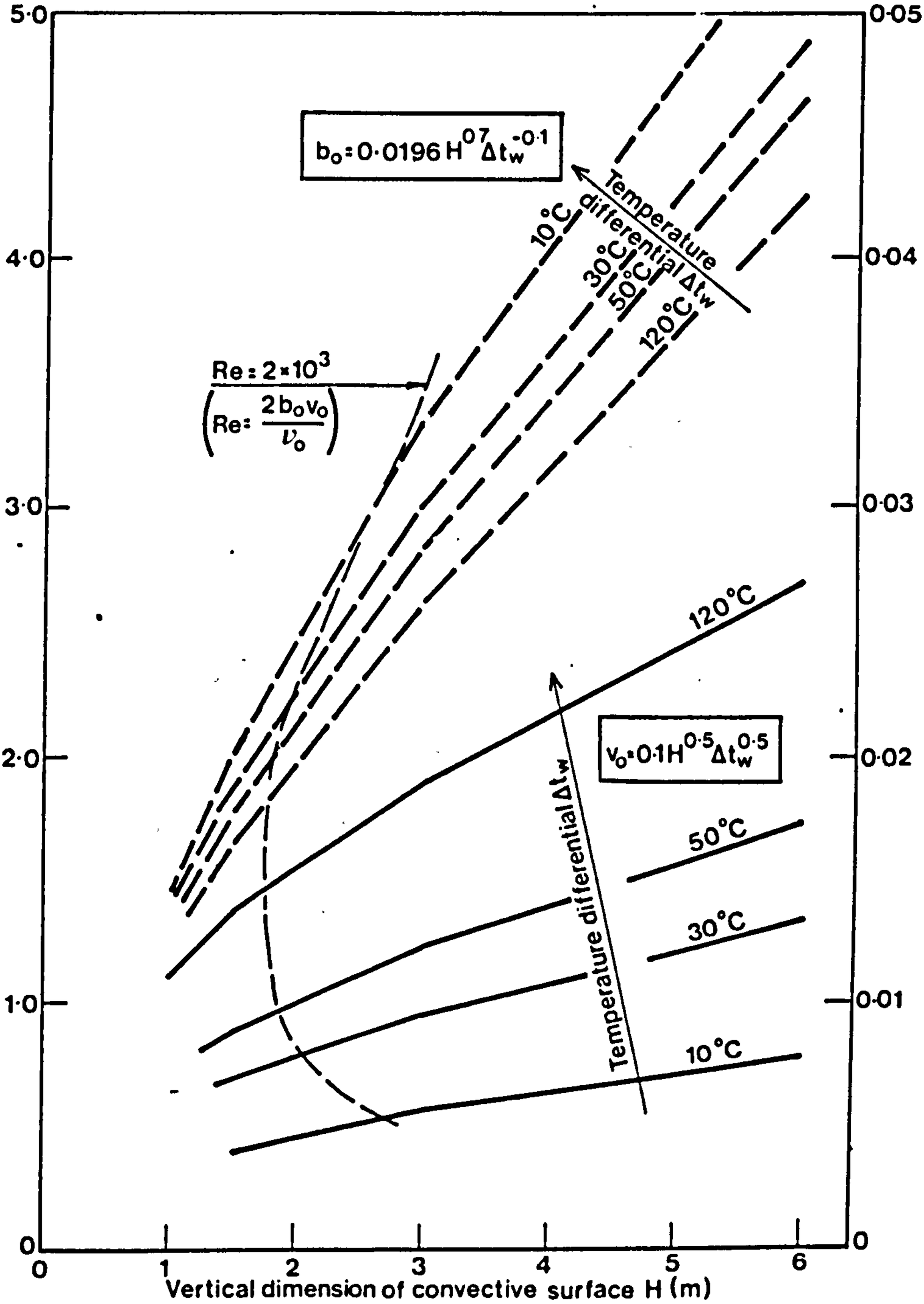

Fig.2.25. VARIATION OF REPLACEMENT JET PARAMETERS v_o AND b_o WITH H AND Δt_w

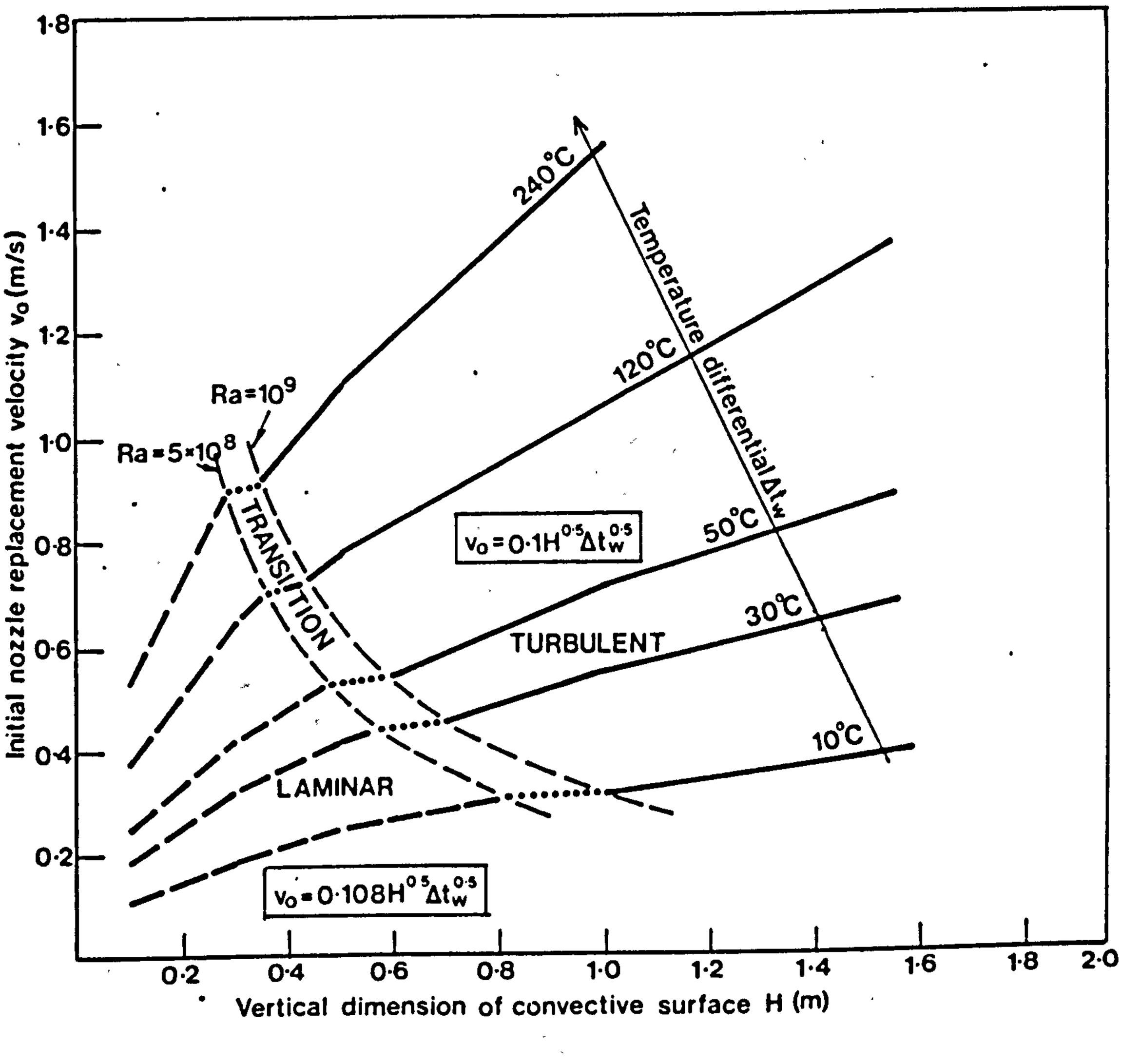

Fig.2.26. VARIATION OF REPLACEMENT JET INITIAL VELOCITY WITH H AND Δt_w (FOR LOWER VALUES OF H)

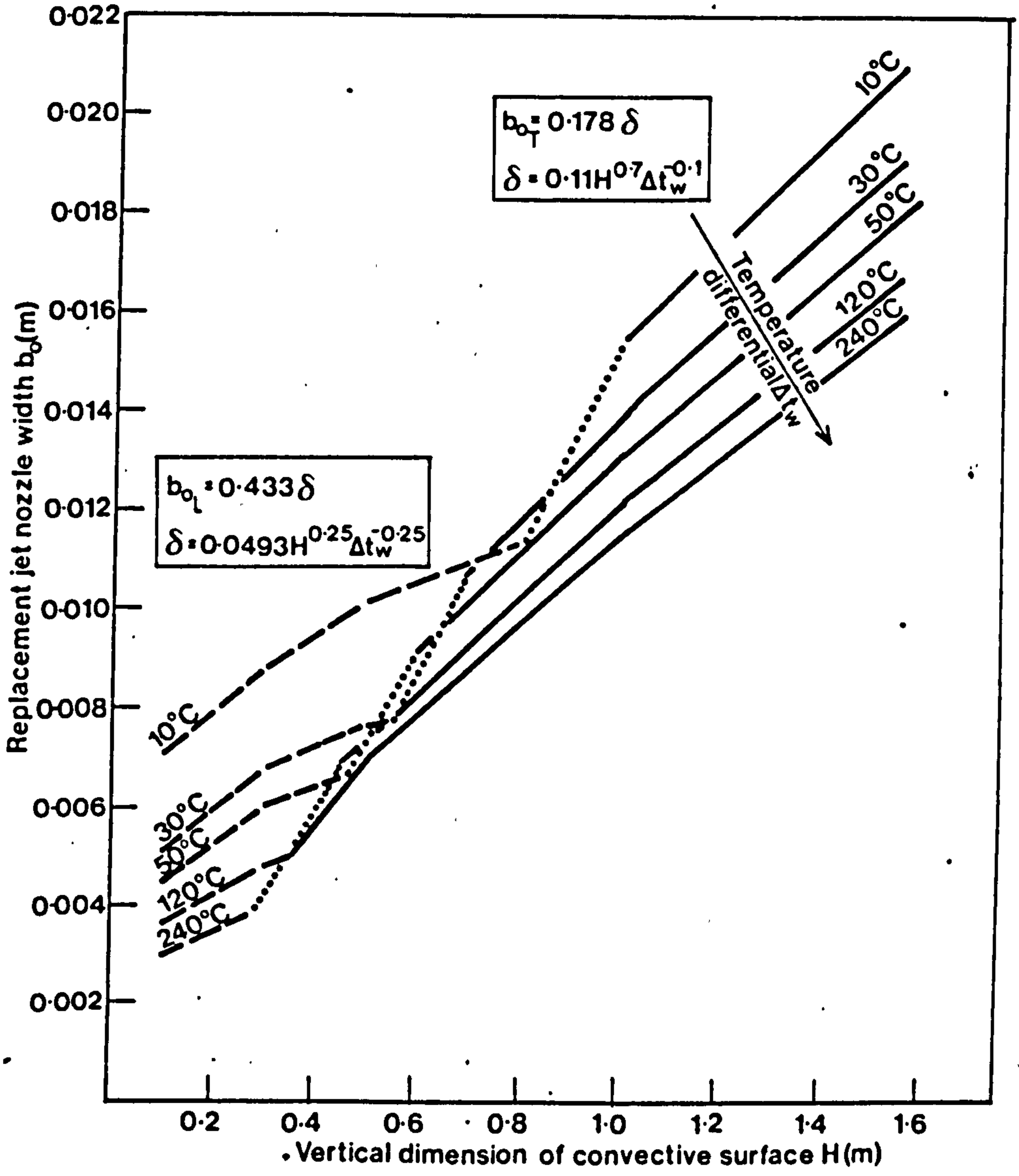

Fig.2.27. VARIATION OF REPLACEMENT JET NOZZLE WIDTH b_o WITH H AND Δt_w (FOR LOWER VALUES OF H)

2.4.2. The effect of buoyancy, room air turbulence and non-uniform initial conditions.

It is exceedingly difficult to predict theoretically the effect of a number of factors that influence convective currents and jets. Three factors considered important are discussed in this chapter. To compensate for their effects the initial replacement jet parameters - b_o, V_o, Δt_o, S - can be varied and it would be convenient to establish empirical or semi-empirical formulae to achieve this.

Buoyancy

Buoyancy affects the replacement jet and, if corrective action were not taken, would distort the required parameters at the replacement cross-section. One of the assumptions made in chapter 2.3.3 was that all energy added by Archimedean forces would be transferred into additional momentum flux of the jet and therefore volume flow would, in essence, remain unaltered. To compensate for the additional momentum, the initial momentum flux of the jet could be reduced. To achieve constant initial volume flow (and therefore also constant heat flux) and reduce momentum flux, the initial velocity has to be lowered and, at the same time, the nozzle width expanded. Strictly, equation (2.66) showsthat nozzle width b_o does affect the relative volume flow at a distance x from the nozzle, but for typical parameters likely to be encountered in replacement jets the influence is insignificant.

A reduction in the initial momentum flux of the replacement jet can be achieved in a number of ways. The available options are illustrated in Fig. 2.28 where the variation of the overall mean square velocity of non-isothermal jets (Δt_o = 20°C) with relative distance S/b_o (i.e. the relative displacement of the nozzle from the edge of the original convective surface) is plotted for three combinations of b_o and v_o giving an identical initial volume flow of V_o = 0.005 m^3/s. The overall mean square velocity was calculated according to equations (2.98), (2.99) and (2.100). For example, if the parameters of the replacement jet are v_o = 1 m/s, b_o = 0.005 m, Δt_o = 20°C and S/b_o = 12, the required mean velocity at x = H, as per equation (67), v_{sq_J} = 0.66 m/s. From Fig. 2.28 it can be seen that the overall mean square velocity, including the buoyancy generated component, is higher v_{sq_T} = 0.71 m/s. The graph shows that a mean square velocity of 0.66 m/s can be achieved by numerous combinations of b_o, v_o and S. If the requirement for identical boundary layer width $\delta = b_s$ (and therefore $V_c = V_s$) at x = H is to be strictly adhered to, any change in the initial parameters of the replacement jet can only be made along the "iso-S" curve. For invariant S, the nozzle parameters in the above example would have to be modified to approximately v_o = 0.9 m/s and b_o = 0.0056m.

As had been mentioned in the previous chapter buoyancy may narrow the angle of spread of the jet and therefore alter the value of the coefficient of turbulence. To compensate, the distance of the nozzle from the edge of the original convective surface would have to be extended. If some variation in the volume flow at x = H is accepted, the graph in Fig. 2.28 indicates that less deformation of the nozzle parameters is necessary if the parameter S is also varied; for example if the value S/b_o is kept constant.

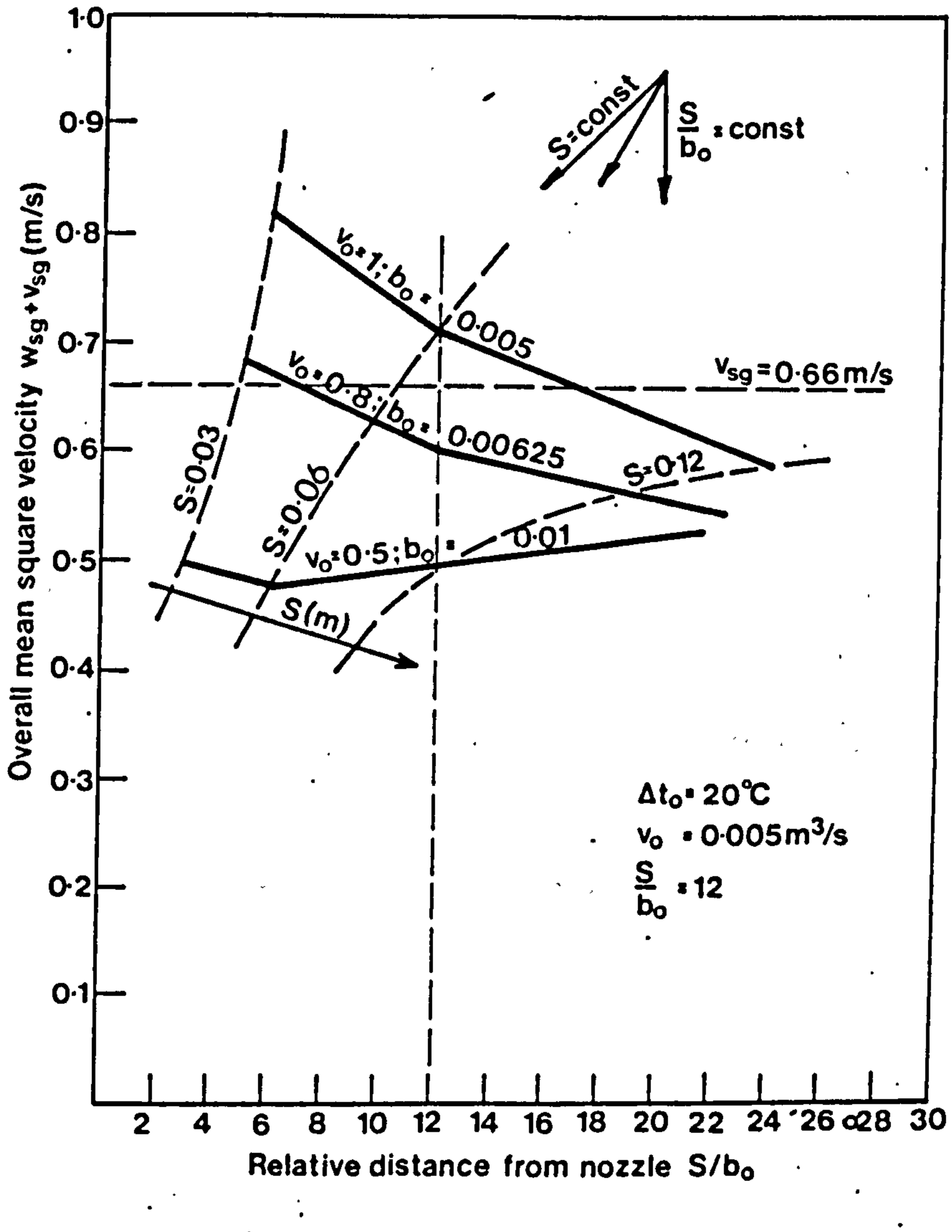

Fig.2.28. VARIATION OF BUOYANCY INFLUENCED OVERALL MEAN SQUARE VELOCITY OF JET WITH RELATIVE DISTANCE FROM NOZZLE

The above discussion had assumed throughout that all additional energy resulting from the action of Archimedean forces would be transformed into additional momentum. However, in practice some of the energy may also be dissipated in additional volume flow and friction on the wall and in the mixing layer and therefore, in many cases,only minimum corrective action may be necessary.

Room air turbulence

Room air turbulence may influence the convective current parameters at the edge of the convective surface. It may also affect the replacement jet but, as H>>S, the influence will not be as prominent.

The convective current parameters (see Fig. 2.24) at x = H when room air turbulence is present (denoted by the subscript e) will differ from the predicted values by the following factors - the maximum velocity of the profile

$$K = \frac{v_e}{v_{max}} \qquad \ldots (2.120)$$

the volume flow

$$K_V = \frac{V_e}{V_c} \qquad \ldots (2.121)$$

the momentum flux

$$K_M = \frac{M_e}{M_c} \qquad \ldots (2.122)$$

and the heat content of the current leaving the convective surface

$$K_Q = \frac{Q_e}{Q_c} \qquad \ldots (2.123)$$

The mean temperature of the current will therefore differ by

$$\frac{\overline{\Delta t_e}}{\Delta t_c} \equiv \frac{K_Q}{K_V} \qquad \ldots (2.124)$$

the mean arithmetic velocity, as defined by equation (2.30)

$$\frac{var_e}{var_c} = Kv \qquad \ldots (2.125)$$

and the mean square velocity, as defined by equation (2.31)

$$\frac{vsq_e}{vsq_c} = \frac{K_M}{K_V} \qquad \ldots (2.126)$$

If it is the purpose of replacement jets to create as near as possible identical flow conditions at x = H, the initial replacement jet parameters have to be adjusted to take into account the effect of room turbulence. The initial nozzle parameters that can be varied

are b_o, Δt_o and V_o. Uniform initial condition, as a first approximation, are assumed, although it is recognised that variation of the initial profile could lead to a more precise solution.

Initial uniform conditions and flow in the initial region demand that the corrected initial velocity v_o' be identical to the maximum velocity of the corrective profile.

$$v_o' = v_e = K\, v_{max} \qquad \ldots (2.127)$$

Substituting equations (2.125), (2.126) and (2.127) into equation (2.106), assuming $^{v}sq_s = {}^{v}sq_c$ and $^{v}ar_s = {}^{v}ar_c$, and rearranging, gives the corrected nozzle width

$$b_o' = \delta\, \frac{^{v}ar_s\ {}^{v}sq_s}{v_o^2}\, \frac{K_M}{K^2} = b_o\, \frac{K_M}{K^2} \qquad \ldots (2.128)$$

With the help of equations (2.127) and (2.128) the corrected initial volume flow can be expressed as

$$V_o' = b_o'\, v_o' = b_o\, v_o\, \frac{K_M}{K} = V_o\, \frac{K_M}{K} \qquad \ldots (2.129)$$

As the heat content of a jet remains constant, the corrected initial heat content assumes the value $Q_o' = Q_e$. Using equations (2.121), (2.123), (2.124) and (2.129) this can be expressed as

$$Q_o' = K_v\, V\, \rho\, \Delta t\, \frac{K_Q}{K_v} = V_o\, \frac{K_M}{K}\, \rho\, \Delta t_o' \qquad \ldots (2.130)$$

Rearranging and substituting the ratio of mean temperatures for the ratio of volume flows (equation (2.54))

$$\Delta t_o' = \Delta t_o\, K\, K_Q\, K_M^{-1} \qquad \ldots (2.131)$$

If the values of all the correction coefficients are less than unity it is probable that the corrected initial velocity will be lower, nozzle width greater, volume flow significantly unchanged and the temperature differential smaller than the original values calculated for non-turbulent room conditions.

Non-uniform initial conditions

As has been previously shown, laminar flow will occur relatively frequently in the nozzle of a replacement jet. Laminar flow, between two parallel walls, by definition, is non-uniform.

When a fluid flow between two parallel walls, see Fig. 2.29, for an element 2 x y x 1 x 1 the pressure loss can be balanced against the sheer stress

$$2\,y\,\Delta p = 2\,\tau\ell \qquad \ldots (2.132)$$

For laminar flow

$$\tau = \mu \frac{dv}{dy} \qquad \ldots (2.133)$$

Substituting equation (2.133) into (2.132), rearranging and integrating from zero to y for the boundary condition of $y = b_o/2$ if $v = 0$, results in

$$v = \frac{1}{2\mu} \frac{\Delta p}{l} \left(\left(\frac{b}{2}\right)^2 - y^2 \right) \qquad \ldots (2.134)$$

The maximum velocity for $y = 0$ is

$$v_{o_{max}} = \frac{1}{2\mu} \frac{\Delta p}{l} \left(\frac{b_o}{2}\right)^2 \qquad \ldots (2.135)$$

The volume flow is defined as

$$V_o = 2 \int_o^{b_o/2} v\, dy \qquad \ldots (2.136)$$

Substituting equation (2.134) and integrating

$$V_o = \frac{2}{3} \frac{1}{\mu} \frac{\Delta p}{l} \left(\frac{b_o}{2}\right)^2 \qquad \ldots (2.137)$$

If the ratio of the mean arithmetic velocity $v_{o_{ar}}$, as defined by equation (2.30), over the maximum profile velocity $v_{o_{max}}$ is denoted as Φ i.e.

$$\Phi = \frac{v_{o_{ar}}}{v_{o_{max}}} = \frac{V_o}{b_o\, v_{o_{max}}} \qquad \ldots (2.138)$$

from equations (2.135) and (2.137) for laminar flow a value of $\Phi = 0.66$ is obtained.

The momentum flux

$$M_o = 2\rho_o \int^{b/2} v^2 dy \qquad \ldots (2.139)$$

and by substitution and integration

$$M_o = \frac{16}{15} \rho \left(\frac{1}{2\mu} \frac{\Delta p}{l} \right)^2 \left(\frac{b}{2}\right)^5 \qquad \ldots (2.140)$$

Similarly, if the ratio of the mean square velocity $v_{o_{sq}}$ (as defined by equation (2.31) to the maximum velocity $v_{o_{max}}$ is

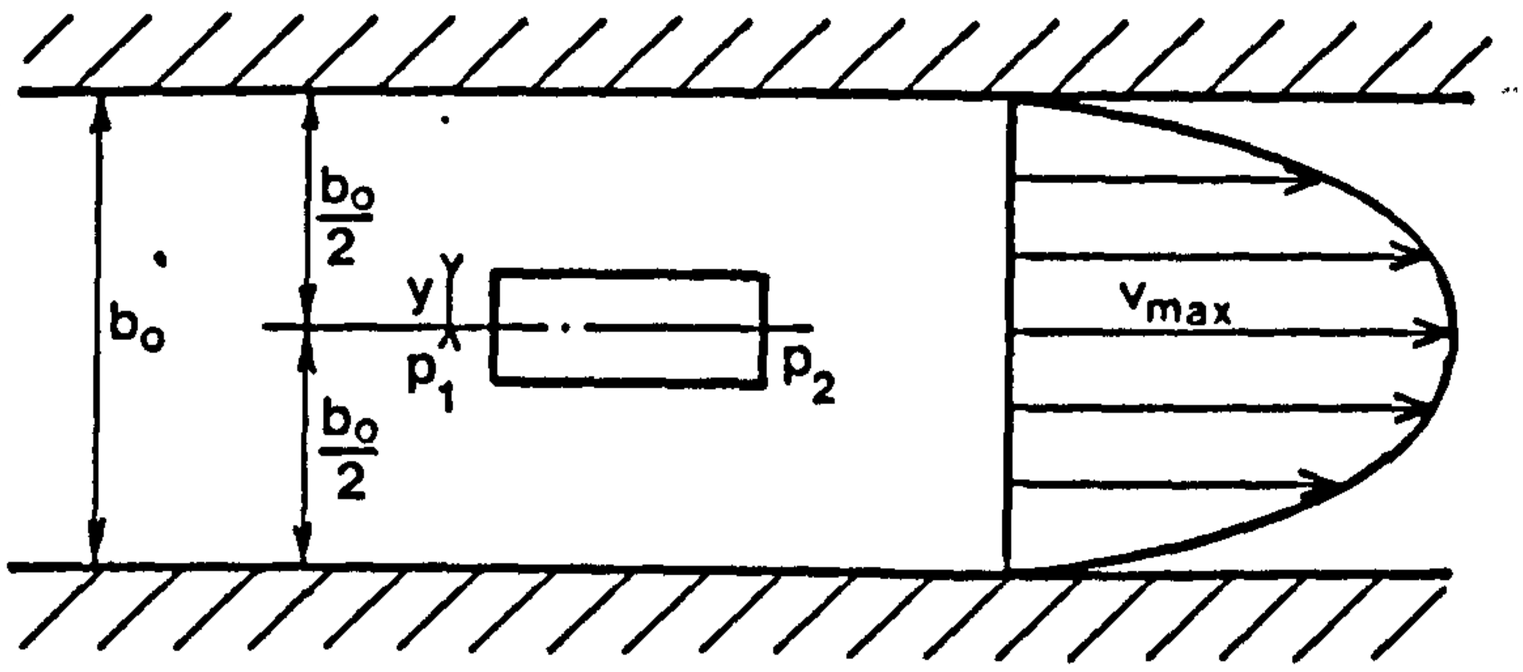

Fig. 2.29. DEFINITION SKETCH OF LAMINAR NOZZLE FLOW

$$\Psi = \frac{v_{o_{sq}}}{v_{o_{max}}} = \frac{M_o}{\rho V_o \, v_{o_{max}}} \qquad \ldots (2.141)$$

the value for laminar flow can be found by substituting equation (2.135), (2.137) and (2.140) to be $\Psi = 0.8$.

The assumption of uniform initial conditions presupposes that the calculated nozzle velocity $v_o = v_{o_{max}} = v_{o_{ar}} = v_{o_{sq}}$. When non-uniform flow,e.g. laminar flow, occurs it is possible to specify only one of the above velocities: the remainder will assume divergent values. If one of the above velocities is to be specified, the obvious choice would be the mean square velocity because, if the initial volume flow V_o also remains unaltered, the identity of the initial momentum flux of the jet is preserved. Therefore

$$v_{o_{sq}} = v_o \qquad \ldots (2.142)$$

and

$$V_o = v_o \, b_o = v_{o_{ar}} \, b_o' \qquad \ldots (2.143)$$

where b_o' is the corrected nozzle width as $v_{o_{ar}} \neq v_o$. Substituting from equations (2.138), (2.141) and (2.142) into equation (2.143), and rearranging, it can be shown that

$$b_o' = \frac{\Psi}{\Phi} \, b_o \qquad \ldots (2.144)$$

For pure laminar flow the value of $\Psi/\Phi = 1.2$. The value Ψ/Φ for turbulent flow or flow in the transition region will be nozzle Reynolds number dependent ($\Psi/\Phi = f\,(Re)$) but will always be less than 1.2.

2.5 CONCLUSIONS

The purpose of Part 2 has been to obtain suitable expressions describing the main parameters of both convective currents and replacement jets in order to facilitate a theoretical calculation of the initial parameters of the replacement jet directly from the convective surface parameters.

Equations describing the main parameters of convective currents were obtained and are summarised in Table 2.1. Appropriate expressions for replacement jets have also been identified and, where not readily available, formulae were deduced theoretically or from existing experimental data. In order to maximise the temperature differential advantage of the concept of replacement jets, the replacement cross-section, i.e. the edge of the original convective surface, should be closest to the nozzle. The closest position that can be considered as practical is where the velocity profile (and temperature profile) is fully developed, that is towards the end of the initial region. For this reason particular attention has been paid to the behaviour of jets in this region. In particular, flow at low Reynolds numbers has been studied and an attempt was made to reconcile theoretically the apparently conflicting data concerning the coefficient of turbulence, the position of the apparent source of the jet and the length of the initial region.

A review of wall jets has shown that for the purposes of calculating replacement jets they can be treated as plane free jets of twice the nozzle width. The only parameter that is significantly affected by the presence of the wall is the length of the initial region. The most appropriate formulae for the calculation of jet parameters are tabulated in Table 2.2.

By definition, the replacement jet is non-isothermal, discharged vertically and the direction of flow of the jet is coincidental with the direction in which buoyancy forces act. Only very limited information is available on the influence of Archimedean forces on the main jet parameters, probably because of the complex nature of the phenomenon. A study based on some simplifying assumptions has shown that for low initial velocities and higher temperature differentials buoyancy forces could modify the main jet parameters. Formulae for the assessment of the effect of buoyancy on replacement jets are given in Table 2.3.

A theoretical calculation of initial replacement jet parameters was then attempted. The replacement jet has to influence room air movements in an identical way as the original convective current and therefore the calculation is based on an identity of momentum flux, maximum velocity and mean temperature at the replacement cross-section. The expressions for the calculation of initial replacement jet parameters (see Fig. 2.24) are tabulated in Table 2.4. When scale factors resulting from the application modelling rules as set out in Part 1 are applied to typical surfaces generating convective currents (windows and radiators), the initial parameters of replacement jets, calculated according to the equations in Table 2.4, yield a surprisingly narrow

range of parameters. The nozzle Reynolds numbers however indicate that the flow in the nozzle will, as a rule, be laminar. A theoretical analysis has shown that if the initial momentum flux and volume flow of the jet as to be retained, the nozzle width has to be widened. The theoretical maximum correction for pure laminar flow was found to be plus 20%: in practice the correction should be much smaller.

To compensate for the effect of buoyancy the initial replacement jet parameters would also have to be altered. A discussion, based on calculations using the approximate formulae in Table 2.3, has shown that there are several strategies available if the requirement for invariant initial volume flow can be relaxed. In practice, especially with room air turbulence present, the non-isothermal jet will not behave strictly as predicted by the equations, i.e. not all additional energy resulting from the action of Archimedean forces will be transformed solely into additional momentum. Some energy may be dissipated in additional volume flow and friction on the wall and in the mixing layer and therefore, in many cases, only minimum corrective action may be necessary.

By definition, room air movements will occur in enclosures having surfaces at unequal temperatures. The introduction of external air, and the corresponding removal of an equal volume of air, will result in even greater levels of room air turbulence. Such turbulence will influence the convective stream flowing over the heated or cooled surface, and therefore the parameters of the current at the replacement cross section, i.e. at the edge of the convective surface, will differ from the predicted values. The replacement jet may also be affected but,as H>>S, the influence of room air turbulence will not be as prominent. To adjust for the impact of room turbulence the initial replacement jet parameters may have to be modified. An analysis of the interdependence of the parameters concerned has shown that probably the corrected initial velocity will be lower, nozzle width greater, volume flow significantly unchanged and the temperature differential smaller than the original values calculated for uniform room conditions.

For the impact of room air turbulence, buoyancy and non-uniform initial conditions to be fully evaluated empirical factors will be required, but, as indicated by the completed analysis, the corrections to values of initial replacement jet parameters calculated according to formulae on Table 2.4 may only be moderate.

TABLE 2.4 Formulae for the calculation of initial replacement jet parameters from convective surface parameters. Uniform initial conditions, minimum room air turbulence and isothermal behaviour of the jet are assumed.

Parameter	Original convective surface flow in		Unit
	Laminar region ($Ra<5 \times 10^5$)	Turbulent region ($Ra>10^9$).	
Initial velocity v_o	v_{max} $0.108H^{0.5} \Delta t_w^{0.5}$	v_{max} $0.1H^{0.5} \Delta tw^{0.5}$	ms^{-1}
Nozzle width b_o	$0.433\ \delta$ $0.0213H^{0.25}\Delta t_w^{-0.25}$	$0.178\ \delta$ $0.0196H^{0.7}\Delta t_w^{0.1}$	m
Distance of nozzle from surface edge S	$0.28\ \frac{\delta}{a_i}$ $\frac{0.0014}{a_i} H^{0.25}\Delta t_w^{-0.25}$	$0.4\ \frac{\delta}{a_i}$ $\frac{0.044}{a_i} H^{0.7}\Delta t_w^{-0.1}$	m
Initial temperature differential Δt_o	$0.52\ \Delta t_w$	$0.354\ \Delta t_w$	^oC
Initial volume flow V_o	$0.433\ v_{max}\ \delta$ $0.0023H^{0.75}\Delta t_w^{0.25}$	$0.178\ v_{max}\ \delta$ $0.00196\ H^{1.2}\Delta t_w^{0.4}$	m^3s^{-1} per m run
Momentum flux M_o	$0.433\ v_{max}^2\ \delta$ $0.000248H^{1.25}\Delta t_w^{0.75}$	$0.178\ v_{max}^2\ \delta$ $0.000196H^{1.7}\Delta t_w^{0.9}$	$kgms^{-2}$ per m run

REFERENCES

1 MÜLLEJANS, H., "Über die Ähnlichkeit der nichtisothermen Strömung und den Wärmübergang in Raümen mit Strahllüftung". Westdeutscherverlag, Köln und Opladen,1966

2 PROBERT, S.D., NEVRALA, D.J., "Modelling of Air Movements in Rooms". J.Mech.Eng.Sci., Vol.19, No.6, 1977, 264-270.

3 NEVRALA, D.J., "Heat Services for Future Housing Part I - The Insulated House Design Requirements". BSE, Vol.45, No.7, 1977, 107 - 117.

4 NEVRALA, D.J., ETHERIDGE, D.W., "Ventilation in Well Insulated Houses". ICHMT Seminar "Heat and Mass Transfer in Buildings" Dubrovnik, Yugoslavia 1977.

5 ETHERIDGE, D.W., NEVRALA, D.J., "Air Infiltration in the U.K. and its Impact on the Thermal Environment" WHO Conference "International Indoor Climate Symposium" Copenhagen, Denmark, 1978.

6 BILLINGTON, N.S., "Air Movement over Hot or Cold Surfaces" HVRA Laboratory Report No. 29, Jan. 1966.

7 CHEESEWRIGHT,R., "Turbulent Natural Convection from a Vertical Plane Surface" Journal of Heat Transfer, Transactions ASME, Paper No.67 - HT-17, Feb. 1968.

8 OSTRACH, S., "An Analysis of Turbulent Free-Convection Heat Transfer about a Flat Plate Parallel to the Direction of the Generating Body Force" NACA TN 2635, 1952.

9 OSTRACH, S., "An Analysis of Laminar Free-Convection Flow and Heat Transfer about a Flat Plate Parallel to the Direction of the Generating Body Force" NACA Report 1111, 1953.

10 ECKERT, E.R.G., JACKSON, T.W., "An Analysis of Turbulent Free-Convection Boundary Layer on Flat Plate" NACA Report 1015, 1951.

11 SCHMIDT, E., BECKMANN, W., "Das Temperatur - und Geschwindig-keitsfeld vor einer Wärme abgebenden senkrechter Platte bei natürlicher Konvektion" Tech. Mech. u Thernodynamik, Bd.1, Nr.10, Okt. 1930, 341-349; cont. Bd.1, Nr.11, Nov.1930, 391-406.

12 ECKERT, E.R.G., "Introduction to the Transfer of Heat and Mass" McGraw-Hill Book Co., Inc., 1950

13 GRIFFITHS, E., DAVIS, A.H., "The Transmission of Heat by Radiation and Convection" British Food Investigation Board, Spec. Report No.9, D.S.I.R., London 1922.

14 WATZINGER,A., JOHNSON, O.G., "Wärmeübertragung von Wasser an Rohrwand bei senkrechter Strömung im Übergangsgebiet zwishen laminarer und turbulenter Strömung". Forsuchung Ingenieurwesen, Bd.10, Helft 4, Juli/August 1939, 182-196.

15 GOLDSTEIN,R.J., ECKERT, E.R.G., "The Steady and Transient Free Convection Boundary Layer on a Uniformly Heated Vertical Plate" Int. Journal of Heat and Mass Transfer, Vol.4, 1960, p.208.

16 BAYLEY, F.J., "An Analysis of Turbulent Free Convection Heat Transfer" Proceedings of I.Mech.E, Vol.169, No.20, 1955, p.361.

17 SZEWCZYK, A.A., "Stability and Transition of the Free Convection Boundary Layer along a Flat Plate" Int. Journal of Heat and Mass Transfer, Vol.5, 1962, p.903.

18 WARNER, C.Y., "Turbulent Natural Convection in Air along a Vertical Flat Plate" Ph.D. Thesis, University of Michigan, Ann Arbor, Mich., Dec.1966.

19 ECKERT, E.R.G., DRAKE, R.M., "Analysis of Heat and Mass Transfer" McGraw-Hill Book Co., Inc., 1972.

20 FANGER, P.O., "Thermal Streaming Along Windows and Cold Walls" Ingeniøren, 19, 580-584, 1964.

21 TOLLMIEN, W., "Berechnung turbulenter Ausbreitungsvorgänge" Z.A.M.M., 6, 1926, 468-478.

22 ABRAMOVICH,G.N., "The Theory of Turbulent Jets" M.I.T. Press, Massachusetts, 1963.

23 GOERTLER, H., "Berechnung von Aufgaben der Freien Turbulens auf Grund eines neuen Naherungsansatzes" Z.A.M.M. 22, 1942, 244-254.

24 GOLDSTEIN, S., "Modern Developments in Fluid Dynamics", Clarendon Press, Oxford, 1938.

25 SCHLICHING, H., "Boundary Layer Theory", McGraw-Hill, New York, 1968.

26 LAUNDER, B.E., SPALDING, D.B., "Mathematical Models of Turbulence" Acadamic Press, London, 1972.

27 REICHARDT, H., "Impuls und Warmeaustauchs in freir Turbulenz" Z.A.M.M., 24, 1944, 268.

28 ABRAMOVICH, G.N., "The Theory of Turbulent Jets", M.I.T. Press, Cambridge, Massachusetts, 1963

29 TAYLOR, G.I., "The Transport of Velocity and Heat through fluids in Turbulent Motion", Proc.R.Soc., 35, 1932, 828.

30 HOWARTH, L., "Concerning the Velocity and Temperature Distribution in Plane and Axially Symmetric Jets", Proc. Cambr. Phil. Soc., 34, 1938, 185.

31 ECKERT, E.R.G., "Heat Transfer in the Constant Property Turbulent Boundary Layer", Intl. J. Heat Mass Transf., 10, 1955.

32 TOWNSEND, A.A., "The Mechanism of Entrainment in Free Turbulent Flows", J. Fluid Mech., 26, 1966,4.

33 TOWNSEND, A.A., "Entrainment and the Structure of Turbulent Flows", J. Fluid Mech., 42, 1970, 1.

34 TOWNSEND, A.A., "The Structure of Turbulent Shear Flow", Cambridge University Press, 1956.

35 FÖRTHMANN, E., "Über turbulenter Strahlausbreitung", Ing. Archiv., V, 1934, 1.

36 ALBERTSON, M.L., DAI, Y.B., JENSEN, R.A., ROUSE, H., "Diffusion of Submerged Jets", Trans. Am. Soc. Civ. Eng., 115, 1950, 639-697.

37 REICHARDT, H., "Gesetzmässigkeiten der freien Turbulenz", VDI - Forschungs., 1951, 414.

38 ZIJNEN, B.G., Van der Hegge, "Measurements of the Velocity Distribution in a Plane Turbulent Jet of Air", Appl.Sci. Res., Sec.A, 7, 1958, 256-276.

39 HESKESTAD, G., "Hot Wire Measurements in a Plane Turbulent Jet", Trans. A.S.M.E., J. Appl.Mech., 1965, 1-14.

40 NEWBERT, G.J., "An Interferometric Study of a Linear Slot Vent", M.Sc. Thesis, Cranfield Institute of Technology, 1973.

41 O'CALLAGHAN, P.W., PROBERT, S.D., NEWBERT, G.J., "Velocity and Temperature Distributions for Cold Air Jets Issuing from Linear Slot Vents into Relatively Warm Air", Journ. Mech. Eng. Sci., Vol.17, No.3, 1975, 139-149.

42 TUVE, G.L., "Air Velocities in Ventilating Jets", Heat. Pip, & Air Cond., 25, 1953, 181-191.

43 SPINAR, B., "Vzduchotechnicka zarizeni" Prace, Prague, 1958.

44 FARQUHARSON, I.M.C, "The Ventilating Air Jet", J.I.H.V.E., 19, 1952, 459.

45 BATURIN, V.V., "Fundamentals of Industrial Ventilation", Pergamon Press, 1972.

46 RAJARATNAM, N., "Turbulent Jets", ElsevierScientific Publishing Co., 1976.

47 TURKUS, B.A., "Otopleniye i Ventilyatsiya", No.5, 1933.

48 NEWMAN, B.G., "The Deflection of Plane Jets by adjacent Boundaries", In. G.V. Lachmann (Editor), Boundary Layer and Flow Control, 2. Pergamon Press, 1961.

49 LIEPMANN, H.W., LAUFER, J., "Investigation of free turbulent mixing", NACA Tech. Note 1257, 1947.

50 WYGNANSKI, I., FIEDLER, H., "The two dimensional mixing region", J. Fluid Mech., 41, 1970, 327-361.

51 FREAN, D.H., BILLINGTON, N.S., "The ventilating air jet", J.I.H.V.E., Dec. 1955, 313-334.

52 PULKRABEK, J., "Vetrani", SNTL, Praha, 1961.

53 ZERBE, J., SELNA, J., "An empirical equation for the coefficient of heat transfer to a flat surface from a plane heated air jet directed tangentically to the surface" NACA, TN 1070, 1946.

54 SIGALLA, A., "Measurements of skin friction in a plane turbulent wall jet", J.A.I.A.A., 8, 1958, 873-877.

55 MYERS, G.E., SCHAUER, J.J., EUSTIS, R.H., "The plane turbulent wall jet. I, Jet development and friction factor." Tech.Rep., 1, Dpt. Mech. Eng., Stanford University, 1961.

56 SCHWARTZ, W.H., COSART, W.P., "The two dimensional turbulent wall jet", J. Fluid Mech., 10, 1961, 481-495.

57 RAJARATNAM, N., SUBRAMAYA, K., "An anotated bibliography of wall jets", Tech. Rep. Dpt. Civil Eng., Univ. of Alberta, Edmonton, 1967.

58 GAUNTER, J.W., LIVINGOOD, J. N.B., HRYCAK, P., "Survey of literature on flow characteristics of a single turbulent jet impinging on a flat plate", NASA, Tn. D-5652, 1970.

59 GLAUERT, M.B., "The Wall Jet", J. Fluid Mech., 1, 1956, 625-643.

60 BAKKE, P., "An experimental investigation of a wall jet", J. Fluid Mech., 2, 1957, 467-472.

61 MATHIEU, J., TAILLAND, A., "Etude d'un jet plan dirigé tangentiellement à une paroi" C.R., Acad. Sci., Paris, 1963, 44-47.

62 VERHOFF, A., "The two dimensional turbulent wall jet with and without external stream", Dep. 626, Princeton Iniv., 1963.

63 GARSTSHORE, I.S., NEWMAN, B.G., "The turbulent wall jet in an arbitary pressure gradient", Aeronaut W., 20, 1969, 25-56.

64 RAJARATNAM, N., SUBRAMANYA, K., "Diffusion of retangular wall jets in wider channels", J. Hydraul. Res., 5, 1967, 281-294.

PART 3 REPLACEMENT OF NATURAL CONVECTIVE CURRENTS BY WALL JETS; EXPERIMENTAL PROCEDURE, RESULTS AND OBSERVATIONS.

CONTENTS

NOTATION

a	coefficient of turbulence	
a'	coefficient of turbulence with buoyancy present	
a_i	coefficient of turbulence in the initial region	
a_i'	coefficient of turbulence in the initial region with buoyancy present	
a_M	coefficient of turbulence in the main region	
b	width of jet	m
b_o	nozzle width	m
b_o'	corrected nozzle width	m
B_M	buoyancy momentum factor $\left(= \frac{V_e}{V_p}\right)$	
B_Q	buoyancy heat flux factor $\left(= \frac{Q_e}{Q_p}\right)$	
B_V	buoyancy volume factor $\left(= \frac{V_e}{V_p}\right)$	
H	vertical dimension of convective surface	m
K	room air turbulence maximum velocity factor $\left(= \frac{v_{max_e}}{v_{max_p}}\right)$	
K_M	room air turbulence momentum factor $\left(= \frac{M_e}{M_p}\right)$	
K_o	nozzle width coefficient $\left(= \frac{K_M}{K^2} \frac{\Psi}{\phi} \frac{K_M + 1 - K_{M(H-S)}}{K_\rho}\right)$	
K_V	room air turbulence volume factor $\left(= \frac{V_e}{V_p}\right)$	
$K_{\frac{}{\Delta t}}$	room air turbulence mean temperature factor $\left(= \frac{\Delta t_e}{\Delta t_p}\right)$	
K_V^*	experimental volume factor $\left(= V_e^*/V_p\right)$	
K_M^*	experimental momentum factor $\left(= M_e^*/M_p\right)$	

K_Q^*	experimental heat flux factor $\left(= Q_e^*/Q_p\right)$	
$K_{\overline{\Delta t}}^*$	experimental mean temperature factor $\left(= \overline{\Delta t_e^*}\ /\overline{\Delta t_p}\right)$	
K_ρ	nozzle momentum buoyancy coefficient $\left(= \frac{M_e}{b_o v_o^2 \rho_o}\right)$	
L_i	length of initial region	m
M	momentum	$kgms^{-2}$ per m run
Pr	Prandtl number	
Q	heat content of flow	W per m run
Ra	Rayleigh number	
Re	Reynolds number	
S	distance of nozzle from replacement cross section	m
S'	distance of nozzle from replacement cross section when buoyancy is neglected	m
t	temperature	^oC
Δt	temperature differential	^oC
u^*	characteristic velocity $\left(= (g\beta\ \Delta t_w\ x)^{0.5}\right)$	ms^{-1}
v	velocity	ms^{-1}
v_m	velocity scale, maximum value of jet velocity profile	ms^{-1}
v^*	characteristic velocity	ms^{-1}
V	volume flow	m^3s^{-1} per m run
w	buoyancy component of velocity	ms^{-1}
x	distance in direction of flow	m
x'	distance in direction of flow when buoyancy is neglected (= x - Δx')	m
Δx'	additional distance travelled due to buoyancy (= x - x')	m
y	transverse distance across flow	m

y_b distance from plate where $v_p = v_a$ m

$y_{0.5}$ length scale, value of y where $v = 0.5v_m$ m

β_o correction coefficient for momentum

δ width of boundary layer m

η dimensionless distance normal to plate
$\left(= \frac{y}{x} Gr^{0.1}\right)$

η dimensionless distance normal to plate
$\left(= \frac{y}{x} \left(\frac{Gr}{4}\right)^{0.25}\right)$

ρ density kgm^{-3}

Φ ratio of mean arithmetic velocity to maximum velocity at the nozzle $\left(= \frac{v_{o_{ar}}}{v_{o_{max}}}\right)$

Ψ ratio of mean square velocity to maximum velocity at the nozzle $\left(= \frac{v_{o\,sq}}{v_{o_{max}}}\right)$

χ ratio of the mean temperature differential to maximum temperature differential at the nozzle $\left(= \frac{\overline{\Delta t_o}}{\Delta t_{max}}\right)$

Subscripts

a denotes experimental values

L laminar

m, max maximum values of flow profile

o with respect to nozzle conditions

p denotes predicted values

T turbulent

w with respect to surface generating convective current

Superscripts

— mean value

' corrected value, with respect to buoyancy

" relates to core values

* with respect to direct measurements

PART 3 REPLACEMENT OF NATURAL CONVECTIVE CURRENTS BY WALL JETS - EXPERIMENTAL PROCEDURE, RESULTS AND OBSERVATIONS

3.1 INTRODUCTION

A new approach to the modelling of room air movements was proposed in Part 1. The method permits the maximum geometric scale factor to be increased whilst the maximum working temperature in the model is limited to acceptable values. The novel ingredient in the proposed method is the replacement of the natural convective currents generated by hot or cold surfaces in full size systems by wall jets in the model. In Part 2 a method by which initial replacement jet parameters can be calculated directly from know convective surface parameters has been evolved. A review of convective currents and jets has shown that there are areas where experimental data are not readily available and which would warrant investigation.

The basic premise of the new approach to modelling of room air movements is that the replacement jet should influence room air movements in the same manner as the original convective current. To be in a position to define the initial parameters of the replacement jet, it is essential to be able to predict the convective current parameters at the edge of the heated or cooled surface. Most observations of convective currents were made under ideal laboratory conditions [1] [2] [3]. Only a limited number of observations of specific applications, such as convective flows from radiators and windows, have been made under less ideal conditions with random laboratory air movements present[4]. Air movements, by definition, will always occur in rooms with surfaces at unequal temperatures and will be augmented by the introduction of external air, whether by mechanical means or by natural infiltration and ventilation. To ascertain the effects of room air turbulence on convective currents under typical conditions it is proposed to investigate convective flows in a test room.

Once it is possible to predict the convective current parameters to a sufficient degree of accuracy, the replacement jet parameters can be calculated according to the expression deduced in Part 2. To validate the theoretically deduced expressions, and any semi-empirical factors that may be necessary, a controlled experiment has to be conducted. The main concern is to conduct the test comparing both natural convection and the replacement wall jet under the same conditions as closely as possible. Because of this requirement, a balance has to be maintained between the desire to conduct the experiment in natural room turbulent conditions and the need for a "standard" environment that would guarantee the repeatibility and comparability of the tests.

It is therefore proposed to conduct two separate experiments. In the first the behaviour of convective currents under naturally turbulent room conditions will be examined to ascertain any need for modification of the theoretically deduced expressions in Part 2. In the second experiment a purpose built test rig enabling a direct comparison of the original convective current and the replacement jet to be made without undue concern for the absolute value of any of the intervening factors will be used.

3.2 EFFECT OF ROOM AIR TURBULENCE ON CONVECTIVE CURRENTS

The effects of room air turbulence, generated by a simulated heated external wall and the compensating cooling air, on a convective current over the surface of a window were studied in a test room.

3.2.1. Test facility

For the experiments a test room representing a typical office located in an office block having one external wall was used. The room was 4.9 m x 3.7 m x 2.75 m high. A plan view is shown in Fig.3.1.

In the end wall representing an external wall, a plate-glass window 2.7 m wide x 1.5 m high was fitted. Outside this wall an insulated compartment accommodated heating or cooling appliances by which the simulated external air temperature could be varied. The test room was enclosed on another two of its sides by a 1.2 m wide enclosed corridor and the floow of the whole structure was suspended 300 mm above the laboratory floor level. The ceiling and the remaining wall of the test room were thermally insulated with expanded polystyrene sheets.

Associated with the test room was an air recirculation and conditioning system. The system included a centrifugal fan, a direct expansion cooling coil connected to refrigeration unit, and an electric heater battery. Regulation of air flow from the fan was achieved with a by-pass system. After the cooling battery the air divided, so that a proportion returned to the fan inlet and the remainder was supplied to the room. From the heater battery the main supply was ducted below the floor and across the diagonal of the room and in this straight section a venturi-type flowmeter, constructed in accordance with BS 1042, was located. The supply system was terminated by a length of flexible ducting connected to the supply opening into the room. A return air aperture was permanently located just above floor level in the centre of the internal end wall. The air recirculation system also included a vent, located in the by-pass circuit, to ensure that the room remained at or only slightly above atmospheric pressure.

Since an on-off thermostat control of the refrigeration system would not give a sufficiently close control of the temperature of the supply air to the room, the refrigeration system was operated continuously and the supply air was reheated to the required temperature by means of the heater battery, the output of which was much more finely controlled. With this arrangement control of the supply air temperature over the range of 10°C to 40°C to within $\pm$ 0.25°C was found possible.

Fan heaters located in the insulating compartment were used to provide a heat load through the external wall of the test room.

3.2.2. Instrumentation

The temperatures of the internal surfaces of the room were measured by thermocouples and displayed on a multi-channel chart recorder for

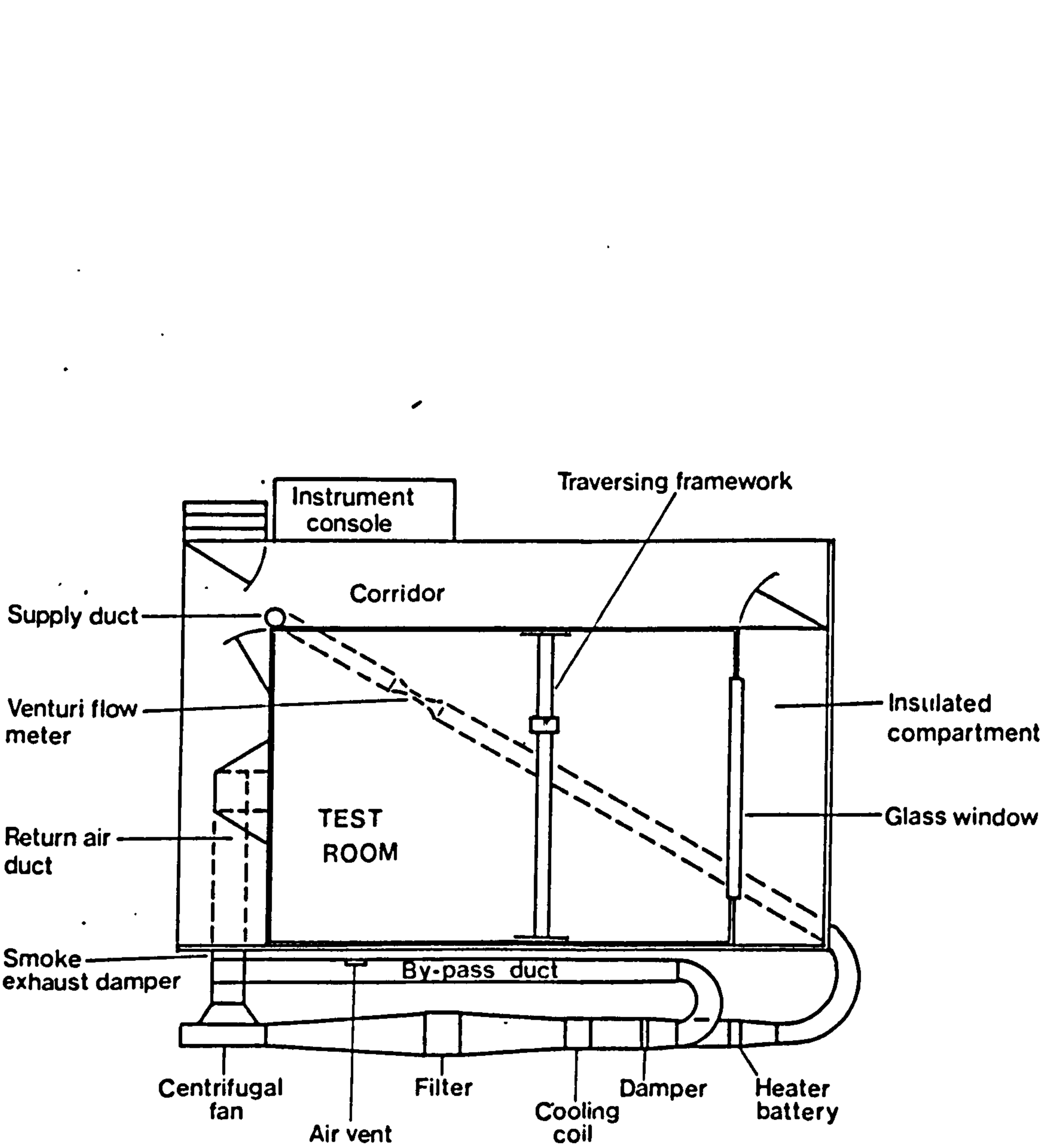

Fig. 3.1. PLAN VIEW OF TEST ROOM

monitoring purposes. Other temperatures similarly recorded included the cooling coil air-temperatures, the room air discharge temperature and laboratory ambient temperature.

An inclined manometer was used in association with the venturi-meter for the measurement of the supply air flow. Air temperatures and speeds within the room were measured by means of thermocouples and anemometers mounted in vertical alignment on a supporting trolley. This in turn was supported on a traversing frame work which enabled manual adjustment of the position of the instruments throughout the room. This positional adjustment was made by means of a pulley system operated from outside the test room. The supporting and traversing arrangement is shown on Fig. 3.2.

The thermocouples were of the chromel-constantan type and the anemometers were heated-thermocouple units.

The operating principle of the heated-thermocouple anemometer is based on the generation of a constant rate of heat at one junction of a thermocouple while the other junction remains at the temperature of the air stream. With both the heated and unheated junctions exposed to an air stream, the difference in the temperatures at the junctions generates an e.m.f. The temperature at the heated junction varies with air speed due to variation in convective heat loss and by suitable interpretation and proper calibration, the generated e.m.f. serves as a measure of the air speed.

Fig.3.3 illustrates the constructional details of the anemometer. The sensing head consists of a manganin-constantan thermocouple with 3.2 mm diameter phosphor-junction and bonded in position. Wound around one of the spheres is a length of 42 S.W.G. manganin wire which, supplied with a constant current, acts as a heater element. Manganin was used because of its very low temperature coefficient of resistance. The sensing head assembly is supported by a manganin wire frame which also conducts the e.m.f. signal from the thermocouple.

While it is the convective heat loss from the heated sphere that is related to air speed, heat loss will also take place by conduction and radiation. To minimise these other losses, relatively long wires of small cross-sectional area have been used in the connection to the heated sphere which was designed to operate at a temperature only some 17°C above the unheated junction.

These instruments, six thermocouples and eleven anemometers, were connected to a data logger, thus enabling sequential scanning of the milli-volt signal from each instrument and the recording of the data on punched tape.

3.2.3 Test procedure

The test condition required the window surface temperature to be 20°C higher than the ambient room temperature, i.e. $\Delta t_w = t_w - t_a = 20°C$. This was accomplished by heating the insulated compartment, see Fig. 3.1 with electric convectors and by supplying cooling air to the test room. To ensure even window surface temperatures, the air inside the insulated compartment was circulated by auxiliary fans. To achieve an even window

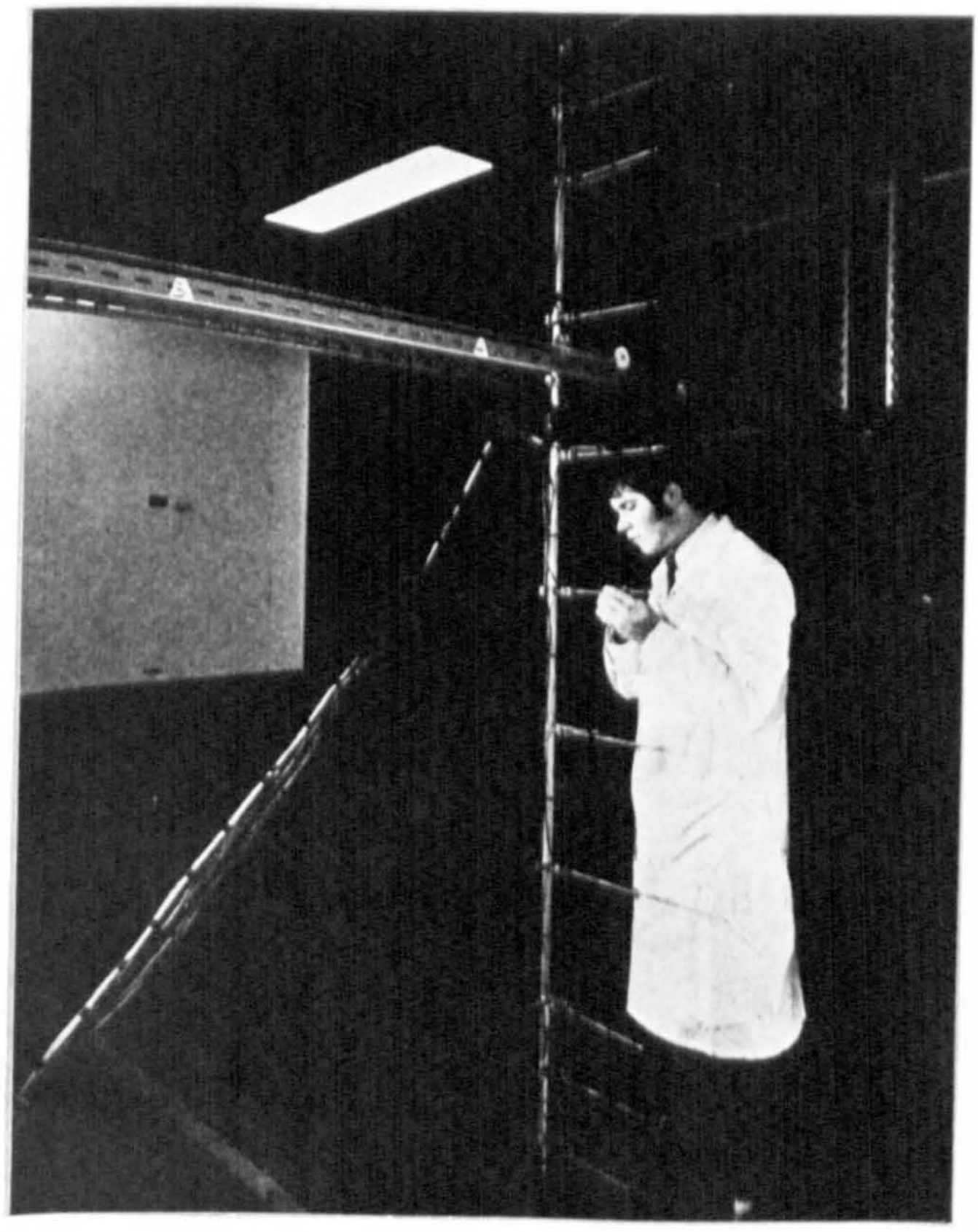

Fig. 3.2. INTERIOR OF TEST ROOM AND INSTRUMENTS

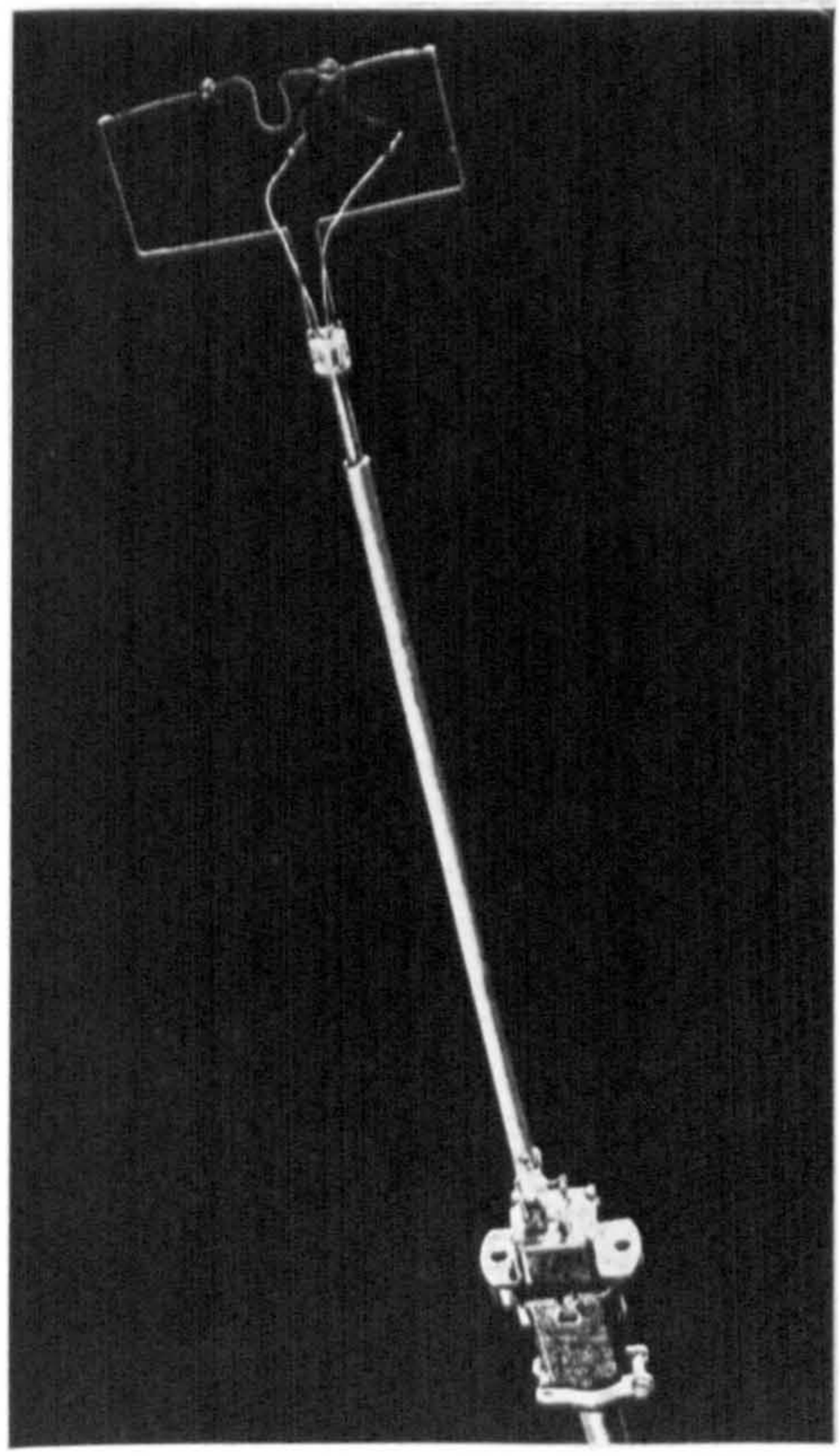

Fig. 3.3. ANEMOMETER SENSING HEAD

surface temperature the surface and ambient air temperatures were constantly monitored; the maximum deviation recorded during the test was 0.4°C. After the test conditions had been established they were maintained for a stabilisation period of at least two hours prior to the commencement of measurements.

The vertical section through the testroom and the insulated compartment, see Fig. 3.4., shows the height at which the velocity profile of the convective current was measured in detail, i.e. at a height of 1.379 m from the bottom of the window (which corresponds to position 10 on the measuring pole).

3.2.4. Results and observations

The velocity profile of a convective current influenced by the presence of room turbulence was measured at a height of 1379 mm from the bottom of a surface (window) at a temperature 20°C higher than the ambient, i.e. $\Delta t_w = 20^oC$. A flow Rayleigh number of $Ra = 5 \times 10^9$ suggests that the flow could be in the turbulent region. The observed velocity profile is shown in Fig. 3.5. Also plotted in the graph is the theoretical velocity profile calculated according to (see also equation 2.20 in Part 2).

$$v = v^* \left(\frac{y}{\delta}\right)^{\frac{1}{7}} \left(1 - \frac{y}{\delta}\right)^4 \qquad \ldots (3.1)$$

where v* can be expressed as (see Table 2.1, Part 2).

$$v^* = 0.187 \times {}^{0.5} \Delta t_w{}^{0.5} \qquad \ldots (3.2)$$

The vertical dimension was x = 1.379 m and the temperature differential $\Delta t_w = 20^oC$.

The graph is Fig.3.5 shows that the measured maximum velocity is probably somewhat lower than predicted. It is unfortunate that because of the physical size of the anemometer sensing head, that velocities at points closer to the surface could not be measured. Observations reported by Billington[4] also indicate that random air movements in the laboratory interfered with the development of the boundary layer flow over a hot surface and probably prevented the theoretical maximum velocity being reached. The boundary layer thickness cannot be defined by the condition v = 0. Good agreement with the predicted value of $\delta = 0.102$ m (calculated according to equation 2.26, Part 2) is reached when the boundary layer thickness is re-defined by $v = v_a = 0.125$ m/s, i.e. when the convective flow velocity is equal to the mean ambient velocity in the room.

In general, relatively good agreement exists between the predicted and measured velocities for the inner part, or the "core" of the convective current. The "core" can approximately be defined by a distance from the heated surface y_b where the predicted velocity is equal to the mean ambient velocity v_a, The outer part of the measured velocity profile, where intensive entrainment ensues, is characterised by higher than predicted velocities, the difference being approximately equal to the value of v_a. The measured volume flow was found to be

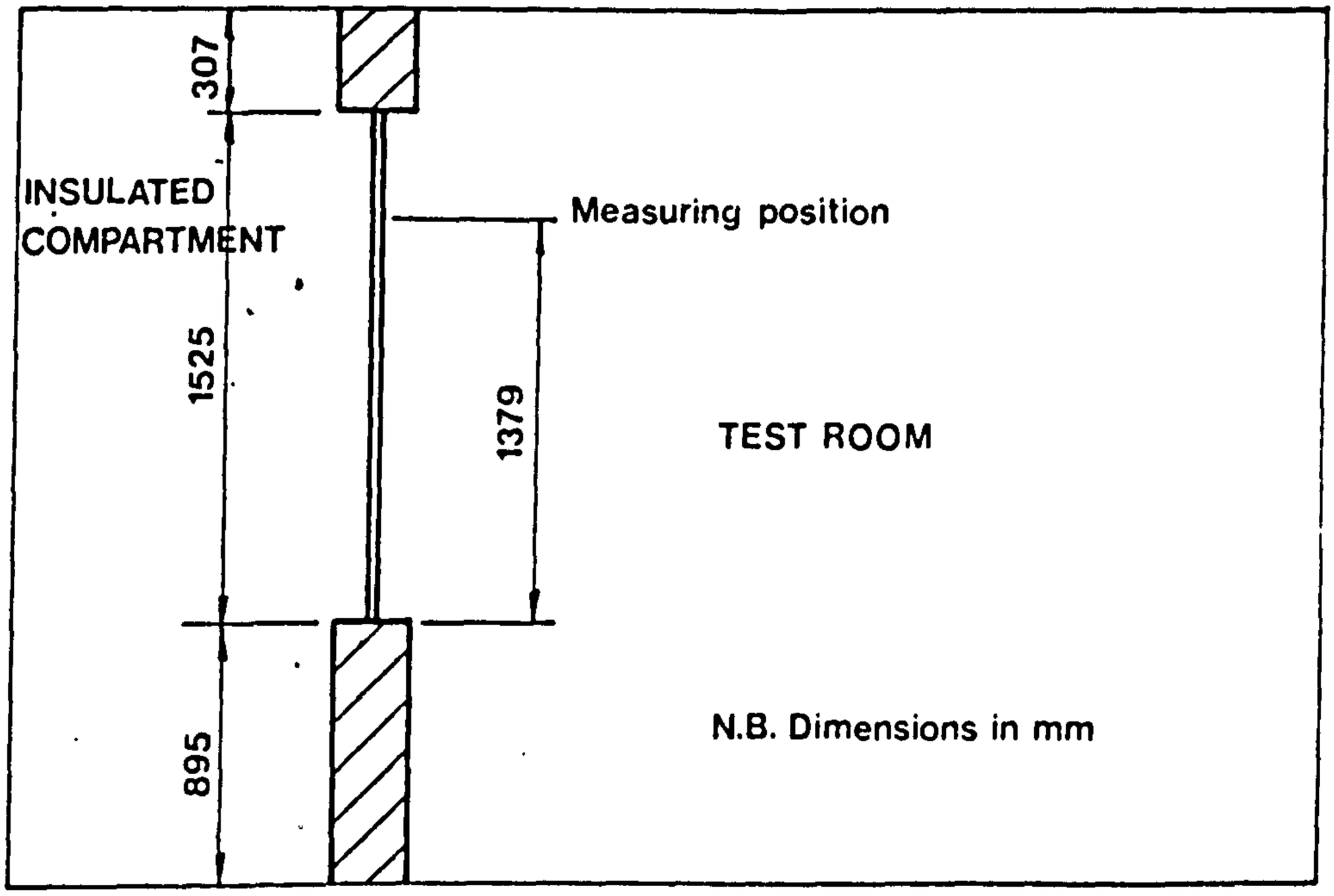

Fig. 3.4. SECTION OF TEST ROOM

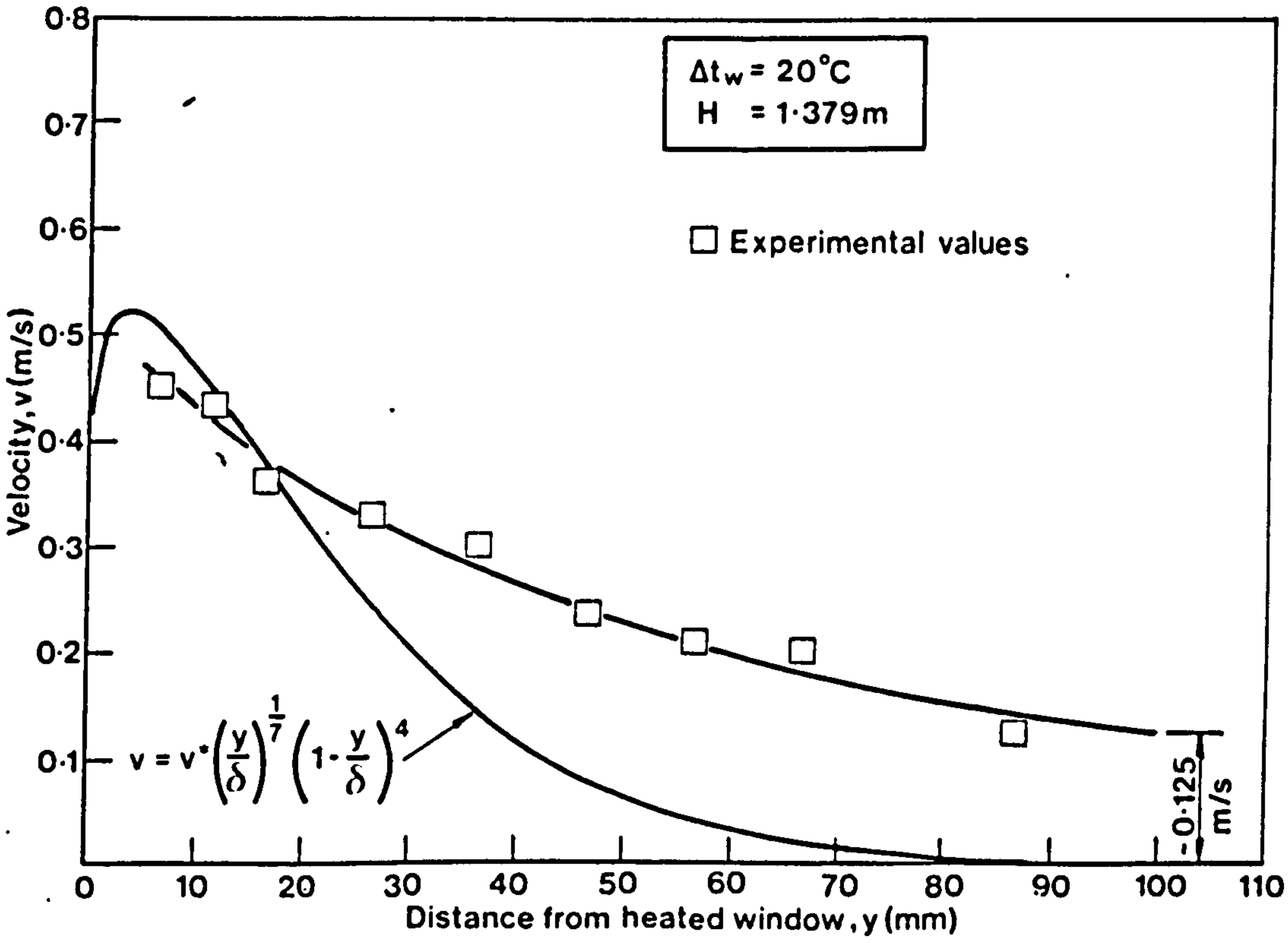

Fig.3.5. VELOCITY DISTRIBUTION ACROSS A CONVECTIVE STREAM FROM A HEATED WINDOW

V_e^* = 0.0224 m^3/s per m run and the momentum flux M_e^* = 0.00683 ρ kgm/s^2. The corresponding predicted values, as calculated from expressions in Table 2.1, are V_p = 0.0142 m^3/s and M_p = 0.00522 ρ kgm/s^2. The measured volume flow, as expected, shows a greater divergence from the predicted value ($K_V^* = V_e^*/V_p$ = 1.58) than momentum flux ($K_M^* = M_e^*/M_p$ = 1.31). In contrast with the high values of K_V^* and K_M^*, the maximum velocity factor shows the opposite trend, $K = {}^{V}max_e/{}^{V}max_p$ = 0.82.

3.2.5. Discussion

The discrepancy between predicted and measured values can be ascribed to two factors. The first, obvious, factor is the influence of room air turbulence on the convective current. The second is in the interpretation of the meaning of the measured values. Tacitly, it had been assumed that, because of the thermal inertia of the velocity sensor, the measured velocity represented the time average velocity of a turbulent flow parallel with the plate. This is probably not so, especially in the outer part of the velocity profile. For example the ambient air velocity reading cannot be interpreted as signifying that the mass of ambient air is moving parallel to the plate. The reading is the result of random air movements in all three dimensions.

More recent studies of the structure of turbulent sheer flows[5] have shown that the mean flow is controlled by large, organised structures - coherent eddies - which are not affected by small scale turbulence at even higher values of Reynolds number. These vortices move at nearly constant speed, which is approximately the average of the velocities of the two streams surrounding the mixing layer. There is evidence[6] that interface convolutions on pictures of wakes are the outer edges of large vortices and it is these spinning vortices that ingest the non-turbulent fluid into the wake. Similarly, the entrainment process associated with convective currents could also be the result of an engulfing action of large coherent vortices. The ambient air is drawn in between vortices and ingested into the convective current where it is made turbulent and digested by the action of the smaller eddies. If the above theory is accepted, the velocity measurements in the outer part of a convective current made by an omni-directional time average sensor cannot be treated as time average values of a flow parallel with the convective surface. The reading would be a time average of the movement of the fluid surrounding the sensor in all three dimensions as there is evidence[5] that the breakdown of vortices in mixing layers where the velocity of one layer is zero is three dimensional. Room air turbulence in the outer part of a convective current will, without doubt, also influence the reading of the velocity sensor.

Without resort to a complex, time consuming and costly study, which would be outside the direct scope of this project, it is not possible to analyse the phenomenon in great detail. The aim of the following discussion is limited to ascertaining the influence of room turbulence on convective current parameters at the edge of a heated or cooled surface so that any variation can be taken into account when replacement jet parameters are calculated. What is most important is the influence a convective current, or the replacement jet, will have on the general, or "macro", room air movement. Whereas it is the "core"

of the current that will influence the "macro" room air movement, the influence of the outer part, where primary ingestion of the ambient fluid takes place, will only be local. It is therefore desirable to define the two parts of a convective current, if only approximately, and ascribe a more appropriate value to the velocity measurement in the outer part.

In the previous chapter, based on the fit of measurement to predicted velocities in Fig. 3.5, the "core" was defined by a distance from the plate y_b where the predicted velocity is equal to the mean ambient velocity v_a. Fig. 3.5 also shows that in the outer part the difference between the measured and predicted velocity profile is approximately equal to the ambient velocity v_a. The two above statements can be combined into a new definition of the boundary between the "core" and the outer region (see Fig. 3.6) - a distance from the convective surface y_b where the measured velocity is equal to twice the mean ambient velocity.

Such a criterion, if applied to the experimental data shown in Fig. 3.5, would result in the "core" being approximately half the boundary layer width. This would seem reasonable as it has been shown[5] that non-turbulent fluid penetrates deep within the mixing region, depending on flow conditions, even over half the distance. Recalculating the basic parameters for the "core", results in $K''_v = 0.88$ and $K''_M = 0.89$. If it is the "macro" impact that is considered important, the "core" values are sufficiently close to theoretical values as to require, as a first approximation, no corrective action to be taken.

In Fig. 3.7 the present data and the experimental results of Cheesewright[3] and Griffiths and Davis[1] are plotted in dimensionless co-ordinates. Also shown is the theoretical velocity profile calculated according to equation (3.1) for the measured temperature differentials. The shape of the velocity profile obtained under turbulent room conditions compares well with the previous laboratory results, but the profile is displaced along the vertical axis by a value approximately equal to the ambient velocity. The discrepancy in the outer part of the velocity profile can be ascribed to the effects of room air turbulence and to the doubts in the interpretation of the measured velocities.

The discrepancy in the inner part of the velocity profile may be due to the difference in Rayleigh numbers. The Rayleigh numbers of the Cheesewright experiments were high ($Ra = 2.2 - 6.2 \times 10^{10}$) and therefore the flow was certainly in the fully developed turbulent region: whereas the Rayleigh number of the present experimental data ($Ra = 5 \times 10^9$) is close to values associated with flow in the transitional region. For comparison, the present data and the experimental results of Schmidt and Beckmann[2] for the large plate (height 0.5 m) are plotted in Fig. 3.8. In the Schmidt and Beckmann experiment, the flow was laminar; the maximum Rayleigh number being $Ra = 2.3 \times 10^8$. Also plotted in Fig. 3.8 are the theoretical predictions of Ostrach[7] for laminar flow at $Pr = 0.72$ and the velocity profile according to equation (3.1). The present measurements agree with those of Schmidt and Beckamnn (and also with the theoretical predictions of Ostrach)up to a value of $n = 2.5$, but in the outer part the agreement between laminar experimental results and theoretical predictions and the present data is, as expected, poor because of the marked difference in laminar and turbulent boundary layer width.

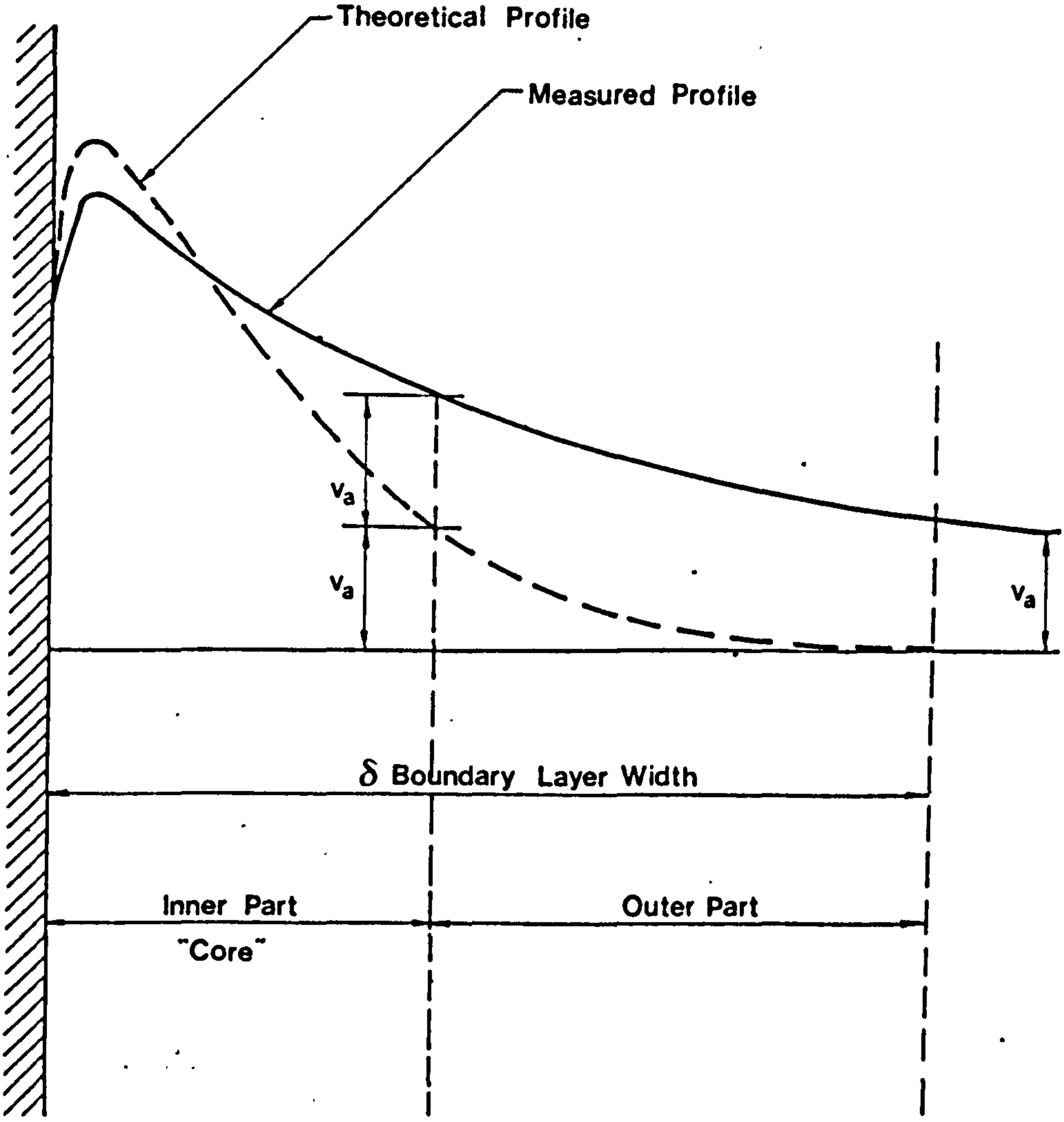

Fig.3.6. DEFINITION SKETCH OF THE CORE AND THE OUTER PART OF A CONVECTIVE STREAM

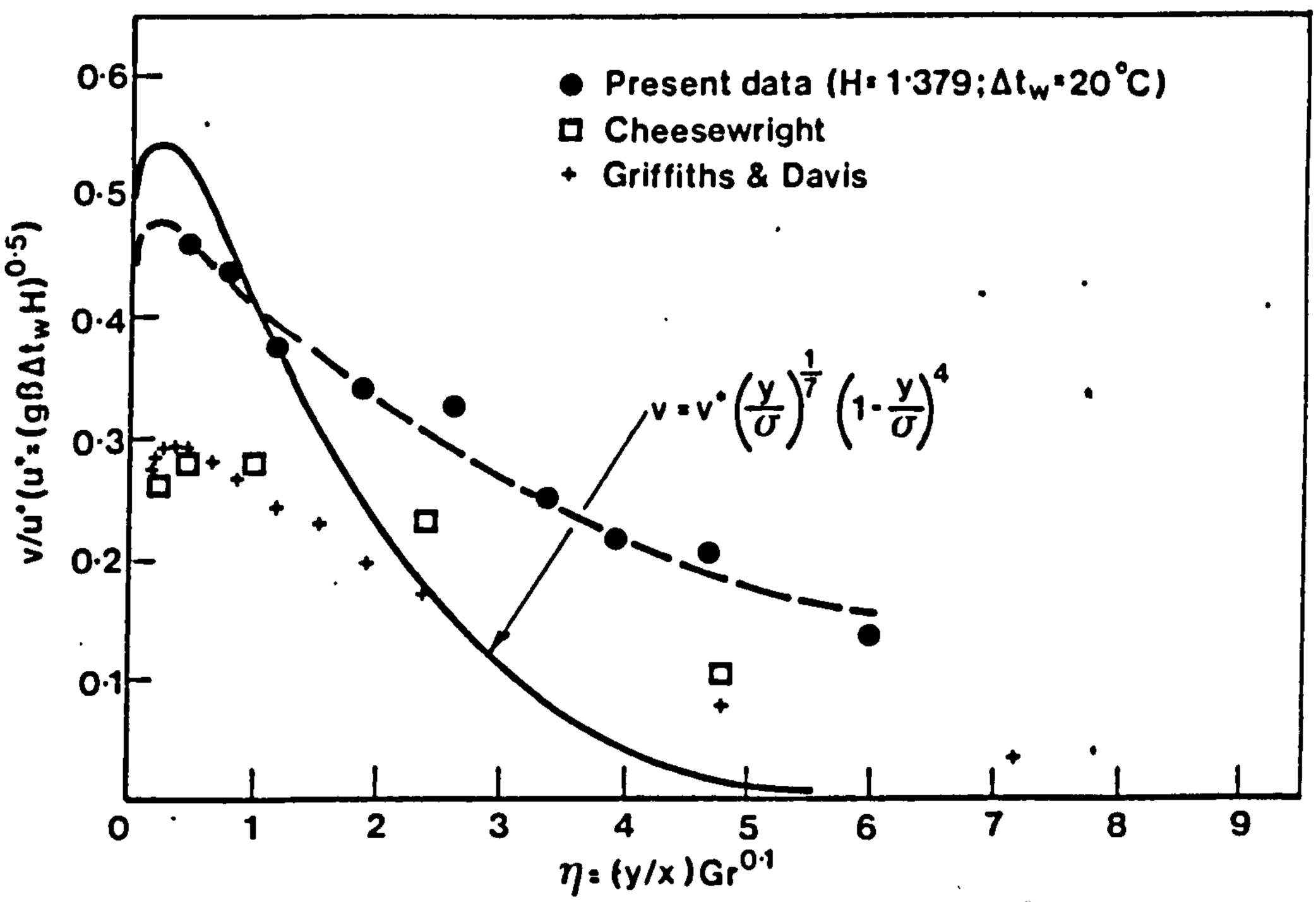

Fig.3.7. NON-DIMENSIONAL VELOCITY DISTRIBUTION: COMPARISON OF HEATED WINDOW RESULTS WITH OTHER TURBULENT EXPERIMENTAL DATA AND PREDICTIONS

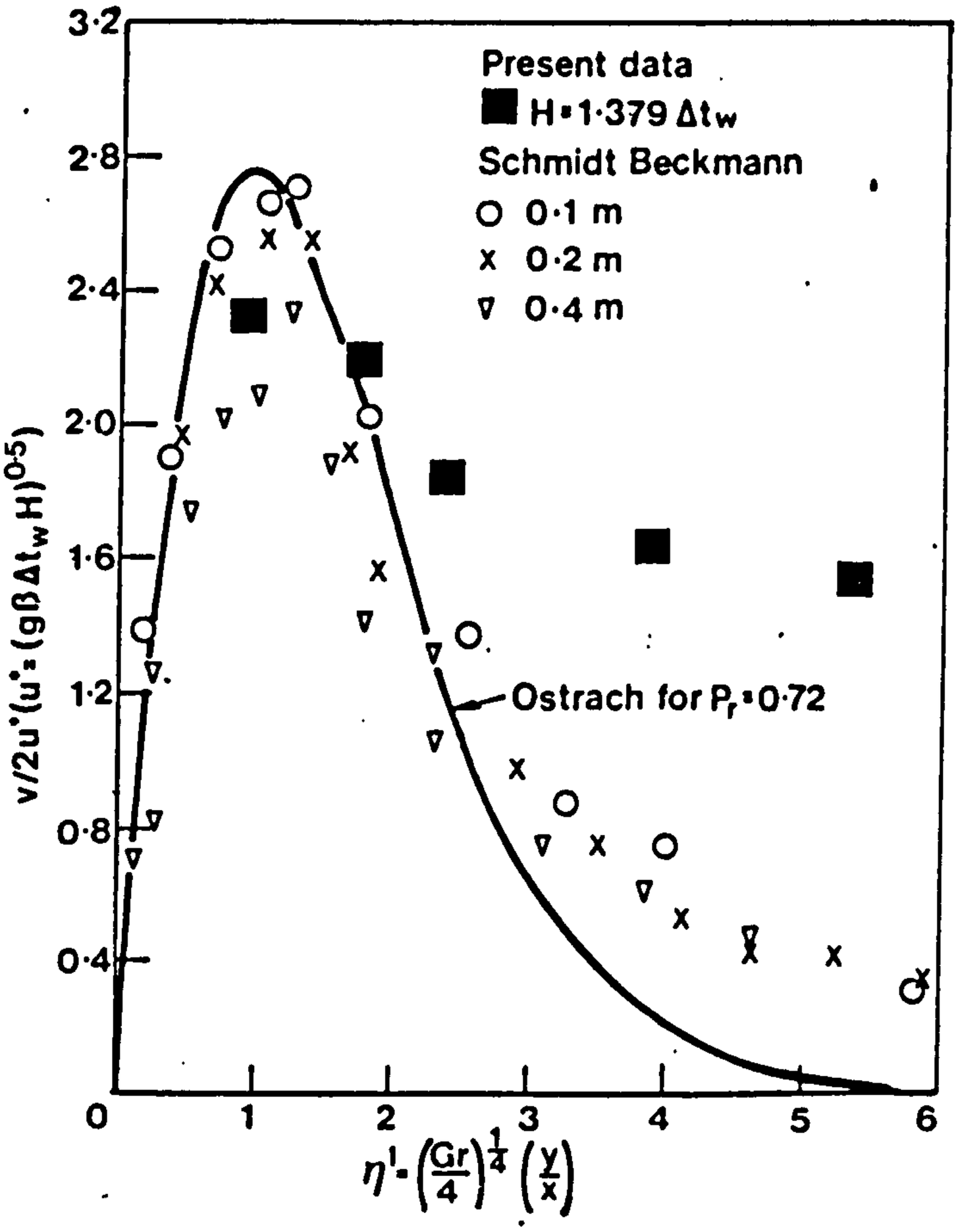

Fig.3.8. NON-DIMENSIONAL VELOCITY DISTRIBUTION: COMPARISON OF HEATED WINDOW RESULTS WITH SCHMIDT AND BECKMAN LAMINAR FLOW RESULTS AND THE OSTRACH PREDICTION

The above comparisons confirm that if it is the "macro" impact of the convective current that is of importance, the theoretical predictions as formulated in Part 2 should provide a sufficiently accurate forecast of the "core" parameters both under turbulent room air conditions and low Rayleigh numbers.

3.3 REPLACEMENT OF CONVECTIVE CURRENTS BY WALL JETS

The purpose of this series of experiments is to validate theoretical expressions for the calculation of replacement jets (as proposed in Part 2) by directly replacing convective currents by wall jets under as near as possible identical ambient conditions. In order to achieve direct compatability of the two phenomena, a purpose built rig was designed and built.

3.3.1. Experimental Facility

The experimental rig was designed specifically to ensure that both the convective current and the replacement wall jet were measured by the same instrumentation, in the same positions and, as far as possible, under identical ambient conditions. The rig was therefore designed to facilitate an exchange of the heated surface for a vertical plane (board) over which the replacement jet could be tested. For reasons of economy, it was decided to use a heated surface instead of a cooled surface to generate the convective current. A requirement that one person should be able to operate the rig as well as financial limitations were factors that influenced the design of the rig.

As the rig was situated in an open laboratory, an effort was made to protect the test area from any excessive air movement. The photograph in Fig. 3.9 is an overall view of the test rig. The heated surface consisted of four electric panel heaters (0.56 x 0.39 m) mounted on a metal frame. The heated surface height and position were chosen to represent a window in a typical office, similar in dimensions to a vertical section through the test room (Fig. 3.4). The area above and below was covered by flush mounted boards and the ceiling was extended 0.3 m from the surface. The side screens were transparent (being constructed of perspex) to enable close observation and the photographic probe was mounted on a sturdy traversing rig, see Fig. 3.10, that enabled movement along both axes and an adjustment of angle.

The temperature of each panel (maximum output 330W) was controlled individually by variable auto transformers. The surface was tested for uniformity of temperature, which was eventually achieved by the application of insulation to the back of the panels. A schematic arrangement of the rig is shown in Fig. 3.11. The surface temperature was sensed by surface mounted thermojunctions and continuously monitored by a multi-channel chart recorder. The air temperature and velocity readings were monitored on a digital vottmeter.

When replacement jets were studied, the heating panels were replaced by a board and provision was made for heated air from an adustable width slot, moveable in the vertical direction, to be discharged vertically upwards over the board, as illustrated in Fig. 3.12. An overall schematic arrangement is shown in Fig. 3.13. Pressurised air from a centrifugal fan was discharged into a plenum box divided by a screen. Coarse volume control was achieved by opening a bleed valve on top of the plenum box; fine adjustment was by means of a three-way valve as shown in Fig. 3.14. This arrangement guaranteed the elimination of pulsations in the flow by allowing the fan to operate in a stable region

Fig. 3.9. VIEW OF CONVECTIVE CURRENT AND REPLACEMENT JET EXPERIMENTAL RIG

Fig. 3. 10. VIEW OF TRAVERSING RIG AND HEATED PANELS

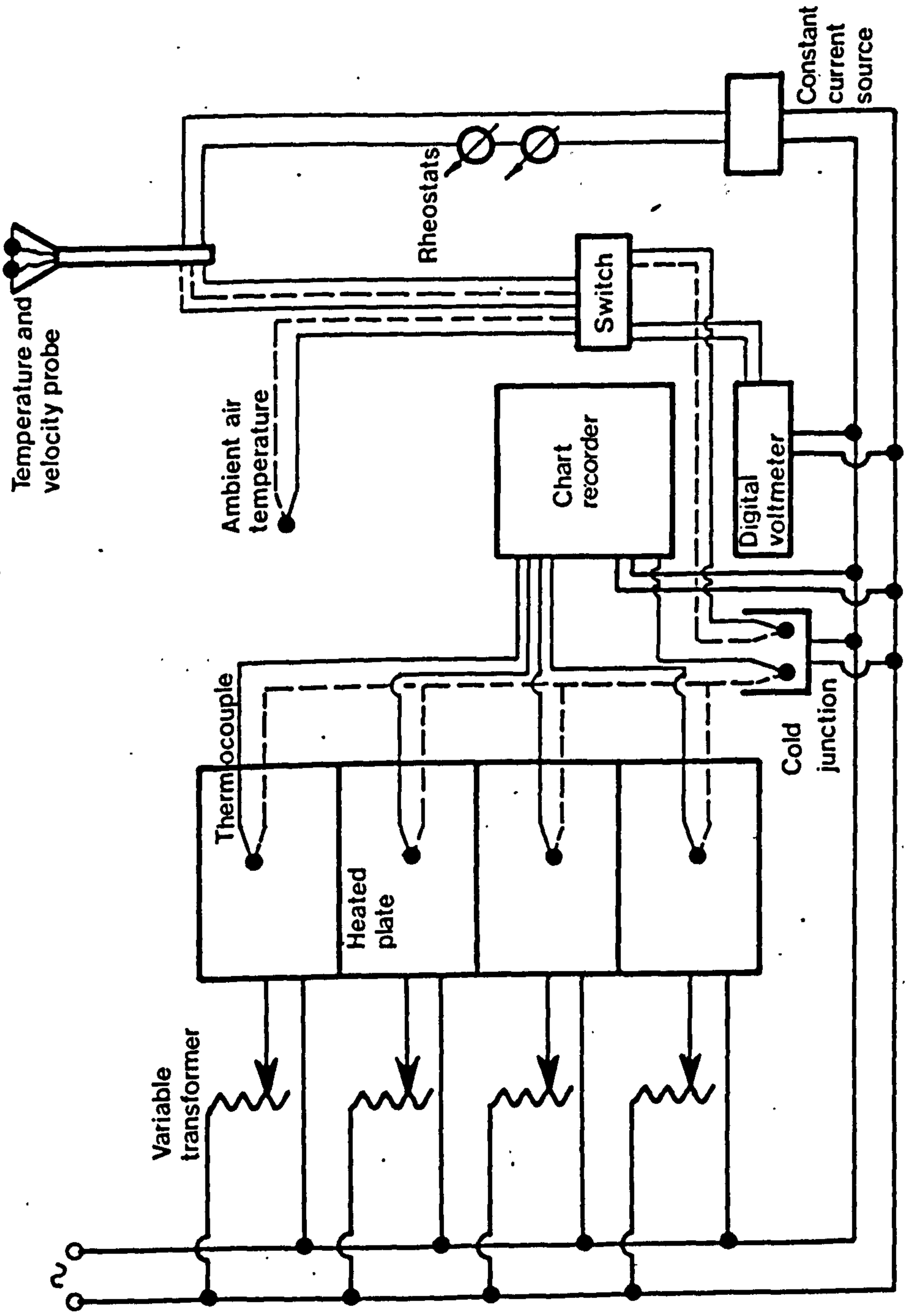

SCHEMATIC DIAGRAM OF HEATED SURFACE EXPERIMENTS

Fig.3.11.

Fig. 3.12. VIEW OF REPLACEMENT WALL JET EXPERIMENTAL ARRANGEMENT

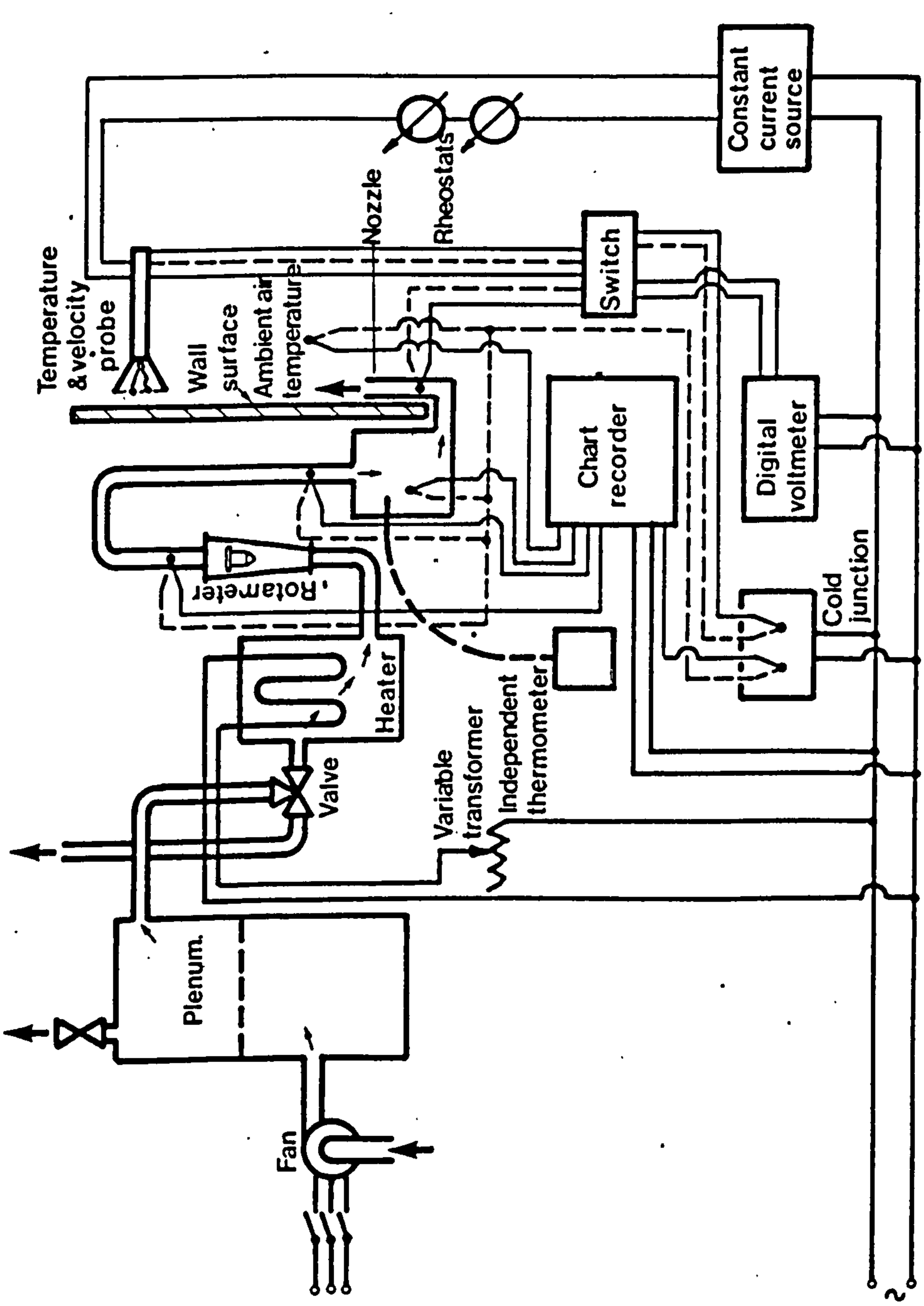

Fig.3.13 SCHEMATIC DIAGRAM OF THE REPLACEMENT WALL JET EXPERIMENTS

Fig. 3. 14. VIEW OF VOLUME CONTROL ARRANGEMENT

in all circumstances. The volume flow was measured by one of two rotameters after it had been heated by a 1.5 kW electric heating element. The output of the heating element was adjusted by a variable auto-transformer. The heated air was introduced into a plenum from which it was finally discharged through the variable width slot. Fig. 3.15 shows that the heating plenum, rotameters, slot plenum and connecting flexible ducting were all well insulated. On the basis of experience gained during the commissioning of the rig, the back of the board was subsequently also well insulated.

The air velocity and temperature readingswere monitored with a digital voltmeter. The multi-channel chart recorder was used to monitor continuously the ambient, slot plenum and two duct temperatures. An independent instrument was used to check the slot plenum temperature.

3.3.2. Instrumentation

After careful consideration, a specification for the temperature and velocity measuring sensor was decided.

The main requirements were:-

- an ability to measure, as far as possible, temperature and velocity in one location and at the same time.
- the signal from the probe to be capable of being monitored a a digital voltmeter. (The instrument would therefore have to have an inherent time constant sufficient for the reading to represent a time average value).
- the ability to measure within 1.5 mm of the heated surface. (This distance was considered to be sufficiently close to the surface to discern the maximum of the velocity profile)
- velocity range of zero to 1.2 m/s.

As the heated-thermocouple anemometer described in chapter 3.2.2 evidently did not fulfil the above requirements (and a survey revealed no suitable alternative instrument) it was decided to design a new sensor.

The probe is a combined heated coil anemometer and temperature measuring thermocouple. A schematic arrangement is shown in Fig. 3.16 and a photograph in Fig. 3.17. The frame and general layout were designed to facilitate an unhindered approach to the heated surface. In principle, the probe consists of two copper-constantan junctions A and B, one of which is heated by a tightly wound coil of 42 S.W.G. manganin wire. (The choice of manganin wire ensures minimum inaccuracy due to a change of resistance with temperatures.) The probe combines two thermocouple circuits in a simple arrangement. The first circuit has junctions at A (see Fig. 3.16) and at C which is the constant temperature cold junction. The temperature difference between A and C generates an e.m.f. that enables the air temperature at A to be calculated. The second circuit has junctions at A and B, junction B being heated at a

Fig. 3.15. REAR VIEW OF REPLACEMENT WALL JET EXPERIMENTAL RIG

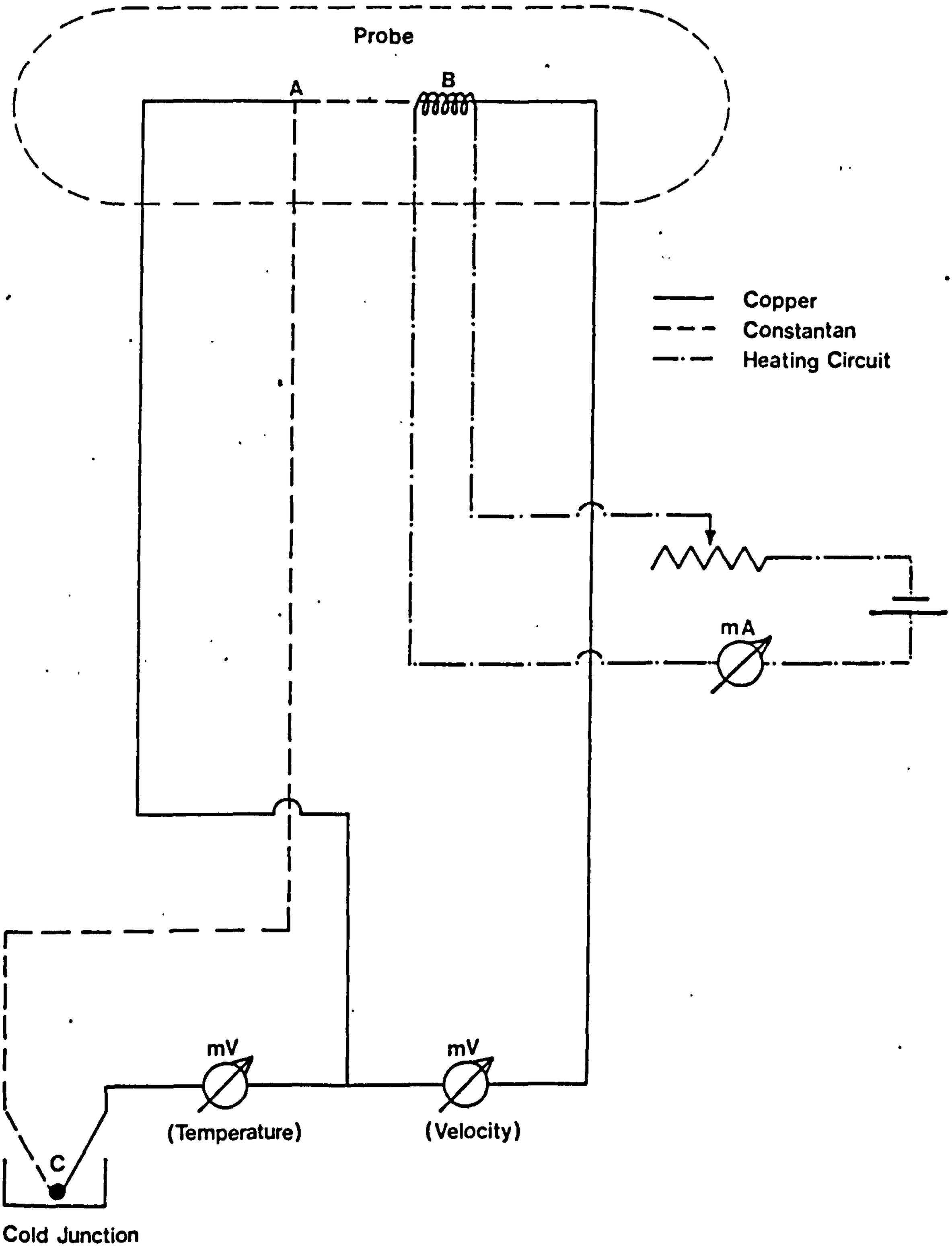

Fig.3.16. SCHEMATIC DIAGRAM OF COMBINED VELOCITY AND TEMPERATURE PROBE

Fig. 3.17. VIEW OF COMBINED VELOCITY AND TEMPERATURE PROBE

constant rate by the heating coil. With both junctions A and B being exposed to the same ambient temperature, any variation in the generated e.m.f. can only be ascribed to a change in the ambient air speed. By careful calibration, the generated e.m.f. can be interpreted in terms of local air speed. If, for the given temperature range, the resistence of the manganin wire can be assumed to be independent of the ambient temperature, the condition of constant heat supply at junction B can be satisfied if the electrical current passing through the heating coil remains invariant. For this purpose a constant current source was provided. As a further check, the voltage across a calibrated 10 Ω resistance was measured by a digital voltmeter, thus ensuring a high degree of accuracy of heating coil current measurement. The measuring equipment can be seen in Fig. 3.18.

The probe was calibrated for both temperatures and velocity. Extensive tests were conducted to ascertain the influence of heat radiation and conduction from junction B on junction A and on the sensitivity of temperature and velocity measurements to radiation from the heated surface. Because of its design and the small cross sectional area of the wires used in its construction, the probe was found to be insensitive to these effects.

The ambient air temperature was measured with a thermocouple and the signal monitored by a digital voltmeter. Readings from thermo-juctions attached to the surface of the heated panels were continuously monitored on a multi-channel chart recorder. When the rig was used to study replacement jets, thermocouples connected to the multi-channel chart recorder were used to monitor continuously the temperature differential between the air temperature in the slot plenum and the ambient air temperature, and two duct temperatures.

3.3.3. Test procedure

The experimental facility was used for two series of tests. In the first series the velocity and temperature profiles of convective currents of a heated plate were measured. In the second series wall jets replacing the convective currents were investigated.

Throughout the tests care was taken to conduct the experiments under favourable conditions. The experiments were carried out after normal working hours in order to minimise any disturbing factors (other test rigs, open doors, convective currents due to solar radiation, ambient temperature fluctuations etc.) The need to conduct the experiments outside normal working hours was one of the main reasons for the requirement that one person should suffice to operate the rig.

In both series of tests the rig was switched on several hours before measurements were taken to ensure that steady state conditions had been attained. During this period frequent checks were made of the temperatures on the multi-channel chart recorder and, if necessary, fine adjustments were made.

Convective tests

In this series of tests the temperature and velocity profiles of con-

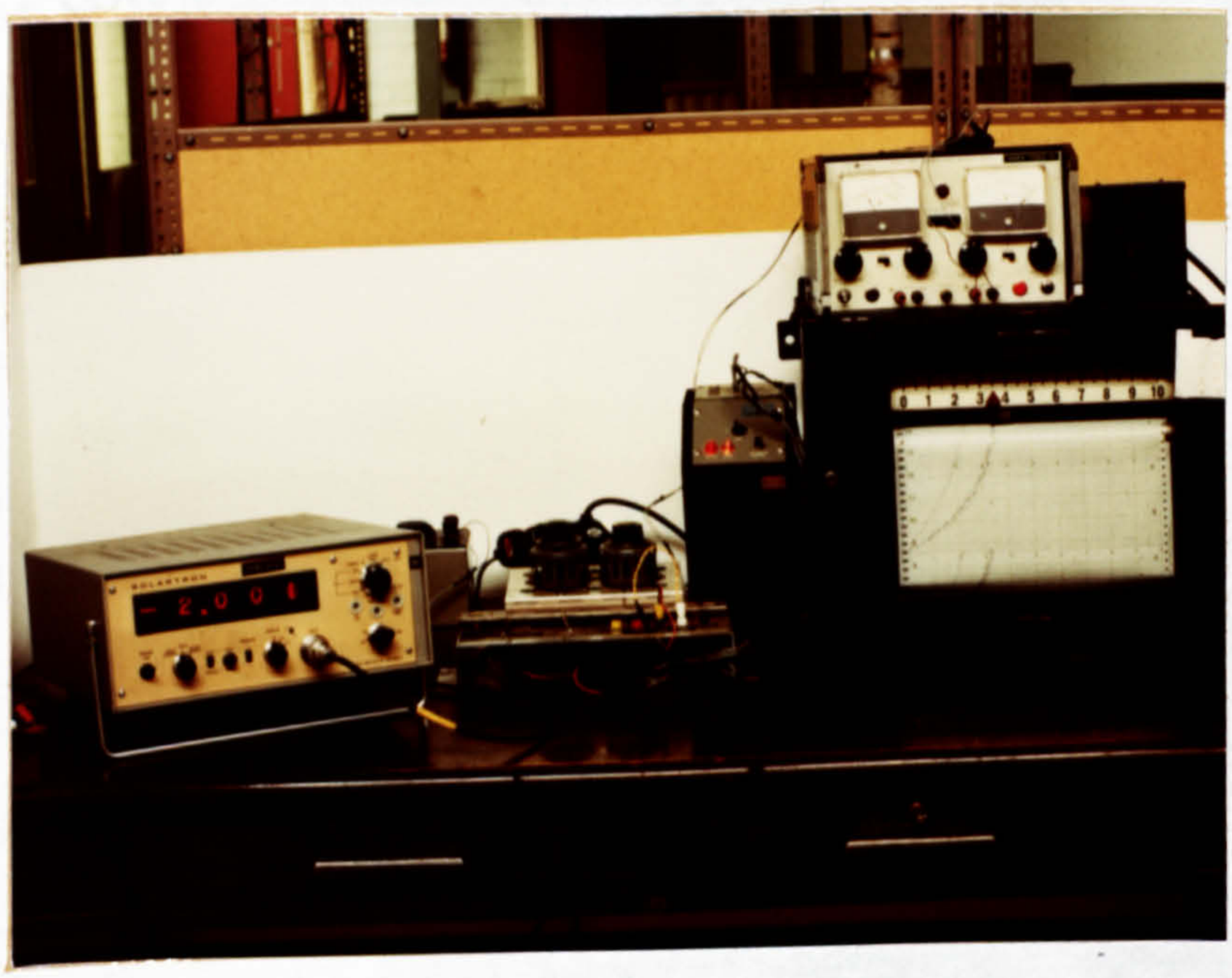

Fig. 3.18. THE INSTRUMENTATION

vective currents generated by the heated surface were measured. Tests were carried out for three nominal values of Δt_w, the temperature differential between the surface temperature of the heated panels and the ambient air temperature, namely 10, 30 and 50° C. Measurements, see Fig. 3.19, were taken at five locations spaced along the height of the heated surface. At least two good experiments conducted independently per nominal Δt_w were required.

The measured velocity and temperature data was punched on paper tape for further processing. Printouts of the data can be seen in Appendix A. The data were then processed by a specially written computer program. For each nominal temperature differential Δt_w the program corrected the velocity and temperature measurements for any minor deviation from the nominal Δt_w, calculated the mean of the two experiments and computed the volume flow, momentum flux, heat content and mean temperature differential of both experiments and of their mean. The program also calculated the theoretical values for the nominal Δt_w (for the maximum velocity, boundary layer thickness,.Grashof number, mean Nusselt number, velocity and temperature profiles, volume flow, momentum flux, heat content and mean temperature differential) and compared these values, in absolute and percentage terms, with the experimental results. Depending on the Grashof number, the program compared the results with either laminar or turbulent theoretical predictions. If the flow was in the transitional region, both comparisons were made. A graphic display of the velocity and temperature profiles, measured and predicted, was also produced. Printouts for nominal temperature differentials of 10, 30 and 50°C are shown in Appendix B.

Replacement jets

After a board and a variable width slot (as described in 3.3.1.) had been substituted for the heated panels, replacement jet tests were carried out. The purpose of this series of tests was to decide experimentally whether replacement jets for the previously measured convective currents could be found.

Initially, the replacement jet parameters were calculated according to the theoretically deduced formulae in Table 2.4, Part 2, and are listed in Table 3.1. Relevant parameters of the replacement jet and the original heated surface as shown in Fig. 3.20.

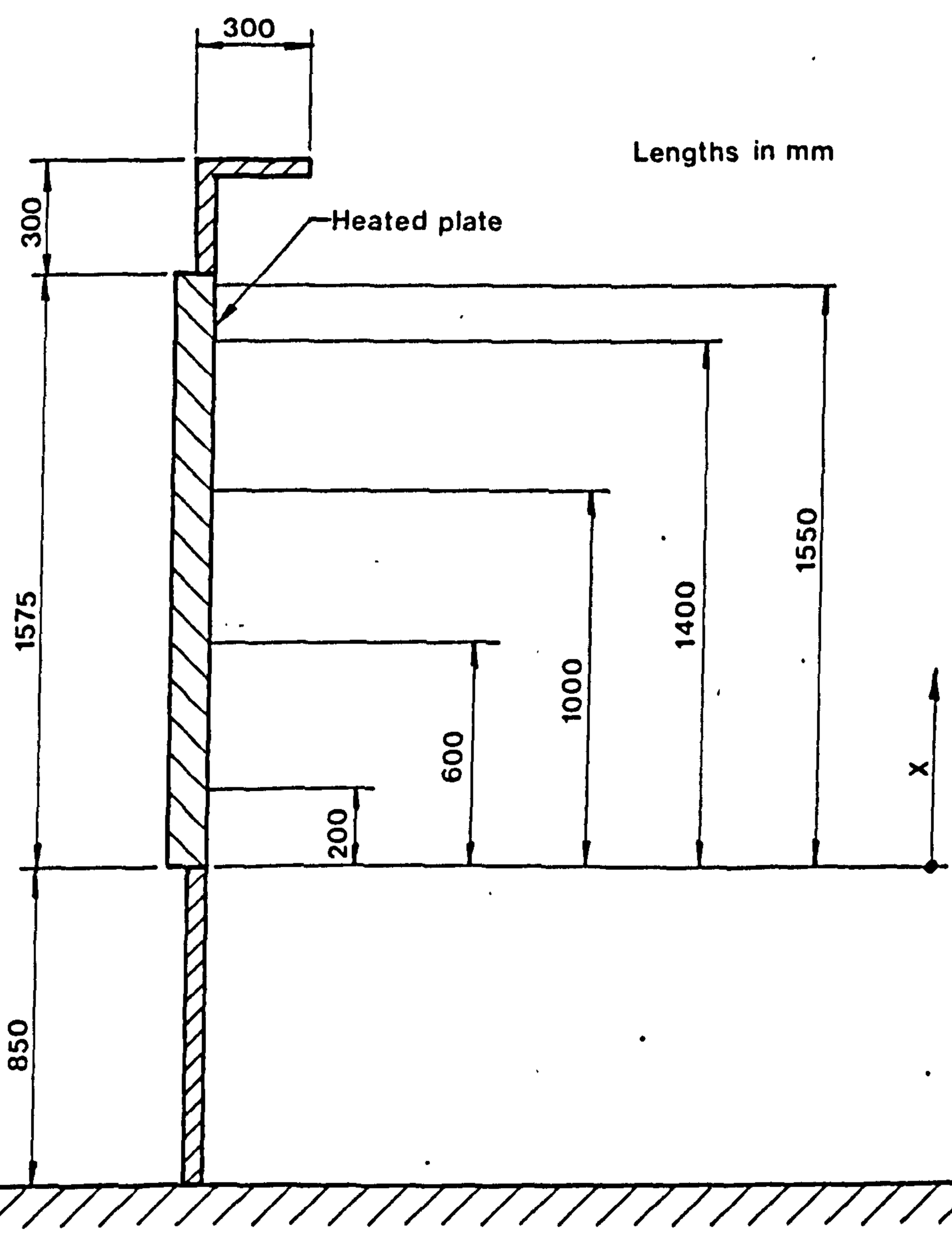

Fig. 3. 19. VERTICAL LOCATION OF VELOCITY AND TEMPERATURE MEASURING PROBES

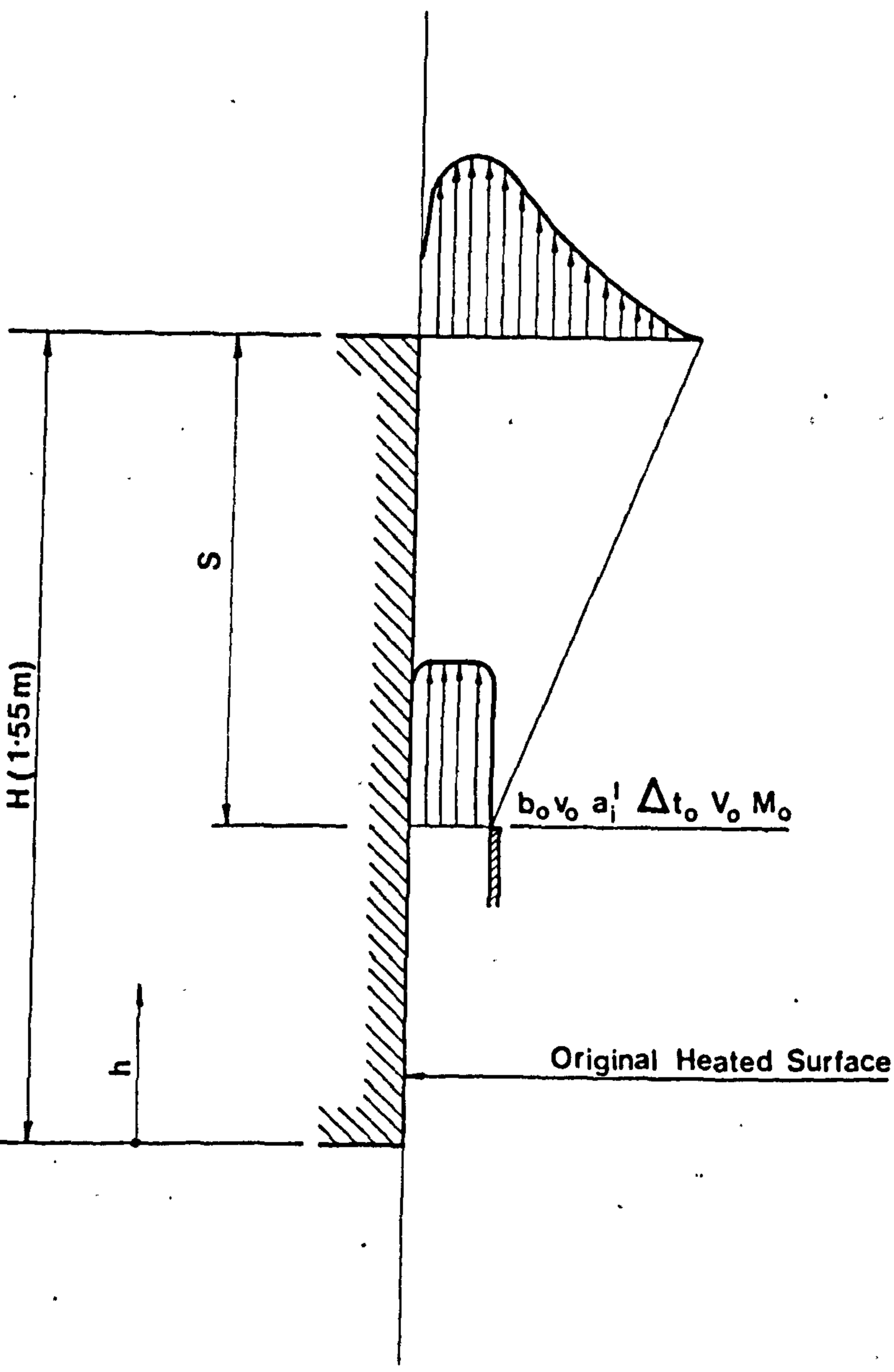

Fig.3.20. DEFINITION SKETCH OF HEATED SURFACE AND REPLACEMENT JET FLOW PARAMETERS

TABLE 3.1 Calculated replacement jet parameters for H = 1.55 m and Δt_w = 10, 30 and 50°C.

	Parameter values for nominal temperature differentials Δt_w of the replaced convective surface (Rayleigh number of convective flow in brackets)		
Δt_w / Replacement jet parameters / Ra	10°C	30°C	50°C
	3.5×10^9	9.1×10^9	1.3×10^{10}
v_o (m/s)	0.394	0.682	0.88
b_o (m)	0.021	0.0189	0.018
$Re_o = \frac{b_o v_o}{\nu_o}$	550	806	943
a_i'	0.06	0.06	0.06
S (m)	0.79	0.71	0.674
Δt_o (°C)	3.5	10.6	17.7
V_o (m^3/s per m run)	0.0074	0.0136	0.0166
M_o (kgm/s^2 per m run)	0.0029	0.0093	0.0146

The low nozzle Reynolds numbers indicate that the flow in the nozzle will be laminar. From Fig. 2.18, Part 2, for Reynolds numbers between 500 and 1000 the coefficient of turbulence has a value of $a_1 = 0.07$. When the influence of buoyancy forces is taken into account (Chapter 2.3.2, Part 2, using an estimated value of $\Delta x/x = 0.16$ in equation 2.101) the value of the modified coefficient of turbulence, $a_1 = 0.06$ used in Table 3.1 is obtained. At this stage no correction for laminar nozzle flow and other effects of buoyancy was attempted.

In a series of tests individual nozzle parameters (v_o, b_o, Δt_o and S) were varied, in order to obtain a best fit to the convection current values at x = H = 1.55 m. Six experimental results, see Table 3.2, were then selected for detailed analysis.

TABLE 3.2 Selected experiments for the comparison of convective and replacement jet parameters.

Experiment	Nominal Δt_w (°C) (H = 1.55 m)	Nozzle parameters			
		$v_{o_{max}}$(m/s)	b_o(m)	S(m)	Δt_w (°C)
50/1	50	0.59	0.01945	0.684	24.3
50/2	50	0.59	0.0182	0.684	34.8
50/3	50	0.59	0.0182	0.684	31.0
30/1	30	0.49	0.0185	0.712	15.9
30/2	30	0.49	0.01984	0.712	14.8
10/1	10	0.36	0.0213	0.805	15.27

Velocity and temperature readings were punched on paper tape for subsequent computer analysis. Printouts of the data are given in Appendix C. The data from the selected experiments were then processed by a second computer program. The program, after correcting for temperature deviation, listed and compared the theoretical and experimental convective values and the respective replacement jet results (velocity and temperature profiles and volume flow, momentum flux, heat content and mean temperature difference in absolute and percentage terms). A graphic comparison of the convective and replacement jet velocity and temperature profiles was also provided. Printouts for the selected experiments are given in Appendix D.

In order to evaluate the extent of non-uniform initial flow, nozzle velocity and temperature profiles were measured. The data were processed manually. Flow visualisation (by smoke) was used to gain an insight into the structure of the outer part of the jet. A photograph in Fig. 3.21 shows a flow visualisation test in progress.

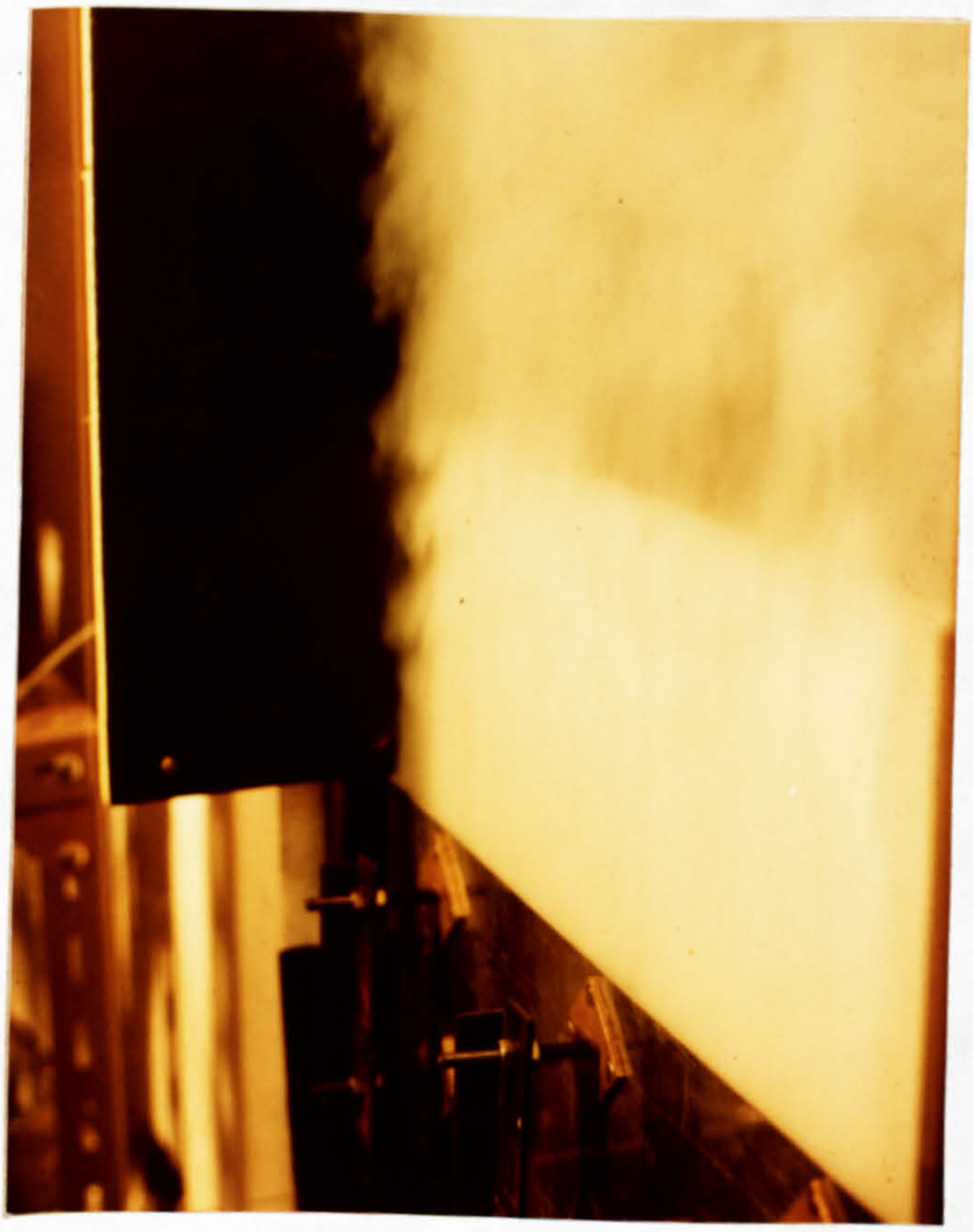

Fig. 3.21. VIEW OF REPLACEMENT WALL JET FLOW VISUALISATION TEST

3.3.4 Results and observations

As had been mentioned, the main purpose of obtaining measurements of convective currents of a heated plate was to provide a datum for the evaluation of the replacement jet results.

The mean values of velocity profile measurements of convective streams leaving the heated plate (H = 1.55 m) for three nominal temperature differentials Δt_w = 10, 30 and 50°C are plotted in Fig. 3.22. Also shown in the graph are the theoretically calculated boundary layer widths. The experimental data are in good agreement with predicted turbulent boundary layer widths if the width of the boundary layer is defined by $v = v_a$ instead of $v = 0$. The corresponding temperature profile measurements are plotted in Fig. 3.23.

The main parameters that characterise a convective stream (and its influence on room air movements) as tabulated in Table 3.3, as are the theoretically predicted values (Table 2.1, Part 2) for flow in the turbulent region. The discrepancy between the predicted and measured maximum profile velocity can be attributed mainly to the presence of room air turbulence. The percentage values (91, 72, 67) indicate that the influence of room air movements increase with temperature difference. The same trend, i.e. a fall in percentage values with temperature difference Δt_w, is also valid for all of the remaining parameters (V, M, Q, $\overline{\Delta t_w}$). The high percentage values, significantly over 100%, of volume flow V and momentum flux M can, as has been discussed in Chapter 3.2.5, be attributed to the difficulties in the interpretation of velocity readings in the outer part of the boundary layer.

The Rayleigh number in Table 3.1 for Δt_w = 10°C ($Ra = 3.5 \times 10^9$) is sufficiently close to values associated with the transitional region to warrant a comparison of the experimental values with predictions based on expressions for laminar flow; the relevant values are tabulated in Table 3.4. The predicted laminar flow values are compared with two sets of experimental values. The sets are the result of integration of the velocity and where appropriate, temperature profiles up to a distance from the heated plate equal to the theoretical width of the laminar or turbulent boundary layer respectively, i.e. $y = \delta_L$ and $y = \delta_T$. As $\delta_L = 0.26\ \delta_T$ (see Fig. 3.22), a significant discrepancy between the two sets of values for $y = \delta_L$ and $y = \delta_T$ indicates that the flow is turbulent.

The velocity and temperature profile measurements of the replacement jet experiments listed in Table 3.2 are shown in Fig. 3.24 to Fig. 3.29. Also shown in the graphs are the mean values of velocity and temperature profile measurements of the replaced convection streams leaving the heated plate. There is goodagreement between jet and convective velocity profiles apart from the region closest to the surface ($y < 10$ mm). The maximum of the convective profile occurs nearer to the surface than that of the replacement wall jet. As expected, agreement of temperature profiles is not possible for a region close to the surface, but for $y > 20$ mm a measure of agreement is reached.

In Table 3.5 the main parameters of convective streams and replacement wall jets are compared. The maximum velocities, throughout, are identical and are also equal (see Table 3.2) to the maximum nozzle velocities.

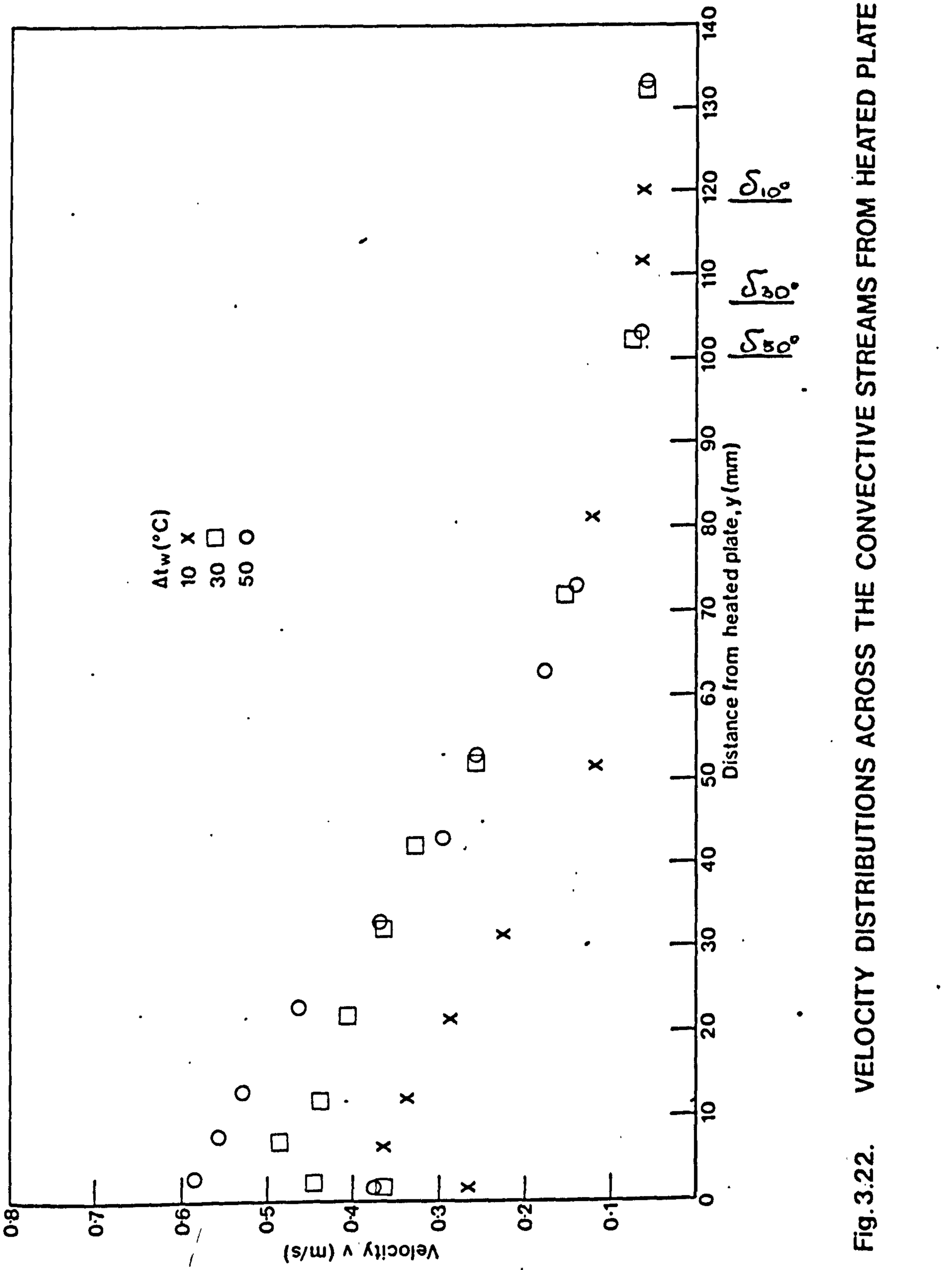

Fig.3.22. VELOCITY DISTRIBUTIONS ACROSS THE CONVECTIVE STREAMS FROM HEATED PLATE

TEMPERATURE DISTRIBUTIONS ACROSS THE CONVECTIVE STREAMS FROM HEATED PLATE
Distance from heated plate y (mm)
Temperature differential Δt (°C)
Δtw(°C)
10 X
30 □
50 O
δ10°
δ30°
δ50°

Fig.3.23. TEMP

TABLE 3.3 Comparison of experimental and predicted values of convective current parameters for H = 1.55 m and Δt_w = 10, 30 and 50°C. Theoretical prediction for flow in the turbulent region.

Parameter	Theoretical prediction (turbulent flow)			Mean values of experimental results		
Δt_w (°C)	10	30	50	10	30	50
Maximum velocity, V_{max} (m/s)	0.394	0.682	0.88	0.36	0.49	0.59
% predicted	100	100	100	91	72	67
Volume flow, V (m^3/s per m run)	0.0125	0.0194	0.0238	0.0195	0.0274	0.0297
% predicted	100	100	100	156	141	125
Momentum flux, M (kgm/s^2 per m run)	0.00402	0.0107	0.0166	0.00498	0.0106	0.0128
% predicted	100	100	100	124	99	77
Heat content, Q (W per m run)	35.6	162.7	336.2	47.6	192.1	276.9
% predicted	100	100	100	134	118	82
Mean temperature differential, $\overline{\Delta t}$ (°C)	2.4	7.1	11.8	2.0	5.9	7.8
% predicted	100	100	100	86	83	66

TABLE 3.4 Comparison of experimental and predicted values of convective current parameters for H = 1.55 and Δt_w = 10°C. Theoretical prediction for flow in the laminar region.

Parameter	Theoretical prediction (laminar flow)	Mean value of experimental results for $y = \delta_L$	$y = \delta_T$
Δt_w (°C)	10	10	10
Maximum velocity, v_{max} (m/s)	0.425	0.36	0.36
% predicted	100	85	85
Volume flow, V (m^3/s per m run)	0.0074	0.00935	0.0195
% predicted	100	126	209
Momentum flux, M (kgm/s^2 per m run)	0.00289	0.00344	0.00498
% predicted	100	119	172
Heat content, Q (W per m run)	3.55	43.4	47.6
% predicted	100	122	134
Mean temperature differential, $\overline{\Delta t_w}$ (°C)	4.0	3.9	2.0
% predicted	100	97	50

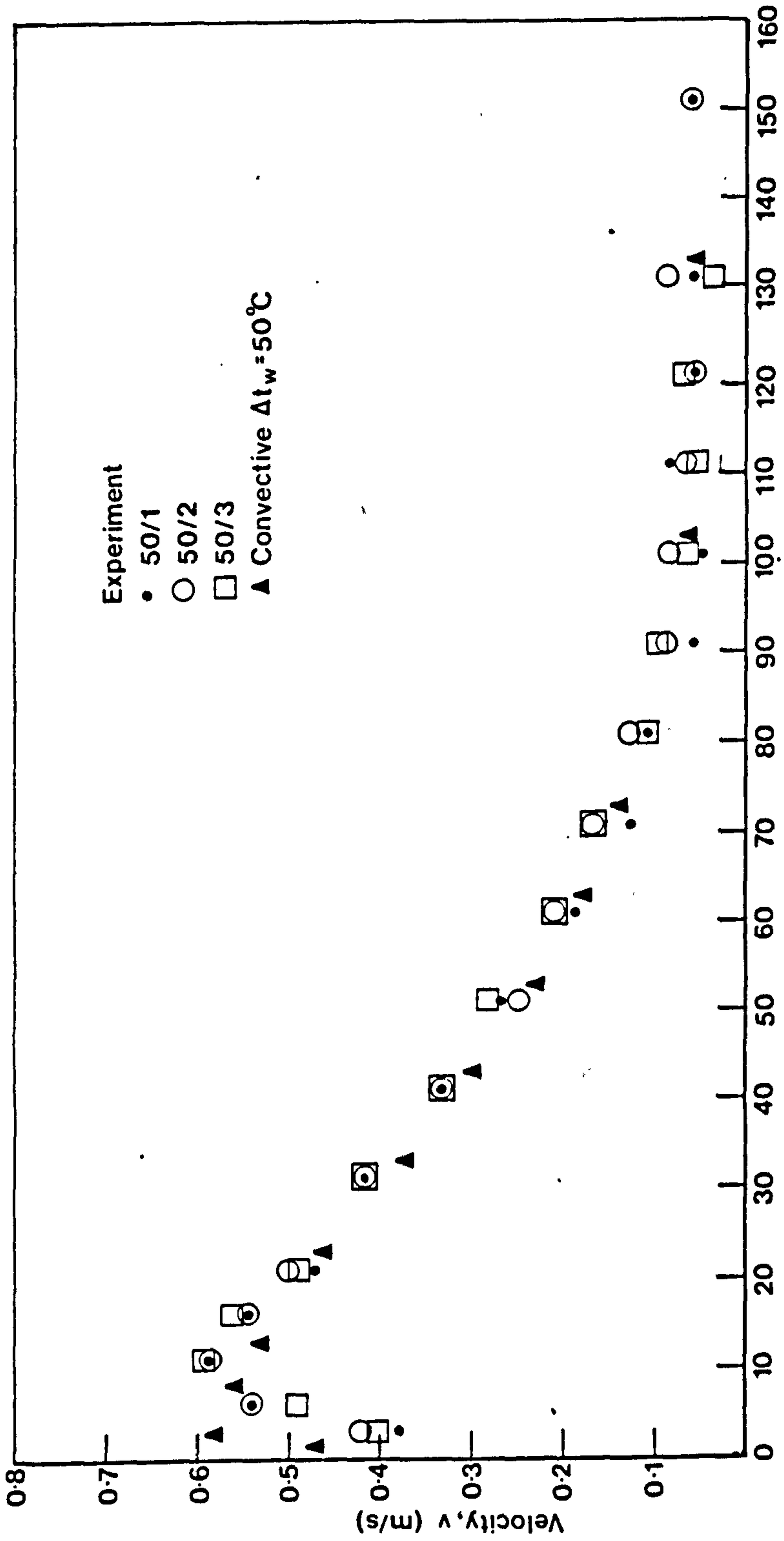

Fig.3.24. VELOCITY DISTRIBUTIONS ACROSS REPLACEMENT WALL JETS FOR $\Delta t_w = 50°C$

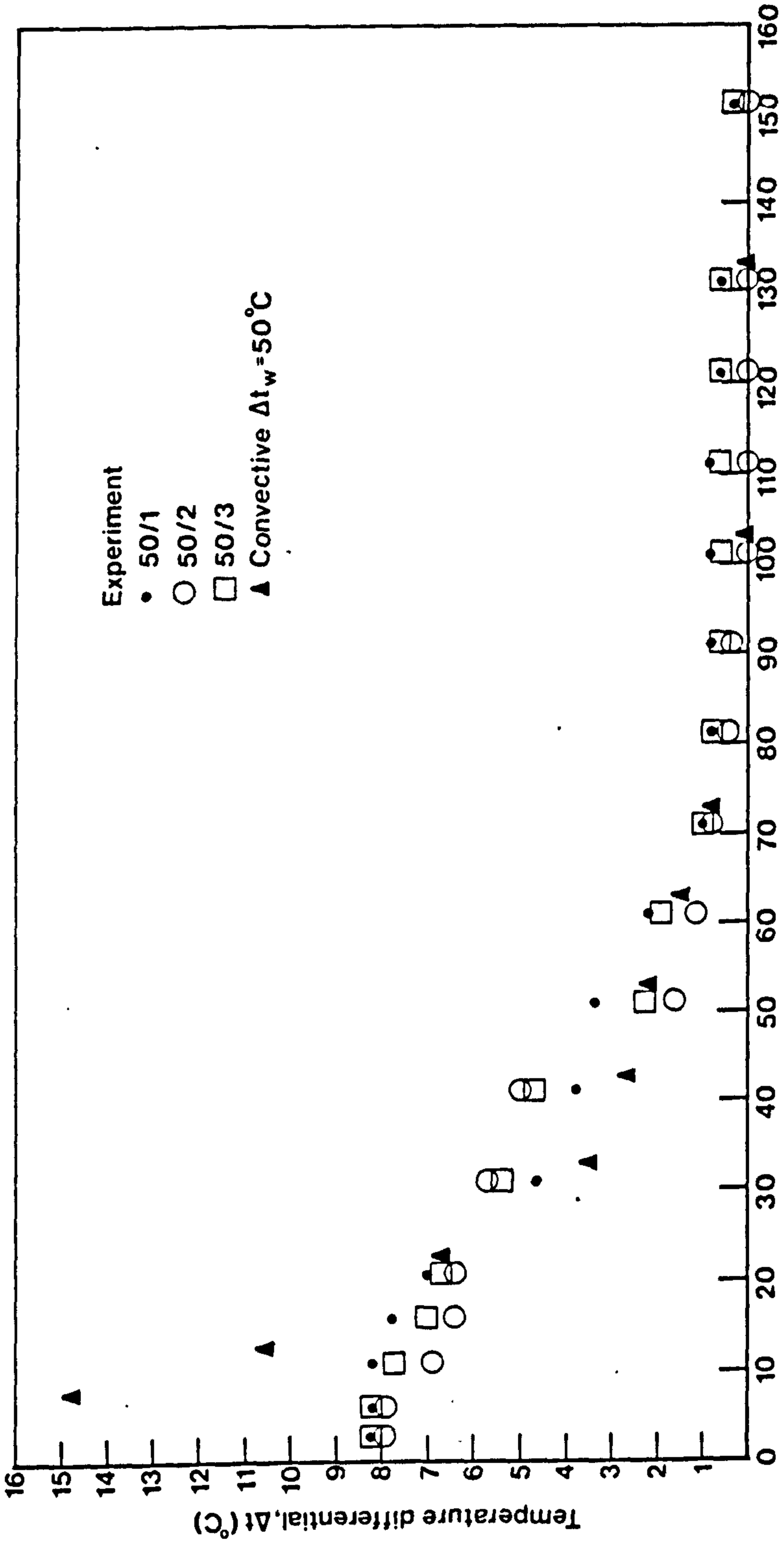

Fig.3.25. TEMPERATURE DISTRIBUTIONS ACROSS REPLACEMENT WALL JETS FOR Δt_w=50°C

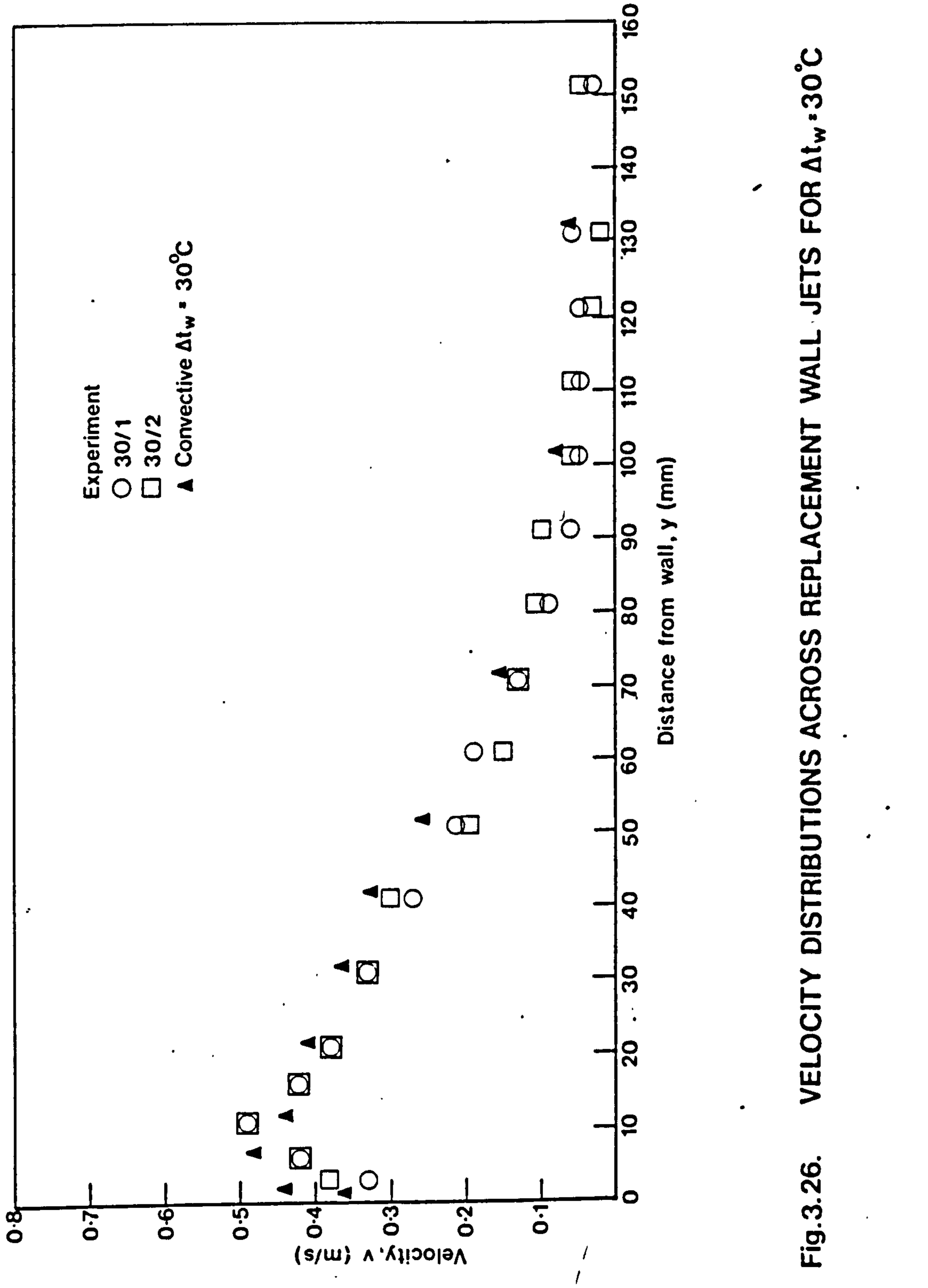

Fig.3.26. VELOCITY DISTRIBUTIONS ACROSS REPLACEMENT WALL JETS FOR Δt_w

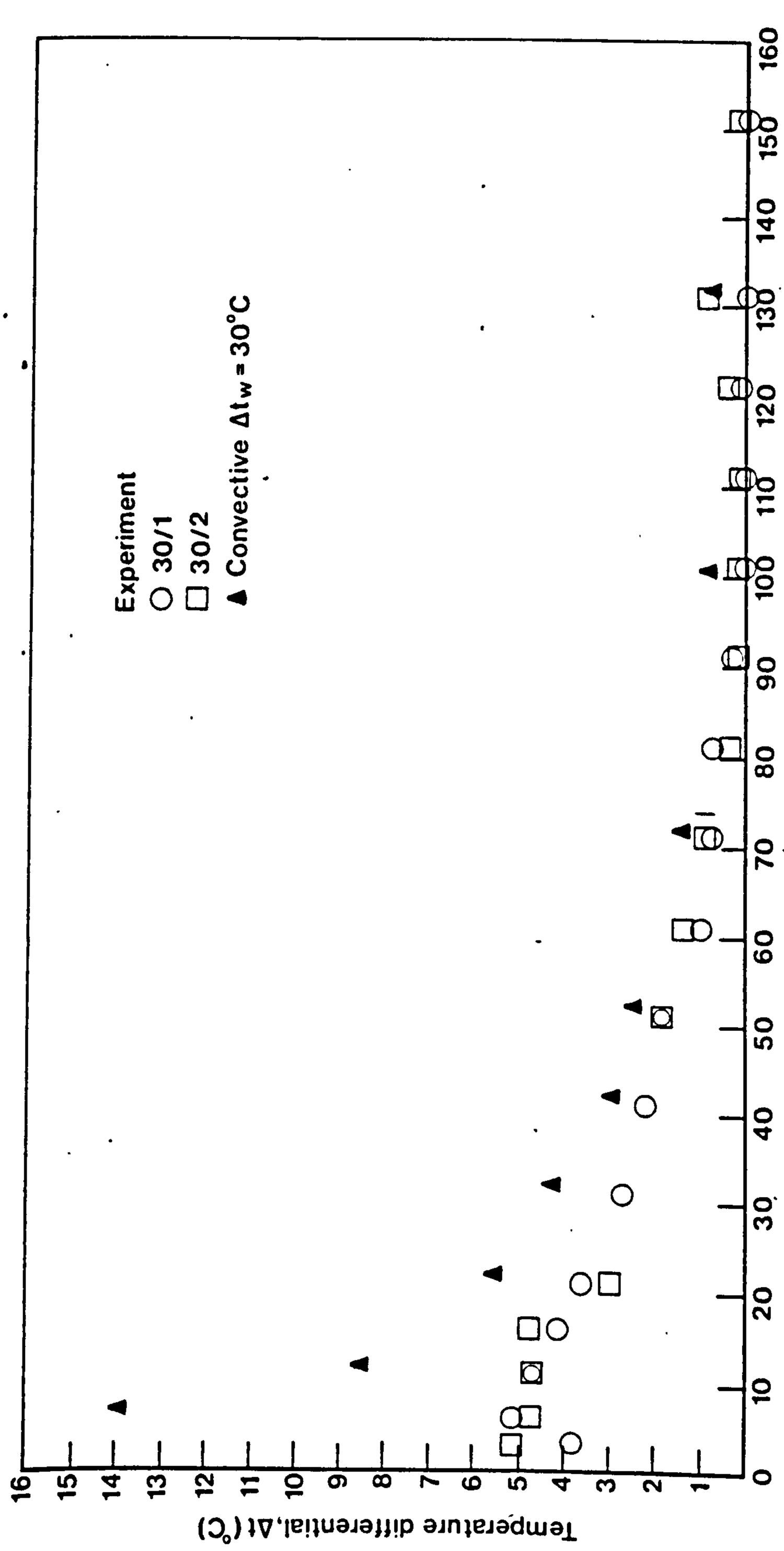

Fig.3.27. TEMPERATURE DISTRIBUTIONS ACROSS REPLACEMENT WALL JETS FOR $\Delta t_w = 30°C$

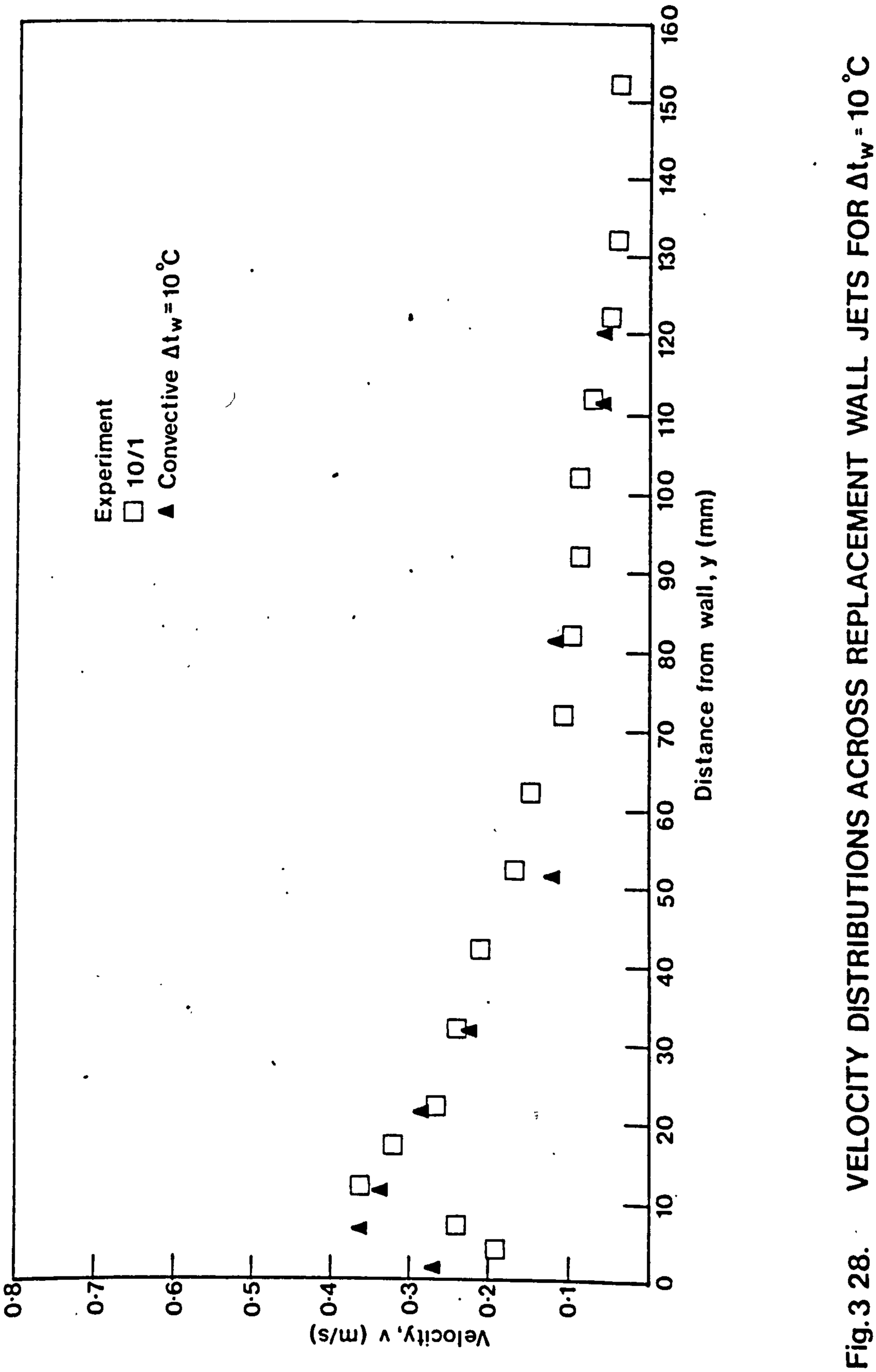

Fig.3 28. VELOCITY DISTRIBUTIONS ACROSS REPLACEMENT WALL JETS FOR $\Delta t_w = 10\,^{\circ}C$

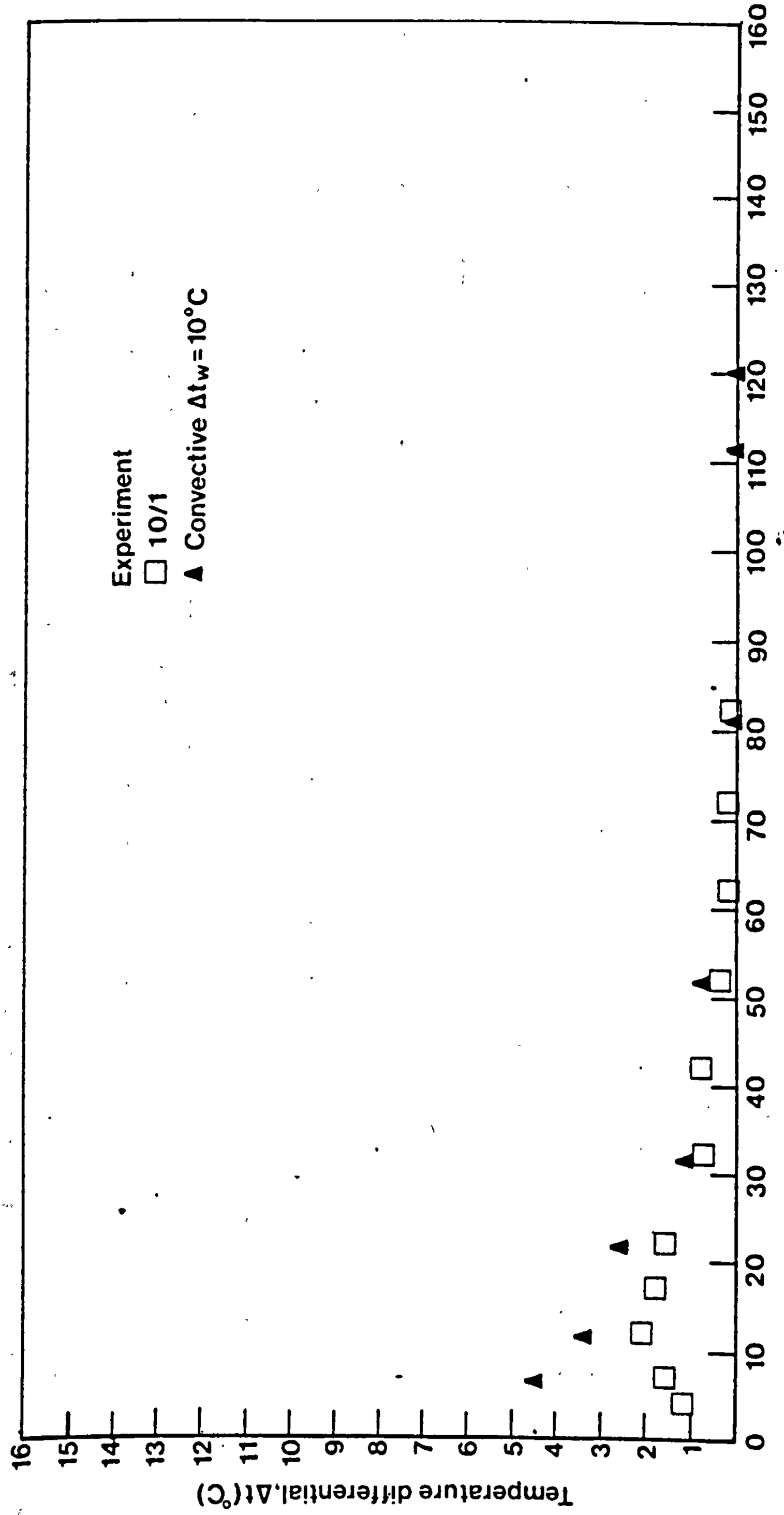

Fig.3.29. TEMPERATURE DISTRIBUTIONS ACROSS REPLACEMENT WALL JETS FOR $\Delta t_w = 10°C$

TABLE 3.5 Comparison of experimental values of replacement jet and convective current parameters for H = 1.55 m and Δt_w = 10, 30 and 50°C. Convective current values = 100%.

Parameter	Nominal temperature differential Δt_w (°C)								
	10		30			50			
Experiment	C	10/1	C	30/1	30/2	C	50/1	50/2	50/3
Maximum velocity, v_{max} (m/s)	0.36	0.36	0.49	0.49	0.49	0.59	0.59	0.59	0.59
%	100	100	100	100	100	100	100	100	100
Volume flow, V (m^3/s per m run)	0.02	0.0196	0.0275	0.0236	0.0241	0.0295	0.028	0.0295	0.0293
%	100	98	100	86	88	100	95	100	99
Momentum flux, M (kg m/s^2 per m run)	0.00526	0.00483	0.0107	0.0084	0.00863	0.0127	0.0124	0.0131	0.013
%	100	92	100	79	81	100	98	103	102
Heat content, Q (W per m run)	50	20.9	196	77.8	81.2	278.5	175.2	167.4	174.7
%	100	42	100	40	41	100	63	60	63
Mean temperature differential, $\overline{\Delta t_w}$ (°C)	2.1	0.9	6.0	2.8	2.8	7.9	5.2	4.7	5.0
%	100	43	100	47	47	100	66	59	63

Good agreement is obtained for volume flow and momentum flux but, due to the inherent difference in the temperature profiles, a moderately worse correlation is obtained for the heat contents and mean temperature differentials of the flows. Better agreement for temperature related parameters is obtained when replacing convective flows having higher temperature differentials between the heated plate and the ambient air. (i.e. better agreement for $\Delta t_w = 50^oC$ than for $\Delta t_w = 10^oC$).

Due to the low nozzle Reynolds numbers (see Table 3.1), non-uniform initial conditions were expected and experienced. The initial velocity and temperature profiles of Experiment 50/2 are given in Fig. 3.30 and Fig. 3.31. The measurements were taken at a distance of 2 mm from the outlet. The velocity profile shows a similarity with theoretical laminar flow between two parallel walls (see Chapter 2.4.2). The ratio of the initial mean arithmetic velocity to the maximum initial velocity (equation (2.138)), for this experiment, has a value of $\Phi = 0.675$ as compared to the theoretical value for laminar flow between two parallel walls of $\Phi = 0.66$. The ratio of initial mean square velocity to maximum initial velocity (equation (2.141)) is $\Psi = 0.75$ as opposed to the theoretical value of $\Psi = 0.8$.

Fig. 3.31 shows that at a distance of only 2 mm from the outlet sufficient mixing must have occured for higher than ambient temperatures to be recorded at distances significantly greater than the nozzle width. Notwithstanding, the asymmetry of the temperature is mainly caused by a convective loss to the parallel plates forming the nozzle. The magnitude of the loss is given by the ratio of the mean initial temperature difference to the maximum temperature difference

$$\chi = \frac{\overline{\Delta t_o}}{\Delta t_{o_{max}}} \qquad \ldots (3.3)$$

which, for Experiment 50/2, has a value of $\chi = 0.915$. The values of Φ, Ψ and χ for the whole range of experiments were near identical.

3.3.5. Discussion

The dicussion of the laboratory test rig results can be conveniently divided into three sections. In the first two, the convective current measurements and the wall jet results are discussed separately. In the third section the actual replacement of convective streams by wall jets is discussed.

Convective tests

In Chapter 3.2.1 the effects of room air turbulence generated by a supply of cool air into the test room on a convective current were investigated. The main purpose of this series of tests, as mentioned before, is to study the replacement of convective streams by wall jets in natural, yet reproducable, ambient conditions. In the environment chosen for the tests the ambient air speed, on the average, was only half the test room value (0.06 m/s instead of 0.125 m/s).

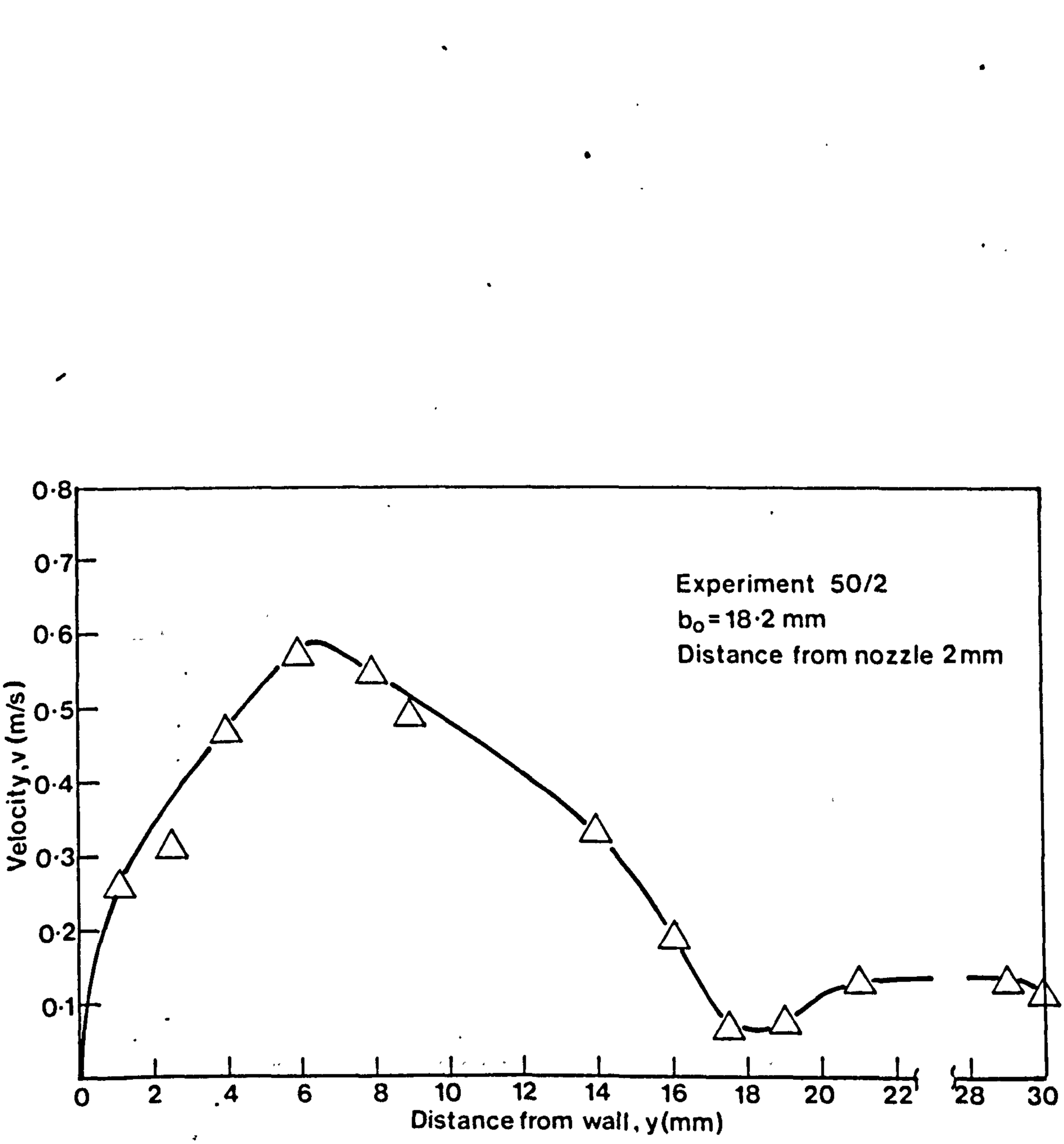

Fig. 3.30. VELOCITY DISTRIBUTION FOR THE INITIAL NOZZLE FLOW

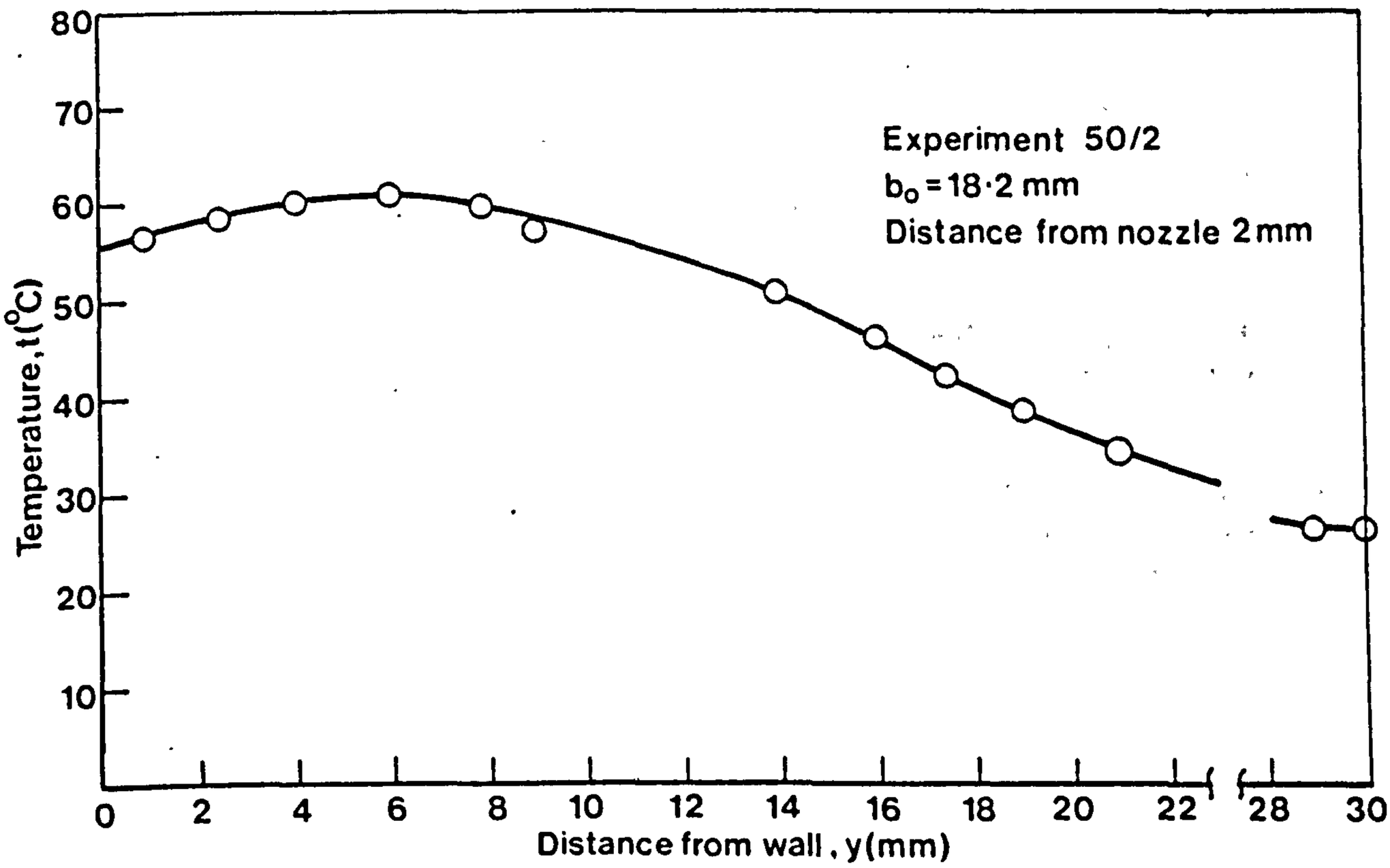

Fig. 3.31. TEMPERATURE DISTRIBUTION FOR THE INITIAL NOZZLE FLOW

In order to compare the test room and open laboratory experiments and evaluate the effect of a change in the level of room air turbulence on convective streams, the results have been plotted in dimensionless co-ordinates in Fig. 3.32. For comparison, a fitted profile to the Cheesewright[3] and Griffiths and Davis[1] results and the theoretical profile are also shown. The present turbulent room results do not fit as neatly on a common curve as do the controlled experiments of Cheesewright and Griffiths and Davis. The discrepancy in the results in the outer part of the boundary layer could be accounted for by the combination of the effect of room air turbulence and by the difficulty in the interpretation of the meaning of the velocity reading, i.e. as has been shown in Chapter 3, Section 2.5, the velocity reading is not identical with the time average velocity of the flow parallel with the heated plate.

It is however, possible to divide the experiments into two groups according to the flow Ra number. The two experiments having the lowest Ra numbers, the heated plate at $\Delta t_w = 10^oC$ ($Ra = 3.5 \times 10^9$) and the test room results ($Ra = 5 \times 10^9$), can be grouped together and are characterised by higher peak relative velocities. The low Ra number experiments follow the theoretical prediction up to a value of $\eta = 0.2$. The other two experiments ($\Delta t_w = 30^oC$, $Ra = 9.1 \times 10^9$ and $\Delta t_w = 50^oC$, $Ra = 12.7 \times 10^9$) show substantially lower peak relative velocities and, in general, are closer to the Cheesewright and Griffiths and Davis experimental results ($Ra = 2.2 - 6.2 \times 10^{10}$).

The Ra number dependent nature of the grouping of the experiments in Fig. 3.32 could be caused by a number of factors - room air turbulence effects are Ra number dependent, incomplete transition from laminar to turbulent flow at lower Ra numbers and inappropriate choice of the independent variable η (perhaps $\eta' = y/x\ (Gr/4)^{0.25}$ would give a better correlation over the inner part of the boundary layer). The inner parts of the velocity profiles of the two low Ra number experiments are plotted in different dimensionless co-ordinates (η' and $v/2u^*$) in Fig. 3.33. The graph shows that the present results definitely follow the turbulent and not the laminar theoretical profile. The test room results ($v_a = 0.125$ m/s) show a tendency towards higher relative velocity values for $\eta' > 5$, i.e. in the outer part of the boundary layer. The data in Fig. 3.32 and Fig. 3.33 indicates that the effect room air turbulence is Ra number dependent, even at low Ra numbers the flow is turbulent and a change in the co-ordinates has no significant effect.

The temperature profile measurements are plotted in dimensionless co-ordinates in Fig. 3.34. The present results tend to agree better with the theoretical prediction in the inner region and with the experimental results of Cheesewright[3] and Griffiths and Davis[1] in the outer region. The overall better agreement of the present temperature profile measurements with theoretical predictions and other experimental results is, in part, due to the greater certainty in the interpretations of the measured values. The readings represent the time average temperature of the medium surrounding the sensor, the difficulty arises only when interpreting the direction and velocity of the flows.

The importance of the exact detail of velocity and temperature profiles when considering the effects of flows on room air movements is, to a degree, secondary. The most important parameters, in this respect, are

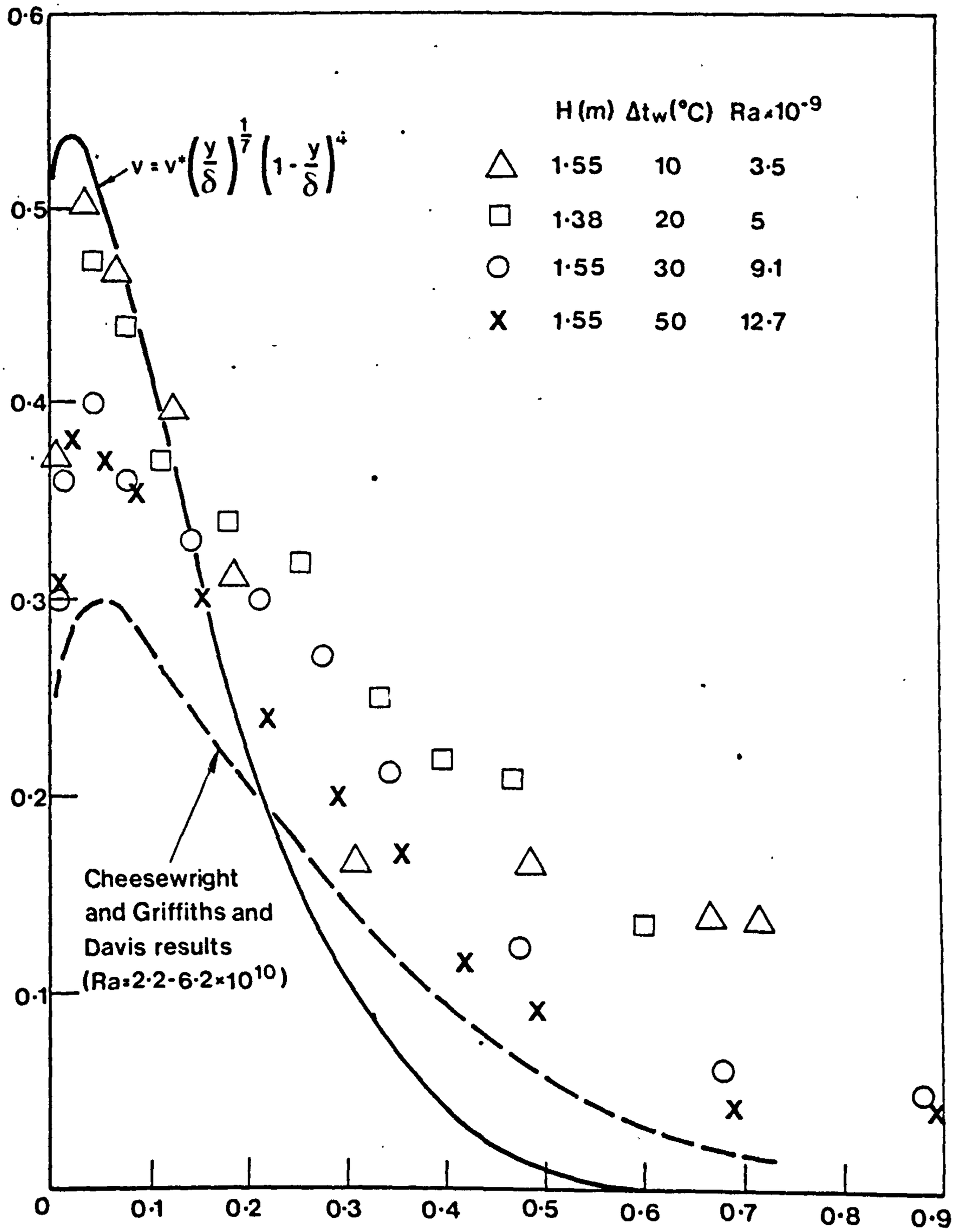

Fig.3.32. NON-DIMENSIONAL VELOCITY PROFILES OF CONVECTION FLOWS-PRESENT DATA COMPARED WITH OTHER TURBULENT EXPERIMENTAL RESULTS

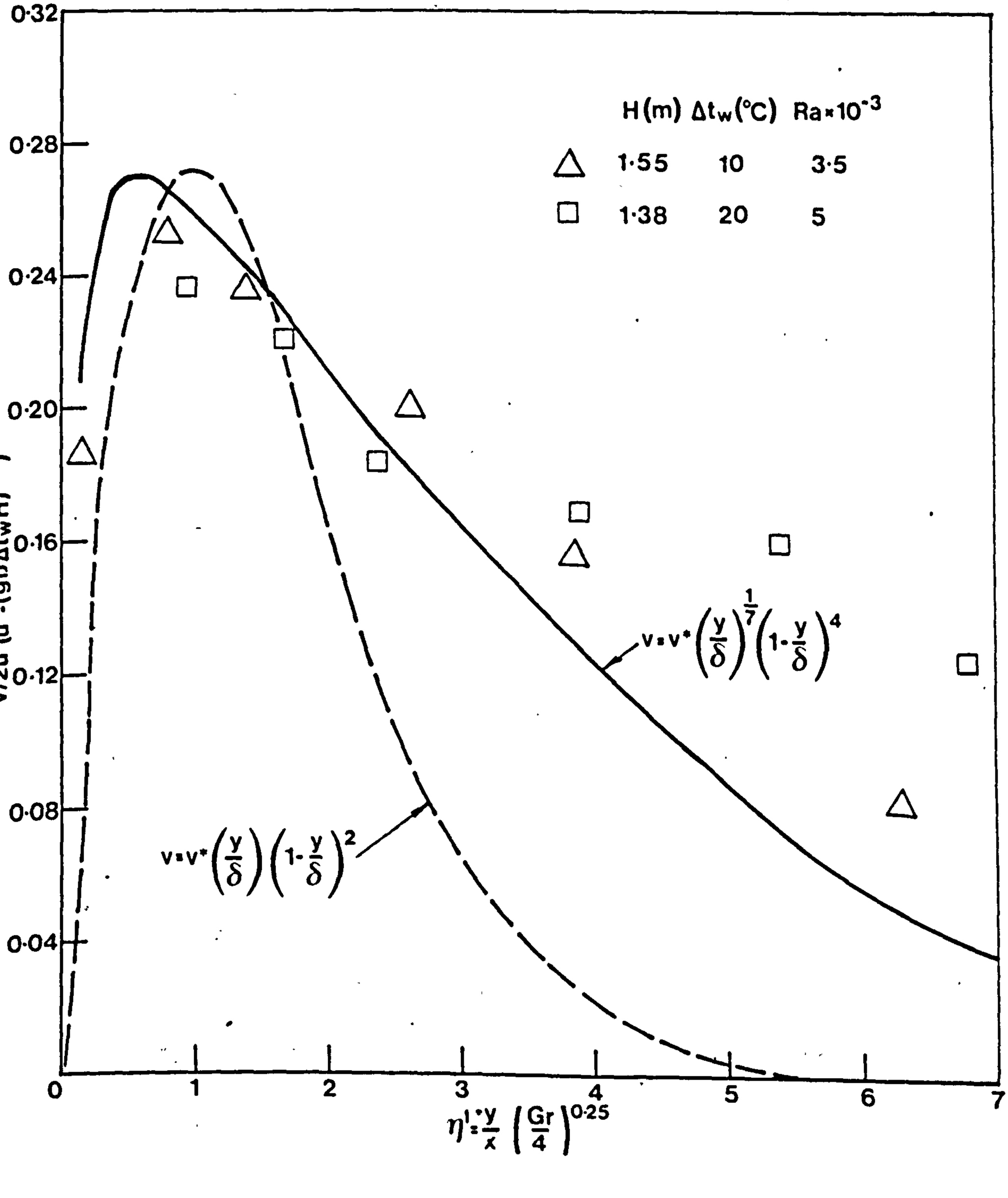

Fig.3.33. NON-DIMENSIONAL VELOCITY PROFILES OF CONVECTIVE FLOWS - PRESENT DATE COMPARED WITH LAMINAR AND TURBULENT PREDICTIONS

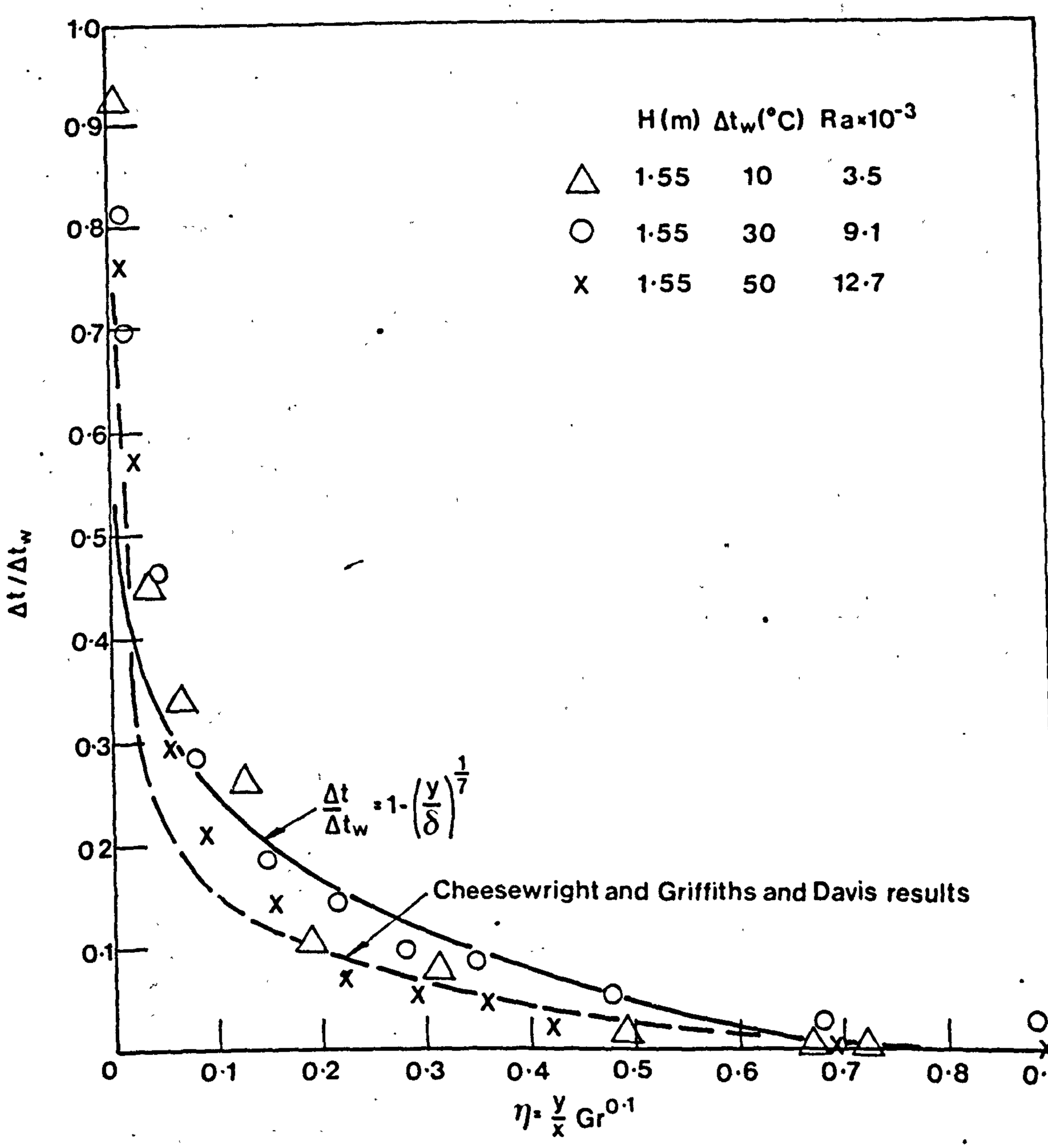

Fig.3.34. NON-DIMENSIONAL TEMPERATURE PROFILES OF CONVECTIVE FLOWS-PRESENT DATA COMPARED WITH PREDICTIONS AND OTHER EXPERIMENTAL RESULTS

momentum flux, profile maximum velocity and the mean temperature, defined as the ratio of heat content to mass flow. The above discussion of velocity profiles plotted in Fig. 3.32 and Fig. 3.33 has shown that the effect of room air turbulence is a function of the Ra number and therefore mainly of the temperature differential between the heated plate and the ambient air Δt_w and of the distance from the bottom of the heated plate x. The variation of the above mentioned five main parameters with $x\Delta t_w$ is plotted in Fig. 3.35 to Fig. 3.39. The parameters are plotted as non-dimensional factors K^*, K^*_V, K^*_M, K^*_Q and $K^* \frac{}{\Delta t}$, defined as ratios of measured to theoretically predicted values (see Chapter 2. 4.2, Part 2). The non-dimensional factors have been calculated for x = 1, 1.4 and 1.55 m and Δt_w = 30 and 50°C and for x = 1.55 and Δt_w = 10°C. Also plotted are values of K^*, K^*_V and K^*_M obtained in the test room.

All of the graphs display the same tendency, i.e. the values of the factors decrease with increasing $x\Delta t_w$. However, the plotted values contain a component dependent on the limitations of the velocity sensor. The reading of the instrument, in the outer part of the boundary layer, is not identical with the time average velocity of a stream flowing parallel with the heated plate. The obvious exception is the ratio of the observed and predicted maximum velocity K as the maximum of the velocity profile lies in the inner region of the boundary layer and therefore the measurement does represent a time average velocity of the flow parallel with the heated plate. The plotted results in Fig. 3.32 and Fig. 3.33 indicate that at low Ra number the velocity measurements in the inner region of the flow follow closely the predicted velocity profile. Discussion in Chapter 3.2.5 has shown that, in all probability only a small part of the velocity reading in the outer part of the boundary layer can be interpreted as a time average flow parallel with the plate. It could therefore be assumed that in the region close to $x\Delta t_w$ = 0 an absolute velocity measuring technique would give values of the non-dimensional factors K^*_V (and K^*_M) near unity. On the other hand at high values of $x\Delta t_w$ the proportional influence of any error in the interpretation of readings in the outer part of the boundary layer will be far less significant. A comparison of velocity profiles in Appendix B suggests that (because the boundary layer width varies little) the error in the interpretation of the readings could be of the same order of magnitude for a wide range of $x\Delta t_w$. If, as an approximation, the difference between the total and "core" values of volume flow of the test room experiment ΔV were subtracted from other, higher $x\Delta t_w$, experimental results and the recalculated parameter K_V joined with K_V = 1 for $x\Delta t_w$ = 0, see Fig. 3.40, a clearer view of the influence of room air turbulence on convective flow parameters could be obtained. The same approach was applied in the recalculation of the remaining non-dimensional factors (K_M, K_Q and $K_{\overline{\Delta t}}$) as plotted in Fig. 3.41.

The recalculated non-dimensional factors, as plotted in Fig. 3.41, are not affected by room air turbulence to the same degree. Volume flow decreases by approximately 20% at $x\Delta t_w$ = 100, whereas momentum flux, the most influenced factor, by double the value. The mean temperature difference $\overline{\Delta t}$ varies only slightly and the variation of the heat content is evidently the result of the compound effect of a decrease both in volume flow and mean temperature difference.

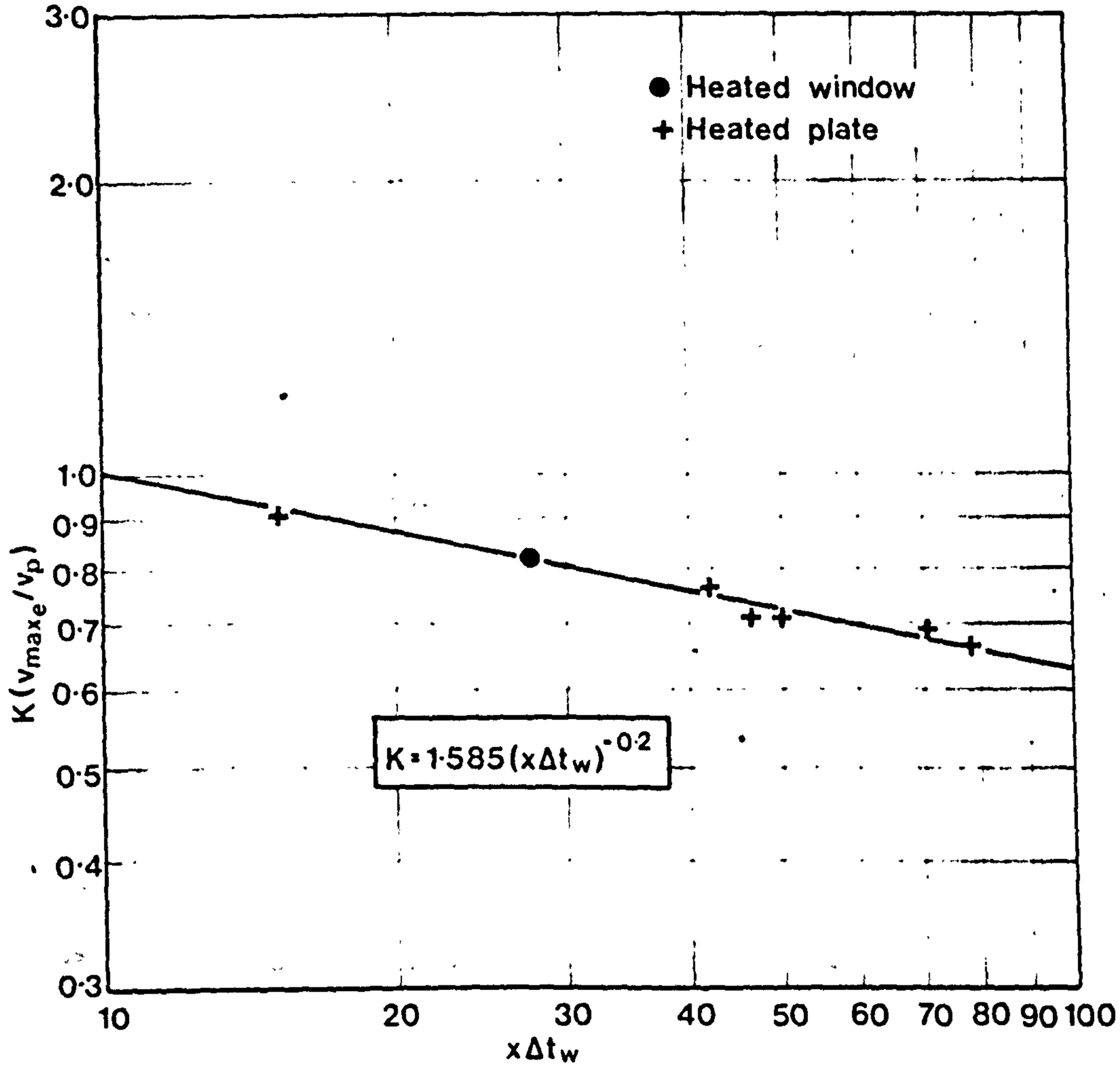

Fig.3.35. VARIATION OF ROOM AIR TURBULENCE MAXIMUM VELOCITY FACTOR K WITH $x\Delta t_w$

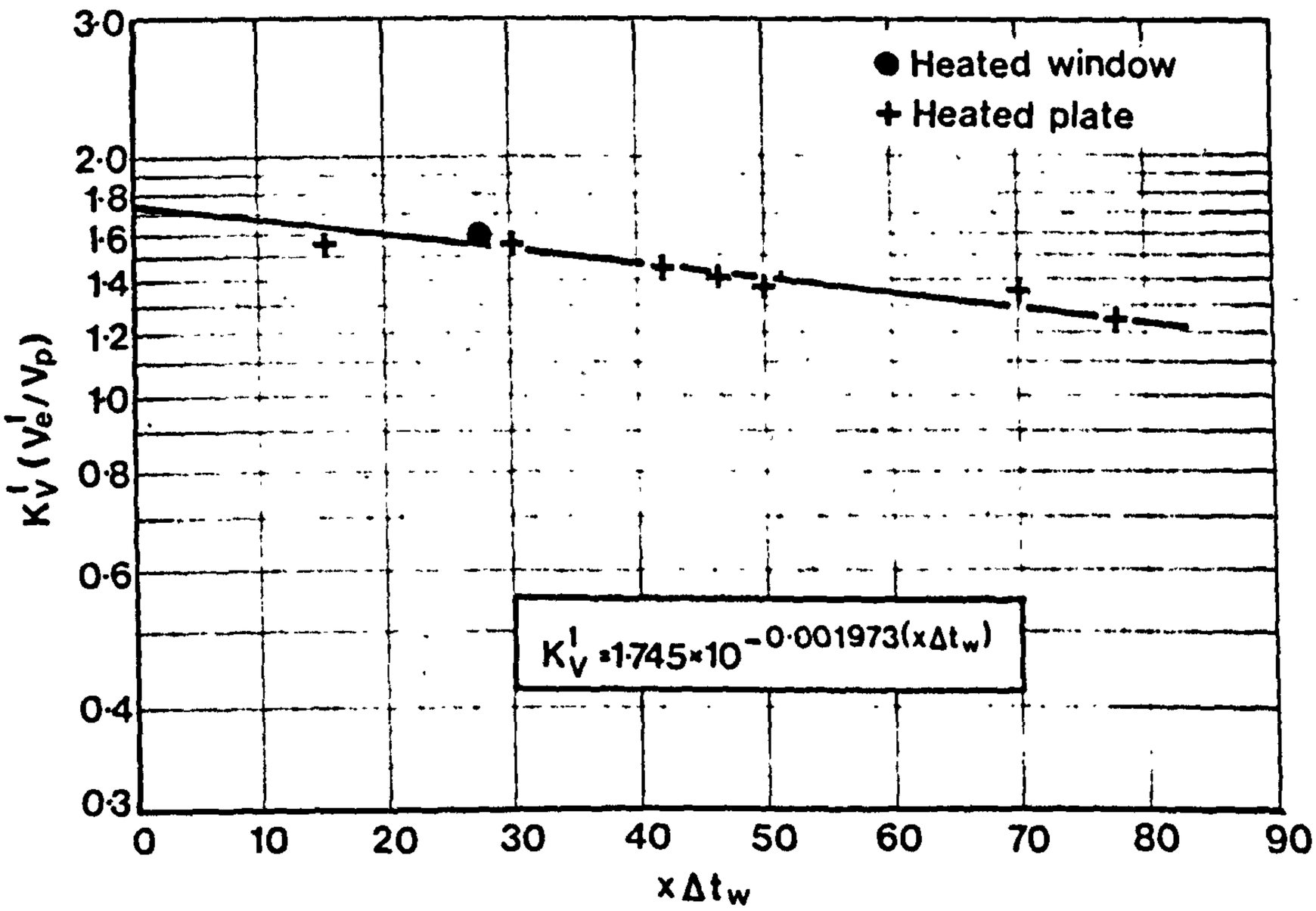

Fig.3.36. VARIATION OF EXPERIMENTAL VOLUME FACTOR K_V^1 WITH $x\Delta t_w$

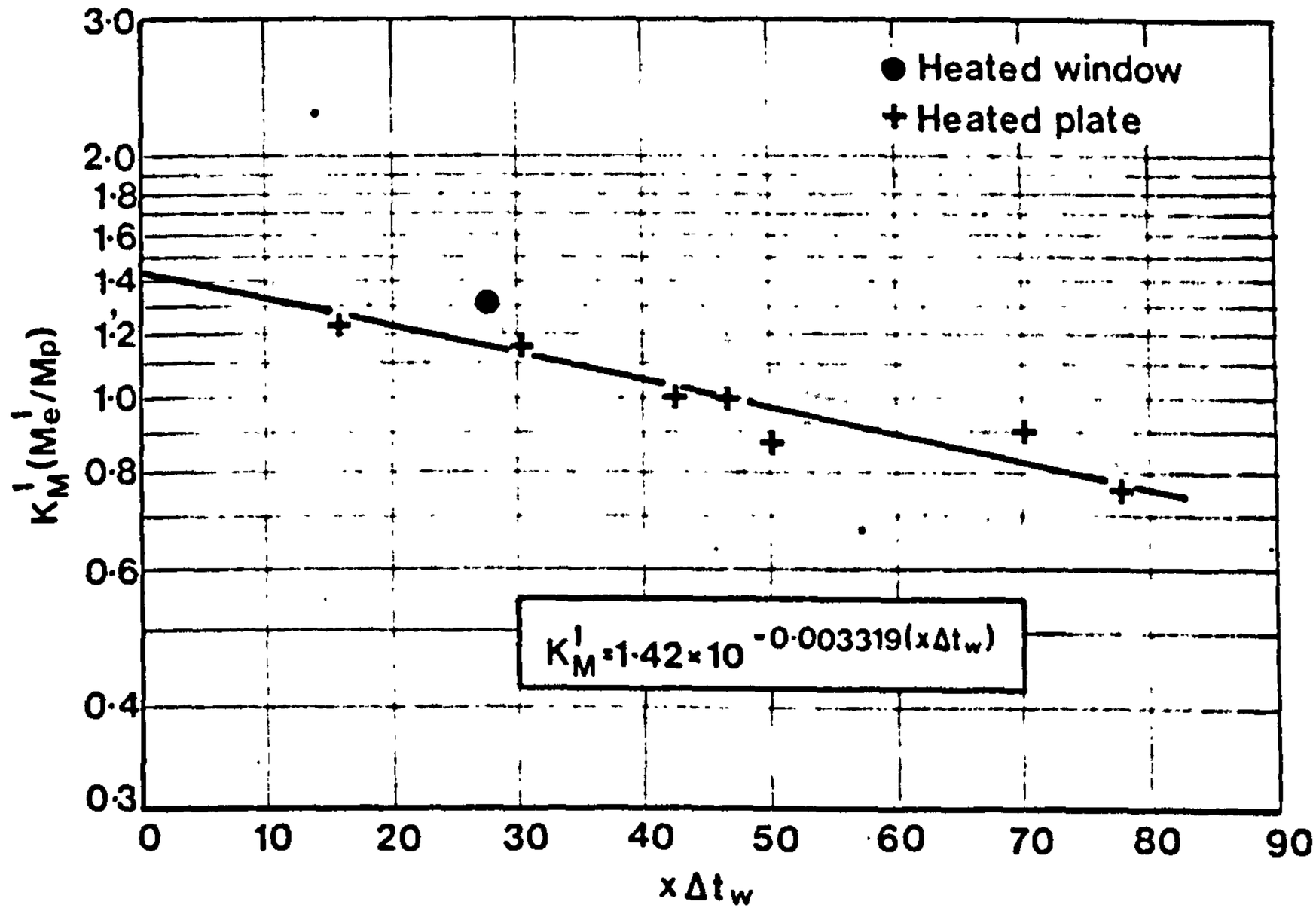

Fig.3.37. VARIATION OF EXPERIMENTAL MOMENTUM FACTOR K_V^1 WITH $x\Delta t_w$

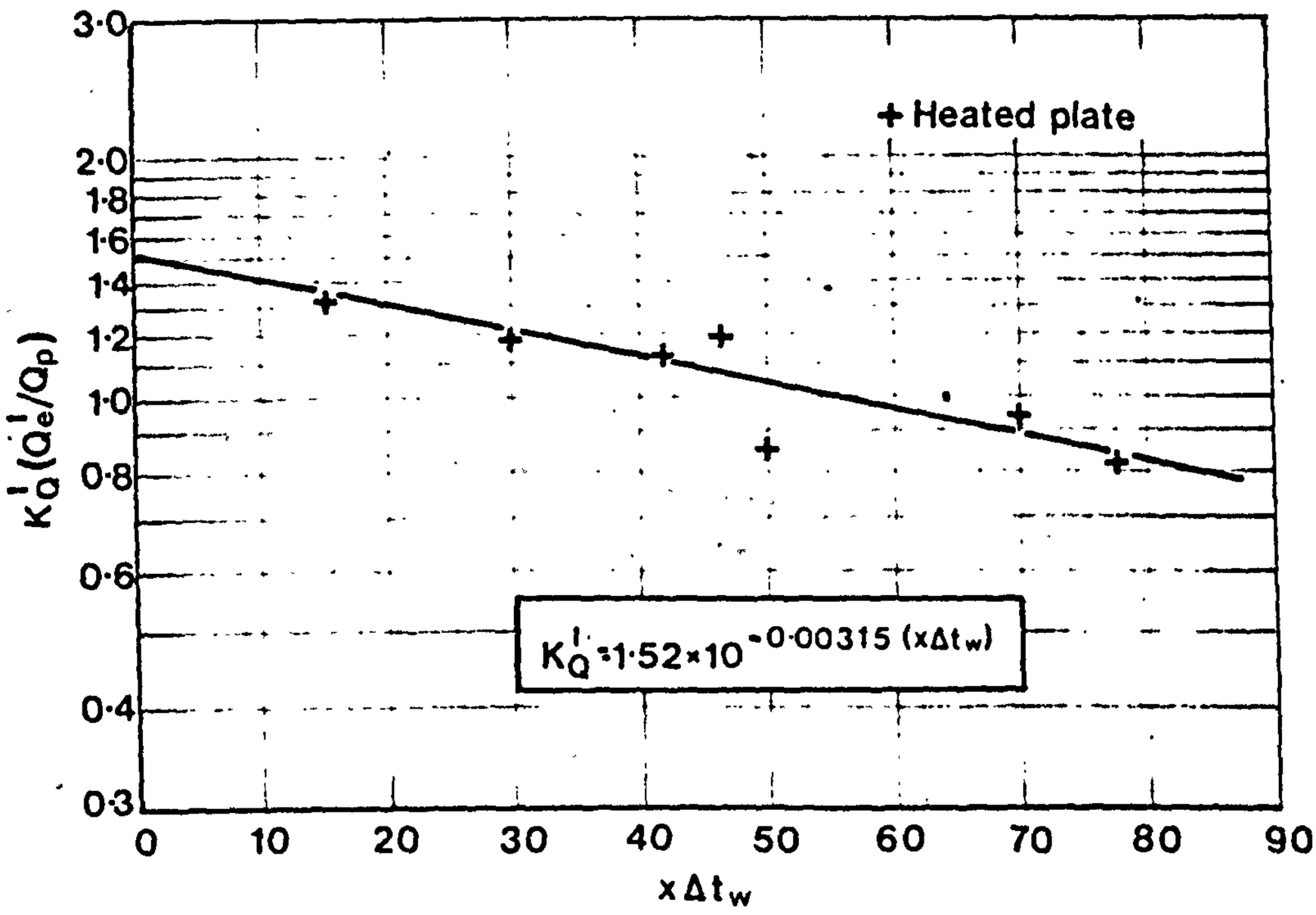

Fig.3.38. VARIATION OF EXPERIMENTAL HEAT FLUX FACTOR K_Q^1 WITH $x\Delta t_w$

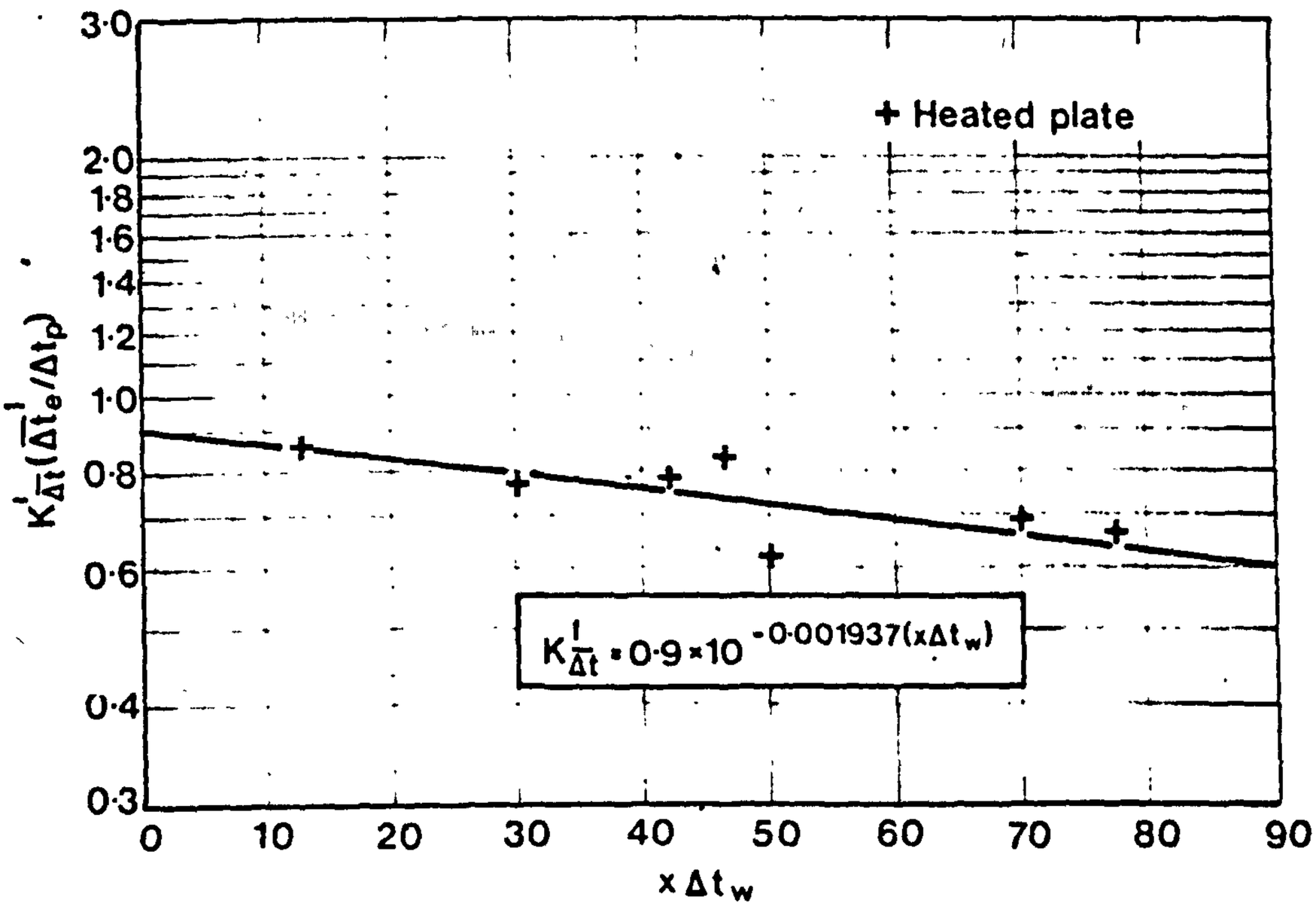

Fig.3.39. VARIATION OF EXPERIMENTAL MEAN TEMPERATURE FACTOR $K'_{\overline{\Delta t}}$ WITH $x\Delta t$

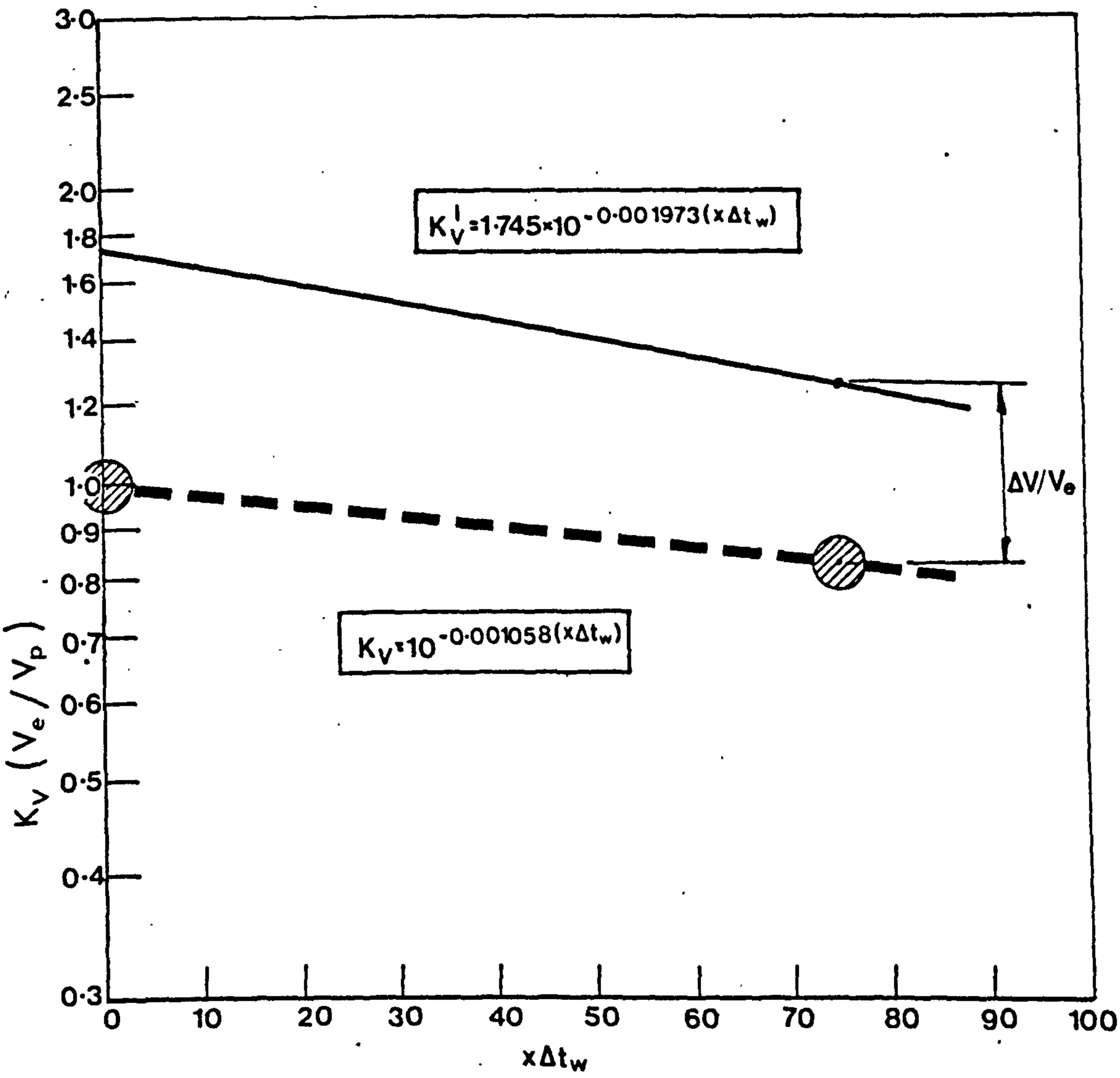

Fig.3.40. DEFINITION SKETCH OF CORRECTION FOR INFLUENCE OF VELOCITY MEASURING INSTRUMENT

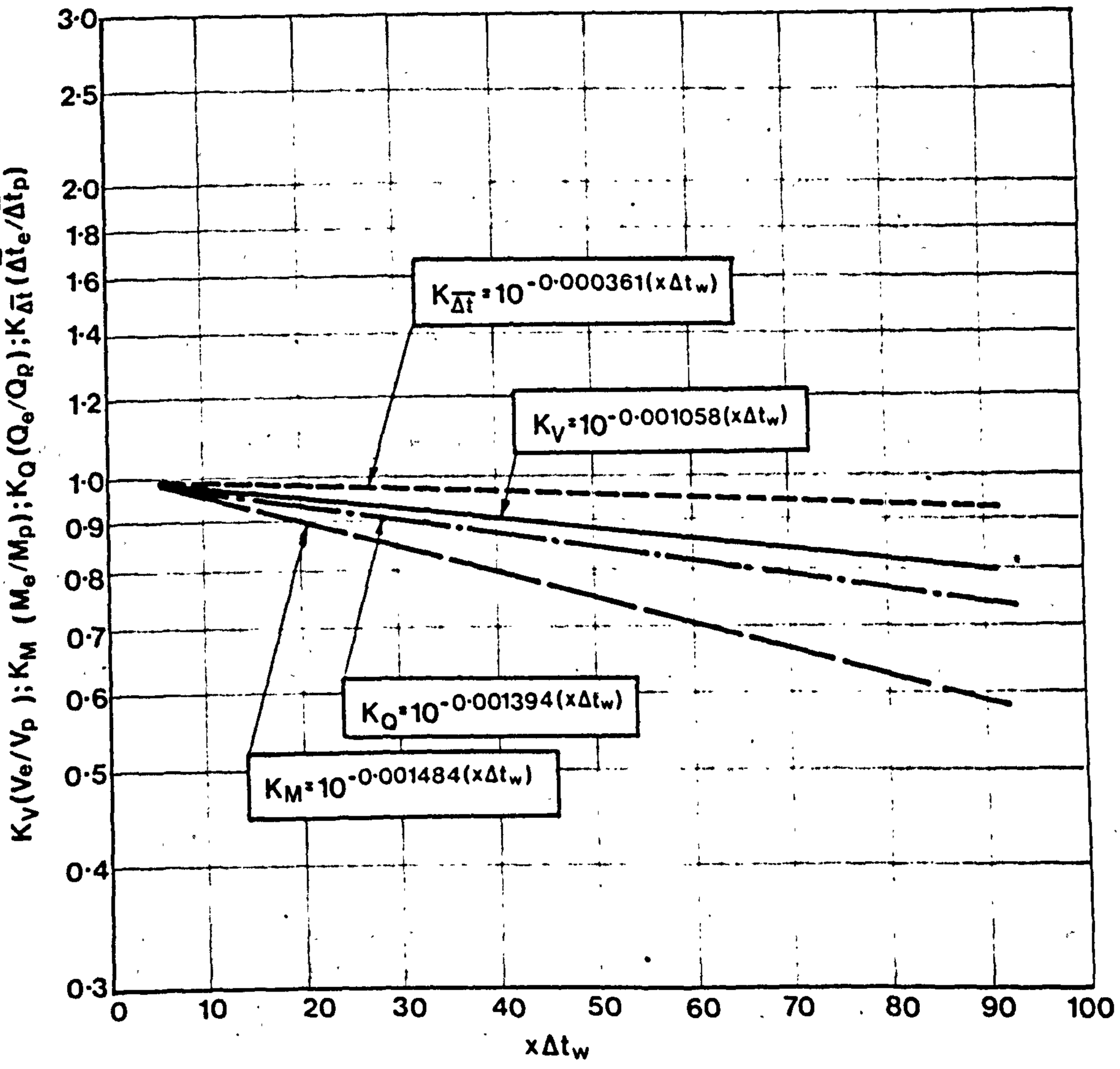

Fig.3.41. VARIATION OF ROOM AIR TURBULENCE FACTORS K_V,K_M,K_Q AND $K_{\bar{\Delta t}}$ WITH $x\Delta t$

Wall Jets

The dimensionless velocity profiles of the replacement wall jets at H = 1.55 m are plotted in Fig. 3.42. The maximum measured velocity was chosen as the velocity scale. Any attempt to predict the course of the velocity profile between measured points would not contribute significnatly to the establishment of a more accurate maximum profile velocity and might introduce an element of subjective judgement. The choice of the length scale presents a greater problem. The exact width of the jet cannot be easily identified and the velocity $v = 0.5 v_m$, used to denote the length scale $y_{0.5}$, may lie in a region of the velocity profile influenced by room air turbulence and subject to the difficulties associated with the interpretation of velocity readings in the outer part of the flow. The width of the jet was therefore chosen to be equal to the predicted boundary layer width of the convective current, namely $b = \delta_p$ (which is in good agreement with an alternative definition of the jet width, $b = y$ where $v = v_a 0$. The length scale $y_{0.5}$ can then be calculated from the Tollmien verlocity distribution for plane turbulent jets.

In view of the somewhat arbitrary choice of velocity and length scales, there is relatively good agreement of the present data (also plotted in Fig. 3.42) with both the Tollimien solution and an empirical similarity curve[8], except at the two extremes of the velocity profile. In the outer part, room air turbulence and the uncertainty in the interpretation of velocity readings can be expected to cause a discrepancy between the present data and the theoretical prediction and experimental results obtained in controlled conditions. In the region close to the wall, the present measurements indicate that the maximum of the velocity profile occurs at a greater distance from the wall then predicted by the empirical similarity curve[8]. The shift in the velocity peak could be caused by buoyancy; the core of the jet having travelled further than in an equivalent isothermal jet with the result that a wider boundary layer on the wall side has developed.

The dimensionless temperature profiles are plotted in Fig. 3.43. The temperature scale, again, is the maximum recorded value and the length scale is identical to that used in Fig. 3.42. Also plotted in the graph are two theoretical profiles, $\Delta t/\Delta t_m = v/v_m$ and $t/\Delta t_m \sqrt{v/v_m}$. The greater scatter of the temperature profiles may be explained by several factors. Perhaps a slightly better correlation could be achieved by a variation of the length factor: some scatter can be attributed to the higher percentage influence of errors on the small values of the temperature differential, but the plotted temperature profiles show a systematic difference in behaviour dependent upon the initial volume flow. Jets having high initial volume flow show no decline in temperature near the wall, whereas those characterised by lower initial volume flow have a definite maximum Δt_m at a distance of $y/y_{0.5} = 0.3$, coincidental with the velocity peaks in Fig. 3.42. Such behaviour can be explained by the heat loss through the wall -this is insignificant at high volume flow but gains in effect at low flows. It is therefore especially important to apply a high degree of insulation to the wall when low initial volume flows are likely to be encountered.

The relative distance of the replacement cross section from the nozzle, S/bo, varies little for the whole range of experiments ($S/b_o = 35 \rightarrow 38$).

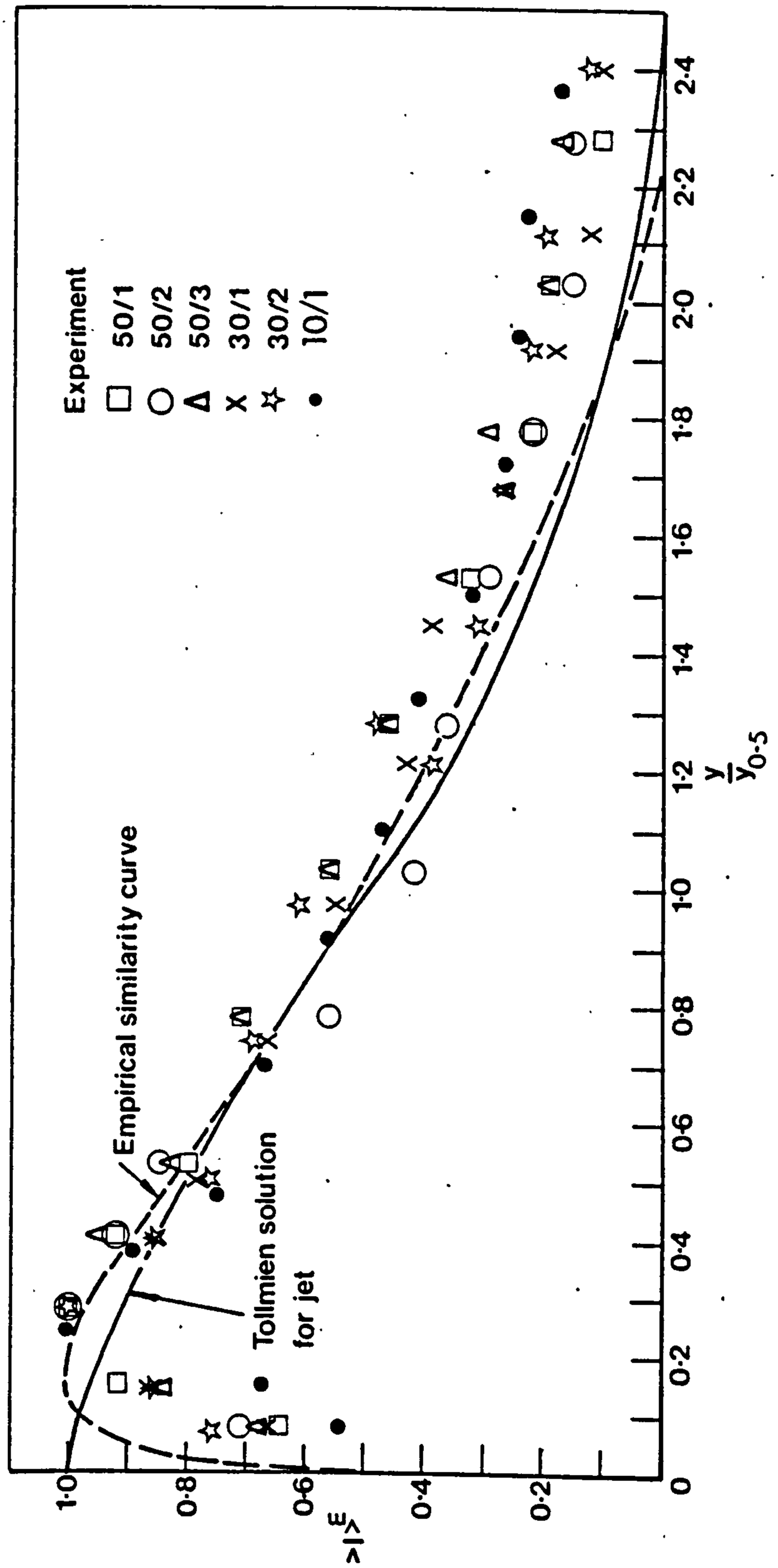

Fig.3.42. NON-DIMENSIONAL VELOCITY PROFILES OF REPLACEMENT JETS

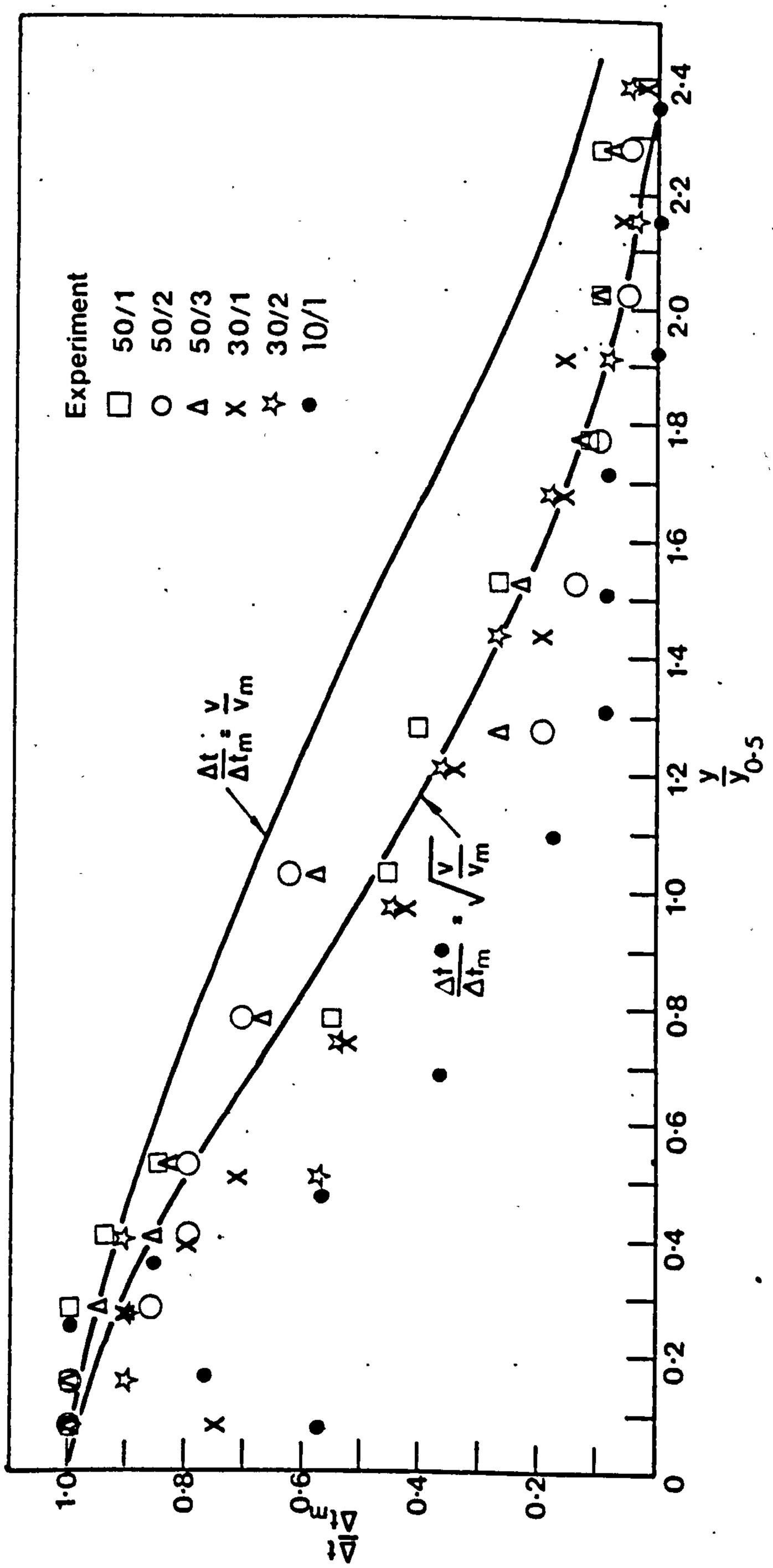

Fig.3.43. NON-DIMENSIONAL TEMPERATURE PROFILES OF REPLACEMENT JETS

The relative distance S/b_o can also be calculated theoretically using the appropriate expressions from Table 2.4, Part 2, viz.,

$$\frac{S}{b_o} = \frac{0.4}{0.178} \frac{1}{a} \qquad \ldots (3.4)$$

Equation (3.4) shows that, for a given value of the coefficient of turbulence a, the relative distance S/b_o is invariant.

The value of the coefficient of turbulence can be cound if the angle of divergence of the jet is known. This angle was found to vary insignificantly for the whole range of experiments ($6^o\ 50' \rightarrow 7^o\ 05'$). The value of the coefficient of turbulence $a' = 0.059$ can therefore, with sufficient accuracy, be assumed for all the experiments. The coefficient of turbulence is denoted as a' because it has been modified by the action of the forces of buoyancy. The value of the non-modified (iso-thermal) coefficient of turbulence a can be calculated from the rearranged equation (2.101).

$$a = a' \left(1 + \frac{\Delta x'}{x'}\right) \qquad \ldots (3.5)$$

where x' is the position that an element of the jet would have reached if forces of buoyancy were not present and $\Delta x'$ is the additional distance travelled due to buoyancy. (Therefore $x = x' + \Delta x'$, and in this case $x = S$). The value of $\Delta x'/x'$ can be calculated using expressions in Table 2.3 by an iterative process. The thus calculated values range from 0.081 to 0.098 for nozzle Reynolds numbers $Re = 0.5 \rightarrow 0.7 \times 10^3$, which agrees well with the values of the coefficient of turbulence for the initial region a_i in Fig. 2.18 (calculated from experimental data of O'Callaghan et al [9]) and not with the main region values a_M. A correlation with a_M would be expected as $S > L_i$.

Experimental results, however, show that, for all the experiments, the maximum profile velocity at S (see Table 3.5) is equal to the initial nozzle velocity. The discrepancy can only be accounted for by buoyancy. As an example, in Fig. 3.44, the relative iso-thermal maximum velocity for Experiment 30/2 (calculated according to equation (2.46) corrected for the influence of the wall and non-uniform initial flow conditions) is plotted against two scales, x/b_o and x'/b_o, where x'/b_o is the iso-thermal scale. When buoyancy forces are present, an element at a given x'/b_o characterised by a value of v_m/v_o will have travelled farther to x/b_o ($x/b_o = x'/b_o\ (1 + \Delta x'/x')$) and have acquired an additional velocity component w'/v_o. The value of w'/v_o has been taken as half the theoretical value calculated according to equation (2.95) because it does not take into account friction and mass interchange with the rest of the jets. The sum of the two components v_m/v_o and w'/v_o, results in the maximum of the velocity profile being practically invariant and equal to the initial velocity over the interval of x/b likely to be encountered. The two plotted experimental results, Experiment 30/2 (for $S/b_o = 36$) and Experiment 30/3 (identical to Experiment 30/2 except $S/b_o = 41$), confirm the invariant behaviour of the maximum velocity.

The velocity and temperature profiles of two pairs of experiments, the two in each pair being identical except for the distance S, are plotted in Fig. 3.45 and Fig. 4.46. Fig. 3.45 shows that there is practically no difference in the velocity profile within each pair and the maximum

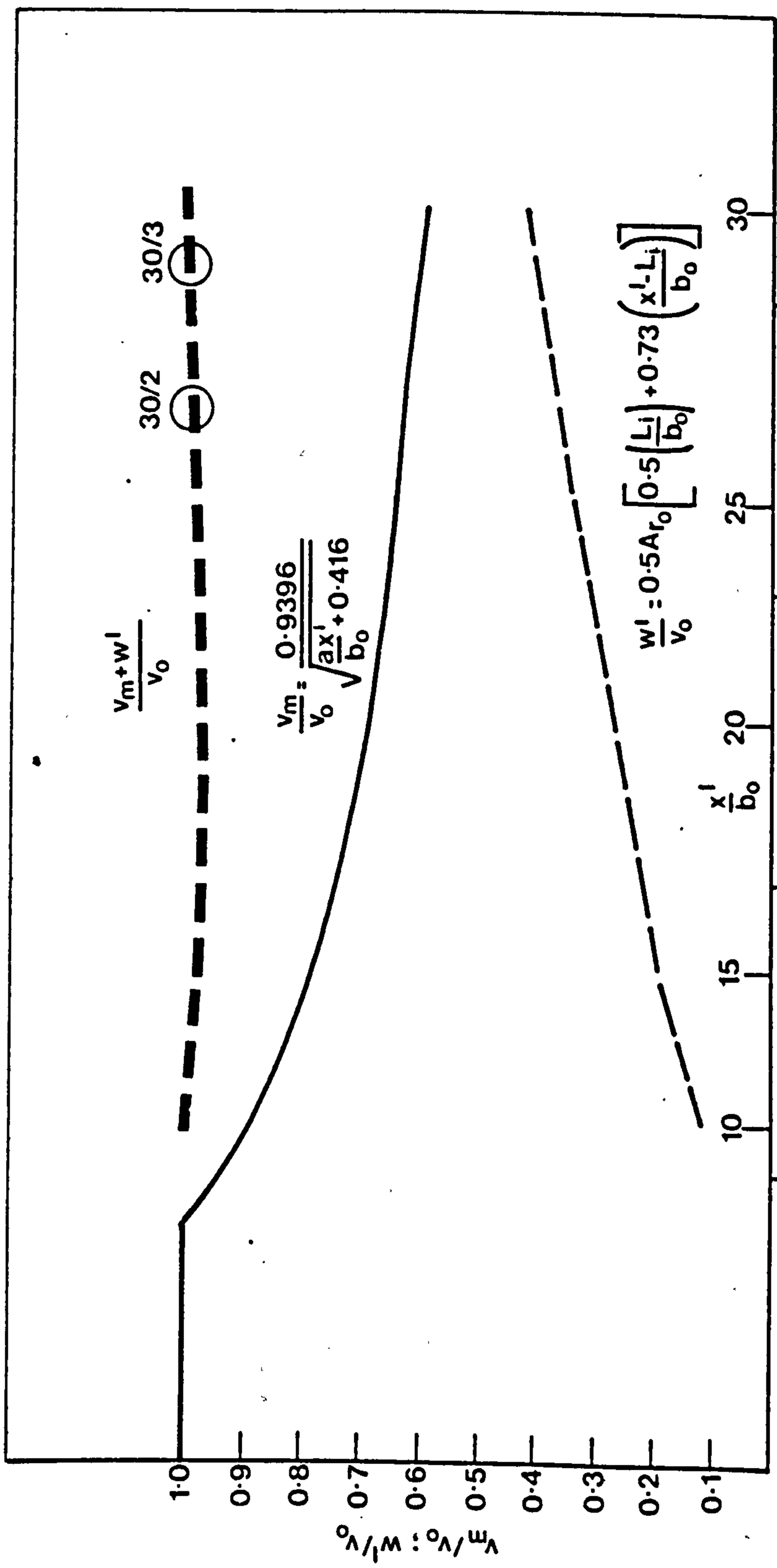

Fig.3.44. VARIATION OF INERTIA AND BUOYANCY COMPONENTS OF THE MAXIMUM WALL JET VELOCITY WITH RELATIVE DISTANCE FROM THE NOZZLE

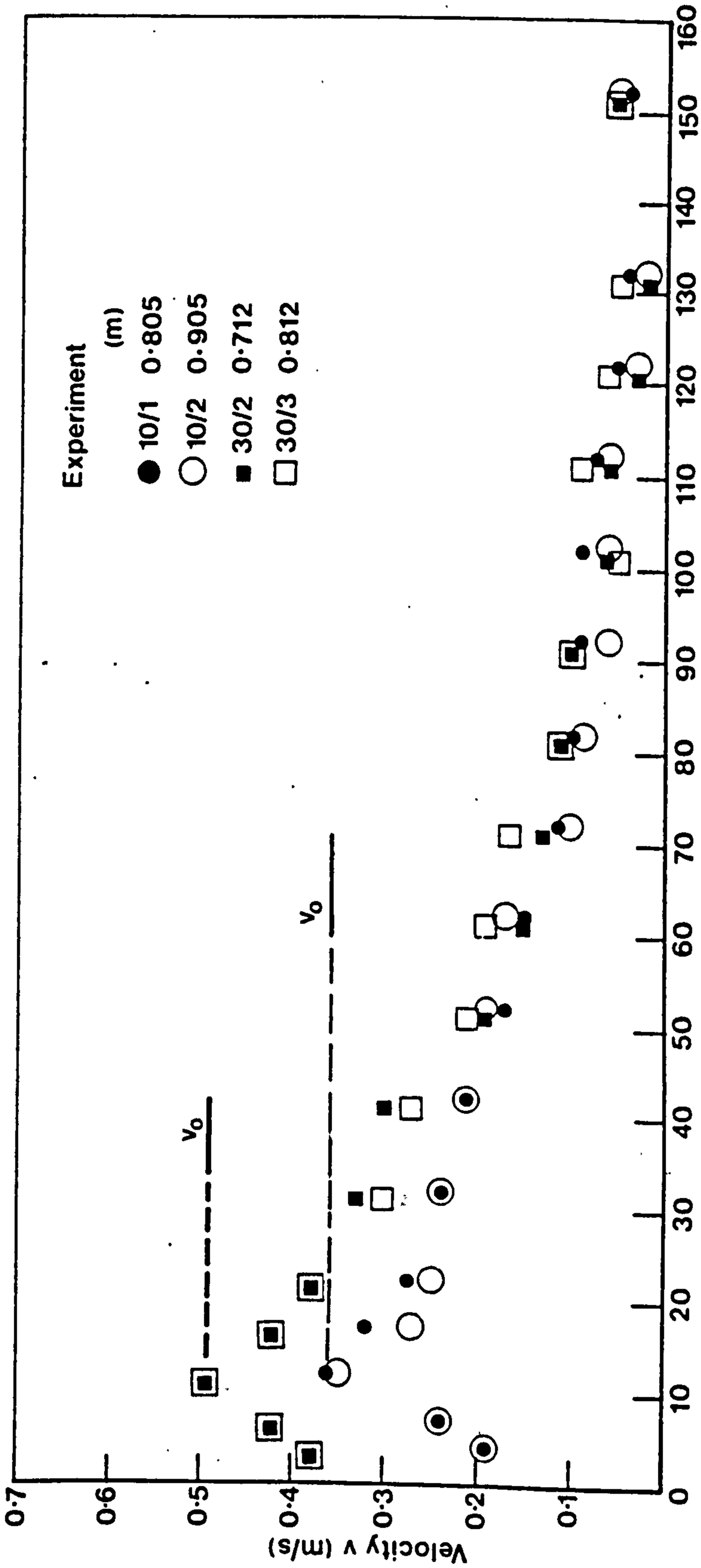

Fig.3.45. EFFECT OF VARIATION OF DISTANCE FROM NOZZLE ON THE VELOCITY PROFILE

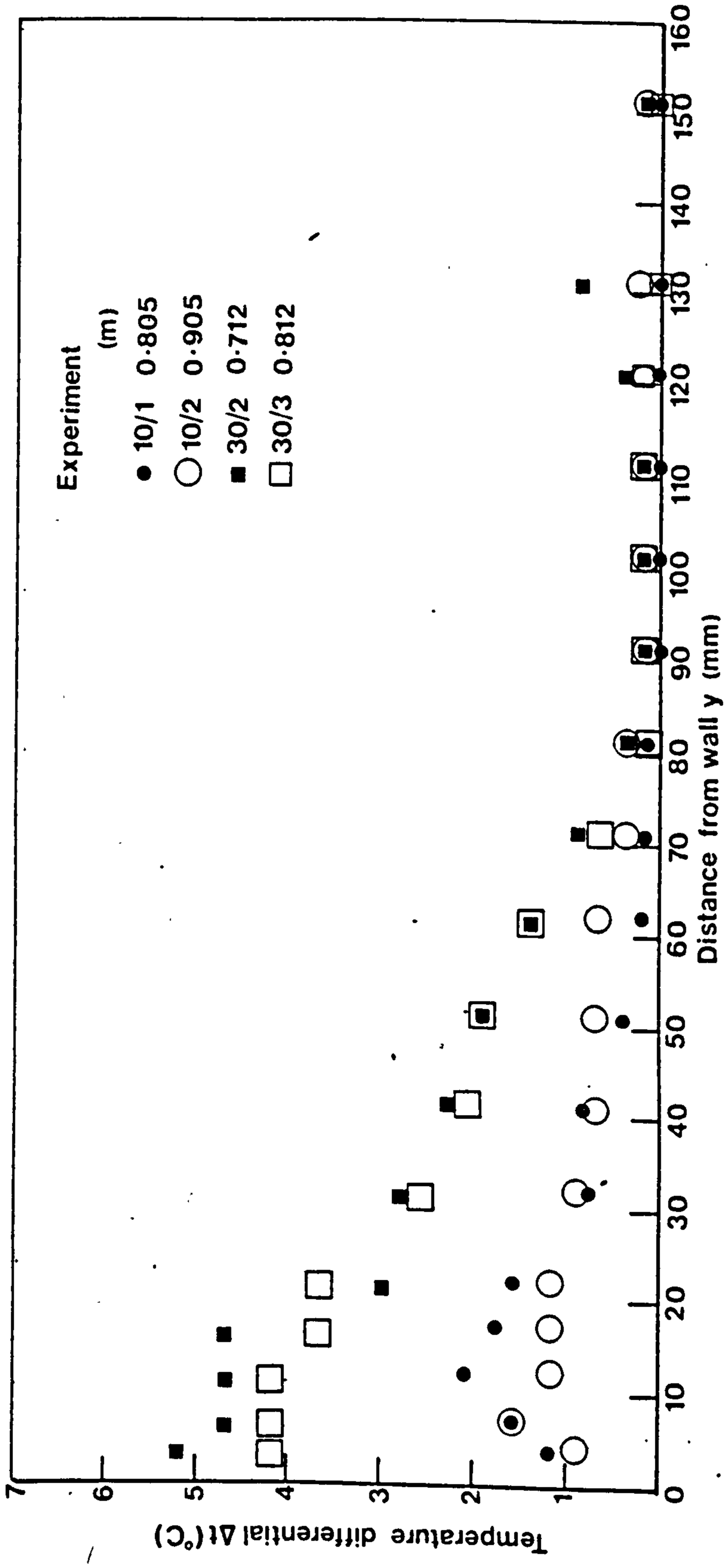

Fig.3.46. EFFECT OF VARIATION OF DISTANCE FROM NOZZLE ON THE TEMPERATURE PROFILE

velocity is equal to the initial velocity. The temperature profiles in Fig. 3.46 show a distinct decline at greater values of S, the maximum recorded temperature being noticeably affected.

In order to assess the influence of the forces of buoyancy on jet parameters at the replacement cross-section, the main results tabulated in Table 3.2 have been analysed in greater detail.

The data, in the first instance, have to be corrected in order to take into account the nature of the flow in the outer part of the jet and its effect on the interpretation of the velocity readings. Flow visualisation tests, see Fig. 3.47, have shown that the mean flow in the outer part of the jet is also controlled by large, organised structures as discussed in Chapter 3, Section 2.5. These observations confirm the similarity of convective and wall jet profiles at the replacement cross-section in Fig. 3.24, Fig. 3.26 and Fig. 3.28. If the similarity of the outer parts of jet and convective flows is accepted, the non-dimensional factors in Fig. 3.36 to Fig. 3.41 can also be applied to the wall jet results. To account for the inaccuracy due to the "false" velocity reading in the outer part of the velocity profile, the following type of correction can be made, the volume flow being used here as an example:-

$$V_e = V_e^* \frac{K_V}{K_V^*} \qquad \ldots (3.6)$$

where K_V is the recalculated dimensionless factor that reflects solely the influence of room air turbulence (Fig. 3.41) and K_V^* is the dimensionless factor that is influenced not only by room air turbulence but also has a "false" velocity reading component.

In the calculation of predicted values at the replacement cross-section, allowances have to be made for non-uniform initial conditions and the effect of room air turbulence on the wall jet. To allow for non-uniform initial conditions the correction factor $\sqrt{\beta_o}$, calculated according to equation (2.59a), was applied. The jet, obviously, is not affected by room air turbulence to the same degree as the original convection current because the length over which it is exposed is significantly shorter. To take the difference in length into account the following formula was used (volume flow, again, being used as an example):-

$$V_p = V_p^* \left[K_V + (1 - K_{V(H-S)})\right] \qquad \ldots (3.7)$$

where $K_{V(H-S)}$ is the dimensionless room air turbulence factor at H-S for the equivalent original Δt_W.

One of the simplifying assumptions made in Chapter 2.3.3. is that all energy added by Archimedean forces is transformed into additional momentum of the jet and therefore no additional volume flow is generated. In order to compare predicted and experimental results, the volume flow at S has to be calculated. The process involves ascertaining the position of the jet S' which would have been reached if buoyancy were not present. The values of S' were calculated, as mentioned before, using expressions from Table 2.3 (and the coefficient of turbulence as per equation (3.5)) by an iterative process. The predicted and measured values of volume flow show a systematic divergence with initial temperature within each

Fig. 3.47. FLOW VISUALISATION OF REPLACEMENT JET

group of tests (i.e. for simulated $\Delta t_w = 50^oC$ and $\Delta t_w = 30^oC$): higher initial temperatures result in greater excesses as measured over the predicted volume flows at S.

In Fig. 3.48, non-dimensional ratios of experimental, V_e, over predicted, V_p, volume flows are plotted against $\Delta t_o V_o$ (which can be interpreted as representing the heat content of the jet). The dependence, expressed by the formula

$$B_V = \frac{V_e}{V_p} = (10 \times \Delta t_o V_o)^{0.157} \qquad \ldots (3.8)$$

shows that with rising $\Delta t_o V_o$ more ambient air than predicted is entrained into the jet. A direct confirmation of this trend is possible: a comparison of Experiment 50/1, Experiment 50/2 and Experiment 50/3 (Table 3.5) shows that the only significant reaction to an approximately 40% rise in initial nozzle temperature is the higher volume flow (and therefore also momentum flux) in spite of a 6% reduction in nozzle width.

The basic property of an isothermal jet is that the momentum flux remains invariant throughout its length. The present results show that the measured momentum flux at S is significantly greater than the initial ($M_e/M_o = 1.5 \rightarrow 2.1$) indicating that the contribution of buoyancy generated momentum is important. The buoyancy component of the total predicted momentum flux at S was calculated according to equation (2.100) for $x' = S'$ and accounted for a higher proportion of the total ($75 \rightarrow 85\%$). In Fig. 3.49, the ratios of measured and predicted values for the six experiments have been plotted against $b_o v_o^2$ (which expresses the initial momentum of the jet). The dependence can be expressed as a simple equation

$$B_M = \frac{M_e}{M_p} = 94\ (b_o\ v_o^2) \qquad \ldots (3.9)$$

Fig. 3.49 shows that better agreement between predicted and measured values exists at higher values of $b_o\ v_o^2$. These higher values can be interpreted as denoting "strong" jets, less likely to be influenced by wall friction or room air turbulence and in general suffering less from rapid temperature decay. A case of rapid temperature decay is illustrated in Fig. 3.46 where for $b_o\ v_o^2 = 4.5 \times 10^{-3}$ (Experiment 30/2 and 30/3) a 20% decay in maximum temperature occurs over a distance of $5x/b_o$, whereas for $b_o\ v_o^2 = 2.8 \times 10^{-3}$ (Experiment 10/1 and 10/2) the decay reaches 25% over $4.7\ x/b_o$. It should be noted that, although the jet as a whole is influenced by the above mentioned factors, the velocity core remains unaffected.

The heat content of a jet, in ideal circumstances, should also be invariant along its length. In the discussion, so far, evidence has been presented showing a rapid temperature decay (faster than the velocity decay), which, as Fig. 3.31 indicates commences immediately the flow leaves the nozzle. The ratio of the measured-to-predicted heat content, Q_e/Q_p, for the six experiments is plotted in Fig. 3.50, against $b_o\ v_o^2$. The equation expressing the relationship, namely

$$B_Q = \frac{Q_e}{Q_p} = 130\ (b_o\ v_o^2) \qquad \ldots (3.10)$$

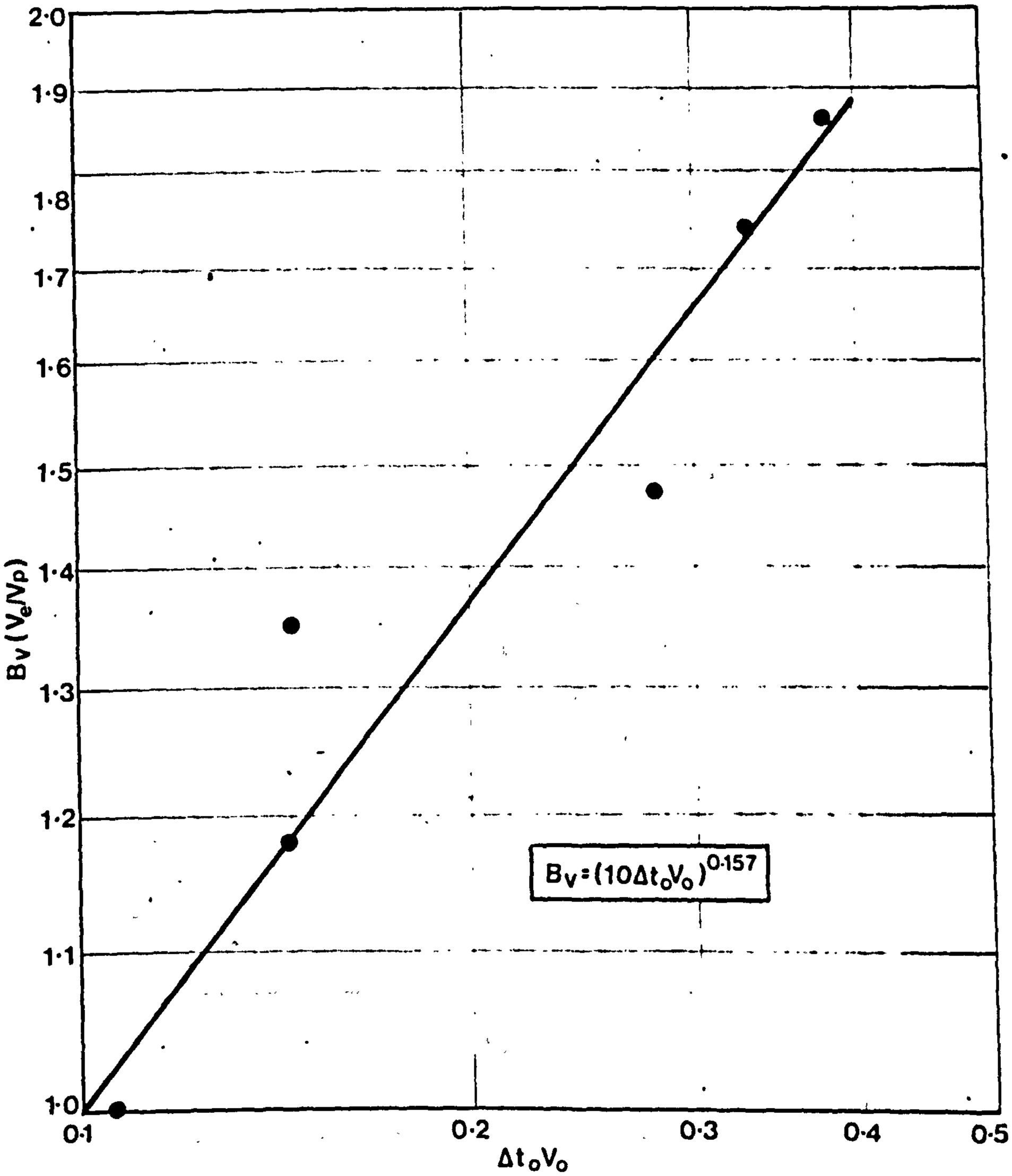

Fig.3.48. VARIATION OF THE BUOYANCY VOLUME FLOW FACTOR B_V WITH $\Delta t_o V_o$

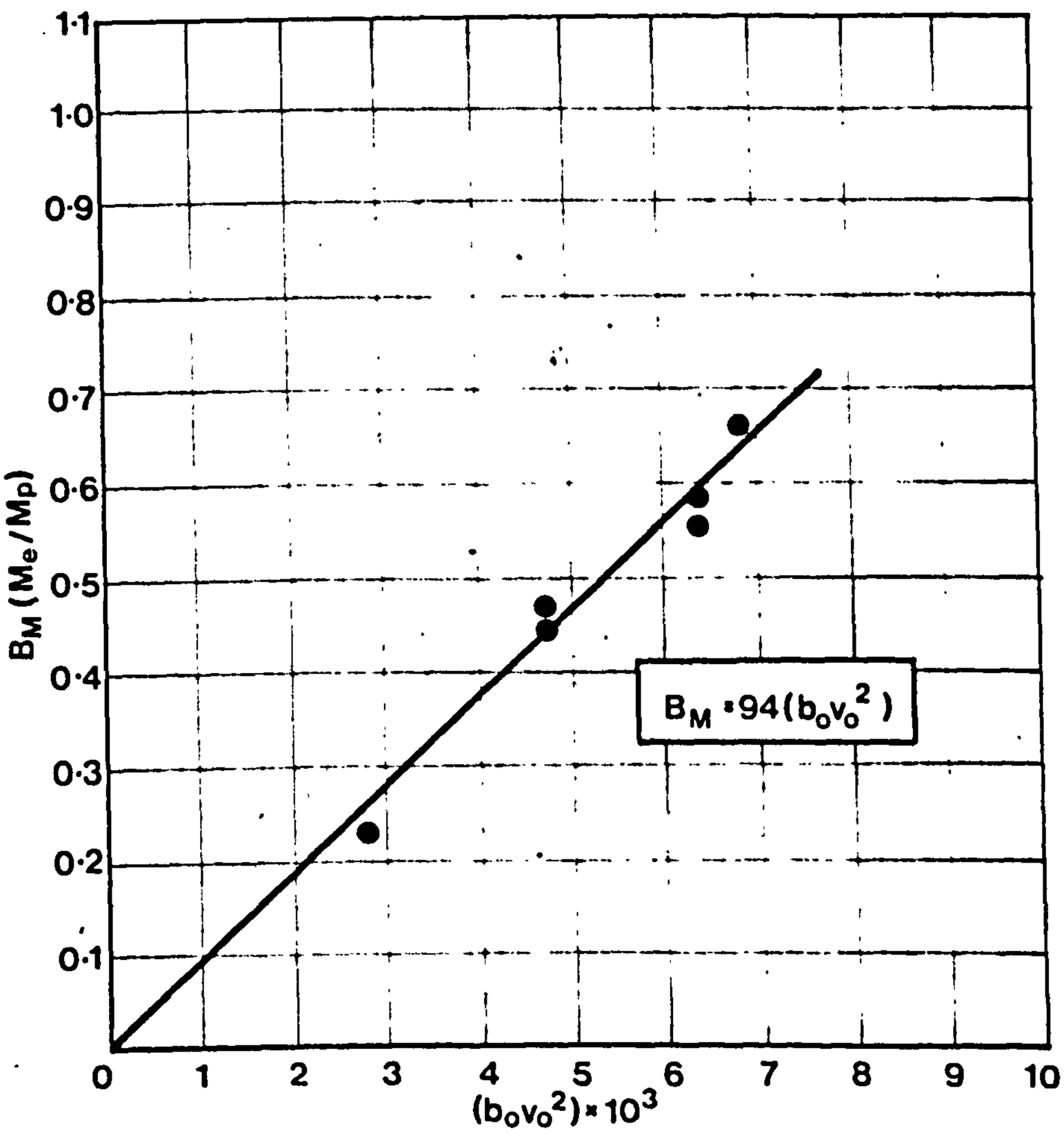

Fig.3.49. VARIATION OF THE BUOYANCY MOMENTUM FACTOR B_M WITH $b_o v_o^2$

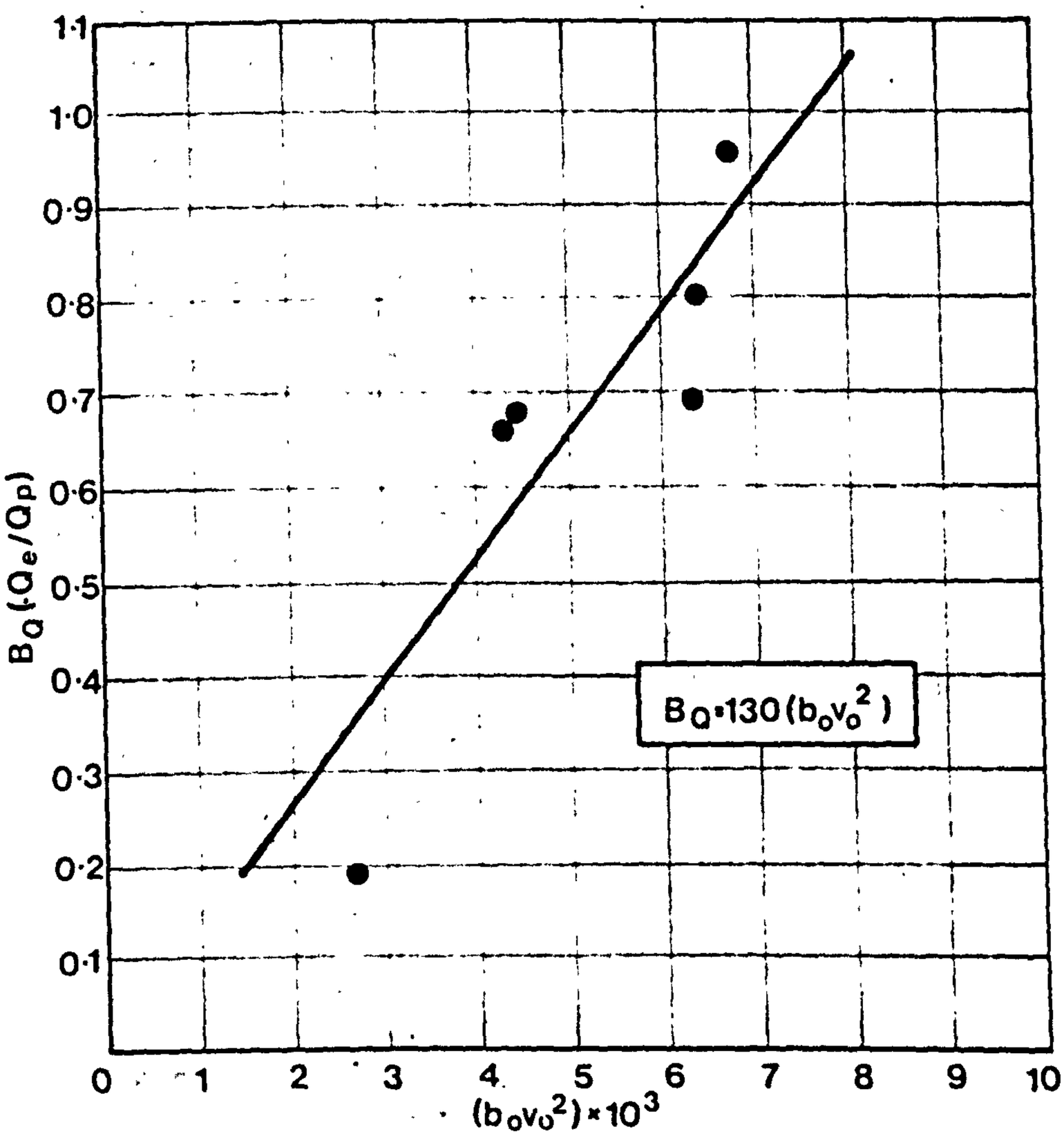

Fig.3.50. VARIATION OF THE BUOYANCY HEAT FLUX FACTOR B_Q WITH $b_ov_o^2$

shows that, as is the case with momentum flux, the "stronger" jets are less influenced by temperature decay.

As has been mentioned above, raising the initial temperature (i.e. increasing the initial heat content) does not result in an increase of the heat content at the replacement cross-section. A plot, in Fig. 3.51, of the ratios of the heat content at S to initial, Q_e/Q_o, against the ratio of initial temperature difference to the nominal convective surface temperature differential, $\Delta t_o/\Delta t_w$, indicates by the slope of the tentative curves for Δt_w 50°C and Δt_w = 30°C that it is counter-productive to raise the initial temperature difference above the value obtained from the formula for the calculation of replacement parameters in Table 2.4.

Replacement of convective currents by wall jets

Three cases of the replacement of convective currents, at a nominal temperature differential betweem the surface and ambient air temperature of 10, 30 and 50°C, by wall jets have been examined. Although the experiments embraced a wide range of Rayleigh numbers (Ra = 3.5×10^9 to 1.3×10^{10}), the flow at the replacement cross-section was always turbulent, and therefore the turbulent region formulae in Table 2.4 were used in the calculation of replacement jet initial parameters (which were listed in Table 3.1).

As has been shown in the discussion of convective flows, the convective current parameters in natural ambient conditions differ from theoretical predictions and experimental data obtained under controlled conditions. The influence of room air turbulence can be described, in a convenient form, by the dimensionless factors K, K_V, K_M and K_Q. A comparison of the influence of room air turbulence at two different levels (one, in the test room, induced by an air-conditioning terminal and the other, in the laboratory, generated solely by natural means) indicates that, once room air turbulence is present, its effect on the main convective flow will not vary significantly. It can therefore we assumed that the values of the dimensionless factors in Fig. 3.35 and Fig. 3.41 have a more general application, and only in unusual circumstances would new, different, factors have to be obtained.

The main aim of the experiments, i.e. the replacement of convective currents by wall jets under as near identical conditions as possible, has been achieved to a degree not envisaged at the onset of the project. A comparison of the main parameters in Table 3.5 and of velocity and temperature profiles in Fig. 3.24 to Fig. 3.29 shows that there is an identity of the maximum velocity, volume flow and momentum flux. The velocity profiles, given the basic dissimilarity of the two flows, are also in surprisingly good agreement. It is only the heat content at the replacement cross-section that shows a shortfall. Fortunately, it is the parameter that, in most circumstances, has the least direct influence on room air movements (compared for example with the momentum flux). The reason for the apparent inability to obtain full agreement of the temperature profiles, as the above discussion has shown, is the rapid decay of temperature along the jet.

To generalise the results, a procedure for the calculation of replacement parameters is suggested below. The application is limited to cases of

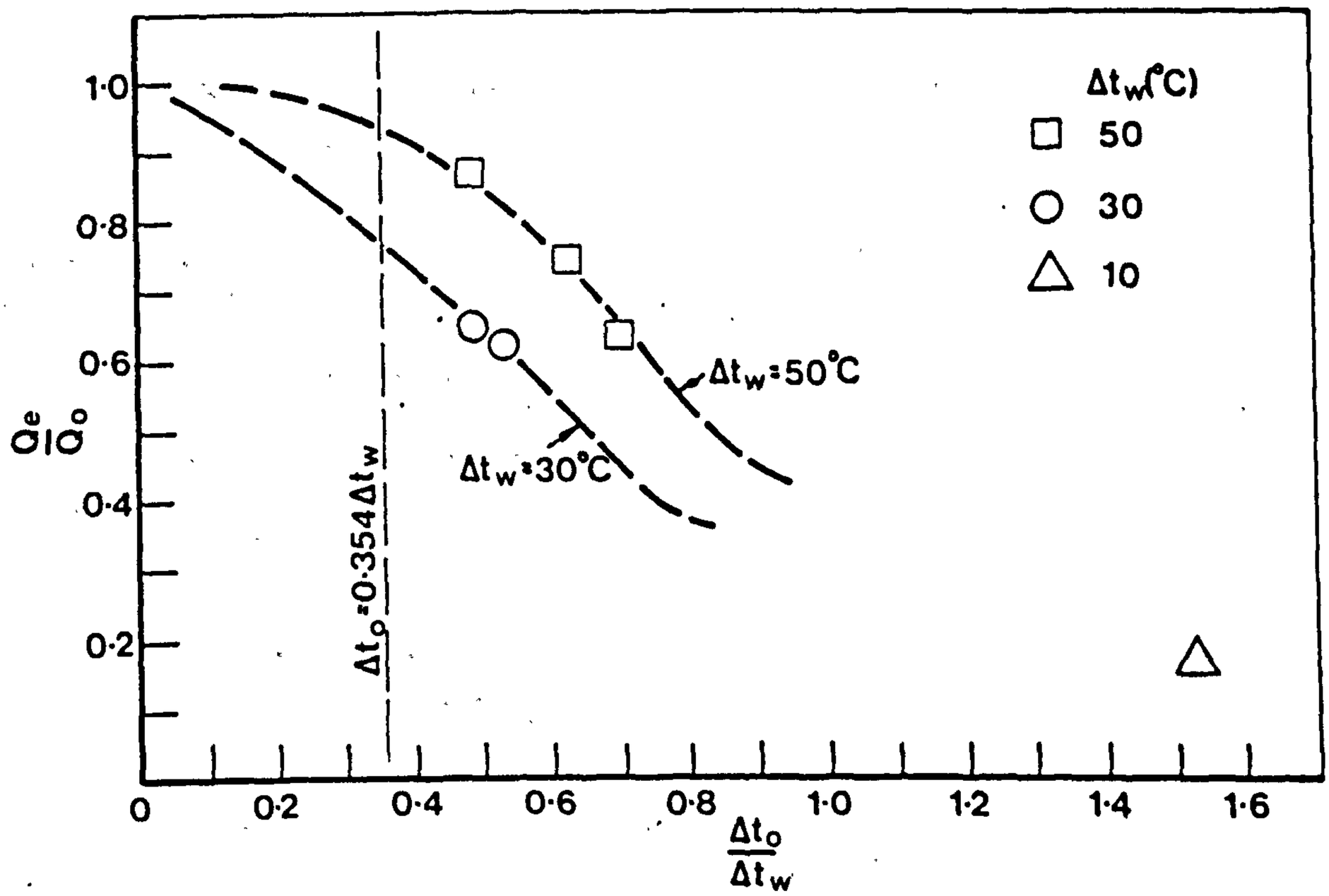

Fig.3.51. VARIATION OF THE RELATIVE HEAT CONTENT OF WALL JETS AT THE REPLACEMENT CROSS SECTION Q_e/Q_o WITH $\Delta t_o/\Delta t_w$

usual room air turbulence levels and turbulent flow in the original convective current at the replacement cross-section. The present experimental results suggest a relative insensitivity of wall jet parameters at the replacement cross-section to variations of the initial parameters, with the exception of the maximum nozzle velocity. This apparently inherent stability can be explained by the configuration of the replacement jet calculation formulae (expressing the nature of the phenomenon) and by the stabilising effect of the forces of buoyancy.

If, as has been shown in the discussion of the replacement wall jets, the initial jet velocity equals the maximum velocity at the replacement cross-section, then

$$v_o = Kv_{max} \qquad \ldots.(3.11)$$

where the value of v_{max} can be determined from the appropriate expression in Table 2.4 and of K from Fig. 3.35.

As any further rise of the initial temperature has been shown to be counterproductive, the initial temperature differential Δt_o can be calculated using the expression given in Table 2.4.

The distance of the nozzle from the replacement cross-section S can, again, be calculated directly from the appropriate formula if the value a_i is substituted by the corrected coefficient of turbulence a_i' which takes into account the effect of buoyancy. For the present series of tests ($Re = 0.5 \rightarrow 0.7 \times 10^3$) the value was found to be $a_i' = 0.059$. In other cases, a_i' can be calculated from equation (2.101), where a value for a_i can be found in Fig. 2.18. As the present test results have shown a particular insensitivity to minor variation of S, so the value $a_i = 0.059$ can be used with confidence.

The initial velocity being subject to the strict requirements expressed by equation (3.11), the only parameter that can be varied to accommodate the influence of room air turbulence, buoyancy and non-uniform initial conditions is the nozzle width b_o. The correction for the effect of room air turbulence on the original convective current (and therefore also requiring a modification of the replacement nozzle width) can be calculated according to equation (2.128) and for non-uniform initial nozzle conditions according to equation (2.144). The presence of Archimedean forces results in additional momentum being imparted to the jet. The calculation of the additional, buoyancy generated, momentum is a complex, iterative, process and therefore a more simple alternative approach, based on a correction coefficient, is suggested. This alternative approach is only known to be strictly valid over the range covered by the experimental data. Nevertheless the range $H\Delta t_w = 15.5 \rightarrow 75.5$ is sufficiently wide for the great majority of applications but in special cases additional buoyancy generated momentum and the compensatory variations of the nozzle width would have to be calculated individually. The experimentally derived nozzle momentum buoyancy coefficient K_ρ is the ratio of the measured momentum flux M_e to initial momentum flux $M_o = b_o v_o^2 \rho_o$. The variation of the nozzle momentum buoyancy coefficient K_ρ with $\Delta t_o V_o$ is shown in Fig. 3.52. The value of $\Delta t_o V_o$ can be calculated from formulae in Table 2.4.

The corrected nozzle width is therefore

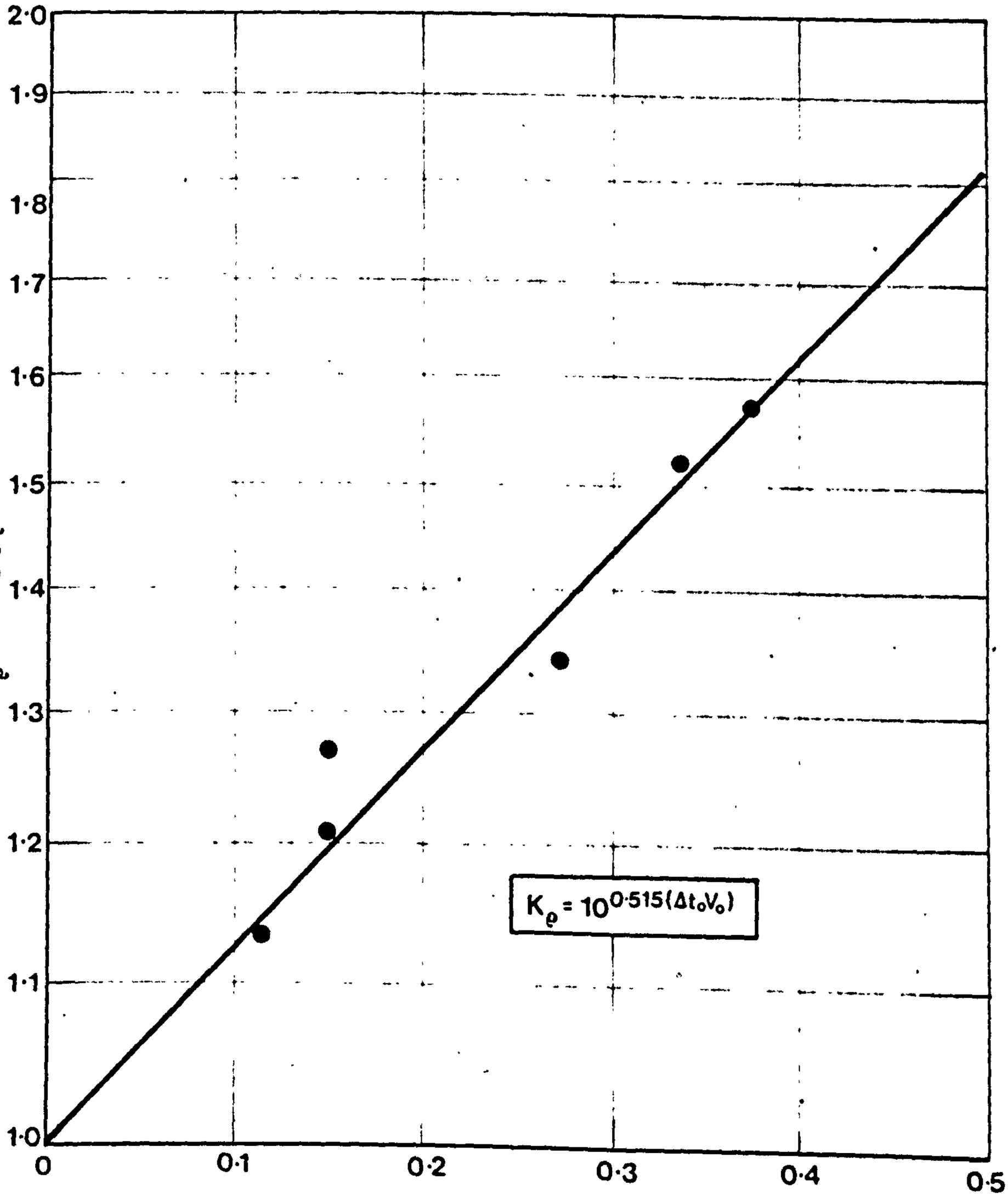

Fig.3.52. VARIATION OF THE NOZZLE MOMENTUM BUOYANCY COEFFICIENT K_e WITH $\Delta t_o V_o$

$$b_o' = b_o \frac{K_M}{K^2} \frac{\Psi}{\Phi} \frac{[K_M + (1-K_{M(H-S)})]}{K_\rho} = K_o b_o \quad \ldots(3.12)$$

where $[K + (1-K_{M(H-S)})]$ has been introduced to compensate for the influence of room air turbulence on the jet. Substituting values of K, K_M, $K_{M(H-S)}$ and K_ρ from the relevant graphs (Fig. 3.34, Fig. 3.41 and Fig. 3.52) shows that, for $H\Delta t_w$ = 15.5 to 77.5 and Ψ/Φ =1.1 (i.e. for Ψ = 0.75; Φ = 0.675), the value of the nozzle width coefficient K_o varies little, i.e. from K_o = 1.11 to 1.09. For the above range of $H\Delta t_w$ and a mean value of K_o = 1.1 the corrected nozzle width can be expressed as

$$b_o' = 0.02156\ H^{0.7}\ \Delta t_w^{0.1} \quad \ldots (3.13)$$

For different values of Φ and $\Psi_\Psi$equation (3.13) can be corrected by multiplying the result by $0.91\ \frac{\Psi}{\Phi}$.

3.4. CONCLUSIONS

The primary aim of the experimental work described in Part 3 has been to test the feasibility of replacing convective streams by wall jets, which is the essence of the new approach to modelling room air movements proposed in Part 1. A secondary objective, once the feasibility and mechanics of the replacement of convective currents by wall jets had been established, was the formulation of a simple procedure for the direct calculation of replacement-jet initial parameters from convective surface parameters that would cover the majority of practical applications.

Before attention could be directed towards the main aims, an important issue concerning convective currents, that had so far received little attention, had to be tackled. The influence of room air turbulence on convective stream parameters, so far only suspected, had to be investigated in detail if convective currents, in conditions as encountered in practice, were to be replaced by jets. Measurements have therefore been made of a convective current generated by a heated window ($\Delta t_w = 20^oC$) in a test room, where room air turbulence was generated by the supply of cooling air (thereby simulating office air conditioning).

The experimental results showed that the "core" of the convective stream was affected less (the maximum velocity reaching 82% of the predicted value) than the outer part of the boundary layer. Nevertheless a comparison of the present data with the results of Cheesewright confirmed a real effect of room air turbulence on the "core".

In the outer part of the boundary layer a direct comparison of experimental results obtained in turbulent room conditions and those obtained in ideal situations, if a less than an "ideal" instrument is used (e.g. an ommidirectional probe), is more difficult due to a need to correctly interpret the meaning of the velocity readings. An analysis, based on comparable phenomena associated with turbulent shear flows, has shown that it is possible to separate the influence of the velocity measuring instrument and to correctly asses the influence of room air turbulence on convective flows. A method, based on this analysis, was subsequently used in the evaluation of the main experimental results. The experiment also showed that, although the Rayleigh number of the flow, $Ra = 5 \times 10^9$, is close to values associated with flows in the transitional region, the flow was turbulent.

The main experiments - the direct replacement of convective currents by wall jets - were carried out in a purpose built experimental facility.

Convective currents from a heated vertical plate (0.39 x 1.55 m) at three nominal temperature differentials between the plate and ambient air of 10, 30 and 50°C were measured. Again although the flow Rayleigh number for one experiment was $Ra = 3.5 \times 10^9$, the flow was, in all instances, found to be turbulent. Good agreement with the predicted boundary layer width was obtained when the boundary layer width was re-defined as the distance y from the plate to where $v = v_a$. The convective velocity profiles, when plotted in dimensionless co-ordinates, show a variation with the flow Rayleigh number; profiles having higher Ra numbers,

Ra = 9.1 x 10^9 to 12.7 x 10^9, being in better agreement with the experimental results of Cheesewright and Griffiths and Davis (Ra = 2.2 → 6.2 x 10^{10}), whereas lower Ra number profiles (Ra = 3.5 to 5 x 10^9) are in better agreement with theoretical predictions. The temperature profiles corroborate the theoretical predictions, especially in the inner part of the boundary layer.

The most important parameters that influence room air movements are momentum flux, maximum velocity and the mean temperature, defined as the ratio of heat content to mass flow. The influence of room air turbulence has been shown to be Rayleigh number dependent (and therefore will vary mainly with the height of the heated surface H and the surface temperature differential Δt_w). The variation of the influence of room air turbulence, expressed as the ratio of measured experimental values to predicted values, with the parameter $H\Delta t_w$ is shown graphically in Fig. 3.35 and Fig. 3.41. The variation can be expressed by the following formulae -

Maximum velocity

$$K = \frac{v_{max_e}}{v_{max_p}} = 1.585\ (x\Delta t_w)^{-0.2}$$

Momentum flux

$$K_M = \frac{M_e}{M_p} = 10^{-0.001484(x\Delta t_w)}$$

Volume flow

$$K_V = \frac{V_e}{V_p} = 10^{-0.001058\ (x\Delta t_w)}$$

Heat content

$$K_Q = \frac{Q_e}{Q_p} = 10^{-0.001394(x\Delta t_w)}$$

Mean flow temperature

$$K_{\overline{\Delta t}} = \frac{\overline{\Delta t_e}}{\Delta t_p} = 10^{-0.00361(x\Delta t_w)}$$

The convective flow parameters are not all affected by room air turbulence to the same extent. Momentum flux and maximum velocity are the most sensitive, volume flow being less affected and the mean flow temperature varying only slightly. The variation of the heat content is, evidently, the result of the compound effect of volume flow and mean flow temperature. The above formulae can have a more general application, as a comparison of the influence of room air turbulence at two different levels (test room and laboratory) indicates that, once room air turbulence is present, its effect varies insignificantly.

Initially the replacement wall jet initial parameters were calculated according to theoretically deduced formulae in Part 2. The initial parameters were subsequently varied in order to take into account

buoyancy, room air turbulence and non-uniform initial conditions. The measured wall jet velocity profiles are in good agreement with both theoretical and empirical similarity curves except for a shift in the velocity peak attributable to the buoyancy. The shape of the temperature profile depends on the initial volume flow. "Strong" jets, i.e. those having a high initial volume flow, show no temperature declines near the wall, the heat loss through the wall, proportionally, being insignificant. It is therefore exceptionally important to apply a high degree of insulation to the walls when low initial volume flows are likely to be encountered.

The coefficient of turbulence a', which includes the effect of buoyancy, was found to vary little for the whole range of experiments (Re_o = 500 → 700). When values of the isothermal coefficient of turbulence a were calculated, they agreed well with the theoretically predicted values in Part 2.

The effect of buoyancy on jet parameters at the replacement cross-section was found to be significant. The maximum velocity at the replacement cross-section remained equal to the initial nozzle velocity although the values of S/b_o indicated flow outside the initial region. Experimental results and theoretical analysis, based on the equations for the assessment of buoyancy effects developed in Part 2, have shown that, when modelling convective currents, the maximum velocity remains stable over a wide range of S/b_o and thereby in effect lengthening the initial region.

Experimental results showed that the volume flow at the replacement cross-section was significantly influenced by the initial nozzle temperature. It can therefore be assumed that higher temperature differentials enhance the mass transfer between the jet and the surrounding air. Rigorous calculations, utilising the buoyancy effect equations developed in Part 2, have enabled the effect to be quantified and expressed, in non-dimensional form, by the following equation

$$B_V = \frac{V_e}{V_p} = (10\ \Delta t_o V_o)^{0.157}$$

where B_V is, in essence, a correction coefficient that would have to be applied to theoretical predictions in order to take into account the temperature-enhanced mass transfer.

Both, momemtum flux and the heat content of the jet, show a tendency to be significantly lower than predicted if the jet is not "strong", i.e. the ratio of the measured values to expected depends on the initial momentum of the jet. The dependence can be expressed by

$$B_M = \frac{M_e}{M_p} = 94\ (b_o v_o^2)$$

and

$$B_Q = \frac{Q_e}{Q_p} = 130\ (b_o v_o^2)$$

where again B_M and B_Q are, in essence, buoyancy correction factors that can be applied to calculated values. As a consequence, raising the

initial jet temperature does not result in an increase in the heat content of a jet at the replacement cross-section.

The main aim of the experiments, i.e. to show that it is feasible to replace convective surrants by wall jets, has been achieved. A virtual identity of the maximum velocity, momentum flux and volume flow at the replacement cross-section has been accomplished and the velocity profiles are in good agreement. Complete identity of the heat content at the replacement cross-section may not be feasible as a rise in the initial jet temperature results in a more rapid temperature decay along the jet.

Based on an understanding of the behaviour of convective currents and their replacement jets exposed to natural room air turbulence, it is possible to formulate practical guidelines for the direct calculation of replacement jets from convective surface parameters. The validity of the following procedure is, strictly, limited to the modelling of convective currents having a Rayleigh number in the interval $Ra = 3.5 \times 10^9$ to 13×10^9 (or $H\Delta t_W = 15.5$ to 75.5), which covers the majority of practical applications. (For applications outside this interval, detailed calculation referred to in the main body of the text would have to be used.)

Initial maximum velocity

$$v_o = 0.1 \; K \; H^{0.5} \; \Delta t_W^{0.5}$$

where $K = 1.585 \; (H\Delta t_W)^{-0.2}$

Initial temperature differential

$$\Delta t_o = 0.354 \; \Delta t_W$$

Distance of nozzle from replacement cross-section

$$S = 0.746 \; H^{0.7} \; \Delta t_W^{-0.1}$$

Nozzle width

$$b_o' = 0.02156 \; H^{0.7} \; \Delta t_W^{-0.1}$$

or $b_o' \doteq \frac{S}{36}$

If values describing non-uniform initial nozzle flow are known, the nozzle width b_o can be multiplied by

$$0.91 \; \frac{\Psi}{\Phi}$$

REFERENCES

1 GRIFFITHS, E., DAVIS, A.H., "The Transmission of Heat by Radiation and Convection" British Food Investigation Board, Spec. Rept. No.9, D.S.I.R. London, 1922.

2 SCHMIDT, E., BECKMANN, W., "Das Temperatur-und Geschwindigkeitsfeld vor einer Wärme abgebenden senkrechten Platte bei natürlicher Konvektion". Tech. Mech. v Thermodynamik, Bd.1, Nr.10, Okt. 1939, 341-349; cont. Bd.1, Nr. 11, Nov. 1930, 391-406.

3 CHEESEWRIGHT, R., "Turbulent Natural Convection from Vertical Plane Surface" Journal of Heat Transfer, Transactions ASME, Paper No. 67-HT - 17, Feb. 1968.

4 BILLINGTON, N.S., "Air Movement over Hot or Cold Surfaces". HVRA Laboratory Report No. 29, Jan. 1966.

5 ROSHKO, A., "Structure of Turbulent Shear Flows": A New Look AIAA Journal, Vol. 14, No. 10, October 1976, p. 1349-1357.

6 BEVILAQUA, P.M., LYKOUDIS, P.S., "Mechanism of Entrainment in Turbulent Wakes", AIAA Journal, Vol. 9, 1971, p. 1657-1659.

7 OSTRACH, S., "An Analysis of Laminar Free-Convection Flow and Heat Transfer About a Flat Plate Parallel to the Direction of the Generating Body Force" NACA Report 1111, 1953.

8 RAJARATNAM, N., "Turbulent Jets", Elsevier Scientific Publishing Co., 1976.

9 O'CALLAGHAN, P.W., PROBERT , S.D., NEWBERT, G.J., "Velocity and Temperature Distributions for Cold Air Jets Issuing from Linear Slot Vents into Relatively Warm Air", Journ. Mech. Eng. Sci., Vol. 17, No. 3, 1975, 139-149.

PART 4. OVERALL MAJOR CONCLUSIONS

The primary objective of this project - the identification of novel methods of extending the scale factor when modelling room air movements - has been achieved.

Accurate predictions of the air flows in full-size air-conditioned rooms may be obtained from observations made with small models if certain criteria are satisfied. The maximum geometric scale-factor can be increased to 8.5, while limiting the maximum working temperature in the model to 100°C, by replacing the convective currents with wall jets of a similar velocity profile, volume flow, momentum flux and heat content. A further improvement may be achieved if the scale-factor adopted for the jet nozzle is smaller than the geometric scale-factor. This approach can lead to scale factors exceeding 11.8. Thus, the aim, namely the worthwhile use of a small model which can be contructed cheaply, can be achieved.

Theoretical studies resulted in the formulation of expressions for the calculation of replacement jet parameters directly from the vertical dimension H of the convective surface and its surface temperature differential Δt_w (Table 2.4). In the course of the study, a detailed investigation of those facts important to the aims of the project, but for which there is a dearth of relevant published information, were undertaken.

An analysis of available data, for jets having low nozzle Reynolds numbers, has resulted in a method for the separation of the coefficients of turbulence for the initial a_i and the main region a_M being evolved. Thus the deduced values of a_i (Fig. 2.18) enable a more accurate calculation of replacement jet parameters to ensue.

The effect of Archimedean forces, acting in the direction of the initial jet flow, was analysed and formulae, based on simplified assumptions, for the additional length travelled by an element of the jet and the additional centreline and mean-square velocities deduced (Table 2.3).

Calculations have shown that, due to non-uniform initial flows at low nozzle Reynolds numbers, up to 20% may have to be added to the nozzle width.

The experimental studies achieved the main aims - the feasibility of a direct replacement of a convective current by a wall jet, the establishment of necessary empirical factors and the formulation of a simple procedure for the calculation of replacement jets, valid for the majority of cases likely to be encountered.

A virtual identity of maximum velocity, momentum flux and volume flow at the replacement cross-section has been achieved (Table 3.5). The correlation of the heat content suffers from the rapid temperature decay above the jet..

The effect of room air turbulence on convective current parameters was found to be significant. The present experimental results obtained in natural room turbulent conditions differ from other results taken

in controlled environments. The effect, expressed as room air turbulence factors (Fig. 3.41), varies with height and temperture of heated surface.

The influence of buoyancy on wall jet parameters has also been quantified. Volume flow (due to enhanced mass transfer) is significantly influenced by nozzle temperature. Values of momentum flux and heat content significantly lower than predicted were found for jets having low initial momentum fluxes.

Based on an understanding of the behaviour of convective currents and their replacement jets, the following modelling procedures are recommended. The application is limited to natural room air movement levels $Ra = 3.5 \times 10^9 \rightarrow 13 \times 10^9$ and nozzle Reynolds numbers

$$Re_o = \frac{b_o v_o}{v_o} = 500 \rightarrow 700.$$

Convective surface

Vertical dimension	H	(m)
Surface temperature differential	$\Delta t_w = t_w - t_a$	(^oC)

Replacement jet

Initial maximum velocity

$v_o = 0.1\ K\ H^{0.5}\ \Delta t_w^{0.5}$ (m/s)

where $K = 1.59(H\Delta t_w)^{-0.2}$

Initial temperature differential

$\Delta t_o = 0.354\ \Delta t_w$ (^oC)

Distance of nozzle from replacement cross-section

$S = 0.746 H^{0.7}\ \Delta t_w^{0.1}$ (m)

Nozzle width

$b_o = 0.0216\ H^{0.7}\ \Delta t_w^{0.1}$ (m)

(If values describing the non-uniform initial nozzle flow are known, b_o should be multiplied by $0.91\ \Psi/\Phi$).

APPENDIX A

COMPUTER PRINTOUTS OF CONVECTIVE MEASUREMENTS

The printouts contain data from six experiments: two each for the three nominal temperature differentials Δt_w = 10, 30 and 50°C.

The first number of each printout (twice underlined) is the nominal temperature differential Δt_w.

Line 1 and Line 2 contain basic data required by the computer program.

Line 3 - The underlined number is the distance from the bottom of the heated surface x; then follow - ambient temperature t_a of Test 1 and Test 2 and actual temperature differential Δt_w of Test 1 and Test 2.

Line 4 - Distances from heated plate y where measurements were taken.

Line 5 - Velocity measurements Test 1.

Line 6 - Velocity measurements Test 2.

Line 7 - Temperature measurements Test 1.

Line 8 - Temperature measurements Test 2.

Lines 3 to 8 are then repeated for other values of x.

```
10,1.57E-05,1.195,1.189,0.288,0.286,
0,0,0,0.143,0,0,0.57,0.57,-7,-7,48,48,
7,0.2,21,22.8,10.6,10.9,
0,0.0015,0.0035,0.0085,0.0135,0.0235,0.0435,0.0635,
0,0.15,0.17,0.15,0.11,0.1,0.1,0.1,
0,0.1,0.15,0.13,0.05,0.06,0.03,0.06,
31.6,30.8,28.4,22,21.7,21,20.8,20.8,
33.7,35,30.3,25.1,23.6,23.4,23.4,23.1,
8,8,0.6,20.8,23.1,10,10.6,
0,0.0015,0.0035,0.0085,0.0135,0.0235,0.0335,0.0535,0.0835,
0,0.24,0.24,0.285,0.19,0.13,0.13,0.13,0.1,
0,0.19,0.27,0.24,0.15,0.06,0.06,0.11,0.07,
30.8,30.8,30.3,24.3,22,21,20.8,20.5,20.5,
33.7,33.7,32.6,26.7,24.3,23.6,23.4,23.1,23.1,
9,9,1,20.8,23.3,11.1,10.5,
0,0.0015,0.0025,0.0075,0.0125,0.0225,0.0325,0.0525,0.0825,0.1125,
0,0.24,0.34,0.34,0.3,0.21,0.19,0.1,0.07,0.06,
0,0.17,0.37,0.3,0.27,0.1,0.09,0.09,0.07,0.1,
31.9,30.3,29.1,25.5,23.1,21.7,20.5,20.5,20.8,20.5,
33.8,35,32.6,27.9,25.5,34.1,23.6,23.6,23.6,23.6,
8,8,1.4,20.6,23.6,11.1,10,
0,0.0015,0.0065,0.0115,0.0215,0.0315,0.0515,0.0815,0.1115,
0,0.21,0.34,0.34,0.3,0.24,0.15,0.11,0.1,
0,0.24,0.38,0.32,0.21,0.13,0.16,0.07,0.06,
31.7,30.3,25.5,23.1,22.7,21.7,21.4,20.5,20.3,
33.6,32.6,27.9,25.5,25.1,24.1,24.1,23.6,23.6,
8,8,1.55,20.4,23.9,10.7,9.4,
0,0.0015,0.0065,0.0115,0.0215,0.0315,0.0515,0.0815,0.1115,
0,0.265,0.34,0.34,0.3,0.24,0.17,0.11,0.06,
0,0.27,0.38,0.33,0.27,0.21,0.07,0.13,0.07,
31.1,30.3,25.5,24.3,23.1,22,21.4,20.5,20.3,
33.3,32.6,27.9,26.9,26.5,24.5,24.5,24.1,24.1,
-500,
```

```
30,1.57E-05,1.177,1.157,0.283,0.286,
9,9,0,0.143,0,0,0.57,0.57,-7,-7,48,48,
7,9.2,18.6,18.9,29.5,29.9,
0,0.0015,0.0025,0.0075,0.0125,0.0225,0.0525,0.0835,
0,0.09,0.19,0.14,0.11,0.13,0.1,0.11,
0,0.21,0.27,0.16,0.1,0.09,0.09,0.11,
48.1,44.2,30.3,20.8,18.6,18.3,18.3,18.3,
48.8,48.7,37.3,22.4,20.8,20.5,20.3,20.3,
8,8,0.6,18.8,18.9,29.4,28.5,
0,0.0015,0.0025,0.0065,0.0125,0.0225,0.0325,0.0525,0.0825,
0,0.19,0.3,0.34,0.21,0.15,0.11,0.13,0.11,
0,0.33,0.47,0.38,0.28,0.13,0.11,0.13,0.07,
48.2,46.5,35,25.5,20.8,19.3,18.8,18.1,18.1,
47.4,46.5,41.9,27.9,25.5,20.8,20.3,20.5,19.8,
10,10,1,18.9,18.8,29.5,28.4,
0,0.0015,0.0025,0.0075,0.0125,0.0225,0.0325,0.0525,0.0825,0.1125,0.1425,
0,0.17,0.34,0.38,0.34,0.265,0.19,0.11,0.11,0.1,0.11,
0,0.38,0.42,0.47,0.42,0.33,0.24,0.15,0.13,0.11,0.1,
48.4,44.2,35,27.9,24.3,20.8,19.5,18.8,18.3,18.3,18.3,
47.2,41.9,35,30.3,25.5,24.1,22.9,21.1,20.3,20,19.8,
11,11,1.4,19.2,18.7,29.2,30.6,
0,0.0015,0.002,0.007,0.012,0.022,0.032,0.042,0.052,0.072,0.102,0.132,
0,0.15,0.265,0.45,0.42,0.34,0.265,0.21,0.17,0.1,0.05,0.1,
0,0.42,0.47,0.54,0.47,0.42,0.33,0.3,0.27,0.17,0.1,0.09,
48.4,44.9,37.3,30.3,25.5,23.6,22,20.8,20.3,19.3,18.8,18.8,
49.3,46.5,41.9,30.3,27.9,25.5,23.1,22.7,22,20.8,20,19.8,
11,11,1.55,19.5,18.3,28.8,30.3,
0,0.0015,0.002,0.007,0.012,0.022,0.032,0.042,0.052,0.072,0.102,0.132,
0,0.3,0.34,0.42,0.4,0.34,0.3,0.265,0.19,0.13,0.06,0.03,
0,0.42,0.54,0.54,0.47,0.47,0.42,0.38,0.32,0.17,0.09,0.09,
48.3,39.6,35,30.3,26.7,24.3,22,20.8,20.8,20,19.5,19.5,
48.6,46.5,44.2,35,27.9,24.5,24.3,22.7,22,20.8,20,20,
-500,
```

48.3 - 19.5 = 28.8

```
50,1.57,-05,1.157,1.128,0.286,0.272,
0,0,0,0.145,0,0,0.57,0.57,-7,-7,48,48,
8,0.2,21.3,19.2,48.6,51.1,
0,0.0015,0.0025,0.0075,0.0125,0.0225,
0.0325,0.0525,0.0825,
0,0.24,0.27,0.15,0.09,0.07,0.06,0.06,0.07,
0,0.24,0.28,0.19,0.15,0.15,0.13,0.11,0.11,
69.9,55.5,41.9,23.6,21.7,21.2,21,21,21,
70.3,55.5,39.6,22.4,20.5,20.5,20.3,20.0,19.3,
10,10,0.6,21.1,19.5,48.9,50.8,
0,0.0015,0.0025,0.0075,0.0125,0.0225,
0.0325,0.0425,0.0525,0.0825,0.1125,
0,0.34,0.38,0.32,0.24,0.16,0.12,0.1,0.06,0.12,0.11,
0,0.42,0.47,0.38,0.27,0.19,0.15,0.15,0.13,0.13,0.1,
70,55.5,44.2,31.5,27.9,24.3,22,22,21.2,21,21,
70.3,55.5,46.5,30.3,22.0,20,20,19.8,19.8,19.3,19.8,
11,11,1,20.7,20.1,48.5,51.3,
0,0.0015,0.0025,0.0075,0.0125,0.0225,
0.0325,0.0425,0.0525,0.0625,0.0825,0.1125,
0,0.42,0.45,0.42,0.38,0.3,0.22,0.16,0.13,0.12,0.1,0.11,
0,0.42,0.52,0.54,0.42,0.33,0.27,0.24,0.21,0.17,0.13,0.11,
69.2,51,44.2,32.6,27.9,24.3,24.1,22,22,21,20.8,20.3,
71.4,57.7,48.7,32.6,30.3,24.1,23.1,22.4,20.8,20,20.5,20.3,
12,12,1.4,20.5,20.1,49.9,50.8,
0,0.0015,0.0025,0.0075,0.0125,0.0225,
0.0325,0.0425,0.0525,0.0625,0.0725,0.1025,0.1325,
0,0.45,0.5,0.5,0.45,0.42,0.38,0.25,0.18,0.12,0.11,0.09,0.09,
0,0.47,0.62,0.64,0.6,0.5,0.45,0.33,0.24,0.21,0.17,0.13,0.1,
70.4,57.7,46.5,35,30.3,27.9,24.3,23.6,22.7,22.2,21.7,21.2,20.5,
70.9,55.5,48.7,35,30.3,27.9,26.7,25.1,23.1,22,21.5,20.8,20.8,
12,12,1.55,21.3,20.6,50.1,49.7
0,0.0015,0.003,0.008,0.013,0.023,
0.033,0.043,0.053,0.063,0.073,0.103,0.133,
0,0.45,0.5,0.475,0.475,0.42,0.355,0.265,0.21,0.11,0.13,0.06,0.06,
0,0.49,0.66,0.64,0.58,0.5,0.38,0.33,0.3,0.24,0.15,0.07,0.06,
71.4,57.7,51,35,30.3,26.7,23.1,22,22,20.8,20.8,19.8,19.8,
70.3,59.9,47.6,36.2,32.6,29.1,25.5,25.1,24.1,22.9,22.7,22,21.5,
-500,
```

APPENDIX B

RESULTS OF COMPUTER ANALYSIS OF CONVECTIVE MEASUREMENTS.

Text cut off in original

XD

DT= 10 DEG. C X= 1.55 M

TURBULENT
BASIC DATA:

KIN VISCOSITY[M2/S]	1.57E-05		
DENSITY[KG/M3]	1.19		
SPECIFIC HEAT CAPACITY[KCAL/M3DEG C]	0.288		
DATA:			
V(MAX)[M/S]	0.394	V(1)[M/S]	0.736
DELTA[M]	0.1187	Y(VMAX)[M]	0.0041
GR	5.058E+09	NU(MEAN)	1.440E+02

VELOCITY

Y (M)	VTH (M/S)	V1 (M/S)	V2 (M/S)	VM (M/S)
0.0000	0.0000	0.0000	0.0000	0.0000
0.0015	0.3747	0.2562	0.2785	0.2673
0.0065	0.3881	0.3287	0.3919	0.3603
0.0115	0.3509	0.3287	0.3404	0.3345
0.0215	0.2594	0.2900	0.2785	0.2843
0.0315	0.1775	0.2320	0.2166	0.2243
0.0515	0.0672	0.1643	0.0722	0.1183
0.0815	0.0068	0.1063	0.1341	0.1202
0.1115	0.0000	0.0580	0.0722	0.0651
0.1200	0.0000	0.0580	0.0722	0.0651

TEMPERATURE DIFFERENCE

Y (M)	DTTH DEG C	DT1 DEG C	DT2 DEG C	DTM DEG C
0.0000	10.00	10.00	10.00	10.00
0.0015	4.64	9.25	9.26	9.25
0.0065	3.40	4.77	4.26	4.51
0.0115	2.84	3.64	3.19	3.42
0.0215	2.17	2.52	2.77	2.64
0.0315	1.73	1.50	0.64	1.07
0.0515	1.12	0.93	0.64	0.79
0.0815	0.52	0.09	0.21	0.15
0.1115	0.09	-0.09	0.21	0.06
0.1200	0.00	-0.09	0.21	0.06

COMPARISON TABLE
DEV., THEOR. =100

QUANTITY	THEOR	TEST 1	TEST2	MEAN
VOLUME(M3/S.M)	1.249E-02	1.998E-02	1.895E-02	1.946E-02
DEVIATION	100	160.0	151.8	155.9
MOMENTUM(KGM/S2.M)	4.023E-03	5.147E-03	4.972E-03	4.979E-03
DEVIATION	100	128.0	123.6	123.8
HEAT CONTENT (W)	3.557E+01	5.026E+01	4.541E+01	4.758E+01
DEVIATION	100	141.3	127.7	133.8

TURBULENT $\Delta t_w = 10^{o}C$

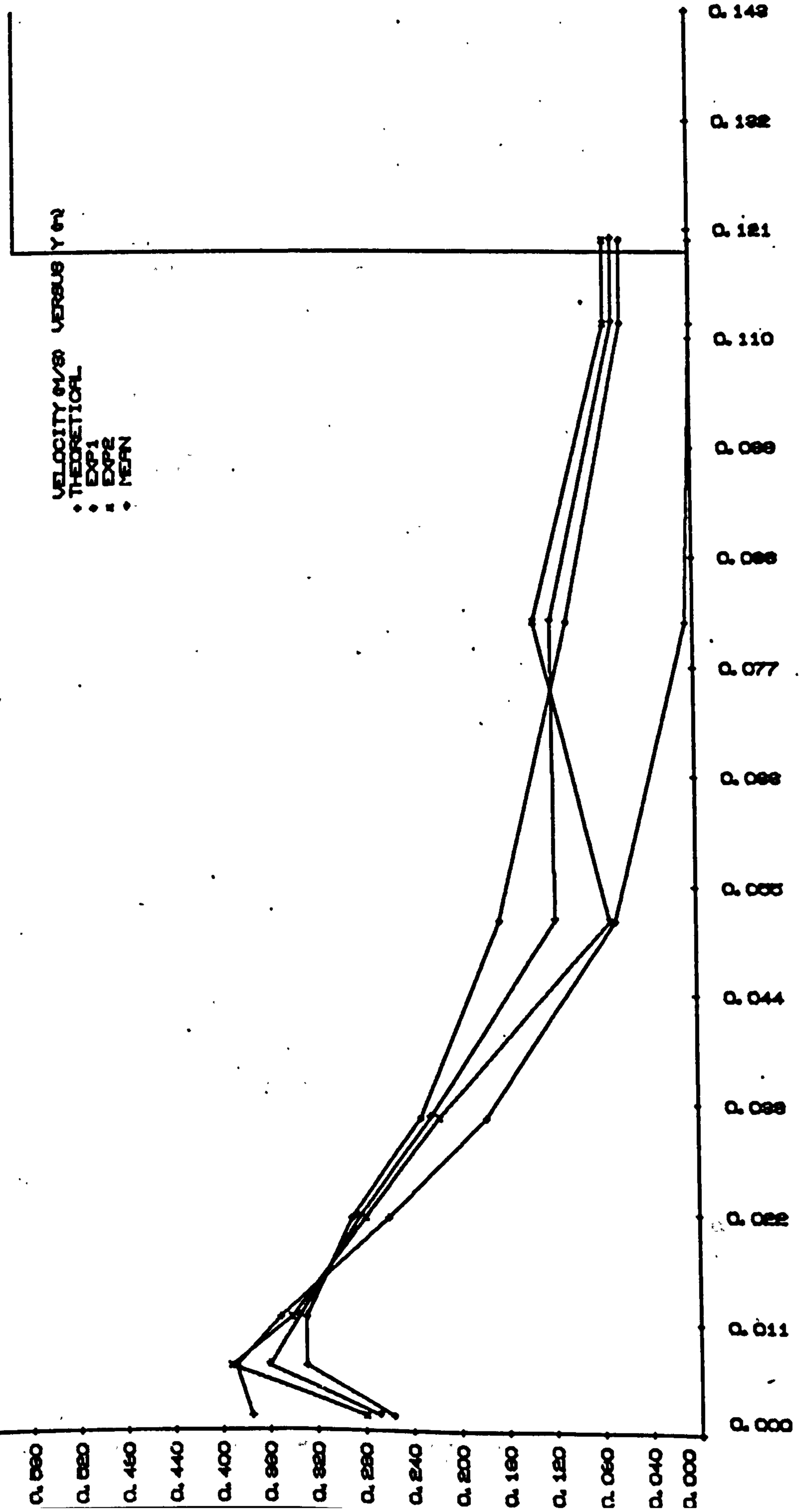

TURBULENT $\Delta t_W \doteq 10^{\circ}C$

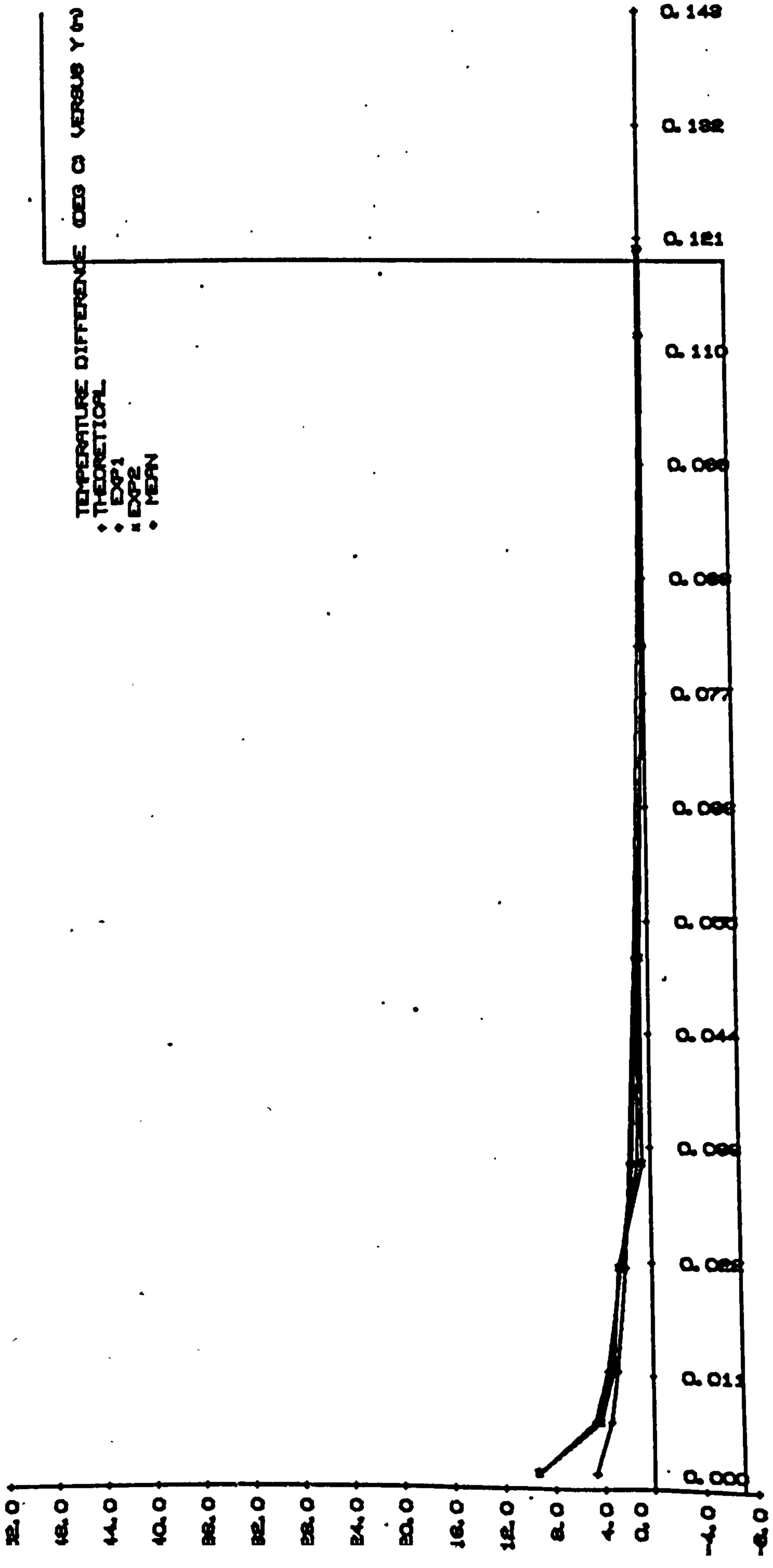

LAMINAR
BASIC DATA:
KIN VISCOSITY[M2/S] 1.57E-05
DENSITY[KG/M3] 1.19
SPECIFIC HEAT CAPACITY[KCAL/M3DEG C] 0.286
DATA:

V(MAX)[M/S]	0.425	V(1)[M/S]	2.870
DELTA[M]	0.0309	Y(VMAX)[M]	0.0103
GR	5.058E+09	NU(MEAN)	1.440E+02

VELOCITY

Y (M)	VTH (M/S)	V1 (M/S)	V2 (M/S)	VM (M/S)
0.0000	0.0000	0.0000	0.0000	0.0000
0.0015	0.1260	0.2562	0.2785	0.2673
0.0065	0.3763	0.3287	0.3919	0.3603
0.0115	0.4211	0.3287	0.3404	0.3345
0.0215	0.1855	0.2900	0.2785	0.2843
0.0315	0.0000	0.2320	0.2166	0.2243
0.0515	0.0000	0.1643	0.0722	0.1183
0.0815	0.0000	0.1063	0.1341	0.1202
0.1115	0.0000	0.0580	0.0722	0.0651
0.1200	0.0000	0.0580	0.0722	0.0651

TEMPERATURE DIFFERENCE

Y (M)	DTTH DEG C	DT1 DEG C	DT2 DEG C	DTM DEG C
0.0000	10.00	10.00	10.00	10.00
0.0015	9.05	9.25	9.26	9.25
0.0065	6.24	4.77	4.26	4.51
0.0115	3.95	3.64	3.19	3.42
0.0215	0.93	2.52	2.77	2.64
0.0315	0.00	1.50	0.64	1.07
0.0515	0.00	0.93	0.64	0.79
0.0815	0.00	0.09	0.21	0.15
0.1115	0.00	-0.09	0.21	0.06
0.1200	0.00	-0.09	0.21	0.06

COMPARISON TABLE
DEV., THEOR. =100

QUANTITY	THEOR	TEST 1	TEST2	MEAN
VOLUME(M3/S.M)	7.398E-03	9.191E-03	9.507E-03	9.349E-03
DEVIATION	100	124.2	128.5	126.4
MOMENTUM(KGM/S2.M)	2.886E-03	3.309E-03	3.585E-03	3.440E-03
DEVIATION	100	114.7	124.2	119.2
HEAT CONTENT (W)	3.550E+01	4.275E+01	4.389E+01	4.339E+01
DEVIATION	100	120.4	123.6	122.2
MEAN TEMP. DIF. (C)	4.0	3.9	3.9	3.9
DEVIATION	100	97.1	96.4	96.9

LAMINAR Δt_w = 10°C

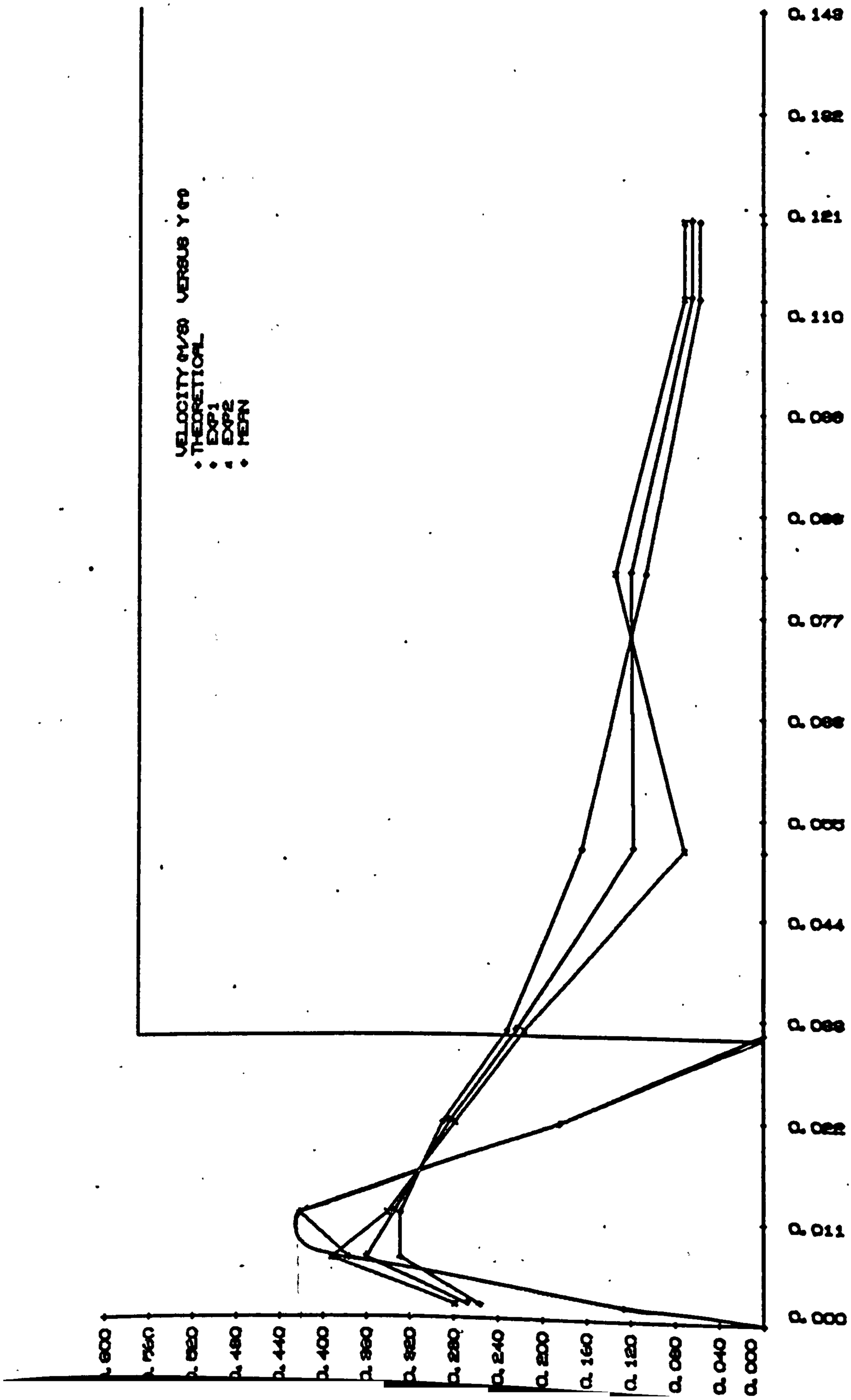

LAMINAR $\Delta t_w = 10^oC$

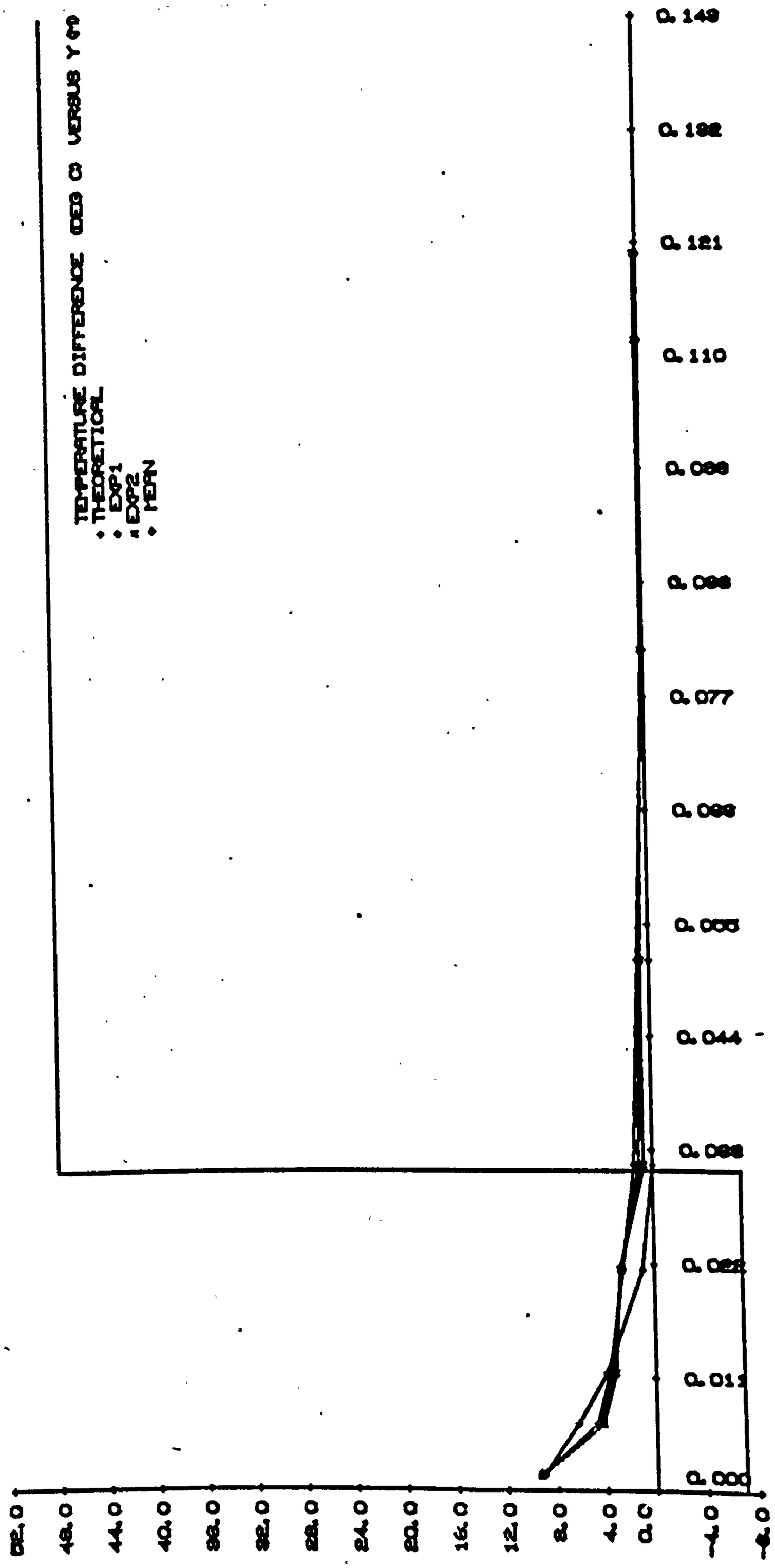

T_DT= 30 DEG. C X= 1.56 CONVECTIVE CURRENT

TURBULENT

BASIC DATA:

KIN VISCOSITY[M2/S]	1.57.-05		
DENSITY[KG/M3]	1.18		
SPECIFIC HEAT CAPACITY[KCAL/M3DEG C]	0.233		
DATA:			
V(MAX)[M/S]	0.682	V(1)[M/S]	1.275
DELTA[M]	0.1064	Y(VMAX)[M]	0.0037
GR	1.517.+10	NU(MEAN)	2.235.+02

VELOCITY

Y (M)	VTH (M/S)	V1 (M/S)	V2 (M/S)	VM (M/S)
0.0000	0.0000	0.0000	0.0000	0.0000
0.0015	0.6554	0.3062	0.4179	0.3621
0.0020	0.6700	0.3470	0.5373	0.4422
0.0070	0.6584	0.4287	0.5373	0.4830
0.0120	0.5785	0.4082	0.4677	0.4330
0.0220	0.4030	0.3470	0.4677	0.4073
0.0320	0.2567	0.3062	0.4179	0.3621
0.0420	0.1498	0.2705	0.3781	0.3243
0.0520	0.0786	0.1939	0.3184	0.2562
0.0720	0.0132	0.1327	0.1692	0.1509
0.1020	0.0000	0.0612	0.0896	0.0754
0.1320	0.0000	0.0306	0.0896	0.0601

TEMPERATURE DIFFERENCE

Y. (M)	DTTH DEG C	DT1 DEG C	DT2 DEG C	DTM DEG C
0.0000	30.00	30.00	30.00	30.00
0.0015	13.68	20.94	27.92	24.43
0.0020	13.00	16.15	25.64	20.89
0.0070	9.66	11.25	16.53	13.89
0.0120	8.04	7.50	9.50	8.50
0.0220	6.05	5.00	6.14	5.57
0.0320	4.73	2.60	5.94	4.27
0.0420	3.73	1.35	4.36	2.86
0.0520	2.92	1.35	3.66	2.51
0.0720	1.63	0.52	2.48	1.50
0.1020	0.18	0.00	1.68	0.84
0.1320	0.00	0.00	1.68	0.84

COMPARISON TABLE
DEV.. THEOR. =100

QUANTITY	THEOR	TEST 1	TEST2	MEAN
VOLUME(M3/S.M)	1.938.-02	2.319.-02	3.157.-02	2.738.-02
DEVIATION	100	119.7	162.9	141.3
MOMENTUM(KGM/S2.M)	1.065.-02	7.711.-03	1.391.-02	1.056.-02
DEVIATION	100	72.4	130.7	99.1
HEAT CONTENT (W)	1.627.+02	1.250.+02	2.740.+02	1.921.+02
DEVIATION	100	76.8	168.4	118.1
MEAN TEMP. DIF. (C)	7.1	4.5	7.3	5.9
DEVIATION	100	64.2	103.4	83.

$\Delta t_w = 30^oC$

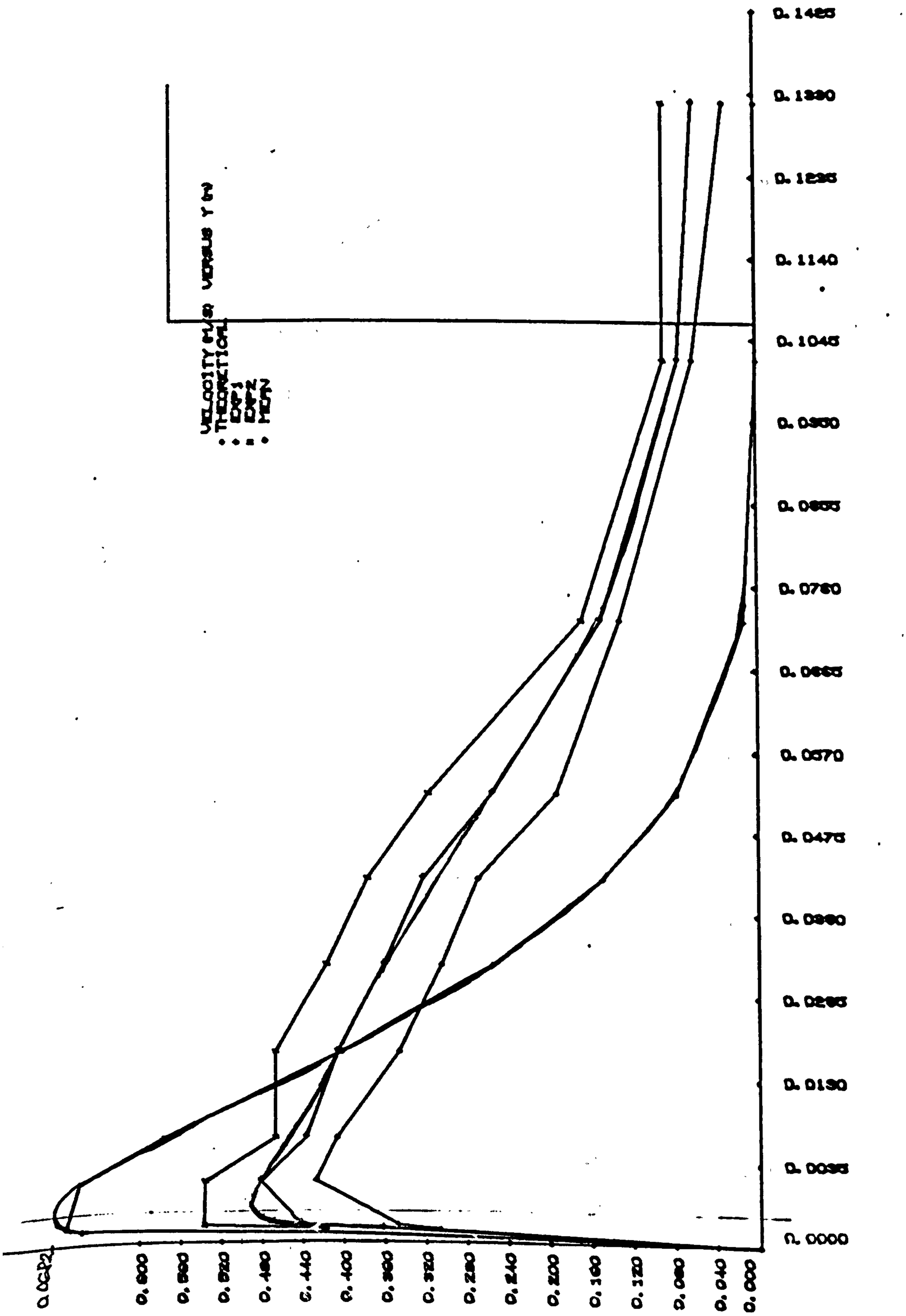

$\Delta t_W = 30^oC$

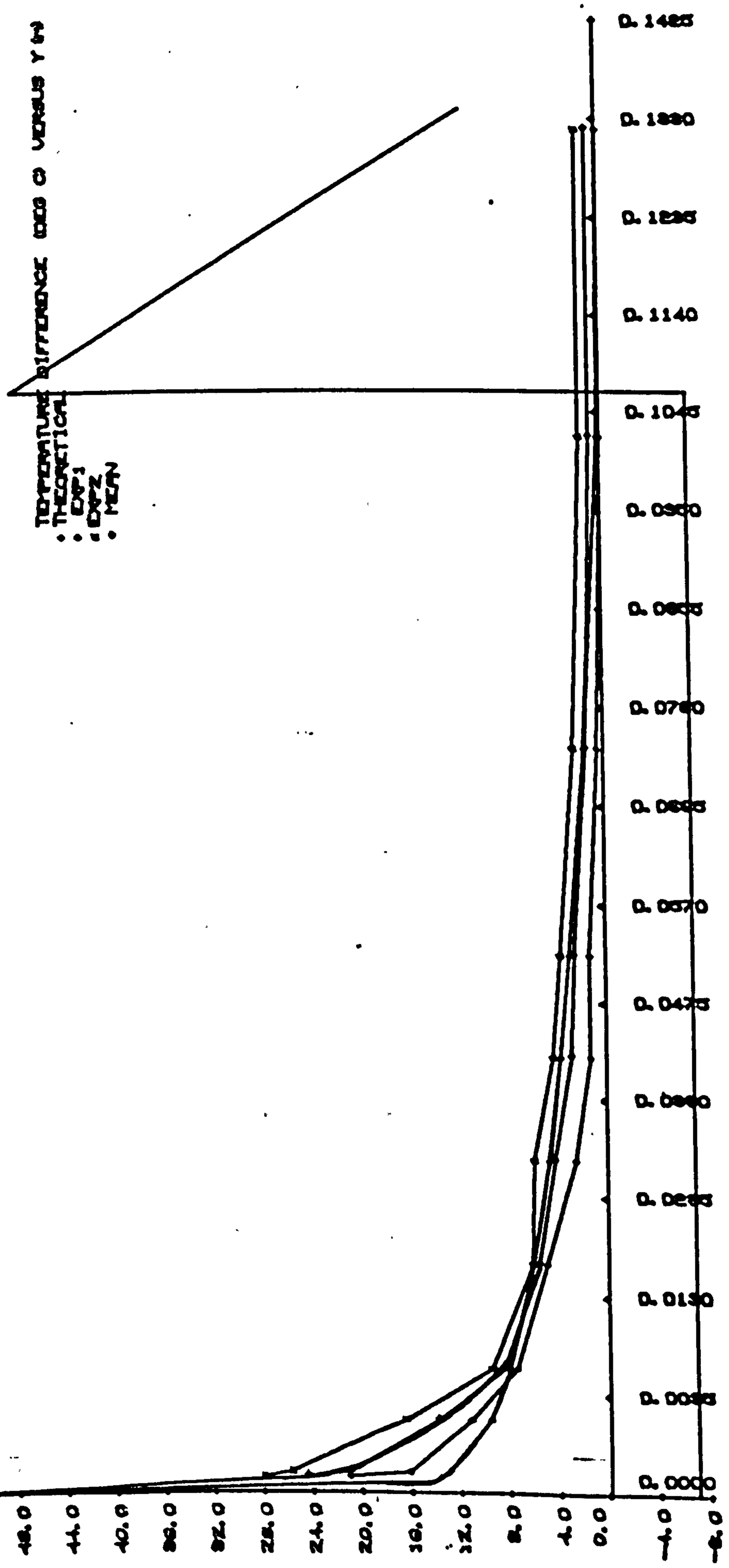

DT= 50 DEG. C X= 1.55 M

TURBULENT

BASIC DATA:

KIN VISCOSITY[M2/S]	1.57E-05		
DENSITY[KG/M3]	1.16		
SPECIFIC HEAT CAPACITY[KCAL/M3DEG C]	0.286		
DATA:			
V(MAX)[M/S]	0.880	V(1)[M/S]	1.646
DELTA[M]	0.1011	Y(VMAX)[M]	0.0035
GR	2.529E+10	NU(MEAN)	2.742E+02

VELOCITY

Y (M)	VTH (M/S)	V1 (M/S)	V2 (M/S)	V4 (M/S)
0.0000	0.0000	0.0000	0.0000	0.0000
0.0015	0.8497	0.4496	0.4915	0.4705
0.0030	0.8829	0.4995	0.6620	0.5807
0.0080	0.8240	0.4745	0.6419	0.5582
0.0130	0.7081	0.4745	0.5917	0.5331
0.0230	0.4745	0.4196	0.5015	0.4605
0.0330	0.2836	0.3546	0.3311	0.3429
0.0430	0.1589	0.2647	0.3310	0.2979
0.0530	0.0769	0.2098	0.3029	0.2563
0.0630	0.0310	0.1699	0.2417	0.1758
0.0730	0.0094	0.1299	0.1505	0.1402
0.1030	0.0000	0.0599	0.0702	0.0651
0.1330	0.0000	0.0599	0.0702	0.0651

TEMPERATURE DIFFERENCE

Y (M)	DTTH DEG C	DT1 DEG C	DT2 DEG C	DT4 DEG C
0.0000	50.00	50.00	50.00	50.00
0.0015	22.60	36.33	39.54	37.93
0.0030	19.75	29.64	27.14	28.41
0.0080	15.20	13.67	15.62	14.64
0.0130	12.70	8.98	12.07	10.53
0.0230	9.53	5.39	8.55	6.97
0.0330	7.39	1.80	4.93	3.36
0.0430	5.75	0.70	4.53	2.61
0.0530	4.41	0.70	3.52	2.11
0.0630	3.27	-0.50	2.31	0.91
0.0730	2.27	-0.50	2.11	1.31
0.1030	0.00	-1.50	1.41	-0.04
0.1330	0.00	-1.50	0.91	-0.30

COMPARISON TABLE
DEV., THEOR. =100

QUANTITY	THEOR	TEST 1	TEST2	MEAN
VOLUME(M3/S.M)	2.377E-02	2.623E-02	3.313E-02	2.968E-02
DEVIATION	100	110.3	139.3	124.8
MOMENTUM(KGM/S2.M)	1.658E-02	1.316E-02	1.585E-02	1.451E-02
DEVIATION	100	61.3	95.6	77.9
HEAT CONTENT (*)	3.362E+02	2.153E+02	3.514E+02	2.834E+02
DEVIATION	100	61.1	136.7	98.9
MEAN TEMP. DIF. (C)	11.8	6.5	9.1	7.8
DEVIATION	100	55.4	76.6	66.

$\Delta t_w = 50^oC$

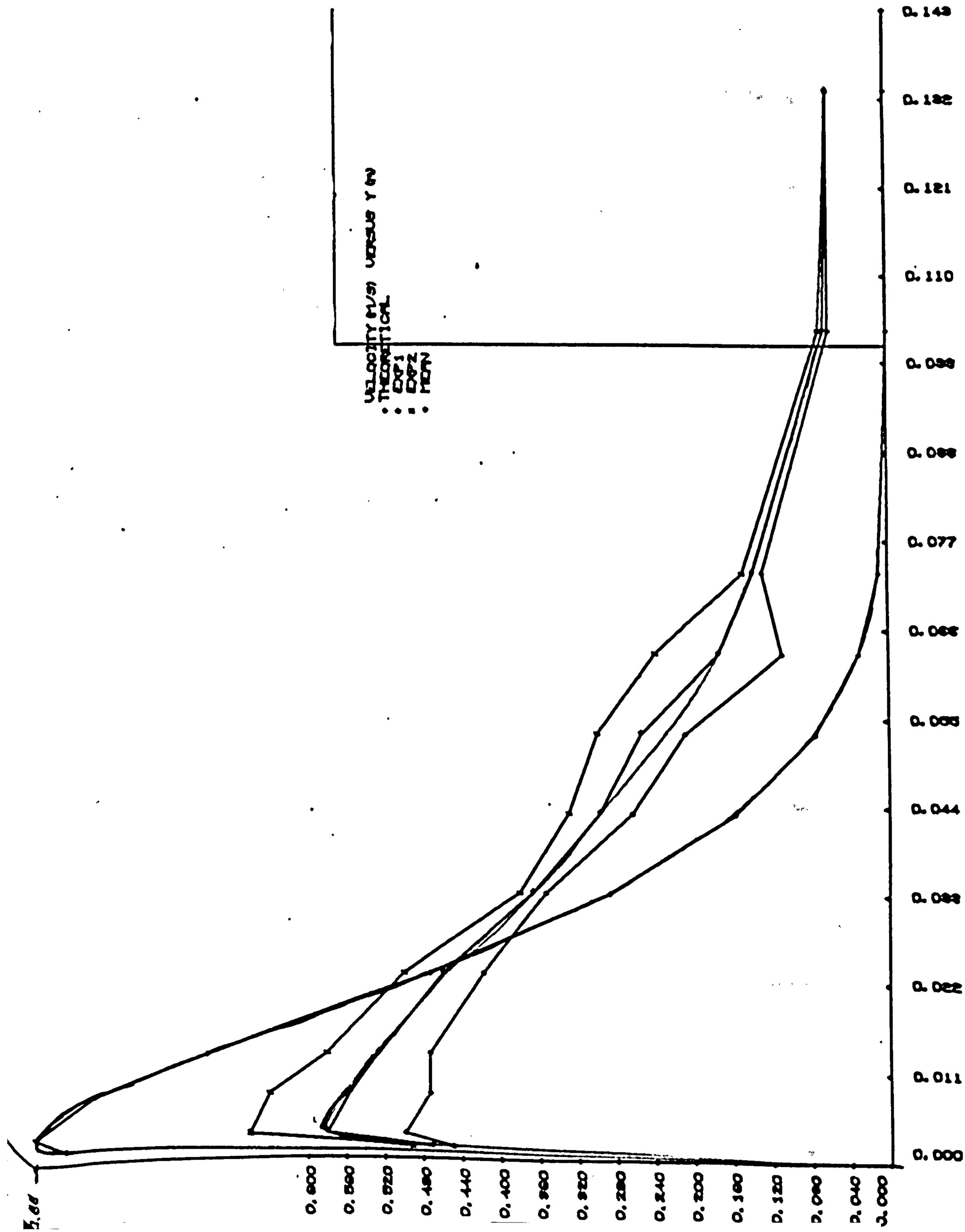

$\Delta t_W = 50^{\circ}C$

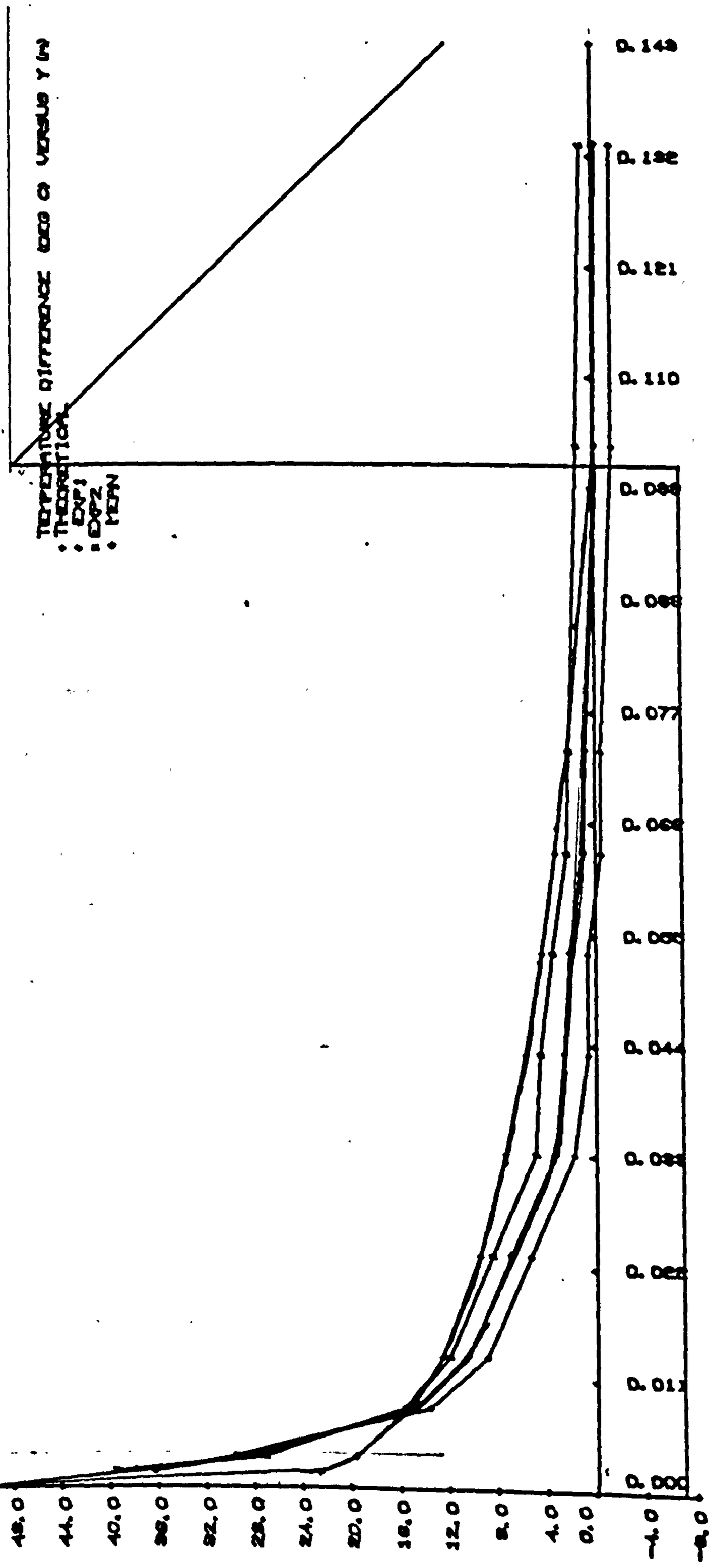

APPENDIX C

COMPUTER PRINTOUTS OF REPLACEMENT JET MEASUREMENTS

The first number on each printout (twice underlined) is the nominal temperature differential Δt_w of the replaced convective surface. The first two lines contain basic data required by the computer program.

Line 1 -	The underlined number is the height of the replaced convective surface H and the following number is the ambient temperature t_a at time of measurement.
Line 2 & Line 3	Distance from heated plate y where convective measurements were taken.
Line 4 & Line 5	Distance from heated plate y where replacement wall jet measurements were taken.
Line 6 & Line 7	Mean values of convective velocity measurements.
Line 8 & Line 9	Replacement wall jet velocity measurements.
Line 10 & Line 11	Mean temperature differential of convective measurements.
Line 12 & Line 13	Replacement wall jet temperature measurements

Line 1 to Line 13 are then repeated.

```
P
10,1.57.-05,1.195,0.288,
0,0,0,0.143,0,0,0.57,0.57,-7,-7,48,48,
17,17,1.55,23.9,
0,0.0015,0.0041,0.0065,0.0115,0.0215,0.0315,0.0515,0.0815,0.1115,
0.12,0.12,0.12,0.12,0.12,0.12,0.12,0.12,
0,0.004,0.007,0.012,0.017,0.022,0.032,0.042,0.052,0.062,0.072,
0.082,0.092,0.102,0.112,0.122,0.132,0.152,
0,0.2673,0.366,0.3603,0.335,0.2843,0.2243,0.159,0.101,0.0651,
0.0645,0,0,0,0,0,0,0,
0,0.19,0.24,0.36,0.32,0.27,0.24,0.21,0.17,.15,0.11,0.1,0.09,
0.09,0.07,0.05,0.04,0.04,
10,9.25,7,4.51,3.42,2.64,1.07,0.79,0.15,0.06,0.06,
0,0,0,0,0,0,0,
25.1,25.1,25.5,26,25.7,25.5,24.7,24.7,24.3,24.1,24.1,24.1,
23.9,23.9,23.9,23.9,23.9,23.9,
17,17,1.55,23.9,
0,0.0015,0.0041,0.0065,0.0115,0.0215,0.0315,0.0515,0.0815,0.1115,
0.12,0.12,0.12,0.12,0.12,0.12,0.12,0.12,
0,0.004,0.007,0.012,0.017,0.022,0.032,0.042,0.052,0.062,0.072,
0.082,0.092,0.102,0.112,0.122,0.132,0.152,
0,0.2673,0.366,0.3603,0.335,0.2843,0.2243,0.159,0.101,0.0651,
0.0645,0,0,0,0,0,0,0,
0,0.19,0.24,0.354,0.27,0.25,0.24,0.21,0.19,0.17,0.1,0.09,0.06,
0.06,0.06,0.03,0.02,0.05,
10,9.25,7,4.51,3.42,2.64,1.07,0.79,0.15,0.06,0.06,
0,0,0,0,0,0,0,
24.8,24.8,25.5,25.1,25.1,25.1,24.8,24.6,24.6,24.6,24.3,24.3,
24.1,24.1,24.1,24.1,24.1,24.1,
```

10/1

10/2

```
10,1.57e-05,1.195,1.189,0.288,0.286,
0,0,0,0.143,0,0,0.57,0.57,-7,-7,48,48,
```

10/3

```
10,10,1.55,0,23.3,10,10,
0,0.0015,0.0041,0.0065,0.0115,0.0215,0.0315,0.0515,0.0815,0.1115,
0.12,
0,0.001,0.006,0.011,0.021,0.031,0.041,0.08,0.09,0.1,0.12,
0,0.2673,0.366,0.3603,0.335,0.2843,0.2243,0.159,0.101,0.0651,
0.0645,
0,0.19,0.354,0.27,0.17,0.04,0,0,0,0,0,
10,9.25,7,4.51,3.42,2.64,1.07,0.79,0.15,0.06,0.06,
30.1,30.1,29.9,27.9,24.8,24.1,23.3,23.3,23.3,23.3,23.3,
```

10/4

```
10,10,1.55,0,23.3,10,10,
0,0.0015,0.0041,0.0065,0.0115,0.0215,0.0315,0.0515,0.0815,0.1115,
0.12,
0,0.002,0.005,0.01,0.02,0.03,0.04,0.08,0.09,0.1,0.12,
0,0.2673,0.366,0.3603,0.335,0.2843,0.2243,0.159,0.101,0.0651,
0.0645,
0,0.21,0.354,0.33,0.19,0.05,0,0,0,0,0,
10,9.25,7,4.51,3.42,2.64,1.07,0.79,0.15,0.06,0.06,
30.3,30.3,30.5,27.9,26,23.9,23.3,23.3,23.3,23.3,23.3,
```

30,1.57,-05,1.177,1.157,0.283,0.286,
0,0,0,0.144,0,0,0.57,0.57,-7,-7,48,48,

30/1

17,17,1.55,23.3,
0,0.0015,0.002,0.0037,0.007,0.012,0.022,0.032,0.042,0.052,0.072,
0.102,0.132,0.132,0.132,0.132,0.132,0.132,
0,0.003,0.006,0.011,0.016,0.021,0.031,0.041,0.051,0.061,0.071,
0.081,0.091,0.101,0.111,0.121,0.131,0.151,
0,0.3621,0.4422,0.493,0.483,0.453,0.4073,0.3621,0.3123,0.2562,
0.1509,0.0754,0.0601,0,0,0,0,0,
0,0.33,0.42,0.49,0.42,0.38,0.33,0.27,0.21,0.19,0.13,0.09,0.06,
0.05,0.05,0.05,0.06,0.03,
30,24.43,20.89,18.9,13.89,8.5,5.57,4.27,2.86,2.51,1.5,0.84,0.84,
0,0,0,0,0,
27.1,27.1,28.4,27.9,27.4,26.9,26,25.5,25.1,24.3,24.1,24.1,23.6,
23.4,23.4,23.4,22.9,23.1,

```
30.1.57,-05,1.177,0.283,
0,0,0,0.144,0,0,0.57,0.57,-7,-7,48,48,
```

30/2

```
17,17,1.55,23.2,
0,0.0015,0.002,0.0037,0.007,0.012,0.022,0.032,0.042,0.052,0.072,
0.102,0.132,0.132,0.132,0.132,0.132,0.132,
0,0.003,0.006,0.011,0.016,0.021,0.031,0.041,0.051,0.061,0.071,
0.081,0.091,0.101,0.111,0.121,0.131,0.151,
0,0.3621,0.4422,0.493,0.483,0.453,0.4073,0.3621,0.3123,0.2562,
0.1509,0.0754,0.0601,0,0,0,0,0,
0,0.38,0.42,0.49,0.42,0.38,0.33,0.3,0.19,0.15,0.13,0.11,0.1,
0.06,0.06,0.03,0.02,0.05,
30,24.43,20.89,18.9,13.89,8.5,5.57,4.27,2.86,2.51,1.5,0.84,0.84,
0,0,0,0,0,
28.4,28.4,27.9,27.9,27.9,26.2,26,25.5,25.1,24.6,24.1,23.6,23.4,
23.4,23.4,23.6,24.1,23.4,
```

30/3

```
17,17,1.55,23.4,
0,0.0015,0.002,0.0037,0.007,0.012,0.022,0.032,0.042,0.052,0.072,
0.102,0.132,0.132,0.132,0.132,0.132,0.132,
0,0.003,0.006,0.011,0.016,0.021,0.031,0.041,0.051,0.061,0.071,
0.081,0.091,0.101,0.111,0.121,0.131,0.151,
0,0.3621,0.4422,0.493,0.483,0.453,0.4073,0.3621,0.3123,0.2562,
0.1509,0.0754,0.0601,0,0,0,0,0,
0,0.38,0.42,0.49,0.42,0.38,0.3,0.37,0.21,0.19,0.17,0.11,0.1,
0.05,0.09,0.06,0.05,0.05,
30,24.43,20.89,18.9,13.89,8.5,5.57,4.27,2.86,2.51,1.5,0.84,0.84,
0,0,0,0,0,
27.6,27.6,27.6,27.6,27.1,27.1,26,25.5,25.3,24.8,24.1,23.6,23.6,
23.6,23.6,23.6,23.4,23.4,
```

```
50,1.57,-05,1.157,0.286,
0,0,0,0.144,0,0,0.57,0.57,-7,-7,48,48,
```

50/4

```
17,17,1.55,0,
0,0.0015,0.003,0.0035,0.008,0.013,0.023,0.033,0.043,0.053,0.063,0.073,
0.103,0.133,0.133,0.133,0.133,0.133,
0,0.003,0.006,0.011,0.016,0.021,0.031,0.041,0.051,0.061,0.071,
0.081,0.091,0.101,0.111,0.121,0.131,0.151,
0,0.4705,0.5807,0.59,0.5582,0.5281,0.4605,0.3679,0.2979,0.2328,
0.1753,0.1402,0.0651,0.0601,0,0,0,0,
0,0.46,0.505,0.6,0.56,0.52,0.42,0.315,0.24,0.19,0.16,0.095,0.095,
0.07,0.065,0.08,0.085,0.07,
50,37.93,28.4,27.2,14.68,10.53,6.97,3.36,2.61,2.11,1.41,0.81,
0,0,0,0,0,0,
7.85,7.85,8.75,7.2,6.8,5.65,5.2,4.4,2.4,1.55,1.3,0.95,0.65,0.35,
0.35,0.35,0.35,0.5,
```

50/5

```
17,17,1.55,21,
0,0.0015,0.003,0.0035,0.008,0.013,0.023,0.033,0.043,0.053,0.063,0.073,
0.103,0.133,0.133,0.133,0.133,0.133,
0,0.003,0.006,0.011,0.016,0.021,0.031,0.041,0.051,0.061,0.071,
0.081,0.091,0.101,0.111,0.121,0.131,0.151,
0,0.4705,0.5807,0.59,0.5582,0.5281,0.4605,0.3679,0.2979,0.2328,
0.1753,0.1402,0.0651,0.0601,0,0,0,0,
0,0.47,0.54,0.6,0.54,0.47,0.38,0.3,0.21,0.17,0.11,0.1,0.09,0.06,
0.05,0.04,0.05,0.05,
50,37.93,28.4,27.2,14.68,10.53,6.97,3.36,2.61,2.11,1.41,0.81,
0,0,0,0,0,0,
29.2,29.2,30.3,30.3,27.9,27.9,25.5,24.3,23.9,23.4,21.7,21.7,21.7,
21.5,21.5,21.5,21.5,21.5,
```

50/6

```
17,17,1.55,20.9,0,50.8,50,
0,0.003,0.006,0.011,0.016,0.021,0.031,0.041,0.051,0.061,0.071,
0.081,0.091,0.101,0.111,0.121,0.131,0.151,
0,0.0015,0.003,0.0035,0.008,0.013,0.023,0.033,0.043,0.053,0.063,0.073,
0.103,0.133,0.133,0.133,0.133,0.133,
0,0.42,0.54,0.6,0.54,0.47,0.42,0.38,0.33,0.21,0.17,0.15,0.11,
0.07,0.07,0.05,0.07,0.07,
0,0.4705,0.5807,0.59,0.5582,0.5281,0.4605,0.3679,0.2979,0.2328,
0.1753,0.1402,0.0651,0.0601,0,0,0,0,
27.9,27.9,29.7,29.2,27.1,26,25.5,25.1,24.6,23.9,23.1,22.7,
21.7,21.7,21.7,21.5,21.5,21.2,
50,37.93,28.4,27.2,24.68,10.53,6.97,3.36,2.61,2.11,1.41,0.81,
0,0,0,0,0,0,
```

50/3

17,17,1.55,0,24.5,50,50,
0,0.0015,0.003,0.0035,0.008,0.013,0.023,0.033,0.043,0.053,0.063,0.073,
0.103,0.133,0.133,0.133,0.133,0.133,
0,0.003,0.006,0.011,0.016,0.021,0.031,0.041,0.051,0.061,0.071,
0.081,0.091,0.101,0.111,0.121,0.131,0.151,
0,0.4705,0.5807,0.59,0.5582,0.5281,0.4605,0.3679,0.2979,0.2328,
0.1753,0.1402,0.0651,0.0601,0,0,0,0,
0,0.4,0.49,0.59,0.56,0.49,0.42,0.33,0.28,0.21,0.17,0.11,0.1,
0.07,0.06,0.07,0.04,0.07,
50,37.93,28.4,27.2,14.68,10.53,6.97,3.36,2.61,2.11,1.41,0.81,
0,0,0,0,0,0,
32.6,32.6,32.6,32.2,31.5,31.2,29.9,29.2,26.7,26.4,25.5,25.3,
25.1,25.1,25.1,25.1,25.1,24.8,

50, 1.57$_{10}$-05, 1.157, 1.128, 0.286, 0.272,
0, 0, 0, 0.144, 0, 0, 0.57, 0.57, -7, -7, 48, 48,

50/1

```
17,17,1.55,23.3,
0,0.0015,0.003,0.0035,0.008,0.013,0.023,0.033,0.043,0.053,0.063,0.073,
0.103,0.133,0.133,0.133,0.133,0.133,
0,0.003,0.006,0.011,0.016,0.021,0.031,0.041,0.051,0.061,0.071,
0.081,0.091,0.101,0.111,0.121,0.131,0.151,
0,0.4705,0.5807,0.59,0.5582,0.5281,0.4605,0.3679,0.2979,0.2328,
0.1753,0.1402,0.0651,0.0601,0,0,0,0,
0,0.38,0.54,0.588,0.54,0.47,0.42,0.33,0.27,0.19,0.13,0.11,0.06,0.05,0.09
0.06,0.06,0.06,
50,37.93,28.4,27.2,14.68,10.53,6.97,3.36,2.61,2.11,1.41,0.81,
0,0,0,0,0,0,
31.5,31.5,31.5,31.5,31,30.3,27.9,27.1,26.7,25.5,24.3,24.1,
24.1,24.1,24.1,23.9,23.9,23.6,
```

50/2

```
17,17,1.55,0,25.3,50,50.
0,0.0015,0.003,0.0035,0.008,0.013,0.023,0.033,0.043,0.053,0.063,0.073,
0.103,0.133,0.133,0.133,0.133,0.133,
0,0.003,0.006,0.011,0.016,0.021,0.031,0.041,0.051,0.061,0.071,
0.081,0.091,0.101,0.111,0.121,0.131,0.151,
0,0.4705,0.5807,0.59,0.5582,0.5281,0.4605,0.3679,0.2979,0.2328,
0.1753,0.1402,0.0651,0.0601,0,0,0,0,
0,0.42,0.54,0.59,0.54,0.5,0.42,0.33,0.25,0.21,0.17,0.13,0.09,
0.09,0.07,0.06,0.09,0.06,
50,37.93,28.4,27.2,14.68,10.53,6.97,3.36,2.61,2.11,1.41,0.81,
0,0,0,0,0,0,
33.3,33.3,33.3,32.2,31.7,31.7,31,30.3,26.9,26.4,26.2,25.7,25.7,
25.3,25.1,25.1,25.1,25.1,
```

APPENDIX D

RESULTS OF COMPUTER ANALYSIS OF REPLACEMENT JET MEASUREMENTS AND COMPARISON WITH CONVECTIVE RESULTS.

V1, DT1, Y	Mean convective values from Appendix B.
VTH, DTTH, Y	Theoretical convective predictions.
V2, DT2, Y2	Replacement jet measurements.

DT= 10 DEG. C X= 1.55 M

12

VELOCITY

10/1

Y (M)	V1 (M/S)	V2 (M/S)	Y2 (M)
0.0000	0.0000	0.0000	0.0000
0.0015	0.2673	0.1900	0.0040
0.0041	0.3660	0.2400	0.0070
0.0065	0.3603	0.3600	0.0120
0.0115	0.3350	0.3200	0.0170
0.0215	0.2843	0.2700	0.0220
0.0315	0.2243	0.2400	0.0320
0.0515	0.1590	0.2100	0.0420
0.0815	0.1010	0.1700	0.0520
0.1115	0.0651	0.1500	0.0620
0.1200	0.0645	0.1100	0.0720
0.1200	0.0000	0.1000	0.0820
0.1200	0.0000	0.0900	0.0920
0.1200	0.0000	0.0900	0.1020
0.1200	0.0000	0.0700	0.1120
0.1200	0.0000	0.0500	0.1220
0.1200	0.0000	0.0400	0.1320
0.1200	0.0000	0.0400	0.1520

TEMPERATURE DIFFERENCE

Y (M)	DT1 DEG C	DT2 DEG C	Y2 M
0.0000	10.00	1.20	0.0000
0.0015	9.25	1.20	0.0040
0.0041	7.00	1.60	0.0070
0.0065	4.51	2.10	0.0120
0.0115	3.42	1.80	0.0170
0.0215	2.64	1.60	0.0220
0.0315	1.07	0.80	0.0320
0.0515	0.79	0.80	0.0420
0.0815	0.15	0.40	0.0520
0.1115	0.06	0.20	0.0620
0.1200	0.06	0.20	0.0720
0.1200	0.00	0.20	0.0820
0.1200	0.00	0.00	0.0920
0.1200	0.00	0.00	0.1020
0.1200	0.00	0.00	0.1120
0.1200	0.00	0.00	0.1220
0.1200	0.00	0.00	0.1320
0.1200	0.00	0.00	0.1520

COMPARISON TABLE
DEV., THEOR. =100

QUANTITY	THEOR	TEST 1	TEST2
VOLUME(M3/S.M)	1.249.-02	2.004.-02	1.960.-02
DEVIATION	100	160.5	157.0
MOMENTUM(KGM/S2.M)	4.023.-03	5.263.-03	4.831.-03
DEVIATION	100	130.8	120.1
HEAT CONTENT (W)	3.557.+01	5.005.+01	2.097.+01
DEVIATION	100	140.7	58.9
MEAN TEMP. DIF. (C)	2.4	2.1	0.9
DEVIATION	100	87.8	37.6

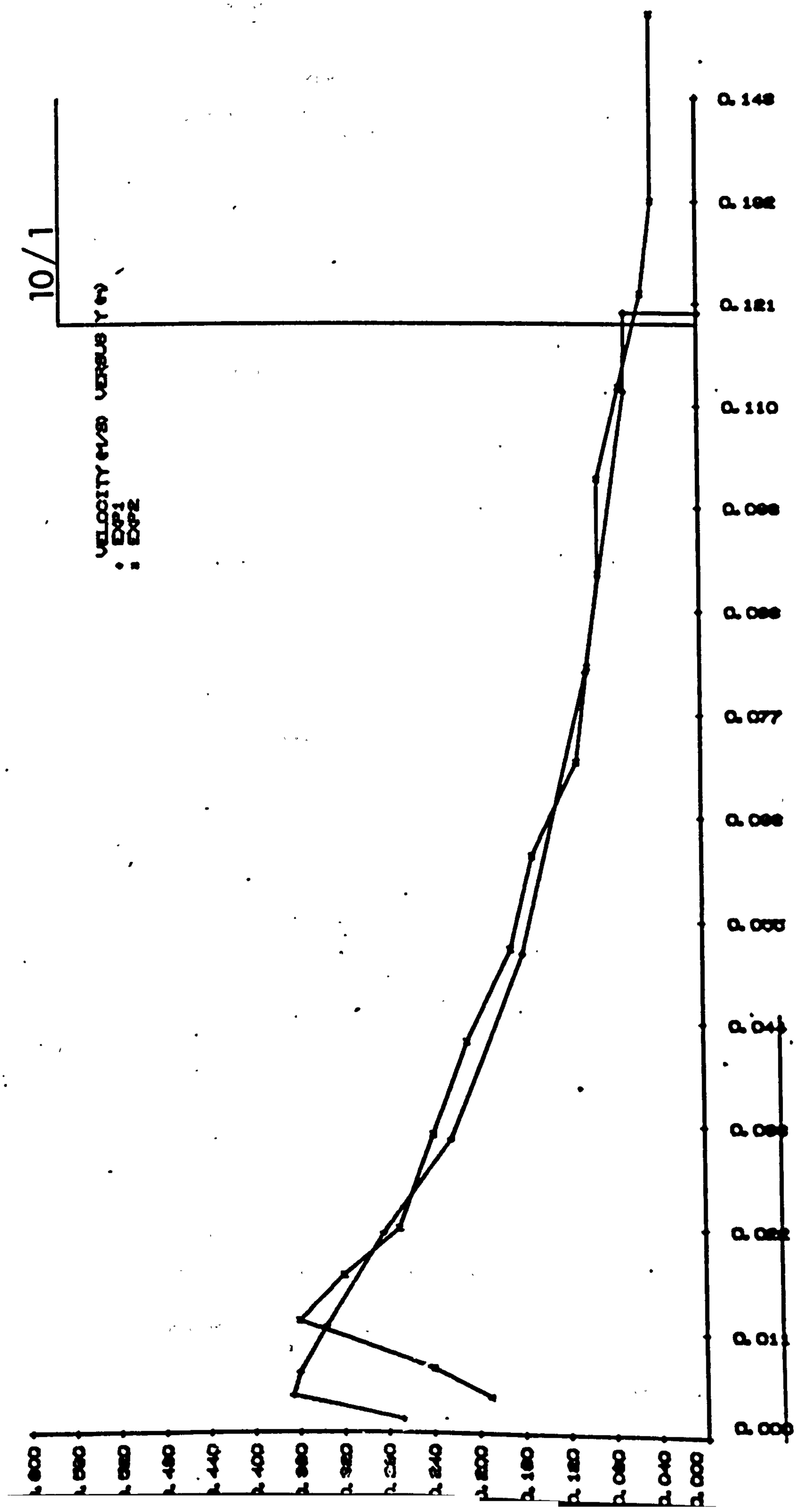
10/1
VELOCITY (FT/SEC) VERSUS Y (IN)
EXP1
EXP2
0.140
0.122
0.121
0.110
0.088
0.066
0.077
0.055
0.044
0.033
0.022
0.011
0.000
800
760
720
680
640
600
560
520
480
440
400
360
320
280
240
200
160
120
080
040
000

DT= 30 DEG. C X= 1.55 M

30/1

TURBULENT
BASIC DATA:
KIN VISCOSITY[M2/S] 1.57.-05

DENSITY[KG/M3] 1.18
SPECIFIC HEAT CAPACITY[KCAL/M3DEG C] 0.283
DATA:

V(MAX)[M/S]	0.682	V(1)[M/S]	1.275
DELTA[M]	0.1064	Y(VMAX)[M]	0.0037
GR	1.517.+10	NU(MEAN)	2.235.+02

VELOCITY

Y (M)	VTH (M/S)	V1 (M/S)	V2 (M/S)	Y2 (M)
0.0000	0.0000	0.0000	0.0000	0.0000
0.0015	0.6554	0.3621	0.3300	0.0030
0.0020	0.6700	0.4422	0.4200	0.0060
0.0037	0.6850	0.4930	0.4900	0.0110
0.0070	0.6584	0.4830	0.4200	0.0160
0.0120	0.5785	0.4530	0.3800	0.0210
0.0220	0.4030	0.4073	0.3300	0.0310
0.0320	0.2567	0.3621	0.2700	0.0410
0.0420	0.1498	0.3123	0.2100	0.0510
0.0520	0.0786	0.2562	0.1900	0.0610
0.0720	0.0132	0.1509	0.1300	0.0710
0.1020	0.0000	0.0754	0.0900	0.0810
0.1320	0.0000	0.0601	0.0600	0.0910
0.1320	0.0000	0.0000	0.0500	0.1010
0.1320	0.0000	0.0000	0.0500	0.1110
0.1320	0.0000	0.0000	0.0500	0.1210
0.1320	0.0000	0.0000	0.0600	0.1310
0.1320	0.0000	0.0000	0.0300	0.1510

TEMPERATURE DIFFERENCE

Y (M)	DTTH DEG C	DT1 DEG C	DT2 DEG C	Y2 M
0.0000	30.00	30.00	3.80	0.00
0.0015	13.68	24.43	3.80	0.003
0.0020	13.00	20.89	5.10	0.006
0.0037	11.43	18.90	4.60	0.011
0.0070	9.66	13.89	4.10	0.016
0.0120	8.04	8.50	3.60	0.021
0.0220	6.05	5.57	2.70	0.031
0.0320	4.73	4.27	2.20	0.041
0.0420	3.73	2.86	1.80	0.051
0.0520	2.92	2.51	1.00	0.061
0.0720	1.63	1.50	0.80	0.071
0.1020	0.18	0.84	0.80	0.081
0.1320	0.00	0.84	0.30	0.091
0.1320	0.00	0.00	0.10	0.101
0.1320	0.00	0.00	0.10	0.111
0.1320	0.00	0.00	0.10	0.121
0.1320	0.00	0.00	-0.40	0.131
0.1320	0.00	0.00	-0.20	0.151

COMPARISON TABLE
DEV., THEOR. =100

QUANTITY	THEOR	TEST 1	TEST2
VOLUME(M3/S.M)	1.938.-02	2.747.-02	2.355.-02
DEVIATION	100	141.7	121.6
MOMENTUM(KGM/S2.M)	1.065.-02	1.069.-02	8.413.-03
DEVIATION	100	100.4	79.0
HEAT CONTENT (W)	1.627.+02	1.956.+02	7.775.+01
DEVIATION	100	120.2	47.8
MEAN TEMP. DIF. (C)	7.1	6.0	2.8
DEVIATION	100	84.9	39.3

30/1
VELOCITY (M/S) VERSUS Y (M)
THEORETICAL
EXP1
EXP2
0.154
0.143
0.132
0.121
0.110
0.099
0.088
0.077
0.066
0.055
0.044
0.033
0.022
0.011
0.00
600
560
520
480
440
400
360
320
280
240
200
160
120
080
040
000

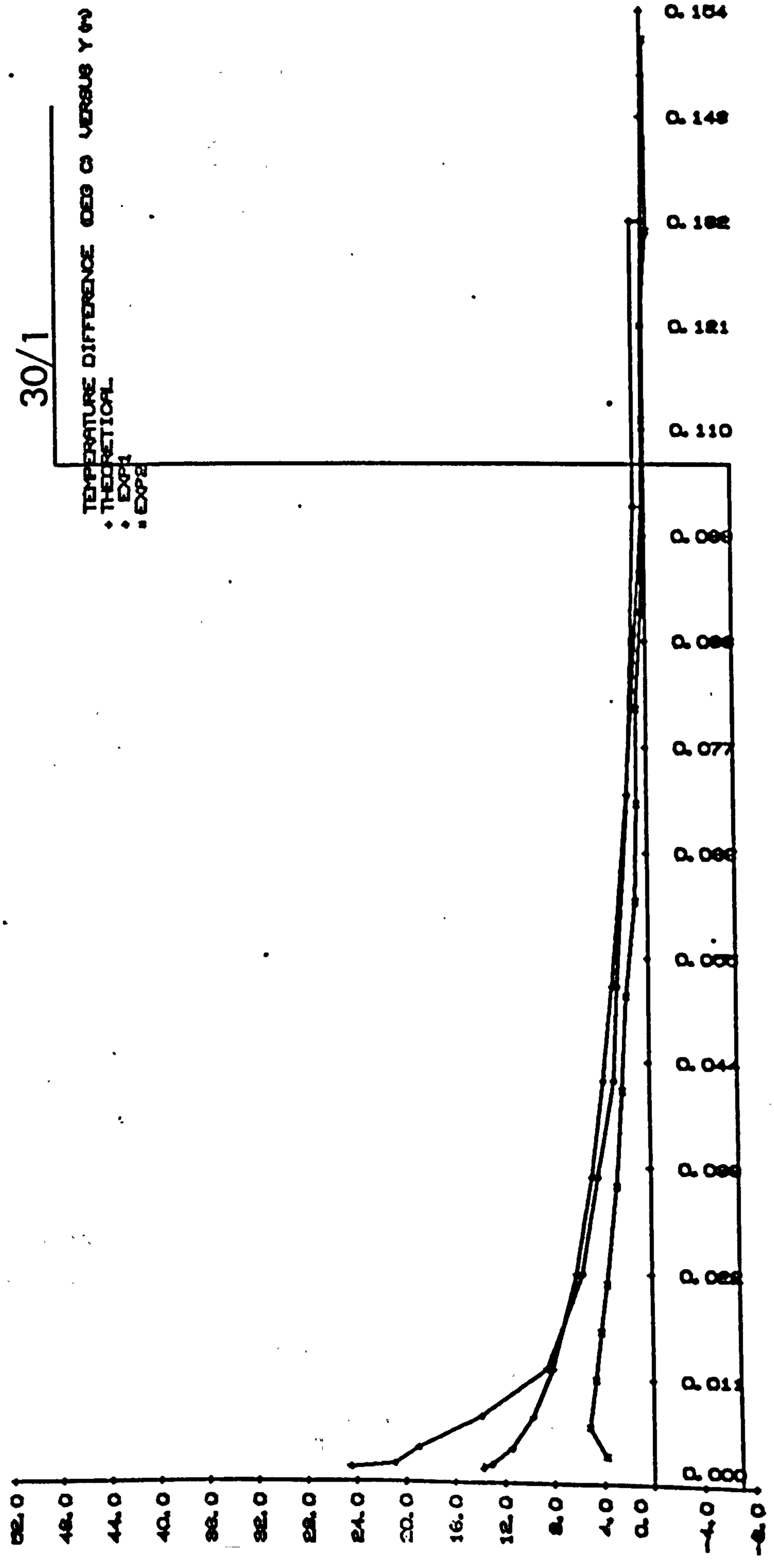
30/1
TEMPERATURE DIFFERENCE (DEG C) VERSUS Y (M)
THEORETICAL
EXP1
EXP2
0.154
0.140
0.126
0.112
0.098
0.084
0.070
0.056
0.042
0.028
0.014
0.000
52.0
48.0
44.0
40.0
36.0
32.0
28.0
24.0
20.0
16.0
12.0
8.0
4.0
0.0
-4.0
-8.0

DT= 30 DEG. C X= 1.55 M

VELOCITY

30/2

Y (M)	V1 (M/S)	V2 (M/S)	Y2 (M)
0.0000	0.0000	0.0000	0.0000
0.0015	0.3621	0.3800	0.0030
0.0020	0.4422	0.4200	0.0060
0.0037	0.4930	0.4900	0.0110
0.0070	0.4830	0.4200	0.0160
0.0120	0.4530	0.3800	0.0210
0.0220	0.4073	0.3300	0.0310
0.0320	0.3621	0.3000	0.0410
0.0420	0.3123	0.1900	0.0510
0.0520	0.2562	0.1500	0.0610
0.0720	0.1509	0.1300	0.0710
0.1020	0.0754	0.1100	0.0810
0.1320	0.0601	0.1000	0.0910
0.1320	0.0000	0.0600	0.1010
0.1320	0.0000	0.0600	0.1110
0.1320	0.0000	0.0300	0.1210
0.1320	0.0000	0.0200	0.1310
0.1320	0.0000	0.0500	0.1510

TEMPERATURE DIFFERENCE

Y (M)	DT1 DEG C	DT2 DEG C	Y2 M
0.0000	30.00	5.20	0.0000
0.0015	24.43	5.20	0.0030
0.0020	20.89	4.70	0.0060
0.0037	18.90	4.70	0.0110
0.0070	13.89	4.70	0.0160
0.0120	8.50	3.00	0.0210
0.0220	5.57	2.80	0.0310
0.0320	4.27	2.30	0.0410
0.0420	2.86	1.90	0.0510
0.0520	2.51	1.40	0.0610
0.0720	1.50	0.90	0.0710
0.1020	0.84	0.40	0.0810
0.1320	0.84	0.20	0.0910
0.1320	0.00	0.20	0.1010
0.1320	0.00	0.20	0.1110
0.1320	0.00	0.40	0.1210
0.1320	0.00	0.90	0.1310
0.1320	0.00	0.20	0.1510

COMPARISON TABLE
DEV., THEOR. =100

QUANTITY	THEOR	TEST 1	TEST2
VOLUME(M3/S.M)	1.938.-02	2.747.-02	2.413.-02
DEVIATION	100	141.7	124.5
MOMENTUM(KGM/S2.M)	1.065.-02	1.069.-02	8.628.-03
DEVIATION	100	100.4	81.0
HEAT CONTENT (W)	1.627.+02	1.956.+02	8.120.+01
DEVIATION	100	120.2	49.9
MEAN TEMP. DIF. (C)	7.1	6.0	2.8
DEVIATION	100	84.9	40.1

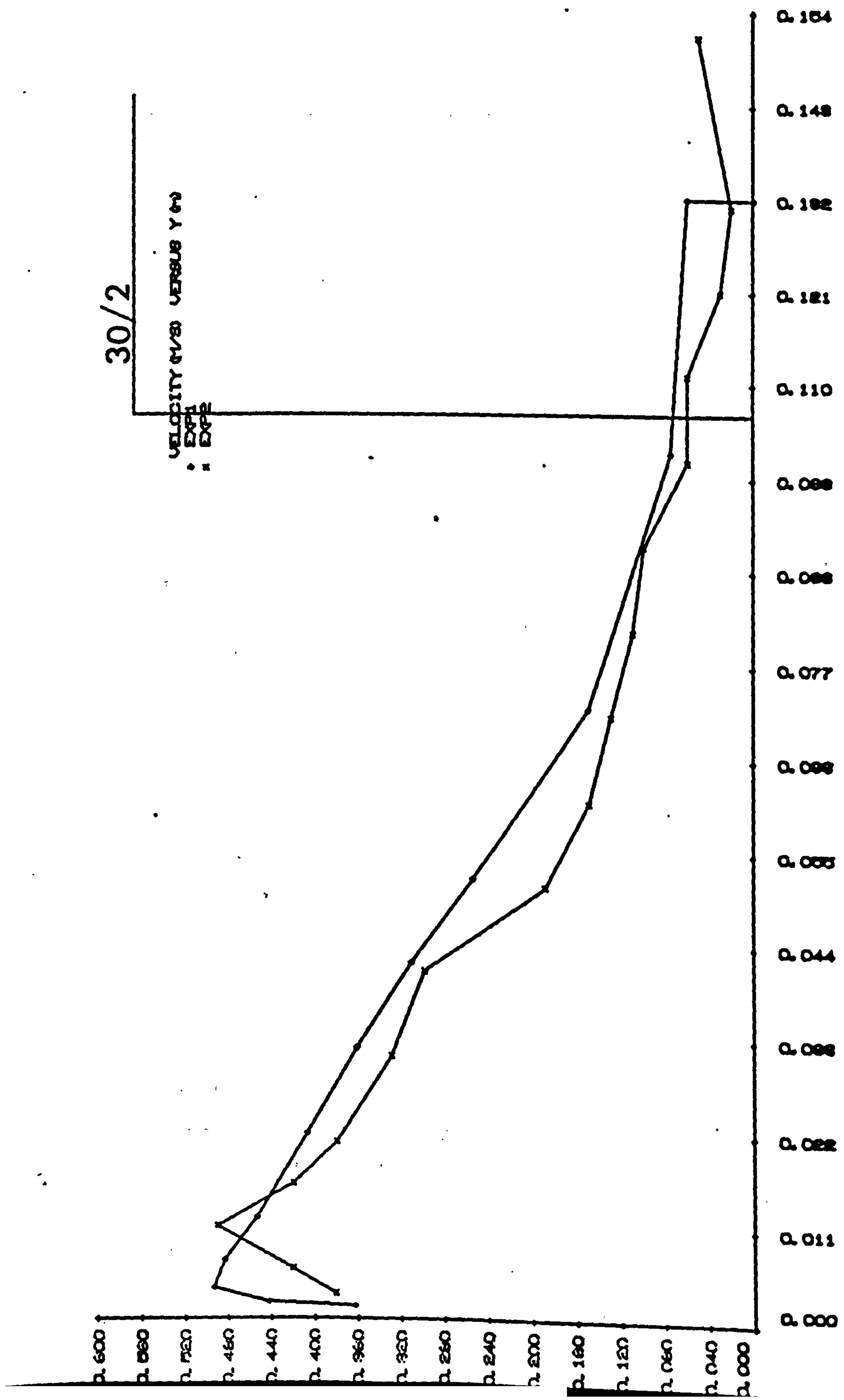
30/2
VELOCITY (M/S) VERSUS Y (M)
EXP1
EXP2
0.600
0.560
0.520
0.480
0.440
0.400
0.360
0.320
0.280
0.240
0.200
0.160
0.120
0.080
0.040
0.000
0.154
0.143
0.132
0.121
0.110
0.099
0.088
0.077
0.066
0.055
0.044
0.033
0.022
0.011
0.00

DT= 50 DEG. C X= 1.55 M

VELOCITY

50/1

Y (M)	V1 (M/S)	V2 (M/S)	Y2 (M)
0.0000	0.0000	0.0000	0.0000
0.0015	0.4705	0.3800	0.0030
0.0030	0.5807	0.5400	0.0060
0.0035	0.5900	0.5880	0.0110
0.0080	0.5582	0.5400	0.0160
0.0130	0.5281	0.4700	0.0210
0.0230	0.4605	0.4200	0.0310
0.0330	0.3679	0.3300	0.0410
0.0430	0.2979	0.2700	0.0510
0.0530	0.2328	0.1900	0.0610
0.0630	0.1753	0.1300	0.0710
0.0730	0.1402	0.1100	0.0810
0.1030	0.0651	0.0600	0.0910
0.1330	0.0601	0.0500	0.1010
0.1330	0.0000	0.0900	0.1110
0.1330	0.0000	0.0600	0.1210
0.1330	0.0000	0.0600	0.1310
0.1330	0.0000	0.0600	0.1510

TEMPERATURE DIFFERENCE

Y (M)	DT1 DEG C	DT2 DEG C	Y2 M
0.0000	50.00	8.20	0.0000
0.0015	37.93	8.20	0.0030
0.0030	28.40	8.20	0.0060
0.0035	27.20	8.20	0.0110
0.0080	14.68	7.70	0.0160
0.0130	10.53	7.00	0.0210
0.0230	6.97	4.60	0.0310
0.0330	3.36	3.80	0.0410
0.0430	2.61	3.40	0.0510
0.0530	2.11	2.20	0.0610
0.0630	1.41	1.00	0.0710
0.0730	0.81	0.80	0.0810
0.1030	0.00	0.80	0.0910
0.1330	0.00	0.80	0.1010
0.1330	0.00	0.80	0.1110
0.1330	0.00	0.60	0.1210
0.1330	0.00	0.60	0.1310
0.1330	0.00	0.30	0.1510

COMPARISON TABLE
DEV., THEOR. =100

QUANTITY	THEOR	TEST 1	TEST2
VOLUME(M3/S.M)	2.377.-02	2.948.-02	2.801.-02
DEVIATION	100	124.0	117.8
MOMENTUM(KGM/S2.M)	1.658.-02	1.272.-02	1.244.-02
DEVIATION	100	76.7	75.0
HEAT CONTENT (W)	3.362.+02	2.785.+02	1.752.+02
DEVIATION	100	82.8	52.1
MEAN TEMP. DIF. (C)	11.8	7.9	5.2
DEVIATION	100	66.9	44.3

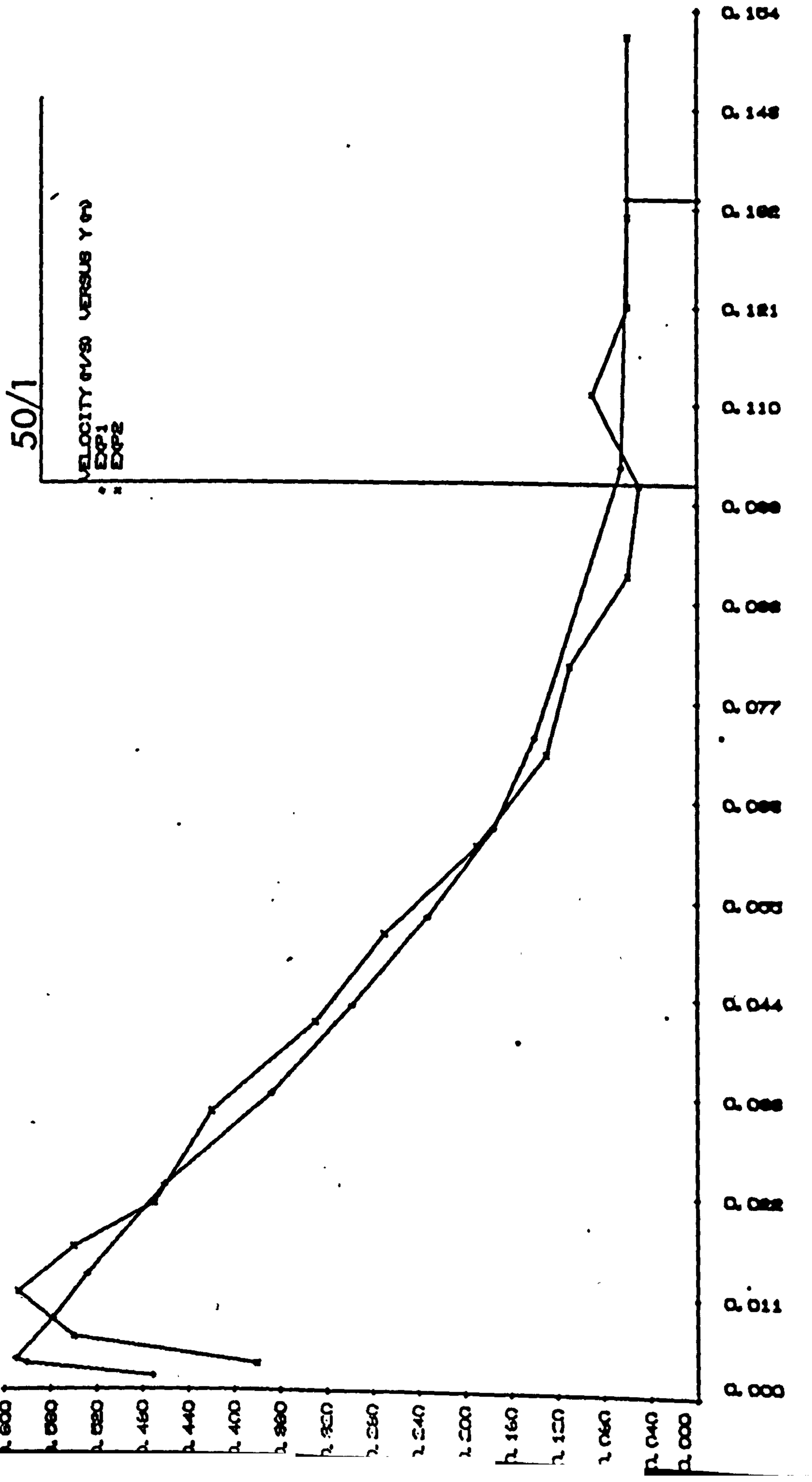
50/1
VELOCITY (M/S) VERSUS Y (M)
EXP1
EXP2
0.104
0.148
0.132
0.121
0.110
0.077
0.044
0.011
1.600
1.560
1.520
1.480
1.440
1.400
1.360
1.320
1.280
1.240
1.200
1.160
1.120
1.080
1.040
1.000

CONVECTIVE CURRENT
DT= 50 DEG. C X= 1.55 M

50/2

TURBULENT
BASIC DATA:

KIN VISCOSITY[M2/S]	1.57.-05		
DENSITY[KG/M3]	1.16		
SPECIFIC HEAT CAPACITY[KCAL/M3DEG C]	0.286		
DATA:			
V(MAX)[M/S]	0.880	V(1)[M/S]	1.646
DELTA[M]	0.1011	Y(VMAX)[M]	0.0035
GR	2.529.+10	NU(MEAN)	2.742.+02

VELOCITY

Y (M)	VTH (M/S)	V1 (M/S)	V2 (M/S)	Y2 (M)
0.0000	0.0000	0.0000	0.0000	0.0000
0.0015	0.8497	0.4705	0.4200	0.0030
0.0030	0.8829	0.5807	0.5400	0.0060
0.0035	0.8843	0.5900	0.5900	0.0110
0.0080	0.8240	0.5582	0.5400	0.0160
0.0130	0.7081	0.5281	0.5000	0.0210
0.0230	0.4745	0.4605	0.4200	0.0310
0.0330	0.2888	0.3679	0.3300	0.0410
0.0430	0.1589	0.2979	0.2500	0.0510
0.0530	0.0769	0.2328	0.2100	0.0610
0.0630	0.0310	0.1753	0.1700	0.0710
0.0730	0.0094	0.1402	0.1300	0.0810
0.1030	0.0000	0.0651	0.0900	0.0910
0.1330	0.0000	0.0601	0.0900	0.1010
0.1330	0.0000	0.0000	0.0700	0.1110
0.1330	0.0000	0.0000	0.0600	0.1210
0.1330	0.0000	0.0000	0.0900	0.1310
0.1330	0.0000	0.0000	0.0600	0.1510

TEMPERATURE DIFFERENCE

Y (M)	DTTH DEG C	DT1 DEG C	DT2 DEG C	Y2 M
0.0000	50.00	50.00	8.00	0.00
0.0015	22.60	37.93	8.00	0.003
0.0030	19.75	28.40	8.00	0.006
0.0035	19.08	27.20	6.90	0.011
0.0080	15.20	14.68	6.40	0.016
0.0130	12.70	10.53	6.40	0.021
0.0230	9.53	6.97	5.70	0.031
0.0330	7.39	3.36	5.00	0.041
0.0430	5.75	2.61	1.60	0.051
0.0530	4.41	2.11	1.10	0.061
0.0630	3.27	1.41	0.90	0.071
0.0730	2.27	0.81	0.40	0.081
0.1030	0.00	0.00	0.40	0.091
0.1330	0.00	0.00	0.00	0.101
0.1330	0.00	0.00	-0.20	0.111
0.1330	0.00	0.00	-0.20	0.121
0.1330	0.00	0.00	-0.20	0.131
0.1330	0.00	0.00	-0.20	0.151

COMPARISON TABLE
DEV.. THEOR. =100

QUANTITY	THEOR	TEST 1	TEST2
VOLUME(M3/S.M)	2.377.-02	2.948.-02	2.949.-02
DEVIATION	100	124.0	124.1
MOMENTUM(KGM/S2.M)	1.658.-02	1.272.-02	1.307.-02
DEVIATION	100	76.7	78.8
HEAT CONTENT (W)	3.362.+02	2.785.+02	1.674.+02
DEVIATION	100	82.8	49.8
MEAN TEMP. DIF. (C)	11.8	7.9	4.7
DEVIATION	100	66.9	40.2

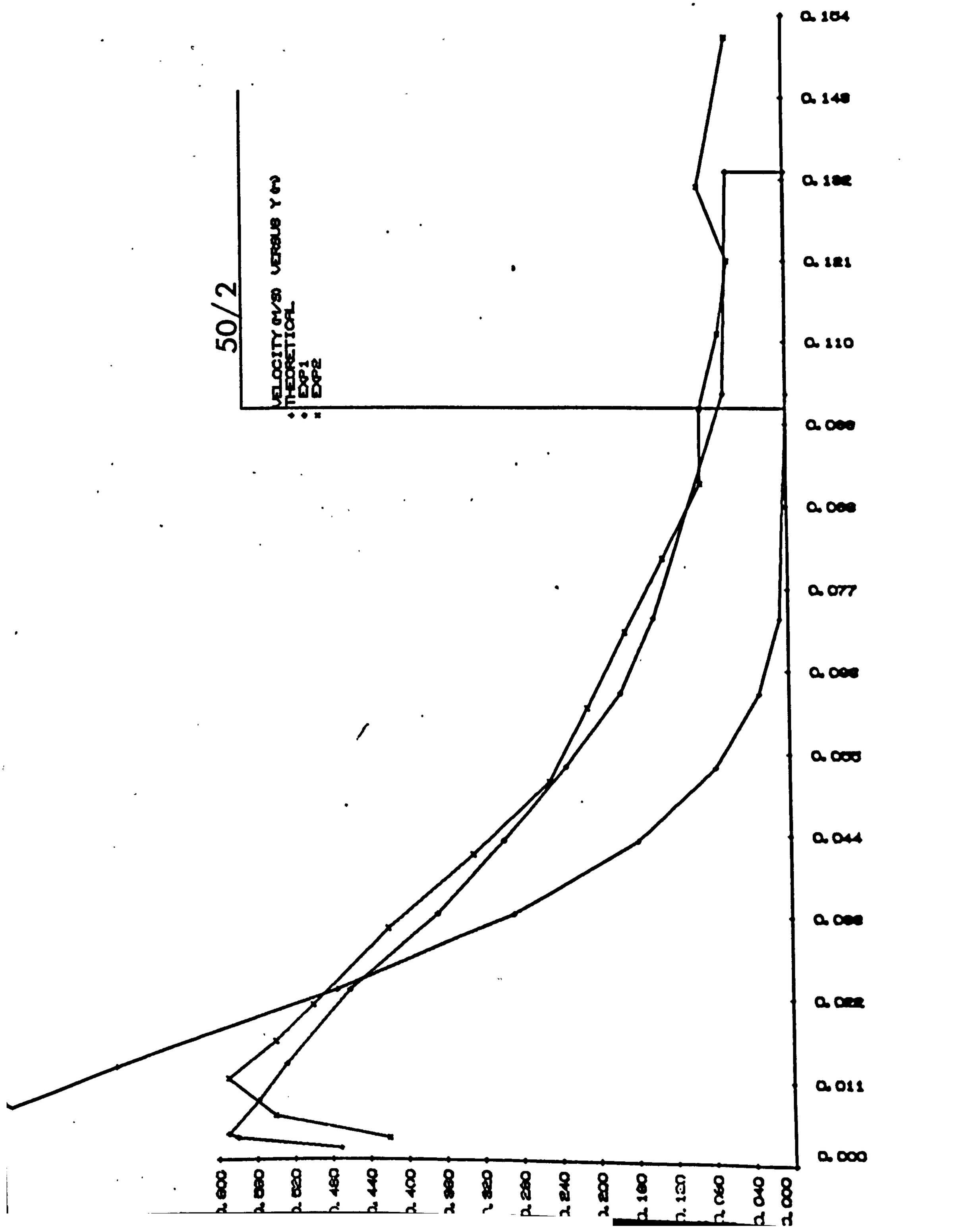
50/2
VELOCITY (M/S) VERSUS Y (M)
THEORETICAL
EXP1
EXP2
0.154
0.143
0.132
0.121
0.110
0.099
0.088
0.077
0.066
0.055
0.044
0.033
0.022
0.011
0.00
2.600
2.560
2.520
2.480
2.440
2.400
2.360
2.320
2.280
2.240
2.200
2.160
2.120
2.080
2.040
2.000

CONVECTIVE CURRENT

DT= 50. DEG. C X= 1.55 M

50/3

TURBULENT
BASIC DATA:

KIN VISCOSITY[M2/S]	1.57.-05		
DENSITY[KG/M3]	1.16		
SPECIFIC HEAT CAPACITY[KCAL/M3DEG C]	0.286		
DATA:			
V(MAX)[M/S]	0.880	V(1)[M/S]	1.646
DELTA[M]	0.1011	Y(VMAX)[M]	0.0035
GR	2.529.+10	NU(MEAN)	2.742.+02

VELOCITY

Y (M)	VTH (M/S)	V1 (M/S)	V2 (M/S)	Y2 (M)
0.0000	0.0000	0.0000	0.0000	0.0000
0.0015	0.8497	0.4705	0.4000	0.0030
0.0030	0.8829	0.5807	0.4900	0.0060
0.0035	0.8843	0.5900	0.5900	0.0110
0.0080	0.8240	0.5582	0.5600	0.0160
0.0130	0.7081	0.5281	0.4900	0.0210
0.0230	0.4745	0.4605	0.4200	0.0310
0.0330	0.2888	0.3679	0.3300	0.0410
0.0430	0.1589	0.2979	0.2800	0.0510
0.0530	0.0769	0.2328	0.2100	0.0610
0.0630	0.0310	0.1753	0.1700	0.0710
0.0730	0.0094	0.1402	0.1100	0.0810
0.1030	0.0000	0.0651	0.1000	0.0910
0.1330	0.0000	0.0601	0.0700	0.1010
0.1330	0.0000	0.0000	0.0600	0.1110
0.1330	0.0000	0.0000	0.0700	0.1210
0.1330	0.0000	0.0000	0.0400	0.1310
0.1330	0.0000	0.0000	0.0700	0.1510

TEMPERATURE DIFFERENCE

Y (M)	DTTH DEG C	DT1 DEG C	DT2 DEG C	Y2 M
0.0000	50.00	50.00	8.10	0.00
0.0015	22.60	37.93	8.10	0.003
0.0030	19.75	28.40	8.10	0.006
0.0035	19.08	27.20	7.70	0.011
0.0080	15.20	14.68	7.00	0.016
0.0130	12.70	10.53	6.70	0.021
0.0230	9.53	6.97	5.40	0.031
0.0330	7.39	3.36	4.70	0.041
0.0430	5.75	2.61	2.20	0.051
0.0530	4.41	2.11	1.90	0.061
0.0630	3.27	1.41	1.00	0.071
0.0730	2.27	0.81	0.80	0.081
0.1030	0.00	0.00	0.60	0.091
0.1330	0.00	0.00	0.60	0.101
0.1330	0.00	0.00	0.60	0.111
0.1330	0.00	0.00	0.60	0.121
0.1330	0.00	0.00	0.60	0.131
0.1330	0.00	0.00	0.30	0.151

COMPARISON TABLE
DEV.. THEOR. =100

QUANTITY	THEOR	TEST 1	TEST2
VOLUME(M3/S.M)	2.377.-02	2.948.-02	2.934.-02
DEVIATION	100	124.0	123.4
MOMENTUM(KGM/S2.M)	1.658.-02	1.272.-02	1.295.-02
DEVIATION	100	76.7	78.1
HEAT CONTENT (W)	3.362.+02	2.785.+02	1.747.+02
DEVIATION	100	82.8	52.0
MEAN TEMP. DIF. (C)	11.8	7.9	5.0
DEVIATION	100	66.9	42.1

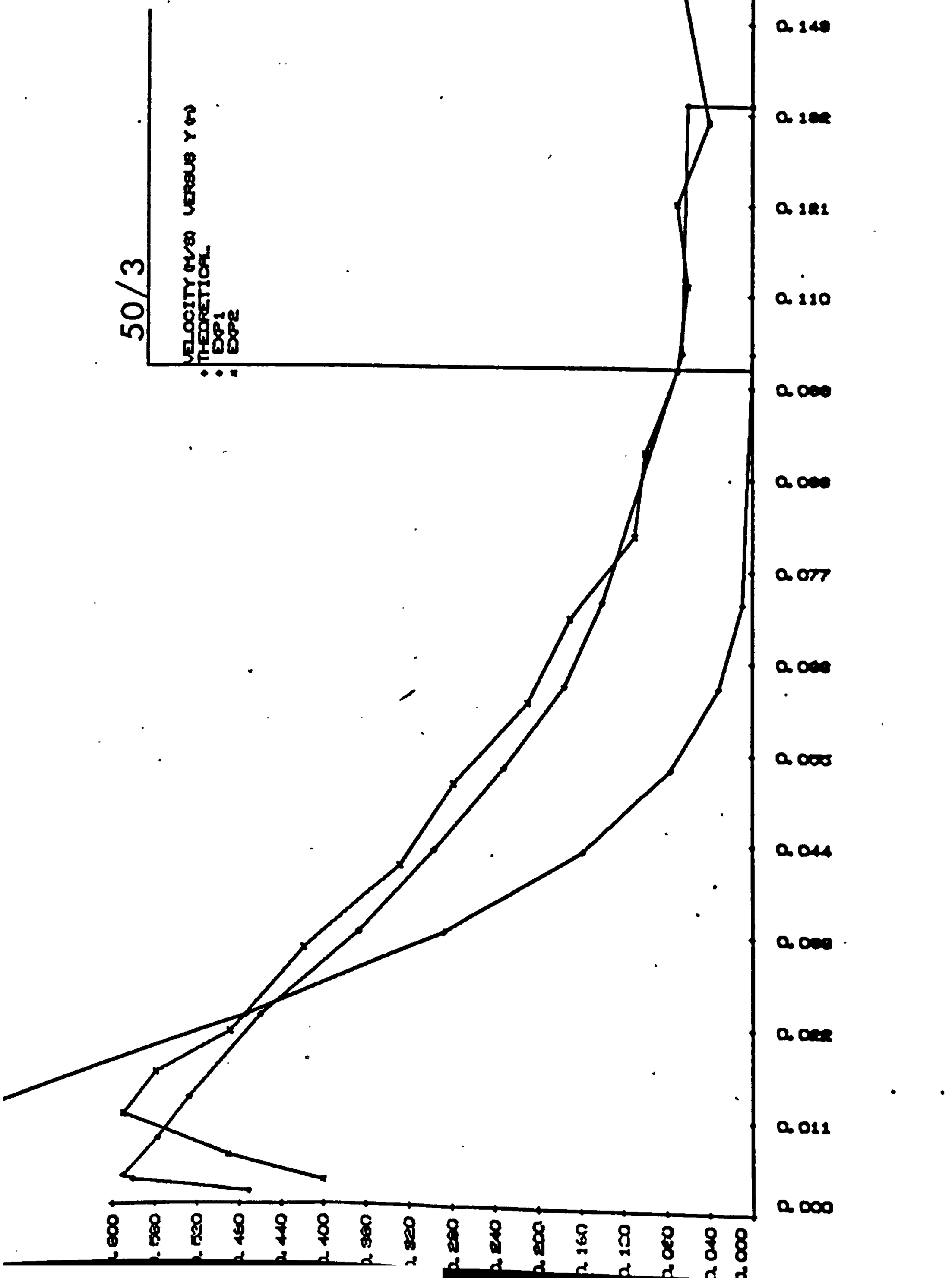
50/3
VELOCITY (M/S) VERSUS Y (M)
THEORETICAL
EXP1
EXP2
0.154
0.143
0.132
0.121
0.110
0.099
0.088
0.077
0.066
0.055
0.044
0.033
0.022
0.011
0.00
1.600
1.580
1.520
1.480
1.440
1.400
1.360
1.320
1.280
1.240
1.200
1.160
1.120
1.080
1.040
1.000